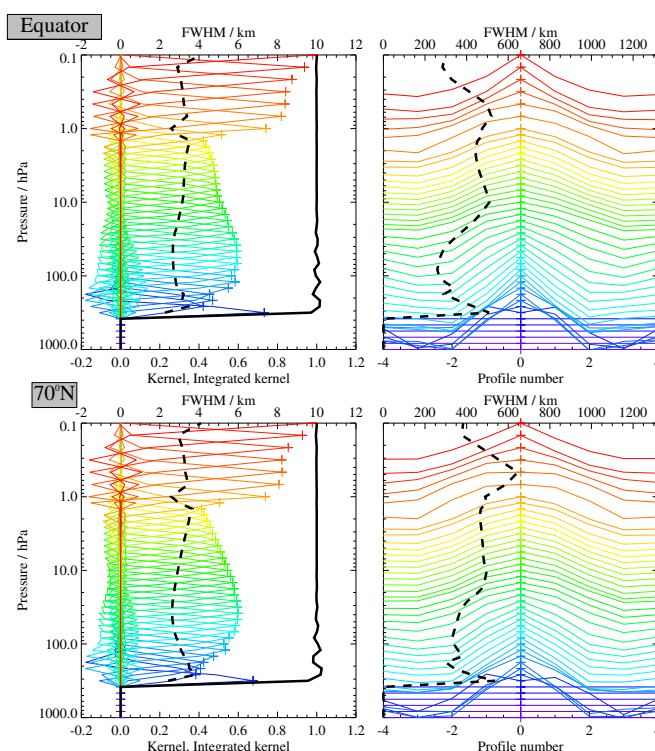
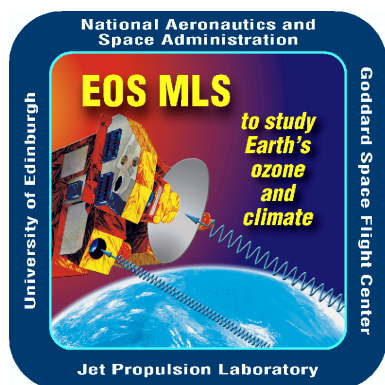


JPL D-33509 Rev. E

## Earth Observing System (EOS)

### Aura Microwave Limb Sounder (MLS)

# Version 4.2x Level 2 and 3 data quality and description document.



Nathaniel J. Livesey, William G. Read, Paul A. Wagner, Lucien Froidevaux, Alyn Lambert, Gloria L. Manney, Luis F. Millán Valle, Hugh C. Pumphrey, Michelle L. Santee, Michael J. Schwartz, Shuhui Wang, Ryan A. Fuller, Robert F. Jarnot, Brian W. Knosp, Elmain Martinez, Richard R. Lay

### Version 4.2x–4.0

April 20, 2020



Jet Propulsion Laboratory  
 California Institute of Technology  
 Pasadena, California, 91109-8099

© 2020 California Institute of Technology. Government sponsorship acknowledged.

## Navigating this document

Clicking on “Help” takes you back to this page.

An overview of the information in this document is given on the next page. You can return to it by clicking on the “Overview” tab in the navigation bar.

First time users of MLS data are advised to read Chapter 1 first. The discussion includes a table summarizing key aspects of each MLS product. This table can be accessed from anywhere in the document by clicking on the “Table” tab in the navigation bar.

Chapter 3 describes each of the MLS data products individually. You can use the navigation bar to skip immediately to any of the product-specific sections.

Each section includes

- A set of rules for screening out data points not recommended for scientific use.
- A table summarizing the precision, accuracy, resolution for each MLS product.

Clicking on the product name in the navigation bar takes you to the beginning of that section; clicking on the “S” and “T” symbols takes you directly to the screening rules and summary table, respectively, for that product.

## Acknowledgment

This research was carried out at the Jet Propulsion Laboratory, California Institute of Technology, under a contract with the National Aeronautics and Space Administration.

Help	
Overview	
Table	
BrO	S T
CH <sub>3</sub> Cl	S T
CH <sub>3</sub> CN	S T
CH <sub>3</sub> OH	S T
ClO	S T
CO	S T
GPH	S T
H <sub>2</sub> O	S T
HCl	S T
HCN	S T
HNO <sub>3</sub>	S T
HO <sub>2</sub>	S T
HOCl	S T
IWC	S T
IWP	S T
N <sub>2</sub> O	S T
O <sub>3</sub>	S T
OH	S T
RHI	S T
SO <sub>2</sub>	S T

## Where to find answers to key questions

This document serves two purposes. Firstly, to summarize the quality of version 4.x Aura MLS Level 2 data. Secondly, to convey important information on how to read and interpret the data to the scientific community.

The MLS science team strongly encourages users of MLS data to thoroughly read this document. Chapter 1 describes essential general information for all users. Chapter 2 is considered background material that may be of interest to data users. Chapter 3 discusses individual MLS data products in detail.

For convenience, this page provides information on how to quickly ascertain answers to anticipated key questions.

### Where do I get v4.2x MLS Level 2 data?

All the MLS Level 2 data described here can be obtained from the NASA Goddard Space Flight Center Earth Science Data and Information Services Center (GES-DISC, see <https://disc.gsfc.nasa.gov/>).

### What format are MLS data files in?

MLS Level 2 data are in HDF-EOS version 5 format (section 1.5, page 4). Level 3 data are in netCDF 4 (section 4.2, page 161).

### Which MLS data points should be avoided? How much should I trust the remainder?

These issues are described in section 1.6 (starting on page 5), and on a product by product basis in chapter 3. The key rules are:

- Only data within the appropriate pressure range (described product by product in chapter 3) are to be used.
- Always consider the precision of the data, as reported in the L2gpPrecision field.
- Do not use any data points where the precision is zero or a negative number. This indicates poor information yield from MLS.

- Do not use data for any profile where the field Status is an odd number.
- Data for profiles where the Status field is non zero should be approached with caution. See section 1.6 on page 5, and the product by product description in chapter 3 for details on how to interpret the Status field.
- Do not use any data for profiles where the Quality field is *smaller* than the threshold given in the section of chapter 3 describing your product of interest.
- Do not use any data for profiles where the Convergence field is *larger* than the threshold given in the section of chapter 3 describing your product of interest.
- Some products require additional screening to remove biases or outliers, as described in chapter 3.
- Information on the accuracy of each product is given in Chapter 3. In the previous versions of this document, the numbers given were for the previous v3.3 dataset. This document has now been updated with the specific v4.2x accuracy estimates.
- Data users are strongly encouraged to contact the MLS science team to discuss their anticipated usage of the data, and are always welcome to ask further data quality questions.

### Why do some species abundances show negative values, and how do I interpret these?

Some of the MLS measurements have a poor signal to noise ratio for individual profiles. Radiance noise can naturally lead to some negative values for these species. It is critical to consider such values in scientific study. Any analysis that involves taking some form of average will exhibit a high bias if the points with negative mixing ratios are ignored.

## Document revision history

### Version 4.x-0.1

A pre-release version of the document, starting from the most recent version 3 document.

### Version 4.x-1.0

The first publicly released version of this document. Released when the MLS v4.20 data set was made publicly available.

### Version 4.x-2.0

The second publicly released version of the document. This describes the minor changes associated with v4.22 (which fixes an issue that gave poor temperature profiles at the end of many days). In addition, this version also include minor corrections and updates (notably a fix to the averaging kernel plots which had the tropical and 70°N cases swapped).

### Version 4.x-3.0

The third released version of the document. The changes mainly reflect updates of systematic error analysis results specific to version 4.

### Version 4.x-3.1

A minor update to reflect the change in recommendation of Quality thresholds for N<sub>2</sub>O (190 GHz) and H<sub>2</sub>O, and an additional screening rule for the latter.

### Version 4.x-4.0

Added a discussion of the new MLS “Level 3” products based on the v4.2x Level 2 input data in a new Chapter (4).

S  
T

BRO

S  
TCH<sub>3</sub>ClS  
TCH<sub>3</sub>CNS  
TCH<sub>3</sub>OHS  
T

ClO

S  
T

CO

S  
T

GPH

S  
TH<sub>2</sub>OS  
T

HCl

S  
T

HCN

S  
THNO<sub>3</sub>S  
THO<sub>2</sub>S  
T

HOCl

S  
T

IWC

S  
T

IWP

S  
TN<sub>2</sub>OS  
TO<sub>3</sub>S  
T

OH

S  
T

RH

S  
TSO<sub>2</sub>S  
TS  
T



3.20	Relative Humidity with respect to Ice (RHI) . . . . .	136
3.21	Sulfur Dioxide (SO <sub>2</sub> ) . . . . .	143
3.22	Temperature (T) . . . . .	150
<b>4</b>	<b>MLS Level 3 datasets</b>	<b>160</b>
4.1	Introduction . . . . .	160
4.2	Level 3 data files . . . . .	161
4.3	Guidance for users of Level 3 data . . . . .	162

Help	S
Overview	T
Table	S
BrO	T
CH <sub>3</sub> Cl	S
CH <sub>3</sub> CN	T
CH <sub>3</sub> OH	S
ClO	T
CO	S
GPH	T
H <sub>2</sub> O	S
HCl	T
HCN	S
HNO <sub>3</sub>	T
HO <sub>2</sub>	S
HOCl	T
IWC	S
IWP	T
N <sub>2</sub> O	S
O <sub>3</sub>	T
OH	S
RHI	T
SO <sub>2</sub>	S
	T

## Chapter 1

# Essential reading for users of MLS version 4.x data

## 1.1 Scope and background for this document

This document describes the quality of the geophysical data products produced by version 4.x of the data processing algorithms for the Earth Observing System (EOS) Microwave Limb Sounder (MLS) instrument on the Aura spacecraft. The intended audience is those wishing to make use of Aura MLS data for scientific study. The bulk of the geophysical products described in this document (this chapter through Chapter 3) are produced by the “Level 2” algorithms, and briefly summarized in Table 1.1.1. In addition Chapter 4 (added in version 4.x-4.0 of this document) describes “Level 3” data products derived from the Level 2 data that provide easier access to collections of MLS observations (e.g., daily zonal means, monthly polar vortex averages) to facilitate simpler studies using MLS observations.

The v4.2x MLS data are the fourth “public release” of MLS data, the first being version 1.5 [Livesey *et al.*, 2005], the second version 2.2, and the third versions 3.3 and 3.4. The v2.2 data are described in a series of validation papers published in a special issue of the *Journal of Geophysical Research* in 2007/2008. This document updates findings from these papers for v4.2x, and gives more general information on the use of MLS data. As always, those wishing to use MLS data are advised to consult the MLS science team concerning their intended use.

In addition to describing the Level 2 data and their quality (this chapter and Chapter 3), Chapter 2 of this document also gives a brief outline of the algorithms used to generate the “Level 2” data (geophysical products reported along the instrument track) from the input “Level 1” data (calibrated microwave radiance observations). Finally, Chapter 4 provides information on MLS Level 3 products.

More information on the MLS instrument can be found in the document *An Overview of the EOS MLS Experiment* [Waters *et al.*, 2004]. A more general discussion of the microwave limb sounding technique and an earlier MLS instrument is given in Waters *et al.* [1999]. The theoretical basis for the Level 2 software is described in Livesey and Snyder [2004]. A crucial component of the Level 2 algorithms is the “Forward Model”, which is described in detail in Read *et al.* [2004] and Schwartz *et al.* [2004]. The document *EOS MLS Retrieved Geophysical Parameter Precision Estimates* [Filipiak *et al.*, 2004] is a very useful source of information on the expected precision of the EOS MLS data, and should be regarded as a companion volume to this document. The impact of clouds on MLS measurements and the use of MLS data to infer cloud properties is described in Wu and Jiang [2004]. All the above documents and papers are available from the MLS web site (<https://mls.jpl.nasa.gov/>).

A subset of the information in those documents is also reported in the *IEEE Transactions on Geoscience and Remote Sensing*. An overview of MLS is given in Waters *et al.* [2006], the algorithms that produce the data described here are reviewed in Livesey *et al.* [2006], Read *et al.* [2006], Schwartz *et al.* [2006], and Wu *et al.* [2006]. Other papers describe the calibration and performance of the various aspects of the MLS instrument [Jarnot *et al.*, 2006; Pickett, 2006; Cofield and Stek, 2006] and the MLS ground data system [Cuddy *et al.*, 2006]. The detailed validation of the MLS v2.2 dataset is described in a collection of papers in the “Aura Validation” special issue of JGR-Atmospheres (papers published in 2007 and 2008). These are cited in Chapter 3 on a product-by-product basis.

## 1.2 Overview of v4.2x and this document

The remainder of this chapter reviews issues that are considered *essential reading* for users of the v4.2x dataset. Chapter 2 details relevant aspects of the MLS instrument design and operations and the theoretical basis for

**Table 1.1.1:** Summary of key information for each MLS standard product. Essential additional information is given in each product section of chapter 3.

Product	Useful vertical range / hPa	Quality threshold <sup>[1]</sup>	Convergence threshold <sup>[2]</sup>	Notes	Contact name
BrO	10 – 3.2	1.3	1.05	A,D,N	Luis Millán Valle
CH3Cl	147 – 4.6	1.3	1.05	N	Michelle Santee
CH3CN	46 – 1.0	1.4	1.05	E,N	Michelle Santee
CH3OH	Not to be used pending further validation				Michelle Santee
ClO	147 – 1.0	1.3	1.05	B	Michelle Santee
CO	100 – 0.0046 215 – 146	1.5	1.03	C	Hugh Pumphrey Michael Schwartz
GPH	83 – 0.001 261 – 100	0.2 0.9	1.03	– C	Michael Schwartz
H2O	83 – 0.002 316 – 100	0.7	2.0	O C,O	Alyn Lambert William Read
HCl	100 – 0.32	1.2	1.05	–	Lucien Froidevaux
HCN	21 – 0.1	0.2	2.0	A,E,N	Hugh Pumphrey
HN03	215 – 1.5	See text	See text	C,O	Gloria Manney
HO2	22 – 0.046	N/A	1.1	A,D,N	Luis Millan & Shuhui Wang
HOC1	10 – 2.2	1.2	1.05	N	Lucien Froidevaux
IWC	215 – 83	N/A	N/A	B	Alyn Lambert
IWP	N/A	N/A	N/A	B	Alyn Lambert
N2O	68 – 0.46	1.0	2.0	–	Alyn Lambert
O3 <sup>[3]</sup>	100 – 0.02 261 – 121	1.0	1.03	C	Lucien Froidevaux Michael Schwartz
OH	32 – 0.0032	N/A	1.1	D	Luis Millan & Shuhui Wang
RHI <sup>[4]</sup>	316 – 0.002	See text	See text	C,O	William Read
SO2	215 – 10	0.95	1.03	E	William Read
Temperature <sup>[5]</sup>	83 – 0.001 261 – 100	0.2 0.9	1.03	– C	Michael Schwartz

**Notes:**

- A Users should consider using alternative versions of this product, produced using different algorithms, as described in the text.
- B This product has significant biases in certain regions that may need to be accounted or corrected for in scientific studies. See text for details.
- C Interference from clouds can affect this product at certain altitudes. See text for details.
- D Biases in this product can be ameliorated (in selected conditions) by taking day/night differences. See text.
- E At some altitudes, this product contains biases of a magnitude that render the product useful only for the study of “enhancement events” (e.g., volcanic plumes, extreme fire pollution). See text for details.

N This is a “noisy” product requiring significant averaging (e.g., monthly zonal mean). See text for details.

O This product contains significant outliers (e.g., spikes or oscillations) in some regions (typically related to clouds in the tropical upper troposphere). These should be screened out as detailed in the text.

[1] Only use profiles with Quality *greater* than this value.

[2] Only use profiles with Convergence *less* than this value.

[3] File also contains a swath giving the column abundance above the (MLS-defined) tropopause.

[4] Relative humidity with respect to ice computed from the MLS H<sub>2</sub>O and Temperature data.

[5] File also contains a swath giving tropopause pressure (WMO definition) inferred from MLS temperatures.



the v4.2x Level 2 algorithms that are considered *background reading*.

Chapter 3 describes the data quality for “Standard” products from the MLS instrument for v4.2x. These are observations of vertical profiles of the abundance of BrO, CH<sub>3</sub>Cl, CH<sub>3</sub>CN, CH<sub>3</sub>OH (a new product on v4.2x) ClO, CO, H<sub>2</sub>O, HCl, HCN, HNO<sub>3</sub>, HO<sub>2</sub>, HOCl, N<sub>2</sub>O, O<sub>3</sub>, and OH and SO<sub>2</sub>, along with temperature, geopotential height, relative humidity (deduced from the H<sub>2</sub>O and temperature data), cloud ice water content and cloud ice water path, all described as functions of pressure. In v4.2x these profiles are mostly output on a grid that has a vertical spacing of six surfaces per decade change in pressure (~2.5 km), thinning out to three surfaces per decade above 0.1 hPa. Exceptions to this are water vapor, temperature, ozone and relative humidity which are on a finer 12 per decade grid from 1000 hPa to 1 hPa. Cloud ice water content is also reported on this fine grid, though these profiles do not extend to the stratosphere and mesosphere. The OH product maintains a 6 per decade grid spacing into the upper mesosphere. Horizontally the profiles are spaced by 1.5° great-circle angle along the orbit, which corresponds to about 160 km. The true vertical and along-track horizontal resolution of the products is typically somewhat coarser than the reporting grid described here. For some of the products, the signal to noise ratio is too low to yield scientifically useful data from a single MLS profile observation. In these cases, some form of averaging (e.g., weekly maps, monthly zonal means etc.) will be required to obtain more useful results.

In addition to these standard products, the algorithms also produce data for many “diagnostic” products. The bulk of these are similar to the standard products, in that they represent vertical profiles of retrieved species abundances. However, the information on these diagnostic products has typically been obtained from a different spectral region than that used for the standard products. These diagnostic products are not discussed in this document. Further information on these is available from the MLS science team.

At the time of writing, the current version of the data processing software is version 4.23, producing files labeled v04-23. Any minor updates for bug fixes, or to reflect changes in input data such as the analysis fields used as *a priori* information for temperature will be referred to as v4.24, v4.25, etc. (similar to the differences between v04.20, v04.21, etc.). This version of the document is intended to be applicable to any v4.2x data files. More substantial changes at a later date (e.g., due to a change in the MLS instrument performance) may necessitate a larger change in the data processing software and/or its configuration. These will be numbered v4.3x etc., and will be accompanied by an updated version of this document (though not necessarily immediately, depending on the circumstances dictating the update).

### 1.3 MLS data validation status

As discussed above, a complete set of MLS validation papers describe the validation state of the earlier v2.2 data. The majority of the v2.2 MLS data products have, accordingly, completed “Stage 3 Validation” defined<sup>1</sup> as:

*Product accuracy has been assessed. Uncertainties in the product and its associated structure are well quantified from comparison with reference in situ or other suitable reference data. Uncertainties are characterized in a statistically robust way over multiple locations and time periods representing global conditions. Spatial and temporal consistency of the product and with similar products has been evaluated over globally representative locations and periods. Results are published in the peer-reviewed literature.*

Work, including that described in this document, has re-validated the v4.2x data, with the level of scrutiny for some (notably ozone and water vapor) establishing them as “Stage 4” validated, defined as:

*Validation results for stage 3 are systematically updated when new product versions are released and as the time-series expands.*

<sup>1</sup>See <https://science.nasa.gov/earth-science/earth-science-data/data-maturity-levels/>

## 1.4 Differences between MLS v4.2x data and earlier v3.x data

The MLS v4.2x data processing software includes a wide range of updates and changes, leading to differences ranging from significant to minor in all the MLS data products. Some of the most important are detailed below.

**Improved composition profiles in cloudy regions:** For the earlier v3.3x and v3.4x datasets, several products (notably O<sub>3</sub>, CO and HNO<sub>3</sub>) showed poor behavior in regions of thick clouds in the upper troposphere (mainly in the tropics). Complex screening approaches enabled users to remove many, but not all of these spurious profiles from consideration. Improved performance in this regard was a key goal for v4.2x, and the manner in which contamination from cloud signals is handled in the MLS gas-phase retrievals was substantially modified. This has resulted not only in a significant reduction in the number of spurious MLS profiles reported in cloudy regions, but also in an appreciable simplification of the steps users need to take to screen out the most cloud-contaminated measurements, and a more effective screening.

**Improvements to O<sub>3</sub> and HCN:** The MLS O<sub>3</sub> and HCN products have been improved in v4.2x through addition of specific retrieval “phases” dedicated to obtaining more accurate estimates for these products, and reducing the impact of contaminating signals from other species.

**Improvements to H<sub>2</sub>O:** The MLS H<sub>2</sub>O product is retrieved in two “phases” with a preliminary phase obtaining a coarse-vertical-resolution initial guess and informing the choice of smoothing constraint for a subsequent more detailed high-resolution retrieval. The use of more channels and more accurate forward model calculations in this initial retrieval have led to improvements in the convergence etc. of the second phase, and thus to improvements in the H<sub>2</sub>O product.

**New CH<sub>3</sub>OH product:** This product, obtained from measurements in the 190- and 640-GHz spectral regions (also from a dedicated retrieval “phase”), has been introduced in v4.2x. This product is scientifically useful in the tropical upper troposphere (see section 3.5).

**More suitable reference surface for geopotential height:** As of v4.2x, the MLS geopotential height (GPH) product has been redefined to be GPH from a reference geoid (a surface of constant geopotential) rather than from an ellipsoid, as was used in previous versions.

**More useful OH retrievals for recent years:** As discussed in section 1.12, MLS observations of OH have been made only sparingly in recent years in light of increased aging in the MLS “THz” subsystem making that measurement. Updates in the v4.2x algorithms have enabled a greater yield of useful OH profiles in the more recent years of observations affected by this aging than was the case in v3.3x and v3.4x.

In addition to these specific changes, changes in all products, including those not listed above, have resulted from updates to spectroscopy and instrument calibration knowledge, and in indirect response to the larger changes detailed above. Note that the threshold values of “Quality” and “Convergence” (see below) to be used in data screening have been updated for all products. All the standard product files (apart from IWC, see below) now also include the *a priori* information used in the retrieval (as an additional “swath”, see below).

## 1.5 Aura MLS file formats, contents, and first order quality information

All the MLS Level 2 data files described here are available from the NASA Goddard Space Flight Center Earth Science Data and Information Services Center (GES-DISC, see <https://disc.gsfc.nasa.gov/>). The standard and diagnostic products are stored in the EOS MLS *Level 2 Geophysical Product* (L2GP) files. These are standard HDF-EOS (version 5) files containing swaths in the Aura-wide standard format. For more information on this format see *Craig et al.* [2003]. A sample reading function for the Interactive Data Language

## 1.6. Additional information given in the Quality, Convergence and Status fields

**Table 1.5.1:** Additional swaths in specific standard product files.

Product	Additional swaths	Notes
HNO3	HNO3-190, HNO3-240	Nitric acid from the 190 and 240 GHz radiometers
IWC	IWP	partial Ice Water Path. (This file has no <i>a priori</i> swath)
O3	O3 column	Ozone column above the tropopause (see below)
RHI	UTRHI, UTRHI-APriori	“Single layer” relative humidity (see Section 3.20)
Temperature	WMOTPPressure	Tropopause (WMO definition, based MLS temperature)

(IDL, version 6.1 or later required), known as `readl2gp.pro` may have been supplied with the data and is available from <https://mls.jpl.nasa.gov/data/readers.php> A reader for MATLAB (`readL2GP.m`) is also available at the same site.

The standard products are stored in files named according to the convention

```
MLS-Aura_L2GP-<product>_v04-20-c01_<yyyy>d<ddd>.he5
```

where `<product>` is BrO, O3, Temperature, etc. The files are produced on a one-day granularity (midnight to midnight, universal time), and named according to the observation date where `<yyyy>` is the four digit calendar year and `<ddd>` is the day number in that year (001 = 1 January).

These files contain the corresponding standard product in an HDF-EOS swath given the same name as the product, e.g., “H2O”. With the exception of IWC, each file also contains the *a priori* values for that product inside a second swath whose name ends with the substring “-APriori”. HNO<sub>3</sub>, IWC, O3, RHI, and Temperature files are special in that they carry extra standard or non-standard products, as detailed in Table 1.5.1.

The files contain an HDF-EOS swath given the same name as the product. In addition, the standard O<sub>3</sub> product files also contain swaths describing column abundances, and the standard Temperature file contains additional swaths describing tropopause pressure. As some L2GP files contain multiple swaths, it is important to ensure that the correct swath in the L2GP files is requested from the file. In the case where the “default” swath is requested (i.e., no swath name is supplied) most HDF software will access the one whose name falls earliest in ASCII order. This generally results in the desired result for all products. For example, for temperature, the standard “Temperature” product will be read in preference to the “WMOTPPressure” swath that gives tropopause pressures.

Each swath contains data fields `L2gpValue` and `L2gpPrecision`, which describe the value and precision (reported at  $1\sigma$ ) of the data, respectively. Data points for which `L2gpPrecision` is set negative or zero *should not be used*, as this flags that the resulting precision is worse than 50% of the *a priori* precision, indicating that instrument and/or the algorithms have failed to provide enough useful information for that point. In addition to these fields, fields such as `latitude` etc. describe geolocation information. The field `time` describes time, in the EOS standard manner, as the number of seconds elapsed (including from five to nine subsequent leap seconds to date) since midnight universal time on 1 January 1993.

The L2GP-DGG (“Diagnostic products on a Geophysical Grid”) file contains a large number of additional swath quantities. The vast majority of these are MLS diagnostic products that will be of little interest to most data users. A few which may be of interest to some users are detailed below.

## 1.6 Additional information given in the Quality, Convergence and Status fields

In addition to the data and their estimated precisions, three quality metrics are output for every profile of each product. The first, called `Quality`, gives a measure of the quality of the product based on the fit achieved by

## 1.6. Additional information given in the Quality, Convergence and Status fields

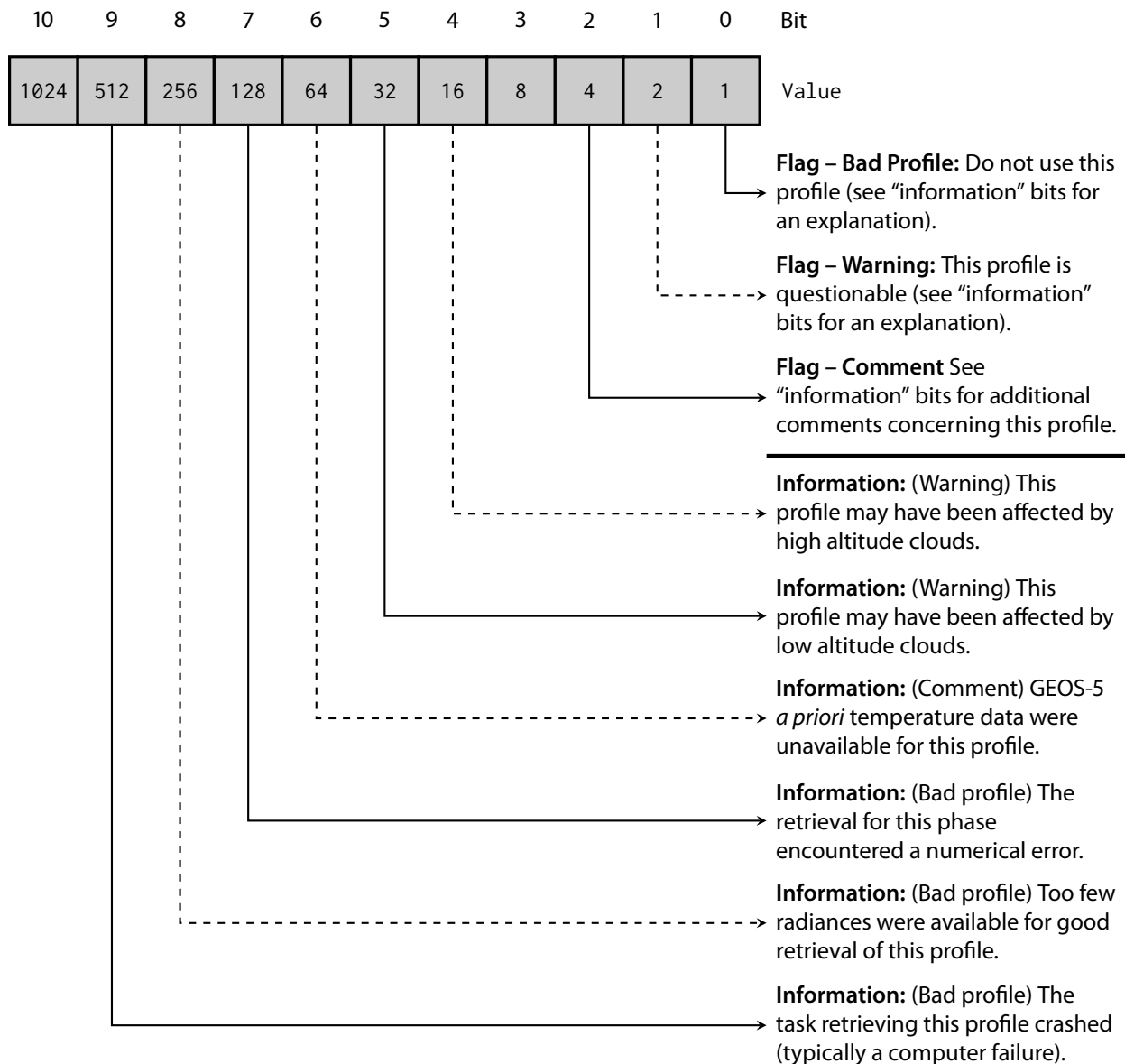


**Figure 1.6.1:** The meaning of the various bits in the Status field. The bits not labeled are not used in v4.2x. Later versions may implement specific meanings for these bits. Note that bit 6 (GEOS-5 data) was not used in v1.5, and that the information in bits 7 and 8 were combined into bit 8 in versions 1.5 and 2.2.

the Level 2 algorithms to the relevant radiances. Larger values of `Quality` generally indicate better radiance fits and therefore more trustworthy data. Values of `Quality` closer to zero indicate poorer radiance fits and therefore less trustworthy data. The value of `Quality` to be used as a “threshold” for rejecting data in scientific studies varies from product to product, and is given later in this document.

The second quality metric is called `Status`. This is a 32 bit integer that acts as a bit field containing several “flags”. Figure 1.6.1 describes the interpretation of these flags in more detail. The first two bits (bits 0 and 1) are “flagging” bits. If the first bit is set it indicates that the profile *should not be used in any scientific study*. Accordingly, any profile for which `Status` is an odd number should not be used. The second bit indicates that data are considered questionable for some reason. Higher bits give more information on the reasons behind the setting of the first two bits. So, for example, a value of `Status` of 18 (2+16) indicates that the data are

questionable (2 ≡ bit 2) because of the possible presence of high altitude clouds (16 ≡ bit 4).

The most commonly set information bits are the “high altitude cloud” and “low altitude cloud” bits. These indicate that the data have been marked as questionable because the Level 2 software believed that the measurements may have been affected by the presence of clouds (clouds alone will never cause a profile to be marked as not to be used, i.e., with odd Status). The implications of this vary from product to product and, more importantly, height to height. For example, situations of either “low cloud” or “high cloud” typically have very little impact on the quality of stratospheric data. Further details of the implications of these flags are given later in this document on a product by product basis.

The third diagnostic field Convergence describes how the fit to the radiances achieved by the retrieval algorithms compared to the degree of fit to be expected. This is quantified as a ratio of an aggregate  $\chi^2$  value to that predicted based on the assumption of a linear system [Livesey *et al.*, 2006]. Values around unity indicate good convergence, the threshold values above which profiles should not be used are given on a product by product basis later in this document.

## 1.7 An important note on negative values

Some of the MLS observations are “noisy” in nature. A consequence of this is that negative values may often be reported for species mixing ratios. It is important that such values *not be ignored or masked*. Ignoring such values will automatically introduce a positive bias into any averages made of the data as part of scientific analysis. Water vapor is retrieved using a logarithmic basis (both vertically and horizontally, as discussed in section 1.9). Accordingly, no negative water vapor abundances are produced by v4.2x.

## 1.8 Averaging kernels for MLS v4.2x profiles

As is common for remote sounding instruments, consideration of the “Averaging Kernel” [e.g., Rodgers, 2000] can be important in some scientific studies. However, the relatively high vertical resolution of the MLS observations (compared, for example, to nadir sounding composition instruments) allows for many scientifically useful studies to be undertaken without reference to the averaging kernels. This section reviews the role averaging kernels play in comparing MLS profiles to other observations and/or model profiles and describes how to obtain representative kernels for the v4.2x data.

The averaging kernel matrix  $\mathbf{A}$  relates the retrieved MLS profiles (given by the vector  $\hat{\mathbf{x}}$ ) to the “true” atmospheric state (the vector  $\mathbf{x}$ ) according to

$$\mathbf{A} = \frac{\partial \hat{\mathbf{x}}}{\partial \mathbf{x}}. \quad (1.1)$$

Rows of the  $\mathbf{A}$  matrix accordingly describe the contributions of the true atmospheric profile to the given level in the retrieved profile. The figures later in this document show these rows as individual colored lines.

Given an independent observation or model estimate of an atmospheric profile  $\mathbf{x}$ , the averaging kernels, in combination with the MLS *a priori* profile  $\mathbf{x}_a$ , can be used to compute the profiles that MLS would observe, were the true profile to be in the state given by  $\mathbf{x}$ , according to

$$\hat{\mathbf{x}} = \mathbf{x}_a + \mathbf{A} [\mathbf{x} - \mathbf{x}_a] \quad (1.2)$$

As of MLS version v4.2x, the *a priori* profile for each MLS observation is available within each of the standard product files, in swaths named according to the product, with the suffix “-APriori” (note the hyphen). Examples are “Temperature-APriori” and “O3-APriori”. This information can also be obtained from the MLS L2GP-DGG files (the only source for this information in v3.3x and v3.4x and earlier versions).

Note that in the case of water vapor where (as described below) a logarithmic interpolation is used for the profile, the calculations in equation 1.2 should be performed in log space, i.e., with  $\mathbf{x}$  and  $\mathbf{x}_a$  containing logarithm of the given H<sub>2</sub>O mixing ratio (leaving the  $\mathbf{A}$  matrix as supplied).

The full MLS averaging kernels are complicated entities, reflecting the two dimensional “tomographic” nature of the MLS retrievals (see section 2.2). We anticipate that few, if any, users will need to apply these full two dimensional kernels, whose interpretation is complex (please contact the MLS team for further information on these). The full kernels can be “collapsed” in the horizontal, to provide a single vertical averaging kernel for each product (as is done for many nadir sounding instruments). Such kernels are shown for each product (along with “horizontal” averaging kernels) in chapter 3. The MLS averaging kernels typically change little with latitude / season / atmospheric state. Accordingly, two representative kernels are shown for each product, one for the tropics and one for polar winter conditions. These representative kernels are available to users as described below. If variability in the averaging kernels is a concern, comparison of  $\hat{\mathbf{x}}$  profiles obtained using the two kernels (likely to represent two extreme cases) can provide a quantitative estimate of the magnitude of differences introduced by kernel variations.

The two averaging kernels for each product are distributed as text files, named according to

```
MLS-Aura_L2AK-<product>-<case>_v04-2x_0000d000.txt
```

where <case> is Eq or 70N for the equator and 70°N, respectively (or Day and Night for OH, see section 3.19). These files are available from the MLS web site at <https://mls.jpl.nasa.gov/data/ak/>.

These files contain comment lines (prefixed with a semicolon) describing their format. The first non-comment line gives the name of the product and the number of levels in the vertical profile. A list of the pressure levels in the profile (matching those in the L2GP files) is then given, followed by all the values of the averaging kernel matrix, with the row index (the level in the retrieved profile) varying most rapidly.

Typically, of course, the MLS profile pressures are not those of the observation or model dataset to which the comparison is being made. In many cases, particularly where the resolution of the other dataset is comparable to that of the MLS profiles, a simple linear interpolation is the most practical manner in which to transform the other dataset into the  $\mathbf{x}$  profile space. However, we note that more formal approaches have been described [Rogers and Connor, 2003] for the case where the comparison dataset is also remotely sounded and has an averaging kernel. In cases where the comparison dataset has high vertical resolution (e.g., sonde or Lidar observations), an additional consideration is described in the following section.

## 1.9 Considerations for comparisons with high vertical resolution datasets

The MLS Level 2 data describe a piecewise linear representation of vertical profiles of mixing ratio (or temperature, GPH, etc.) as a function of pressure, with the tie points given in the L2GP files (in the case of water vapor, the representation is piecewise linear in log mixing ratio). This contrasts with some other instruments, which report profiles in the form of discrete layer means. This interpretation has important implications that may need to be considered when comparing profiles from MLS to those from other instruments or models, particularly those with higher vertical resolution.

It is clearly not ideal to compare MLS retrieved profiles with finer resolution data by simply “sampling” the finer profile at the MLS retrieval surfaces. One might expect that instead one should do some linear interpolation or layer averaging to convert the other dataset to the MLS grid. However, in the MLS case where the state vector describes a profile at infinite resolution obtained by linearly interpolating from the fixed surfaces, it can be shown that the appropriate thing to do is to compare to a least squares fit of the non-MLS profile to the lower resolution MLS retrieval grid.

Consider a high resolution profile described by the vector  $\mathbf{z}_h$ , and a lower resolution MLS retrieved profile described by the vector  $\mathbf{x}_l$ . We can construct a linear interpolation in log pressure that interpolates the low resolution information in  $\mathbf{x}_l$  to the high resolution grid of  $\mathbf{z}_h$ . We describe that operation by the (typically highly sparse)  $n_h \times n_l$  matrix  $\mathbf{H}$  such that

$$\mathbf{x}_h = \mathbf{H}\mathbf{x}_l \quad (1.3)$$

where  $\mathbf{x}_h$  is the high resolution interpolation of the low resolution  $\mathbf{x}_l$ . It can be shown that the best estimate profile that an idealized MLS instrument could obtain, were the true atmosphere in the state described by  $\mathbf{z}_h$ , is given by

$$\mathbf{z}_l = \mathbf{W}\mathbf{z}_h \quad (1.4)$$

where

$$\mathbf{W} = [\mathbf{H}^T\mathbf{H}]^{-1}\mathbf{H}^T \quad (1.5)$$

In other words,  $\mathbf{z}_l$  represents a least squares linear fit to  $\mathbf{z}_h$ . This operation is illustrated by an example in Figure 1.9.1. Precision uncertainty on high resolution measurements may be similarly converted to the MLS grid by applying

$$\mathbf{S}_l = \mathbf{W}\mathbf{S}_h\mathbf{W}^T \quad (1.6)$$

where  $\mathbf{S}_h$  is the covariance of the original high resolution data (typically diagonal) and  $\mathbf{S}_l$  is its low resolution representation on the MLS pressure grid. Following this transfer of the high-resolution profile onto the state vector vertical grid, the profile can be multiplied by the averaging kernels, as described above, according to equation 1.2.

In some cases, the application of this least-squares “smoothing” is as important, if not more important, than the application of the averaging kernels described above. This is particularly true when the averaging kernels are close to delta functions, indicating that the vertical resolution is comparable to the retrieved profile level spacing.

In the case of water vapor, where a logarithmic vertical basis is used, the  $\mathbf{x}$  and  $\mathbf{z}$  vectors should describe the logarithm of the mixing ratio.

## 1.10 A note on the HCl measurements in v4.2x

Starting in February 2006, the primary MLS band for measuring HCl (specifically the HCl<sup>35</sup> isotopologue) (R4:640.B13F:HCl or “band 13”) began to exhibit symptoms of aging and was deactivated to conserve life. This is likely to be due to a radiation susceptibility issue for a batch of transistors identified shortly before launch. Useful observations of HCl are still made with the adjacent band (R4:640.B14F:O3 or “band 14”) which, as can be seen from Figures 2.1.1 and 2.1.2 also observe the HCl<sup>35</sup> line (and a smaller line for the HCl<sup>37</sup> isotopologue).

In order to avoid undesirable discontinuities in the v4.2x HCl dataset, the band 13 radiances are not considered in the retrieval of the standard HCl product, even on days for which it was active. For days prior to the 16 February 2006 deactivation of band 13, and the few subsequent days when band 13 has been (or may be) reactivated, the v4.2x algorithms also produce a second HCl product (in the HCl-640-B13 swath in the L2GP-DGG) file which includes the band 13 radiances, giving a product with improved precision and resolution in the upper stratosphere and mesosphere. See section 3.10 for more information.

As discussed in section 3.10, while the band 14 and band 13 data show very good agreement in the lower stratosphere, they disagree on the magnitude of the declining trend in upper stratospheric HCl (reflecting cuts in emissions of ozone depleting substances). At these high altitudes the HCl line is significantly narrower than the single channel in band 14 in which it resides, whereas the band 13 channels (by design, as this band was targeted to HCl) resolve the line shape. Accordingly, the band 13 trend is judged to be the more accurate one.

## 1.11 A note on N<sub>2</sub>O measurements in v4.2x

The preferred MLS band for measuring N<sub>2</sub>O (band 12 in the 640 GHz region, N20-640) began to show signs of aging in June 2013 (although more slowly than the rapid decline observed in the HCl band 13 in 2006). Band 12 was subsequently turned off on August 6, 2013. However, the level-2 processing stream for the N<sub>2</sub>O standard product in v3.x was switched to output the band 3 (190 GHz, N20-190) retrieval on 7 June 2013 and later data for N20-640 are not recommended for scientific use.

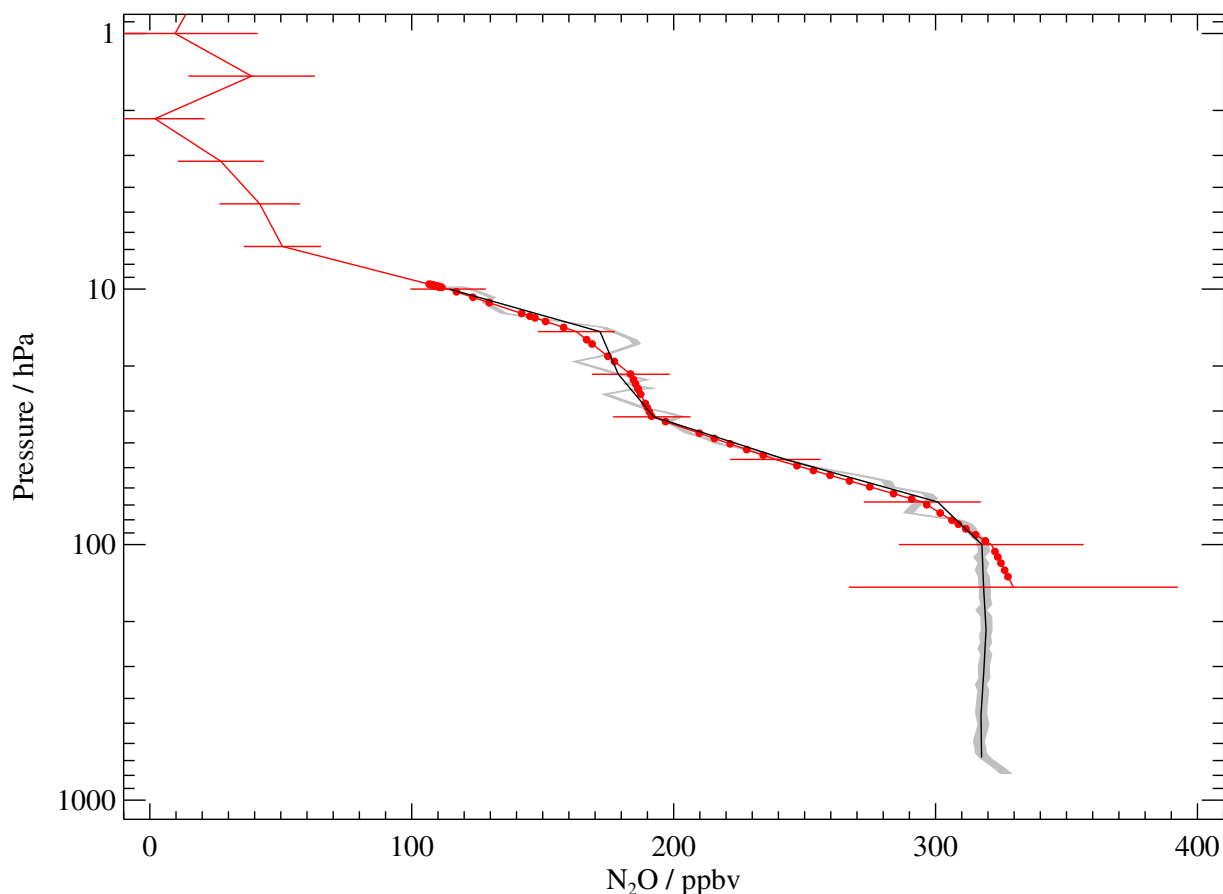


**Figure 1.9.1:** Comparisons of MLS (v1.5)  $\text{N}_2\text{O}$  observations with in-situ balloon data (courtesy of J. Elkins). The raw balloon data ( $\mathbf{z}_h$ ) are shown as the grey shaded region (shading indicates precision). A coincident MLS profile ( $\mathbf{x}_l$ ) is shown in red with the red error bars indicating precision. The red dots show the MLS data linearly interpolated to the balloon pressures using the  $\mathbf{H}$  matrix (i.e.,  $\mathbf{x}_h$  from equation 1.3). The black line shows the “least squares” interpolation of the balloon data onto the MLS grid using the  $\mathbf{W}$  matrix as described in the text (i.e.,  $\mathbf{z}_l$  from equation 1.4). The black line therefore represents the closest possible match at this resolution to the original grey line, and is the appropriate quantity to compare to the red MLS profile, and to be multiplied by the averaging kernels for formal comparison.

For v4.x the decision was taken to assign the band 3 (190 GHz, N20–190) retrieval as the standard product from launch, whereas the band 12 (640 GHz, N20–640) retrieval is now only available in the N20–640 swath in the L2GP–DGG file.

As discussed in section 3.17, the band 3 and band 12 data show good agreement except at 100 hPa where there is a >30% high bias in the  $\text{N}_2\text{O}$  values from band 3.

## 1.12 A note on OH measurements in v4.2x

The MLS OH measurements derive from observations in the 2.5-THz region of the spectrum. The local oscillator signal driving the MLS 2.5-THz radiometers is provided by a methanol laser (pumped by a  $\text{CO}_2$  laser). In December 2009, following more than five years of operation, this laser began to show signs of aging and was temporarily deactivated (prior to the 2004 Aura launch, the expected lifetime of this laser was only eighteen months).

Upper stratospheric and mesospheric OH is strongly affected by solar activity [Wang *et al.*, 2013], which was low during the solar 11-year minimum in 2009. In order to conserve the remaining lifetime of the THz



instrument for valuable measurements when the Sun becomes more active, we suspended OH measurements from December 2009 to August 2011. As the Solar Cycle 24 rises with increasing solar activity, we reactivate THz instrument for a 30-day continuous measurement during August – September in each year. The reasons of having this measurement at this time of year are:

1. Since MLS OH measurements started in early August in 2004, in order to achieve the longest possible annual OH data record for trend studies, we have to choose a time no earlier than August.
2. The ground-based instrument used for MLS OH validation [Wang *et al.*, 2008], located at 34.4°N, has the best OH measurement signal in summer (June – August) and the lowest signal in winter. Having the annual MLS OH measurement starting in August allows for continuing validation with the best possible collocated ground-based data.

We have performed the 30-day OH measurement in each August – September during 2011 – 2014 and plan to continue it during the declining phase of Solar Cycle 24. However, due to the aging of the instrument, OH data acquired since 2014 are significantly noisier than the previous years and have poor spatial coverage at mid-low latitudes.

Help

Overview

Table

S  
BRO  
TS  
CH<sub>3</sub>Cl  
TS  
CH<sub>3</sub>CN  
TS  
CH<sub>3</sub>OH  
TS  
ClO  
TS  
CO  
TS  
GPH  
TS  
H<sub>2</sub>O  
TS  
HCl  
TS  
HCN  
TS  
HNO<sub>3</sub>  
TS  
HO<sub>2</sub>  
TS  
HOCl  
TS  
IWC  
TS  
IWP  
TS  
N<sub>2</sub>O  
TS  
O<sub>3</sub>  
TS  
OH  
TS  
RHI  
TS  
SO<sub>2</sub>  
TS  
T

## Chapter 2

# Background reading for users of MLS version 4.x data

## 2.1 Aura MLS radiance observations

Figures 2.1.1 and 2.1.2 show the spectral coverage of the MLS instrument. The instrument consists of seven radiometers observing emission in the 118 GHz (R1A and R1B), 190 GHz (R2), 240 GHz (R3), 640 GHz (R4) and 2.5 THz (R5H and R5V) regions. With the exception of the two 118 GHz devices, these are “double sideband” radiometers. This means that the observations from both above and below the local oscillator frequencies are combined to form an “intermediate frequency” signal. In the case of the 118-GHz radiometers, the signals from the upper sideband (those frequencies above the ~126 GHz local oscillator) are suppressed. These intermediate frequency signals are then split into separate “bands”. The radiance levels within these bands are quantified by various spectrometers.

In operation, the instrument performs a continuous vertical scan of both the GHz (for R1A–R4) and THz (R5H, R5V) antennæ from the surface to about 90 km in a period of about 20 s. This is followed by about 5 s of antenna retrace and calibration activity. This ~25 s cycle is known as a *Major Frame* (MAF). During the ~20 s continuous scan, radiances are reported at 1/6 s intervals known as *Minor Frames* (MIFs).

## 2.2 Brief review of theoretical basis

The Level 2 algorithms implement a standard *Optimal Estimation* retrieval approach [Rodgers, 1976, 2000] that seeks the “best” value for the state vector (the profiles of temperature and abundances) based on an optimal combination of the fit to the MLS radiance observations, *a priori* estimates of the state vector (from climatological information and, for temperature in the troposphere and lower stratosphere, analysis fields), and constraints on the smoothness of the result. This fit must often be arrived at in an iterative manner because of the non-linear nature of the Aura MLS measurement system.

An innovative aspect of the retrieval algorithms for Aura MLS arises from taking advantage of the fact that the MLS instrument looks in the forward direction from the spacecraft. Figure 2.2.1 reviews the Aura MLS measurement geometry and shows that each radiance observation is influenced by the state of the atmosphere for several consecutive profiles. In the v4.2x Level 2 algorithms, the state vector consists of “chunks” of several profiles of atmospheric temperature and composition, which are then simultaneously retrieved from radiances measured in a similar number of MLS scans. Results from these “chunks” are then joined together to produce the products at a granularity of one day (the chunks overlap in order to avoid “edge effects”).

The retrieval state vector consists of vertical profiles of temperature and composition on fixed pressure surfaces. Between these fixed surfaces, the forward models assume that species abundances and temperature vary from surface to surface in a piecewise-linear fashion (except for the abundance of H<sub>2</sub>O, which is assumed to vary linearly in the logarithm of the mixing ratio). This has important implications for the interpretation of the data as was described in section 1.9. In addition to these profiles, the pressure at the tangent point for the mid-point of each minor frame is retrieved, based on both radiance observations and knowledge of tangent point height from the MLS antenna position encoder and the Aura spacecraft ephemeris and attitude determination.

Most of the MLS data products are deduced from observations of spectral contrast, that is, variations in radiance as a function of frequency for a given limb pointing. Many of the systematic errors in the MLS measurement system manifest themselves as a spectrally flat or slowly spectrally varying error in radiance. This is true of effects arising both from the instrument (such as gain and offset during the limb scan) and from the “forward model” (such as knowledge of continuum emission and the impact of some approximations



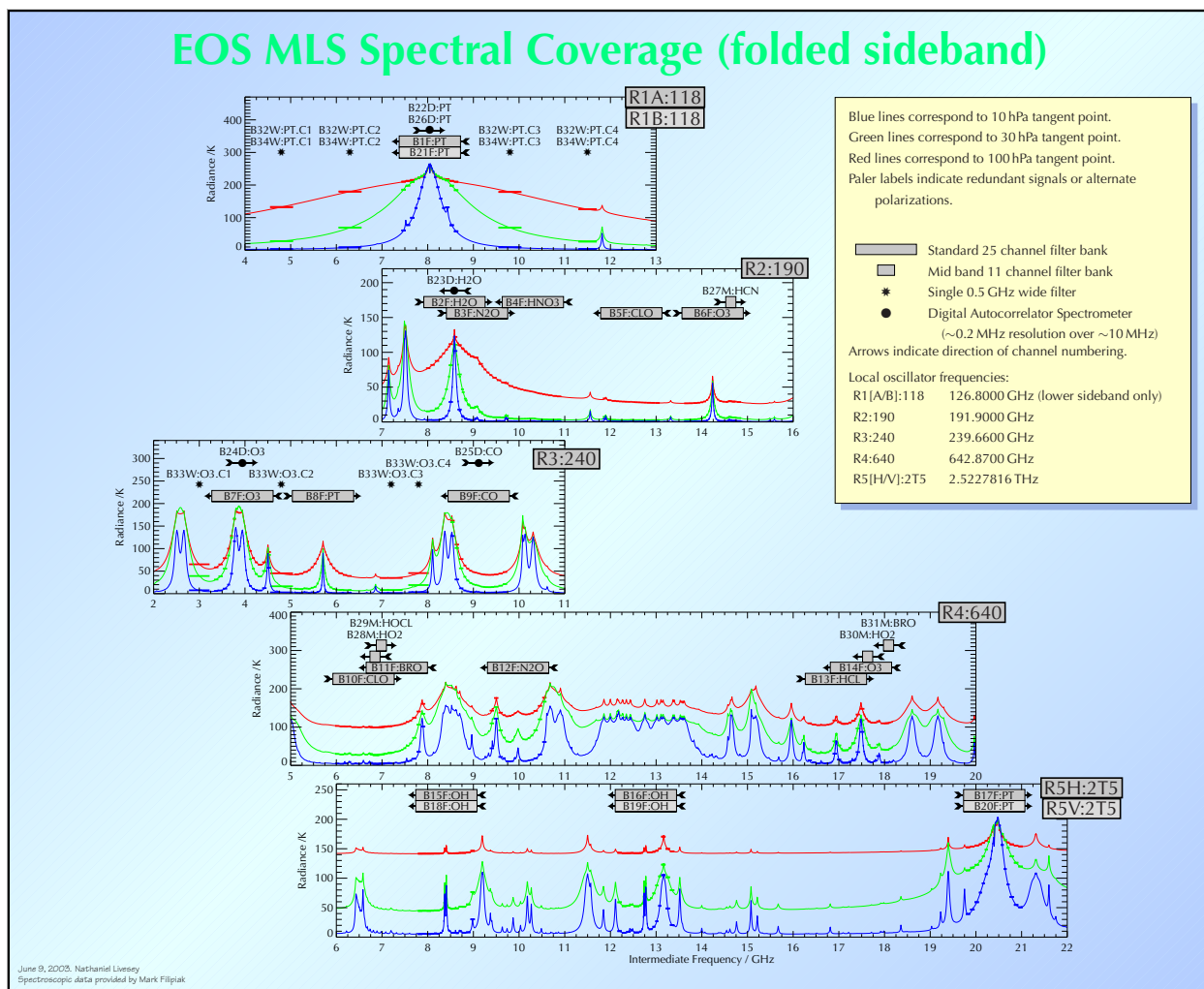


**Figure 2.1.2:** This is similar to figure 2.1.1, except that x-axes represent “intermediate frequency”. The signal at each intermediate frequency represents a sum of the signals observed at that frequency both above and below the local oscillator (below only in the case of the 118 GHz receivers.)

made in the forward model in order to increase its speed). In order to account for such effects, the v4.2x algorithms also retrieve spectrally flat (or slowly spectrally varying) corrections to the MLS radiances, either in terms of an additive radiance offset or an additive atmospheric extinction.

## 2.3 The Core, CorePlusRn approach

### 2.3.1 The need for separate “phases”

Many aspects of the MLS measurement system are linear in nature. In other words, there is a linear relationship between changes in aspects of the atmospheric state and consequent changes in the MLS radiance observations. However, there are some components of the state vector whose impact on the radiances is non-linear. The most non-linear of these is the estimate of the tangent pressure for each MIF of observation. The impact of water vapor in the upper troposphere on the MLS radiance observations is also highly non-linear. Solving for these aspects of the state vector therefore requires several iterations.

The computational effort involved in retrieval and forward models scales very rapidly (arguably as high as cubically) as a function of the size of the measurement system (i.e., the number of elements in the state

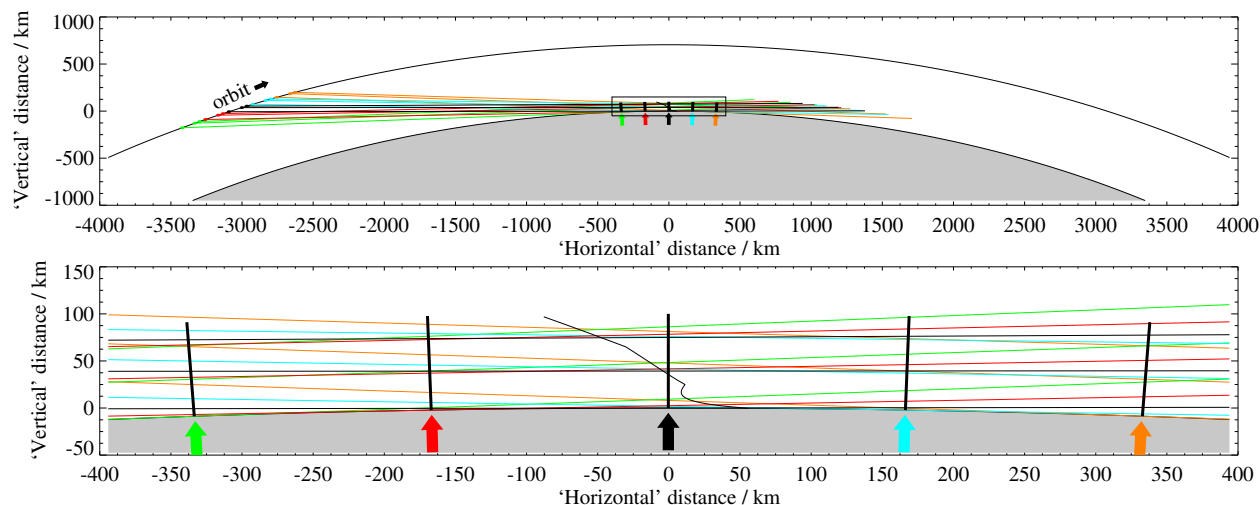


**Figure 2.2.1:** The top diagram shows a section of one orbit. Three of the 120 limb ray paths per scan are indicated by the “horizontal” lines. The lower diagram shows an expansion of the boxed region above. The straight radial lines denote the location of the retrieved atmospheric profiles. The limb ray scan closest to each profile is that whose color is the same as that of the arrow underneath. The thin black line under the central profile indicates the locus of the limb tangent point for this scan, including the effects of refraction.

and measurement vectors). Thus it is desirable to simplify retrievals involving strongly non-linear variables to a small subset of the complete system, in order to cut down on the effort involved in retrievals that require many iterations.

For this and other reasons, most retrieval algorithms are split into *phases*. In the case of the MLS v4.2x retrievals, there are many such phases. The first group of phases (collectively known as “Core”) use the 118 GHz and 240 GHz observations of  $O_2$  and  $O^{18}O$ , respectively, to establish estimates for temperature and tangent pressure. Upper tropospheric 190 GHz radiances are used in these early phases to establish a first order estimate of upper tropospheric humidity. The “Core” phases also include “cloud screening” computations (based on differences between observed and estimated clear-sky radiances). These identify minor frames where radiances in a given radiometer have been subject to significant (and currently poorly modeled) cloud scattering. Such minor frames are ignored in v4.2x processing in certain radiometers. Including information in such cloud-contaminated conditions is a goal for future MLS data processing versions.

The “Core” phases are followed by phases such as CorePlusR3 and CorePlusR5, where composition profiles are retrieved from a given radiometer. Sometimes (e.g., for CorePlusR3) these later phases continue to retrieve temperature and pressure, continuing using information from the 118 GHz radiometers, as in “Core”. In other phases (e.g., the CorePlusR2 and CorePlusR4 families of phases), the 118 GHz information is neglected and temperature and pressure are constrained to the results of “Core”. This choice is made based on extensive testing aimed at maximizing the information yield from MLS while minimizing the impact of inevitable systematic disagreements among the different radiometers, introduced by uncertain spectroscopy and/or calibration knowledge.

Table 2.3.1 describes the phases in more detail. Many products (e.g., ozone) are produced in more than one phase. All the separate measurements of these species are produced as diagnostic quantities, and labeled according to the spectral region from which they originated. For example, the ozone obtained from the CorePlusR2 retrieval is known in the v4.2x dataset as O3-190. In v4.2x in order to reduce confusion for users of MLS data, the algorithms also output “standard products”, which is typically a copy of one of the products from the CorePlusRn phases. For example, the “standard” chlorine monoxide product is a copy of the C10-640 product. In the case of v4.2x nitric acid, the standard product represents a hybrid of the results

from two phases. Details of which standard product is obtained from which phase are given in table 2.3.2.

## 2.4 Forward models used in v4.2x

The retrieval algorithms in v4.2x make use of a variety of different forward models. The most accurate is the so-called “full” forward model described in *Read et al.* [2004] and *Schwartz et al.* [2004]. This is a hybrid line-by-line and channel averaged model that computes radiances on appropriate grids of frequency and tangent pressure that are then convolved with the MLS frequency and angular responses.

This model is generally very time consuming, although for some comparatively “clean” spectral regions the computational burden is small enough that the full forward model can be used in the operational retrievals. In the v4.2x retrieval algorithms, its use is restricted mainly to radiance channels whose focus is the upper troposphere and lower stratosphere, as these radiances generally have a non-linear relationship to the state vector.

For many of the MLS channels, a simpler “Linearized” forward model can be used. This model invokes a simple first-order Taylor series to estimate radiances as a function of the deviation of the state from one of several pre-selected representative states. The inputs to this model are pre-computed radiances and derivatives corresponding to the pre-selected states, generated by “off-line” runs of the full forward model.

This model is by its nature approximate, and its use is generally confined to the upper stratosphere and mesosphere where retrievals are more linear in nature. In addition, a “cloud” forward model can be invoked to model the effects of scattering from cloud particles in the troposphere and lower stratosphere [*Wu and Jiang*, 2004]. This model was used in the simulation of radiances based on known model atmospheres for the v4.2x testing, but is not invoked in the v4.2x retrieval algorithms (the handling of clouds is described in more detail in section 2.5).

## 2.5 The handling of clouds in v4.2x

Thin clouds and atmospheric aerosols do not affect MLS atmospheric composition measurements as the typical particle sizes are much smaller than the wavelengths of the radiation being observed. The MLS v4.2x algorithms can reliably retrieve composition in moderately cloudy cases (having small limb radiance perturbations) and in the case of the Core+R3 retrieval this is handled by retrieving a frequency squared dependent extinction (including background atmospheric absorption from N<sub>2</sub>, H<sub>2</sub>O and unknown emitters). In the other retrieval phases, by contrast, a spectrally-flat baseline is used. Thick clouds can affect the MLS radiances beyond the modeling capability of this approach, mainly through scattering processes. Such situations and the affected radiances are excluded from the retrievals, or their influence down-weighted.

The first aspect of handling clouds in v4.2x is therefore the flagging of radiances that are believed to be significantly contaminated by cloud effects. To determine if a cloud is present in each MLS radiance measurement, we estimate the so-called cloud-induced radiance ( $T_{cir}$ ). This is defined as the difference between the measured radiance and the radiance from a forward model calculation assuming clear-sky conditions. Specific window channels (those that are most transparent deepest into the atmosphere) in each radiometer are chosen to set these flags.

Cloud screening in the Core+R2 and Core+R3 phases is based on determining the highest altitude limb view contaminated by cloud signals and either rejecting all radiances below that altitude or, in the case of less impacted channels, inflating their estimated radiance precisions. Clouds are detected by a combination of a radiance fit  $\chi^2$  quantity from Band 8 (240 GHz isotopic oxygen line) retrieval of temperature and pointing, and a cloud induced radiance calculation, also using 240 GHz measurements. Cloud radiance scattering causes severe line shape distortions which are most reliably detectable in the Band 8 O<sup>18</sup>O line fit, based on extrapolating a tangent pressure estimate into the upper troposphere from the pressure information obtained from the 118 GHz Band 1 measurements (unaffected by clouds). RHi from a previous phase is used to compute

Table 2.3.1: The phases that form the v4.2x retrieval algorithms.

Phase	Target species <sup>[1]</sup>	Measurements	Comment
InitPTan	T, pTan (GHz), GPH	R1A & R1B (118 GHz)	Initial estimate of P/T, lower limit 261 hPa
InitR2	H <sub>2</sub> O, N <sub>2</sub> O, CH <sub>3</sub> CN, HCN, ClO, HNO <sub>3</sub> , O <sub>3</sub> , SO <sub>2</sub>	R2 (190 GHz)	Initial trace gas estimator, lower limit 100 hPa
R3InitRHi	RHi, T <sub>cir</sub>	R3 (240 GHz)	Retrieves RHi profile from 316 hPa and up, used mostly for “near field” cloud detection and to compute R3 T <sub>cir</sub>
CloudDetector	none	R3 (240 GHz)	Determines cloud screening for R2 (190 GHz) and R3 (240 GHz)
FinalPTan	T, pTan (GHz), GPH	R1A & R1B (118 GHz), R3 (240 GHz)	Best P/T retrieval, lower limit 261 hPa
InitLowCloud	T <sub>cir</sub>	All radiometers	Determines cloud flags for all phases
InitRHi	UT RHi	R2 (190 GHz)	Retrieve RHi in a ~6 km-layer centered 400 – 600 hPa. Uses only saturated radiances
InitUTH	Upper tropospheric H <sub>2</sub> O	R2 (190 GHz)	Low vertical resolution (6/decade)
CorePlusR3	T, pTan (GHz), GPH, O <sub>3</sub> <sup>[2]</sup> , CO, HNO <sub>3</sub> , SO <sub>2</sub> , RHi <sup>b</sup>	R1A & R1B (118 GHz), R3 (240 GHz)	Retrievals down to 316 hPa
OzoneOnly	O <sub>3</sub> , CO	R3 (240 GHz)	Retrievals down to 316 hPa
CorePlusR2	H <sub>2</sub> O, N <sub>2</sub> O, HNO <sub>3</sub> , ClO, O <sub>3</sub> , HCN, CH <sub>3</sub> CN, SO <sub>2</sub>	R1A & R1B (118 GHz), R2 (190 GHz)	H <sub>2</sub> O retrieved down to 316 hPa, other species 100 hPa (note no T, pTan, GPH retrieval)
Hydrogen Cyanide	HCN, O <sub>3</sub> , HNO <sub>3</sub>	R2 (190 GHz)	Retrievals down to 100 hPa
CorePlusR4AB14	ClO, BrO, HO <sub>2</sub> , HOCl, HCl, O <sub>3</sub> , HNO <sub>3</sub> , CH <sub>3</sub> CN, SO <sub>2</sub> , CH <sub>3</sub> Cl	R4 (640 GHz)	Retrievals down to 147 hPa
Methanol	CH <sub>3</sub> OH, ClO, BrO, HO <sub>2</sub> , HOCl, HNO <sub>3</sub> , SO <sub>2</sub> , CH <sub>3</sub> Cl	R2 (190 GHz) and R4 (640 GHz)	Retrievals down to 147 hPa
CorePlusR4AB13	HCl, O <sub>3</sub> , SO <sub>2</sub>	R4 (640 GHz)	Retrievals down to 147 hPa. This phase only performed when MLS band 13 is operating
CorePlusR4B	N <sub>2</sub> O, SO <sub>2</sub>	R4 (640 GHz)	Retrievals down to 147 hPa
HighCloud	Cloud induced radiance, IWC, IWP	—	Used for flagging clouds in Core+R3 and later phases and forms basis for cloud ice products.
CorePlusR5	T, pTan (GHz, THz), GPH, OH, O <sub>3</sub>	R1A & R1B (118 GHz), R5H and R5V (2.5 THz)	Retrievals down to 68 hPa (147 hPa for Temperature)

<sup>[1]</sup>Tangent pressure and Geopotential height have been abbreviated to pTan (GHz/THz) and GPH respectively. Minor state vector components such as “baseline” and/or ‘extinction’ have been omitted unless they are the specific focus of the phase. Temperature, IWC, H<sub>2</sub>O, RHi are “high resolution” (12 surfaces per decade change in pressure from 1000 hPa to 1 hPa) unless otherwise stated. O<sub>3</sub> is low resolution except for the Core+R3 phase.

<sup>[2]</sup>On high vertical resolution grid

**Table 2.3.2:** The origin of each of the “standard products” from v4.2x.

Product	Origin	Spectral region
BrO	CorePlusR4AB14	640 GHz
CH <sub>3</sub> Cl	CorePlusR4AB14	640 GHz
CH <sub>3</sub> CN	CorePlusR4AB14	640 GHz
CH <sub>3</sub> OH	Methanol	640 GHz
ClO	CorePlusR4AB14	640 GHz
CO	CorePlusR3	240 GHz
GPH	CorePlusR3	118 & 240 GHz
H <sub>2</sub> O	CorePlusR2	190 GHz
HCl	CorePlusR4AB14	640 GHz
HCN	HydrogenCyanide	190 GHz
HNO <sub>3</sub>	CorePlusR2 (15 hPa and less)	190 GHz
	CorePlusR3 (larger than 15 hPa)	240 GHz
HO <sub>2</sub>	CorePlusR4AB14	640 GHz
HOCl	CorePlusR4AB14	640 GHz
IWC	HighCloud	240 GHz
IWP	HighCloud	240 GHz
N <sub>2</sub> O	CorePlusR2	190 GHz
O <sub>3</sub>	OzoneOnly	240 GHz
OH	CorePlusR5	2.5 THz
RHi	Computed from Temperature and H <sub>2</sub> O	190 GHz
SO <sub>2</sub>	CorePlusR3	240 GHz
Temperature	CorePlusR3	118 & 240 GHz



**Table 2.5.1:** MLS frequency channels and thresholds for cloud flag

Radiometer	Cloud channel	USB/LSB frequency / GHz	Low threshold	High threshold
R1[A/B]:118	B[32/34]W:PT.C4	115.3 (LSB only)	$T_{\text{cir}} < -4 \text{ K}$	none
R2:190	B5F:C10.C1	178.8 / 204.9	$T_{\text{cir}} < -20 \text{ K}$	$T_{\text{cir}} > 10 \text{ K}$
R3:240	B8F:PT	233.4 – 234.5 / 244.8 – 245.9	none	$\chi^2 > 30$
R4:640	B11F:BrO.C23	635.9 / 649.8	$T_{\text{cir}} < -10 \text{ K}$	none

a cloud induced radiance ( $T_{\text{cir}}$ ). The vertical profiles of  $\chi^2$  and  $T_{\text{cir}}$  are analyzed to find the highest limb view affected by cloud scattering, and radiances below are handled accordingly.

The other aspect of cloud handling in v4.2x is the estimation of cloud ice water content (IWC) and ice water path (IWP) products from the final  $T_{\text{cir}}$  computed by the retrieval in the HighCloud phase. More information on these products and their derivation is given in section 3.15.

## 2.6 The quantification of systematic uncertainty in MLS Level 2 data

A major component of the validation of MLS data is the quantification of the various sources of systematic uncertainty. These can arise from instrumental issues (e.g., radiometric calibration, field of view characterization), spectroscopic uncertainty, and through approximations in the retrieval formulation and implementation. A comprehensive quantification of these uncertainties has been performed for the v4.2x MLS products, updated from that described in the MLS validation papers (which were based on v2.2). The individual sections of Chapter 3 detail the results of this quantification product-by-product.

For each identified source of systematic uncertainty, its impact on MLS measurements of radiance (or pointing where appropriate) has been quantified and modeled. These modeled impacts correspond to either  $2\sigma$  estimates of uncertainties in the relevant parameter(s), or an estimate of their maximum reasonable error(s) based on instrument knowledge and/or design requirements. Accordingly, the numbers reported for each product in Chapter 3 reflect  $2\sigma$  estimates of potential systematic error.

For most of the uncertainty sources, the impact on MLS standard products has been quantified by running perturbed radiances through the MLS data processing algorithms. Other (typically smaller) uncertainty sources have been quantified by simple perturbation calculations.

Although the term “systematic uncertainty” is often associated with consistent biases and/or scaling errors, many sources of “systematic” error in the MLS measurement system give rise to additional scatter. For example, an error in the  $\text{O}_3$  spectroscopy, while being a bias on the fundamental parameter, will have an impact on the retrievals of species with weaker signals (e.g., CO) that is dependent on the amount and morphology of atmospheric ozone. The extent to which such terms can be expected to average down is estimated to first order by these “full up studies” through their separate consideration of the bias and scatter each uncertainty source introduces.

The results of these studies are summarized as “accuracy” (and in some cases additional contributions to “precision”) on a product by product basis in the next chapter. More details on the quantification for each product are given in the MLS validation papers. In addition Appendix A of *Read et al.* [2007] gives more specific details of the perturbations used in the study.

## 2.7 A brief note on the Quality field

As described in section 1.6, the Quality field in the L2GP files gives a measure of the fit achieved between the observed MLS radiances and those computed by the forward model given the retrieved MLS profiles. Quality is computed from a  $\chi^2$  statistic for all the radiances considered to have significantly affected the

retrieved species (i.e., those close to the relevant spectral lines), normalized by dividing by the number of radiances. Quality is simply the reciprocal of this statistic (i.e., low values indicate large  $\chi^2$ , i.e., poor fits).

Ideally, the typical values of these normalized  $\chi^2$  statistics will be around one, indicating that radiances are typically fitted to around their noise levels. Quality will therefore also ideally have a typical value of one. For some species, however, because of uncertain knowledge of spectroscopy and/or instrument calibration, the v4.2x algorithms are known to be consistently unable to fit some observed radiances to within their predicted noise. In many of these cases, the noise reported on the radiances has been “inflated” to allow the retrieval more leeway in fitting to radiances known to be challenging. As the noise level is the denominator in the  $\chi^2$  statistic, these species will have typical  $\chi^2$  statistics that are less than one and thus typical values of Quality higher than one. Accordingly, differences in Quality from one species to another do not reflect the species’ relative validity, nor do version-to-version increases in Quality for a given product necessarily indicate improvements (or vice versa)

Help

Overview

Table

S  
TS  
TS  
TS  
TS  
TS  
TS  
TS  
TS  
TS  
TS  
TS  
TS  
TS  
TS  
TS  
TS  
TS  
TS  
TS  
TS  
TS  
TS  
TS  
TS  
TS  
TS  
TS  
TS  
T

## Chapter 3

### Product-specific information

#### 3.1 Overview of species-specific discussion

This section describes each MLS v4.2x “standard product” in more detail. An overview is given of the expected resolution, precision and accuracy of the data. The resolution is characterized by the averaging kernels described below. Precision is quantified through a combination of the precision estimated by the MLS v4.2x algorithms, through reference to the systematic uncertainty budget described in section 2.6, and through study of the actual MLS data (e.g., consideration of the observed scatter in regions where little natural variability is anticipated).

The systematic uncertainty reported is generally based on the study described in section 2.6. However, in some cases larger disagreements are seen between MLS and correlative observations than these quantifications would imply. In such cases (e.g., MLS 215 hPa CO) the uncertainty quoted reflects these disagreements.

#### A note on the averaging kernel plots

The averaging kernels shown in this section describe both the horizontal (along track) and vertical (pressure) resolution of the MLS v4.2x data. While the averaging kernels vary somewhat from profile to profile, their variation is sufficiently small that these samples can be considered representative for all profiles. The averaging kernel plots are accompanied by estimates of the horizontal and vertical resolution of the product defined by the full width at half maximum of the kernels. Each kernel plot also shows the integrated areas under the kernels.

Help
Overview
Table
BrO
CH <sub>3</sub> Cl
CH <sub>3</sub> CN
CH <sub>3</sub> OH
ClO
CO
GPH
H <sub>2</sub> O
HCl
HCN
HNO <sub>3</sub>
HO <sub>2</sub>
HOCl
IWC
IWP
N <sub>2</sub> O
O <sub>3</sub>
OH
RHI
SO <sub>2</sub>

## 3.2 Bromine monoxide (BrO)

**Swath name:** BrO

**Useful range:** 10 – 3.2 hPa (day/night differences needed)

**Contact:** Luis Millan, **Email:** <Luis.F.Millan@jpl.nasa.gov>

### 3.2.1 Introduction

The standard product for BrO is taken from the 640-GHz CoreR4AB13 retrieval. The spectral signature of BrO in the MLS radiances is very small, leading to a very poor signal-to-noise ratio on individual MLS observations. Significant averaging (e.g., monthly zonal means) is required to obtain scientifically useful results. Large biases of between 12 to 43 pptv (typical BrO abundances range from 5 to 15 pptv) are seen in the data. These biases can be minimized by taking day/night differences. For pressures of 4.6 hPa and greater, nighttime BrO is negligible; however, for smaller pressures, nighttime BrO needs to be taken into account. Table 3.2.1 summarizes the precision, accuracy, and resolution of the MLS v4.2x BrO product. The accuracy assessment is based on v2.2 data, as described in the validation paper [Kovalenko *et al.*, 2007].

Note, the v4.2x “standard” BrO product (as with earlier versions) contains systematic biases and horizontal oscillations that present a larger challenge than for other species. Those interested in using MLS BrO in scientific studies are strongly advised to contact the MLS team before embarking on their research. Different algorithms for BrO have been developed by the MLS team, aimed at ameliorating some of these artifacts [Millán *et al.*, 2012], and those products are available from the GSFC DISC. The product short name is “ML3DZMBRO” and it is available from: [https://disc.gsfc.nasa.gov/datacollection/ML3DZMBRO\\_004.html](https://disc.gsfc.nasa.gov/datacollection/ML3DZMBRO_004.html).

### 3.2.2 Vertical Resolution

Figure 3.2.1 shows that the vertical resolution for the v4.2x MLS BrO is about 5.5 km in the 10 to 4.6 hPa pressure region, degrading to 6 km at 3.2 hPa.

### 3.2.3 Precision

The expected precision in a retrieved profile is calculated from radiance noise and reported for each retrieved data point. The value of the expected precision is flagged negative or zero if it is worse than 50% of the value of the a priori precision. Figure 3.2.2 compares the expected precision (thick line) on an individual MLS BrO measurement with that deduced from observations of scatter in night-time observations (expected to be zero). Also shown are the expected precisions for daily, monthly, and yearly 10° zonal means. For the minimal averaging recommended, a monthly 10° zonal mean, which corresponds to about 3,000 measurements, the precision is about ±4 ppt. See Table 3.2.1 for more details.

### 3.2.4 Accuracy

The accuracy of the MLS BrO product is summarized in Table 3.2.1. The effect of each identified source of systematic error on MLS measurements of radiance has been quantified and modeled [Read *et al.*, 2007]. These quantified effects correspond to either 2σ estimates of uncertainties in each MLS product, or an estimate of the maximum reasonable uncertainty based on instrument knowledge and/or design requirements. More discussion is given in Kovalenko *et al.* [2007]. While that paper described v2.2 BrO, findings are expected to be applicable also to v4.2x. The potential systematic bias in MLS BrO measurements can be as high as about ±43 ppt at 10 hPa, decreasing to about ±12 pptv at 3.2 hPa. The systematic bias is dramatically reduced by subtracting the nighttime signal from the daytime signal. Taking the day/night difference reduces the systematic biases to ±16 pptv at 10 hPa and to ±9 pptv at 3.2 hPa. If the MLS BrO data is used at 3.2 hPa, the day/night difference value will need to be adjusted to compensate for the non-negligible nighttime BrO. We note that this method of taking day/night differences is not applicable for polar summer and winter during periods of continuous sunlight or darkness.

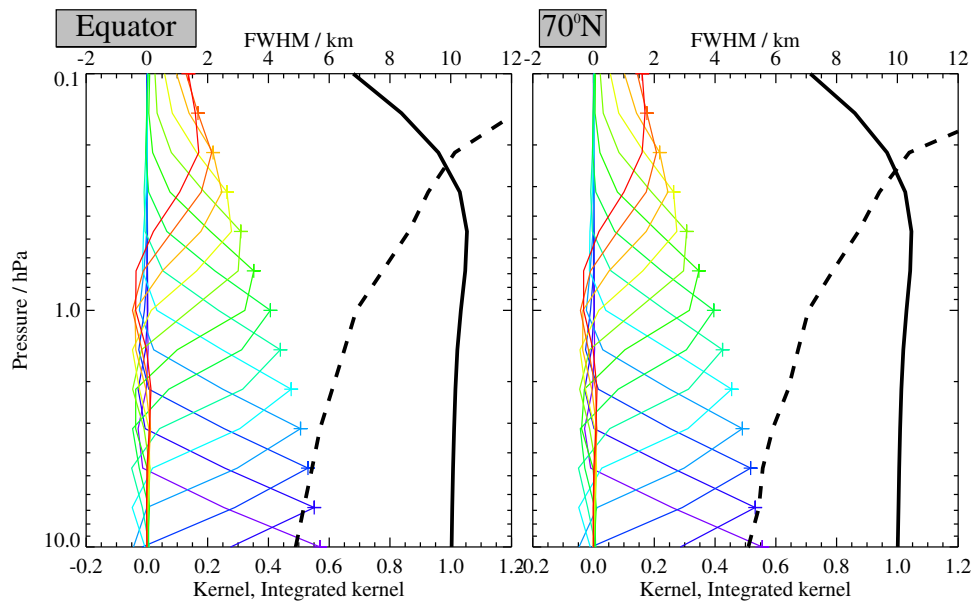


**Figure 3.2.1:** Typical vertical averaging kernels for the MLS v4.2x BrO data at the equator (left) and at 70°N (right); variation in the averaging kernels is sufficiently small that these are representative of typical profiles. Colored lines show the averaging kernels as a function of MLS retrieval level, indicating the region of the atmosphere from which information is contributing to the measurements on the individual retrieval surfaces, which are denoted by plus signs in corresponding colors. The dashed black line indicates the vertical resolution, determined from the full width at half maximum (FWHM) of the averaging kernels, approximately scaled into kilometers (top axes). The solid black line shows the integrated area under each kernel; values near unity imply that the majority of information for that MLS data point has come from the measurements, whereas lower values imply substantial contributions from a priori information. The low signal to noise for this product necessitates the use of significant averaging (e.g., monthly zonal mean), making horizontal averaging kernels largely irrelevant.

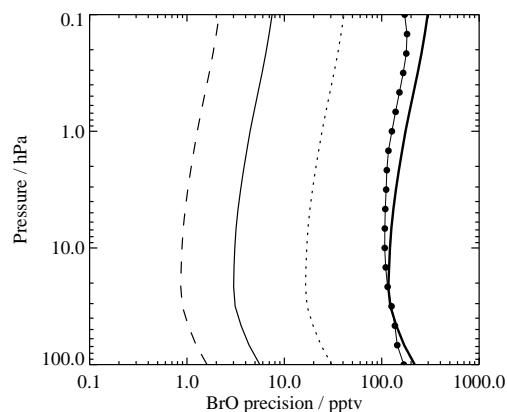


**Figure 3.2.2:** Comparison of the MLS v4.2x BrO precision as estimated from scatter in the retrieved data (circles) with that expected from the retrieval (thick line), for a single profile. Also shown is the expected precision for the day/night difference of 10° zonal mean profiles averaged over a day (dotted line), a month (thin line) and a year (dashed line).

### 3.2.5 Data screening

**Pressure range:** 10 – 3.2 hPa

Values outside this range are not recommended for scientific use.

**Averaging required:** Significant averaging (such as monthly zonal means) is required if useful scientific data are sought.

**Diurnal differences:** For use in any scientific study, day / night or ascending / descending differences should be used to alleviate biases.

Note that, for 3.2 hPa, the non-zero nighttime expected abundances BrO needs to be taken into account.

**Estimated precision:** Only use values for which the estimated precision is a positive number.

Values where the *a priori* information has a strong influence are flagged with negative or zero precision, and should not be used in scientific analyses (see Section 1.5).

**Status flag:** Only use profiles for which the **Status** field is an even number.

Odd values of Status indicate that the profile should not be used in scientific studies. See Section 1.6 for more information on the interpretation of the Status field.

**Clouds:** Profiles identified as being affected by clouds can be used with no restriction.

**Quality:** Only profiles whose **Quality** field is greater than 1.3 should be used.

**Convergence:** Only profiles whose **Convergence** field is less than 1.05 should be used.

### 3.2.6 Artifacts

Significant biases exist in the BrO data, as discussed above. Day / night (or ascending / descending) differences must be used to reduce these. For 3.2 hPa, nighttime BrO needs to be taken into account [Kovalenko *et al.*, 2007].

A systematic horizontal (i.e., profile-to-profile) oscillation has been discovered in MLS v4.2x (and earlier) standard BrO product. This presents a significant challenge to the interpretation of the BrO observations. Users are strongly advised to contact the MLS team before embarking on research involving the MLS standard BrO product. As described above, use of other BrO products is preferable to using the Level 2 BrO data.

### 3.2.7 Review of comparisons with other data sets

We have calculated total bromine, Br<sub>y</sub>, from MLS measurements of BrO using a photochemical model, and compared this with Br<sub>y</sub> similarly inferred from balloon-borne measurements of BrO; good agreement is seen [Kovalenko *et al.*, 2007].

<

**Table 3.2.1:** Summary of the Aura MLS v4.2x BrO product.

Pressure range	Vertical res. / km	Precision <sup>a</sup> / pptv	Day/night difference accuracy <sup>b</sup> / pptv	Comments
2.2 hPa and less	–	–	–	Unsuitable for scientific use
3.2 hPa	6	±5	±9	Need to account for non-negligible night time BrO
4.6	5.5	±4	±12	
6.8	5.5	±4	±14	
10	5.5	±4	±16	
150 – 15 hPa	–	–	–	Unsuitable for scientific use
1000 – 215 hPa	–	–	–	Not retrieved

<sup>a</sup>The precision quoted is for a 10° monthly zonal mean

<sup>b</sup>Because of large biases in the data, the daytime and nighttime BrO data are unsuitable for scientific use, so day/night differences must be used. Note that day/night differences are not useful for polar winter and summer, where BrO does not undergo a diurnal variation.

Help	S
Overview	S
Table	S
BrO	T
<b>CH<sub>3</sub>Cl</b>	<b>S</b>
CH <sub>3</sub> CN	T
CH <sub>3</sub> OH	S
ClO	T
CO	S
GPH	T
H <sub>2</sub> O	S
HCl	T
HCN	S
HNO <sub>3</sub>	T
HO <sub>2</sub>	S
HOCl	T
IWC	S
IWP	T
N <sub>2</sub> O	S
O <sub>3</sub>	T
OH	S
RHI	T
SO <sub>2</sub>	S
	T

### 3.3 Methyl chloride (CH<sub>3</sub>Cl)

**Swath name:** CH3Cl

**Useful range:** 147 – 4.6 hPa

**Contact:** Michelle Santee, **Email:** <Michelle.L.Santee@jpl.nasa.gov>

#### 3.3.1 Introduction

The v2.2 MLS ClO measurements were characterized by a substantial (~0.1 – 0.4 ppbv) negative bias at retrieval levels below (i.e., pressures larger than) 22 hPa. *Santee et al.* [2008] suggested that contamination from an interfering species such as CH<sub>3</sub>Cl, which has lines in two wing channels of the 640-GHz band used to measure ClO, could have given rise to the bias; they showed results from early v3 algorithms in which CH<sub>3</sub>Cl was also retrieved that demonstrated significant reduction in the bias in lower stratospheric ClO. Further refinements in the v3.3x and v3.4x algorithms yielded not only an improved ClO product, but also a reliable retrieval of CH<sub>3</sub>Cl. The quality and reliability of the v3.3x and v3.4x MLS CH<sub>3</sub>Cl measurements were assessed in detail by *Santee et al.* [2013].

As is the case for ClO, the standard CH<sub>3</sub>Cl product is derived from radiances measured by the radiometer centered near 640 GHz. The MLS v4.2x CH<sub>3</sub>Cl data are scientifically useful over the range 147 to 4.6 hPa. A summary of the estimated precision, resolution (vertical and horizontal), and systematic uncertainty of the v4.2x CH<sub>3</sub>Cl measurements as a function of altitude is given in Table 3.3.1.

#### 3.3.2 Differences between v3.3x/v3.4x and v4.2x

Changes in CH<sub>3</sub>Cl between v4.2x and v3.3x/v3.4x result from modifications to upstream retrievals of tangent pressure etc., and small updates to the spectroscopy database for some molecules. Differences in the retrieved CH<sub>3</sub>Cl abundances between the two versions range from less than 10 pptv at 68 hPa and lower pressures to ~50 pptv at 147 hPa (Figure 3.3.1), or typically within ±10%, with v4.2x mixing ratios generally smaller.

#### 3.3.3 Resolution

The resolution of the retrieved data can be described using “averaging kernels” [e.g., *Rodgers*, 2000]; the two-dimensional nature of the MLS data processing system means that the kernels describe both vertical and horizontal resolution. Values of the integrated kernel near unity indicate that the majority of information for that level has come from the measurements themselves and not the a priori; Figure 3.3.2 shows that the measurements dominate at pressures greater than 3.2 hPa, above which level the integrated kernel drops below 0.5. Smoothing, imposed on the retrieval system in both the vertical and horizontal directions to enhance retrieval stability and precision, degrades the inherent resolution of the measurements. Thus, although CH<sub>3</sub>Cl measurements are reported at six pressure levels per decade change in pressure (spacing of ~2.7 km), the vertical resolution of the v4.2x CH<sub>3</sub>Cl data as determined from the full width at half maximum of the rows of the averaging kernel matrix shown in Figure 3.3.2 is ~4 – 6 km in most of the lower stratosphere, degrading to ~8 – 10 km at and above (i.e., at pressures less than) 15 hPa. The averaging kernels are fairly symmetric, and for the most part they peak at their nominal position. However, overlap in the averaging kernels for the 100 and 147 hPa retrieval surfaces indicates that the 147 hPa retrieval does not provide as much independent information as is given by retrievals at higher altitudes. Figure 3.3.2 also shows horizontal averaging kernels, from which the along-track horizontal resolution is determined to be ~600 km at 147 hPa, ~450 – 500 km from 100 to 22 hPa, and ~550 – 850 km at and above 15 hPa. The cross-track resolution, set by the width of the field of view of the 640-GHz radiometer, is ~3 km. The along-track separation between adjacent retrieved profiles is 1.5° great circle angle (~165 km), whereas the longitudinal separation of MLS measurements, set by the Aura orbit, is 10° – 20° over low and middle latitudes, with much finer sampling in the polar regions.



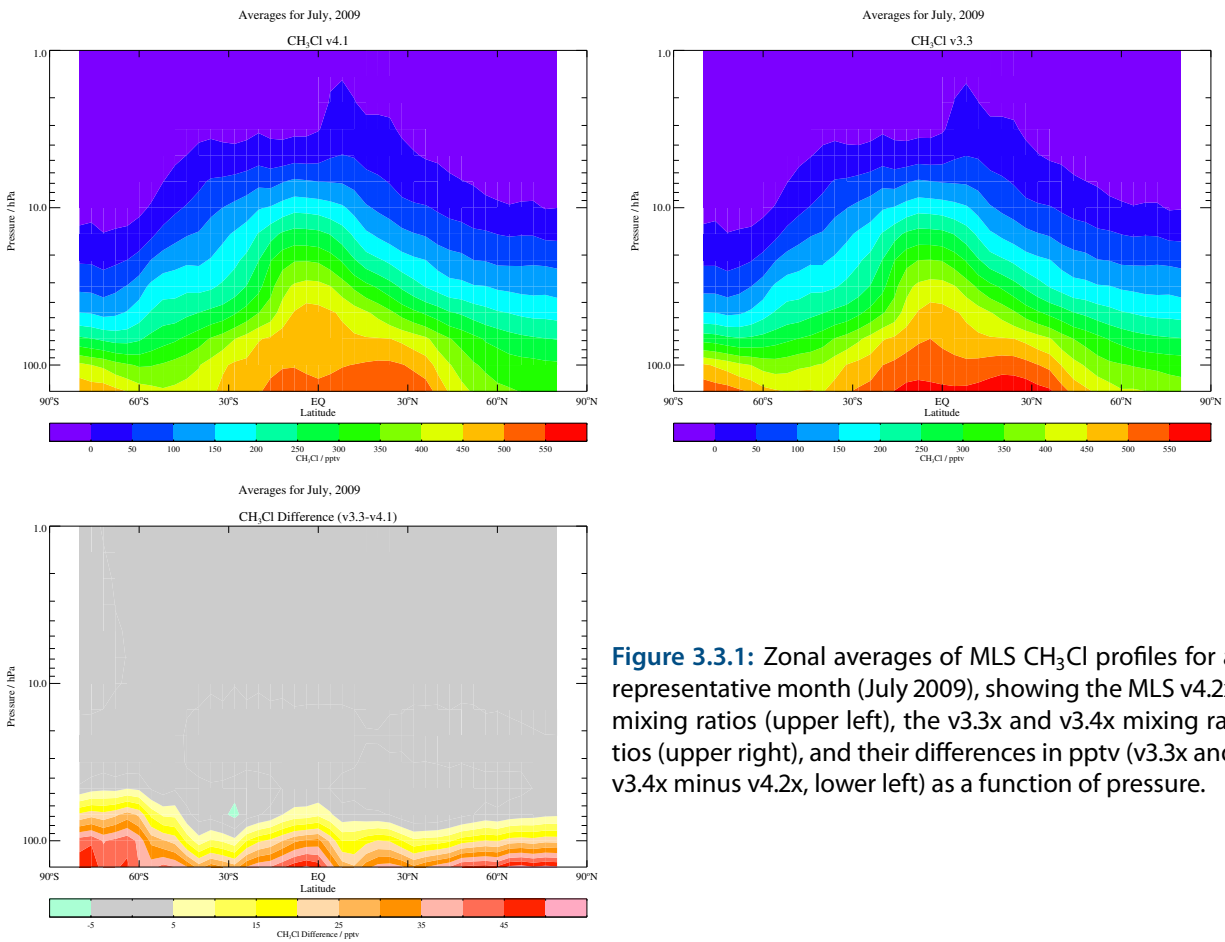


**Figure 3.3.1:** Zonal averages of MLS CH<sub>3</sub>Cl profiles for a representative month (July 2009), showing the MLS v4.2x mixing ratios (upper left), the v3.3x and v3.4x mixing ratios (upper right), and their differences in pptv (v3.3x and v3.4x minus v4.2x, lower left) as a function of pressure.

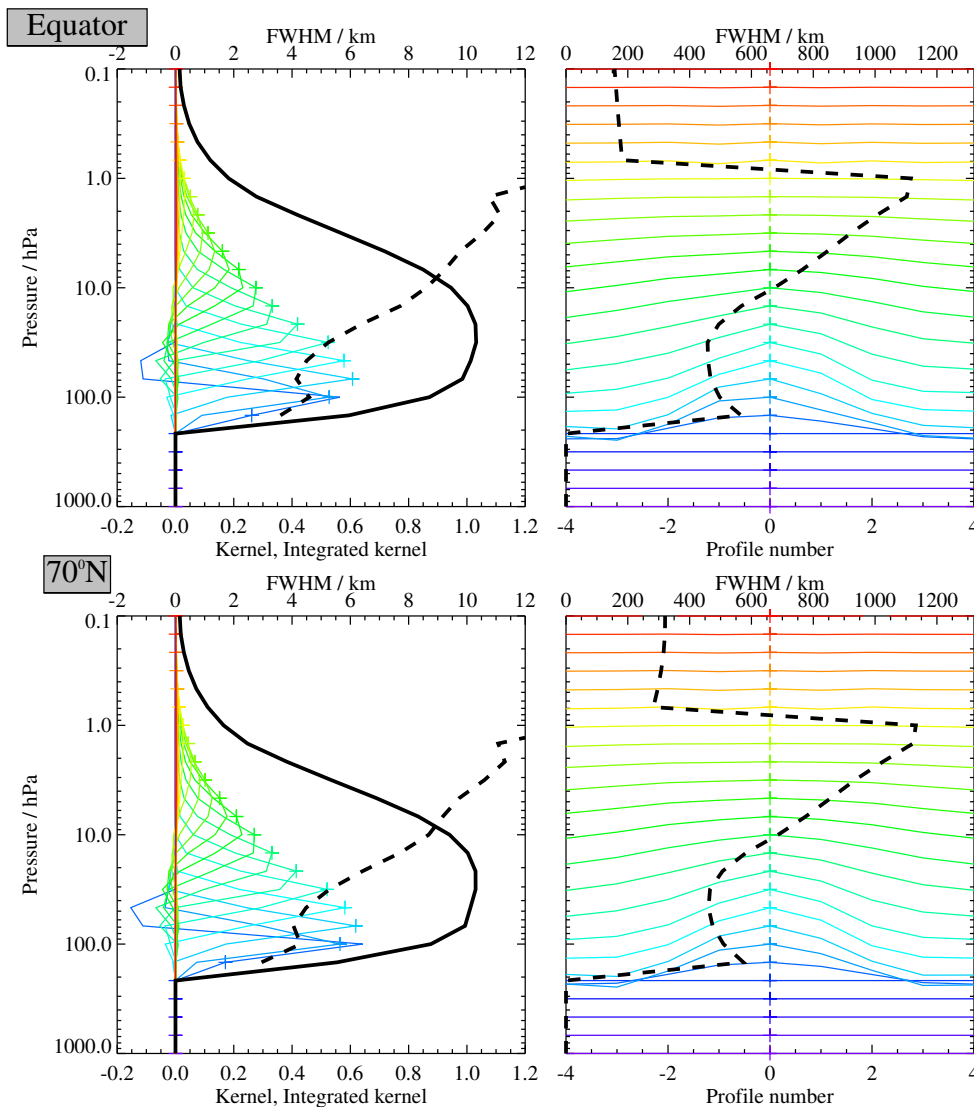


**Figure 3.3.2:** Typical two-dimensional (vertical and horizontal along-track) averaging kernels for the MLS v4.2x CH<sub>3</sub>Cl data at the equator (upper) and at 70°N (lower); variation in the averaging kernels is sufficiently small that these are representative of typical profiles. Colored lines show the averaging kernels as a function of MLS retrieval level, indicating the region of the atmosphere from which information is contributing to the measurements on the individual retrieval surfaces, which are denoted by plus signs in corresponding colors. The dashed black line indicates the resolution, determined from the full width at half maximum (FWHM) of the averaging kernels, approximately scaled into kilometers (top axes). (Left) Vertical averaging kernels (integrated in the horizontal dimension for five along-track profiles) and resolution. The solid black line shows the integrated area under each kernel (horizontally and vertically); values near unity imply that the majority of information for that MLS data point has come from the measurements, whereas lower values imply substantial contributions from a priori information. (Right) Horizontal averaging kernels (integrated in the vertical dimension) and resolution. The horizontal averaging kernels are shown scaled such that a unit averaging kernel amplitude is equivalent to a factor of 10 change in pressure.

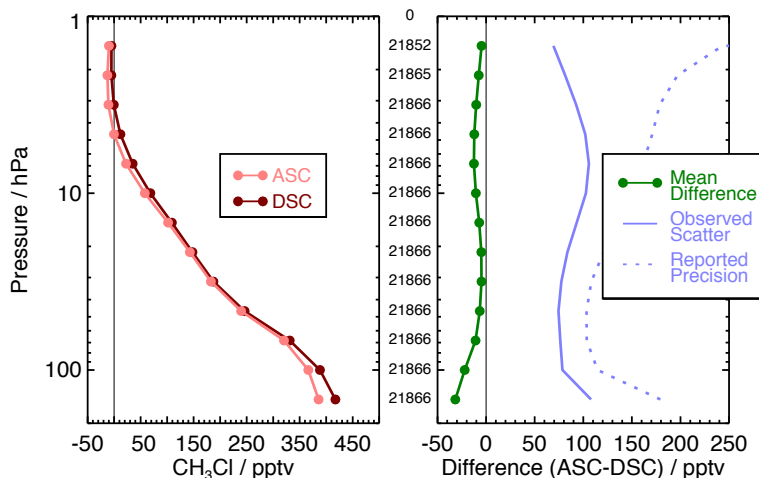


**Figure 3.3.3:** (left) Ensemble mean profiles for ascending (light red) and descending (dark red) orbit matching pairs of MLS v4.2x CH<sub>3</sub>Cl profiles averaged over several months of a representative year of data (2005). Symbols indicate MLS retrieval pressure levels. (right) Mean differences (ascending–descending) in pptv (green solid line). Also shown are the standard deviations about the mean differences (light blue solid line) and the root sum square (RSS) of the precisions calculated by the retrieval algorithm for the two sets of profiles (light blue dashed line). The observed scatter about the mean differences and the reported precision values have been scaled by  $1/\sqrt{2}$  (to convert from standard deviations of differences into standard deviations of individual data points); hence the light blue solid line represents the statistical repeatability of the MLS measurements, and the light blue dashed line represents the expected  $1\sigma$  precision for a single profile. The thin black lines mark zero in each panel. The number of crossing pairs of measurements being compared at each pressure level is noted in the space between the panels.

### 3.3.4 Precision

The precision of the MLS CH<sub>3</sub>Cl data is estimated empirically by comparing profiles measured at the intersections of ascending (day) and descending (night) portions of the orbit. Under ideal conditions (i.e., a quiescent atmosphere), the standard deviation about the mean differences between such matched profile pairs provides a measure of the precision of the individual data points. In practice, however, real changes in the atmosphere may occur over the 12 h interval between the intersecting measurement points, in which case the observed scatter provides an upper limit on the estimate of precision, assuming that the a priori has a negligible influence on the retrieval (a reasonable assumption at least at pressures greater than 3.2 hPa). The precision estimates were found to be essentially invariant with time; results for a representative year of data are shown in Figure 3.3.3. The observed standard deviation values are  $\sim 100$  pptv or less throughout the vertical domain. Mean differences between paired crossing profiles are  $\sim 10$  pptv or less except at the lowest two levels, where they reach 20–25 pptv. Given the large number of data points being compared, these ascending–descending differences are substantially larger than the standard error of the mean, implying the presence of significant systematic biases. These biases likely arise from the cumulative effect of various factors in the retrieval system that can vary diurnally or along the orbit, such as interferences from temperature or other atmospheric constituents (e.g., H<sub>2</sub>O and ClO), or thermal emissions from the MLS antenna.

The precision reported for each data point by the Level 2 data processing system exceeds the observationally determined precision throughout the vertical range (Figure 3.3.3), indicating that the vertical smoothing (regularization) applied to stabilize the retrieval system and improve the precision has a non-negligible influence. Because the reported precisions take into account occasional variations in instrument performance, the best estimate of the precision of an individual data point is the value quoted for that point in the L2GP files, but it should be borne in mind that this approach slightly overestimates the actual measurement noise. The estimates reported here represent the precisions at each pressure level of a single profile; precision can

generally be improved by averaging, with the precision of an average of  $N$  profiles being  $1/\sqrt{N}$  times the precision of an individual profile (although the actual standard error of the mean can in some cases be even smaller [Toohey and von Clarmann, 2013]).

### 3.3.5 Range

Although CH<sub>3</sub>Cl is retrieved over the range 147 to 0.001 hPa, because of the degradation in resolution and expected precision, the reduction in independent information contributed by the measurements, and the results of simulations using synthetic data as input radiances to test the closure of the retrieval system, the data are not deemed reliable at retrieval pressures less than 4.6 hPa. Despite the overlap in the averaging kernels for the 147 and 100 hPa surfaces discussed above, the simulations show that the retrieved CH<sub>3</sub>Cl values track the variations in the “truth” field at both levels. Moreover, the retrievals (of real data) at 147 hPa display significant features not seen at 100 hPa (not shown) that are believed to represent actual atmospheric variations. Thus, we recommend that the v4.2x CH<sub>3</sub>Cl data may be used for scientific studies between 147 and 4.6 hPa (inclusive), although the reduced sensitivity at the extremes of this range, as well as the relatively coarse vertical resolution of the retrieved profiles, should be borne in mind.

### 3.3.6 Accuracy

The effects of various sources of systematic uncertainty (e.g., instrumental issues, spectroscopic uncertainty, and approximations in the retrieval formulation and implementation) on the MLS v4.2x CH<sub>3</sub>Cl measurements have been quantified through a comprehensive set of retrievals of synthetic radiances; see *Santee et al.* [2013] for details of a similar analysis conducted on MLS v3.3x and v3.4x CH<sub>3</sub>Cl data. The overall systematic uncertainty, or accuracy, is calculated by combining (RSS) the contributions from both the expected biases and the additional scatter each source of uncertainty may introduce into the data. In aggregate, the factors considered in these simulations are estimated to give rise to total systematic uncertainty of approximately 30–45% in the MLS v4.2x CH<sub>3</sub>Cl data in the upper troposphere / lower stratosphere (see Table 3.3.1).

### 3.3.7 Review of comparisons with other datasets

Extensive comparisons of MLS v3.3x and v3.4x CH<sub>3</sub>Cl data with a variety of different platforms (balloon-borne, aircraft, and satellite instruments) were presented by *Santee et al.* [2013].

### 3.3.8 Data screening

**Pressure range:** 147 – 4.6 hPa

Values outside this range are not recommended for scientific use.

**Estimated precision:** Only use values for which the estimated precision is a positive number.

Values where the *a priori* information has a strong influence are flagged with negative or zero precision, and should not be used in scientific analyses (see Section 1.5).

**Status flag:** Only use profiles for which the **Status** field is zero.

We recommend that all profiles with nonzero values of **Status** be discarded, because of the potential impact of cloud artifacts at lower levels. Note, however, that rejecting in their entirety all profiles with nonzero **Status** may be unnecessarily severe at and above (i.e., at pressures equal to or smaller than) 46 hPa, where clouds have negligible impact; thus otherwise good-quality profiles with nonzero but even **Status** values may be used without restriction at those levels as long as they are removed at larger pressures. See Section 1.6 for more information on the interpretation of the **Status** field.

**Quality:** Only profiles whose **Quality** field is greater than 1.3 should be used.

This threshold for **Quality** (unchanged from v3.3x and v3.4x) typically excludes less than 1% of CH<sub>3</sub>Cl profiles on a daily basis; note that it potentially discards some “good” data points while not necessarily identifying all “bad” ones.

**Convergence:** Only profiles whose **Convergence** field is less than 1.05 should be used.

On a typical day this threshold for Convergence (unchanged from v3.3x and v3.4x) discards very few (0.3% or less) of the CH<sub>3</sub>Cl profiles, most (but not all) of which are also filtered out by the other quality control measures.

### 3.3.9 Artifacts

- Significant ascending–descending differences imply the presence of systematic biases at the bottom two retrieval pressure levels. However, various analyses performed separately on sets of ascending-only and descending-only measurements suggest that, although significant, these biases will have little or no impact on most scientific conclusions based on the MLS CH<sub>3</sub>Cl measurements.

### 3.3.10 Desired improvements for future data version(s)

- Minimize the impact of thick clouds on the retrievals to further improve the CH<sub>3</sub>Cl measurements in the upper troposphere and lowermost stratosphere.

**Table 3.3.1:** Summary of Aura MLS v4.2x CH<sub>3</sub>Cl Characteristics

Pressure / hPa	Resolution $V \times H^a$ / km	Precision <sup>b</sup> / pptv	Systematic Uncertainty <sup>c</sup> / %	Known Artifacts or Other Comments
3.2 – 0.001	—	—	—	Unsuitable for scientific use
15 – 4.6	8 – 10 × 550 – 850	±100	±30 – 75	
100 – 22	4.5 – 6.5 × 450 – 500	±100	±30 – 50	
147	4 × 600	±100	±45	
1000 – 215	—	—	—	Not retrieved

<sup>a</sup>Vertical and Horizontal resolution in along-track direction.

<sup>b</sup>Precision on individual profiles.

<sup>c</sup>Values should be interpreted as 2- $\sigma$  estimates of the probable magnitude.

## 3.4 Methyl cyanide (CH<sub>3</sub>CN)

**Swath name:** CH<sub>3</sub>CN

**Useful range:** 46 – 1.0 hPa

**Contact:** Michelle Santee, **Email:** <Michelle.L.Santee@jpl.nasa.gov>

### 3.4.1 Introduction

In v4.2x, as in v3.3x and v3.4x, the standard CH<sub>3</sub>CN product is taken from radiances measured by the radiometer centered near 640 GHz. The CH<sub>3</sub>CN retrieval is largely unchanged in v4.2x. Although the data have not been validated extensively, the v4.2x CH<sub>3</sub>CN retrievals are deemed to be scientifically useful over the range 46 to 1 hPa, except in the winter polar regions, where they may exhibit large biases below 10 hPa. Data retrieved at higher pressures may be used with caution in certain circumstances. A summary of the estimated precision, resolution (vertical and horizontal), and systematic uncertainty of the v4.2x CH<sub>3</sub>CN measurements as a function of altitude is given in Table 3.4.1.

### 3.4.2 Differences between v3.3x/v3.4x and v4.2x

Changes in CH<sub>3</sub>CN between v4.2x and v3.3x/v3.4x result from modifications to upstream retrievals of tangent pressure etc., and small updates to the spectroscopy database for some molecules. Differences in the retrieved CH<sub>3</sub>CN abundances between the two versions are typically less than 10 pptv, but can reach 20 pptv (still within ±5%) at 147 hPa, particularly at higher latitudes (Figure 3.4.1).

### 3.4.3 Resolution

The resolution of the retrieved data can be described using “averaging kernels” [e.g., Rodgers, 2000]; the two-dimensional nature of the MLS data processing system means that the kernels describe both vertical and horizontal resolution. Values of the integrated kernel near unity indicate that the majority of information for that level has come from the measurements themselves and not the a priori; Figure 3.4.2 shows that the measurements dominate throughout most of the vertical range. Smoothing, imposed on the retrieval system in both the vertical and horizontal directions to enhance retrieval stability and precision, degrades the inherent resolution of the measurements. Thus, although CH<sub>3</sub>CN measurements are reported at six pressure levels per decade change in pressure (spacing of ~2.7 km), the vertical resolution of the v4.2x CH<sub>3</sub>CN data as determined from the full width at half maximum of the rows of the averaging kernel matrix shown in Figure 3.4.2 degrades from 4 km at 147 hPa to ~5 – 6 km in the lower stratosphere, and then further worsens to ~7 – 8 km in the upper stratosphere. Substantial overlap in the averaging kernels for the 100 and 147 hPa retrieval surfaces (which both peak at 100 hPa) indicates that the 147 hPa retrieval does not provide as much independent information as is given by retrievals at higher altitudes. Figure 3.4.2 also shows horizontal averaging kernels, from which the along-track horizontal resolution is determined to be ~400 – 700 km over most of the vertical range. The cross-track resolution, set by the width of the field of view of the 640-GHz radiometer, is ~3 km. The along-track separation between adjacent retrieved profiles is 1.5° great circle angle (~165 km), whereas the longitudinal separation of MLS measurements, set by the Aura orbit, is 10° – 20° over low and middle latitudes, with much finer sampling in the polar regions.

### 3.4.4 Precision

The precision of the MLS CH<sub>3</sub>CN data is estimated empirically by comparing profiles measured at the intersections of ascending (day) and descending (night) portions of the orbit. Under ideal conditions (i.e., a quiescent atmosphere), the standard deviation about the mean differences between such matched profile pairs provides a measure of the precision of the individual data points. In practice, however, real changes in the

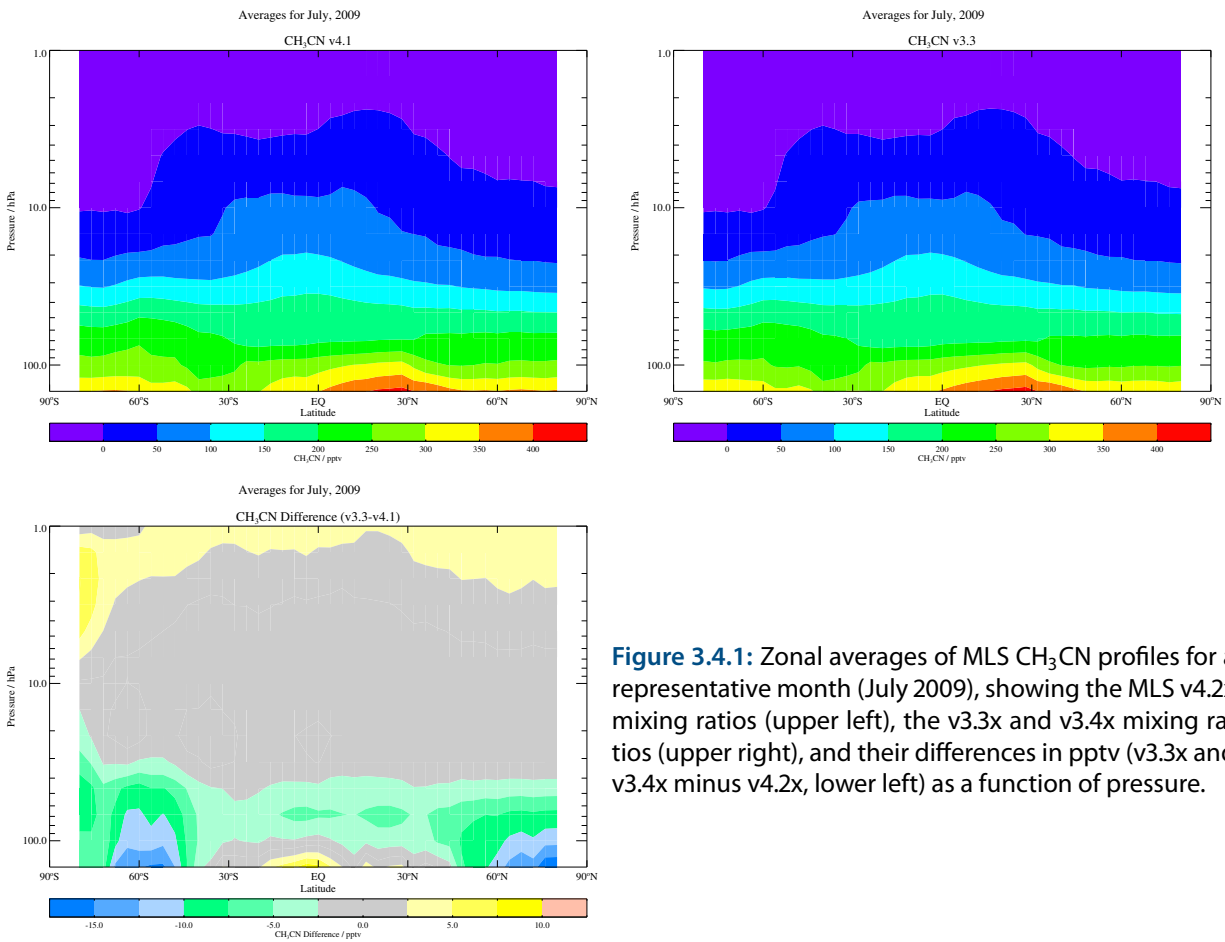


**Figure 3.4.1:** Zonal averages of MLS CH<sub>3</sub>CN profiles for a representative month (July 2009), showing the MLS v4.2x mixing ratios (upper left), the v3.3x and v3.4x mixing ratios (upper right), and their differences in pptv (v3.3x and v3.4x minus v4.2x, lower left) as a function of pressure.

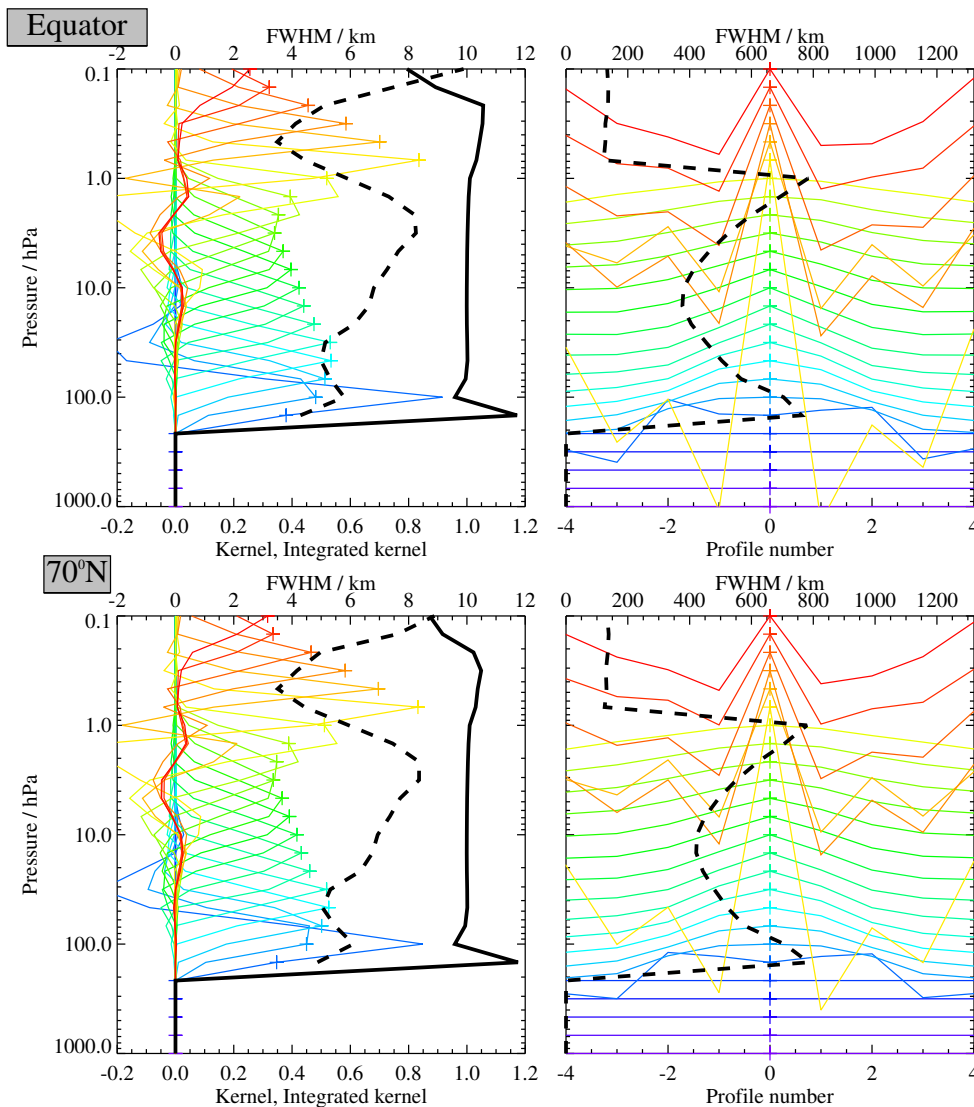


**Figure 3.4.2:** Typical two-dimensional (vertical and horizontal along-track) averaging kernels for the MLS v4.2x CH<sub>3</sub>CN data at the equator (upper) and at 70°N (lower); variation in the averaging kernels is sufficiently small that these are representative of typical profiles. Colored lines show the averaging kernels as a function of MLS retrieval level, indicating the region of the atmosphere from which information is contributing to the measurements on the individual retrieval surfaces, which are denoted by plus signs in corresponding colors. The dashed black line indicates the resolution, determined from the full width at half maximum (FWHM) of the averaging kernels, approximately scaled into kilometers (top axes). (Left) Vertical averaging kernels (integrated in the horizontal dimension for five along-track profiles) and resolution. The solid black line shows the integrated area under each kernel (horizontally and vertically); values near unity imply that the majority of information for that MLS data point has come from the measurements, whereas lower values imply substantial contributions from a priori information. (Right) Horizontal averaging kernels (integrated in the vertical dimension) and resolution. The horizontal averaging kernels are shown scaled such that a unit averaging kernel amplitude is equivalent to a factor of 10 change in pressure.



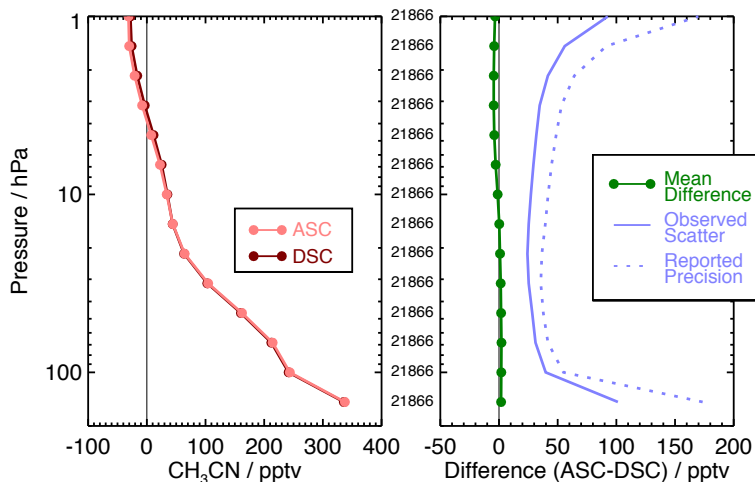


**Figure 3.4.3:** (left) Ensemble mean profiles for ascending (light red) and descending (dark red) orbit matching pairs of MLS v4.2x CH<sub>3</sub>CN profiles averaged over several months of a representative year of data (2005). Symbols indicate MLS retrieval pressure levels. (right) Mean differences (ascending–descending) in pptv (green solid line). Also shown are the standard deviations about the mean differences (light blue solid line) and the root sum square (RSS) of the precisions calculated by the retrieval algorithm for the two sets of profiles (light blue dashed line). The observed scatter about the mean differences and the reported precision values have been scaled by  $1/\sqrt{2}$  (to convert from standard deviations of differences into standard deviations of individual data points); hence the light blue solid line represents the statistical repeatability of the MLS measurements, and the light blue dashed line represents the expected  $1\sigma$  precision for a single profile. The thin black lines mark zero in each panel. The number of crossing pairs of measurements being compared at each pressure level is noted in the space between the panels.

atmosphere may occur over the 12 h interval between the intersecting measurement points, in which case the observed scatter provides an upper limit on the estimate of precision, assuming that the a priori has a negligible influence on the retrieval (a reasonable assumption throughout the retrieval range for CH<sub>3</sub>CN). The precision estimates were found to be essentially invariant with time; results for a representative year of data are shown in Figure 3.4.3. The observed standard deviation values are  $\sim 50$  pptv or less throughout most of the vertical domain, increasing to 100 pptv at 147 and 1 hPa. Mean differences between paired crossing profiles are negligible, indicating the absence of significant ascending–descending offsets.

The precision reported for each data point by the Level 2 data processing system exceeds the observationally determined precision throughout the vertical range (Figure 3.4.3), indicating that the vertical smoothing (regularization) applied to stabilize the retrieval system and improve the precision has a non-negligible influence. Because the reported precisions take into account occasional variations in instrument performance, the best estimate of the precision of an individual data point is the value quoted for that point in the L2GP files, but it should be borne in mind that this approach slightly overestimates the actual measurement noise. The estimates reported here represent the precisions at each pressure level of a single profile; precision can generally be improved by averaging, with the precision of an average of  $N$  profiles being  $1/\sqrt{N}$  times the precision of an individual profile (although the actual standard error of the mean can in some cases be even smaller [Toohey and von Clarmann, 2013]).

### 3.4.5 Range

Although CH<sub>3</sub>CN is retrieved (and reported in the L2GP files) over the range 147 to 0.001 hPa, on the basis of the drop off in precision and resolution, the lack of independent information contributed by the measurements, and the results of simulations using synthetic data as input radiances to test the closure of the retrieval system, the data are not deemed reliable at the extremes of the retrieval range. Thus we recommend that v4.2x

Help	
Overview	
Table	
BrO	S
CH <sub>3</sub> Cl	S
CH <sub>3</sub> CN	S
CH <sub>3</sub> OH	S
ClO	S
CO	S
GPH	S
H <sub>2</sub> O	S
HCl	S
HCN	S
HNO <sub>3</sub>	S
HO <sub>2</sub>	S
HOCl	S
IWC	S
IWP	S
N <sub>2</sub> O	S
O <sub>3</sub>	S
OH	S
RHI	S
SO <sub>2</sub>	S
T	S
T	S

CH<sub>3</sub>CN be used for scientific studies only at the levels between 46 and 1 hPa, except in the winter polar regions, where they may exhibit large biases below 10 hPa. However, although the 147, 100, and 68 hPa retrievals are not generally recommended, they may be scientifically useful in some circumstances. For example, the data display unphysical sharp latitudinal gradients at  $\pm 30^\circ$  at 100 and 68 hPa, yet the large-scale longitudinal variations within the tropics are probably robust. Similarly, confined regions of significant enhancement at 147 hPa unaccompanied by comparably enhanced values at 100 hPa may reflect real atmospheric features. Indeed, many of the “hotspots” apparent in MLS CH<sub>3</sub>CN measurements in the upper troposphere / lower stratosphere closely track similar enhancements in other pollution markers measured by MLS, such as CO and CH<sub>3</sub>Cl. The v4.2x CH<sub>3</sub>CN data at the lowest retrieval levels (147 – 68 hPa) should only be used in consultation with the MLS science team.

### 3.4.6 Accuracy

The effects of various sources of systematic uncertainty (e.g., instrumental issues, spectroscopic uncertainty, and approximations in the retrieval formulation and implementation) on the MLS v4.2x CH<sub>3</sub>CN measurements have been quantified through a comprehensive set of retrievals of synthetic radiances. The overall systematic uncertainty, or accuracy, is calculated by combining (RSS) the contributions from both the expected biases and the additional scatter each source of uncertainty may introduce into the data. In aggregate, the factors considered in these simulations are estimated to give rise to total systematic uncertainty of approximately 100–200% in the MLS v4.2x CH<sub>3</sub>CN data (see Table 3.4.1).

### 3.4.7 Review of comparisons with other datasets

Detailed quantification of differences from correlative data sets has not been performed, but preliminary comparisons suggest that the MLS CH<sub>3</sub>CN measurements are biased substantially high in the UTLS relative to airborne [Singh *et al.*, 2003], balloon-borne [Kleinböhl *et al.*, 2005], and ACE-FTS satellite [Harrison and Bernath, 2013] CH<sub>3</sub>CN measurements, as do results from a two-dimensional chemistry transport model and (noncoincident) CH<sub>3</sub>CN retrievals from the predecessor MLS instrument on the Upper Atmosphere Research Satellite (UARS) [Livesey *et al.*, 2001] (not shown). Furthermore, the zonal-mean morphology of the Aura MLS CH<sub>3</sub>CN at the lowest levels does not agree well with that either observed by UARS MLS or predicted by the model.

### 3.4.8 Data screening

#### Pressure range: 46 – 1.0 hPa

Values outside this range are not recommended for scientific use. The CH<sub>3</sub>CN data at 147 – 68 hPa may be useful under certain circumstances but should not be analyzed in scientific studies without significant discussion with the MLS science team.

#### Estimated precision: Only use values for which the estimated precision is a positive number.

Values where the *a priori* information has a strong influence are flagged with negative or zero precision, and should not be used in scientific analyses (see Section 1.5).

#### Status flag: Only use profiles for which the Status field is zero.

We recommend that all profiles with nonzero values of Status be discarded, because of the potential impact of cloud artifacts at lower levels. Note, however, that rejecting in their entirety all profiles with nonzero Status may be unnecessarily severe at and above (i.e., at pressures equal to or smaller than) 46 hPa, where clouds have negligible impact; thus otherwise good-quality profiles with nonzero but even Status values may be used without restriction at those levels as long as they are removed at larger pressures. See Section 1.6 for more information on the interpretation of the Status field.

#### Quality: Only profiles whose Quality field is greater than 1.4 should be used.

This threshold for Quality (unchanged from v3.3x and v3.4x) typically excludes less than 1% of CH<sub>3</sub>CN profiles on a daily basis; note that it potentially discards some “good” data points while not necessarily identifying all “bad” ones.

**Convergence:** Only profiles whose Convergence field is less than 1.05 should be used.

On a typical day this threshold for Convergence (unchanged from v3.3x and v3.4x) discards very few (0.3% or less) of the CH<sub>3</sub>CN profiles, many (but not all) of which are filtered out by the other quality control measures.

### 3.4.9 Artifacts

- The retrievals at 100 and 68 hPa are characterized by unphysical sharp latitudinal gradients at  $\pm 30^\circ$ .
- Substantial biases may be present in the mixing ratios in the winter polar regions for retrieval levels in the range 100 – 15 hPa.

### 3.4.10 Desired improvements for future data version(s)

- Improve the CH<sub>3</sub>CN retrievals at 147 – 68 hPa.

**Table 3.4.1:** Summary of Aura MLS v4.2x CH<sub>3</sub>CN Characteristics

Pressure / hPa	Resolution V × H <sup>a</sup> / km	Precision <sup>b</sup> / pptv	Systematic Uncertainty <sup>c</sup> / %	Known Artifacts or Other Comments
0.68 – 0.001	—	—	—	Unsuitable for scientific use
1.0	6 × 800	±100	±200	Consult with MLS science team
10 – 1.5	7 – 8 × 400 – 700	±50	±100 – 200	Consult with MLS science team
46 – 15	5 – 6.5 × 400 – 500	±50	±100 – 200	Consult with MLS science team
100 – 68	5.5 × 550 – 700	±50	±100	Consult with MLS science team
147	4 × 750	±100	±200	Consult with MLS science team
1000 – 215	—	—	—	Not retrieved

<sup>a</sup>Vertical and Horizontal resolution in along-track direction.

<sup>b</sup>Precision on individual profiles.

<sup>c</sup>Values should be interpreted as 2- $\sigma$  estimates of the probable magnitude.

## 3.5 Methanol (CH<sub>3</sub>OH)

**Swath name:** CH<sub>3</sub>OH

**Useful range:** 147 – 100 hPa

**Contact:** Michelle Santee, **Email:** <Michelle.L.Santee@jpl.nasa.gov>

### 3.5.1 Introduction

The standard CH<sub>3</sub>OH product is taken from radiances measured by the radiometer centered near 640 GHz. However, as the methanol spectral signature in this region is very similar to that of ClO, additional measurements from the 190-GHz radiometer (which has channels sensitive to ClO but not CH<sub>3</sub>OH) are used to decouple the CH<sub>3</sub>OH and ClO information. CH<sub>3</sub>OH is a new product in v4.2x, and it has not been fully validated. Thus the scientific utility of the v4.2x MLS CH<sub>3</sub>OH measurements remains to be determined. A summary of the estimated precision, resolution (vertical and horizontal), and systematic uncertainty of the v4.2x CH<sub>3</sub>OH measurements as a function of altitude is given in Table 3.5.1.

### 3.5.2 Resolution

The resolution of the retrieved data can be described using “averaging kernels” [e.g., *Rodgers*, 2000]; the two-dimensional nature of the MLS data processing system means that the kernels describe both vertical and horizontal resolution. Values of the integrated kernel near unity indicate that the majority of information for that level has come from the measurements themselves and not the a priori; Figure 3.5.1 shows that the measurements dominate throughout most of the vertical range. Smoothing, imposed on the retrieval system in both the vertical and horizontal directions to enhance retrieval stability and precision, degrades the inherent resolution of the measurements. Thus, although CH<sub>3</sub>OH measurements are reported at six pressure levels per decade change in pressure (spacing of ~2.7 km), the vertical resolution of the v4.2x CH<sub>3</sub>OH data as determined from the full width at half maximum of the rows of the averaging kernel matrix shown in Figure 3.5.1 is ~4–5 km at 147 and 100 hPa. Figure 3.5.1 also shows horizontal averaging kernels, from which the along-track horizontal resolution is determined to be ~350 km. The cross-track resolution, set by the width of the field of view of the 640-GHz radiometer, is ~3 km. The along-track separation between adjacent retrieved profiles is 1.5° great circle angle (~165 km), whereas the longitudinal separation of MLS measurements, set by the Aura orbit, is 10°–20° over low and middle latitudes, with much finer sampling in the polar regions.

### 3.5.3 Precision

The precision of the MLS CH<sub>3</sub>OH data is estimated empirically by comparing profiles measured at the intersections of ascending (day) and descending (night) portions of the orbit. Under ideal conditions (i.e., a quiescent atmosphere), the standard deviation about the mean differences between such matched profile pairs provides a measure of the precision of the individual data points. In practice, however, real changes in the atmosphere may occur over the 12 h interval between the intersecting measurement points, in which case the observed scatter provides an upper limit on the estimate of precision, assuming that the a priori has a negligible influence on the retrieval (a reasonable assumption throughout the retrieval range for CH<sub>3</sub>OH). The precision estimates were found to be essentially invariant with time; results for several months of a representative year of data are shown in Figure 3.5.2. For the most part, differences between paired profiles are small, implying the absence of significant systematic ascending / descending biases. The observed standard deviation is ~1 ppbv at 147 hPa. The observationally determined precision agrees well with that reported for each data point by the Level 2 data processing system. The estimates reported here represent the precisions at each pressure level of a single profile; precision can generally be improved by averaging, with the precision of an average of  $N$  profiles being  $1/\sqrt{N}$  times the precision of an individual profile (although the actual standard error of the mean can in some cases be even smaller [*Toohey and von Clarmann*, 2013]).

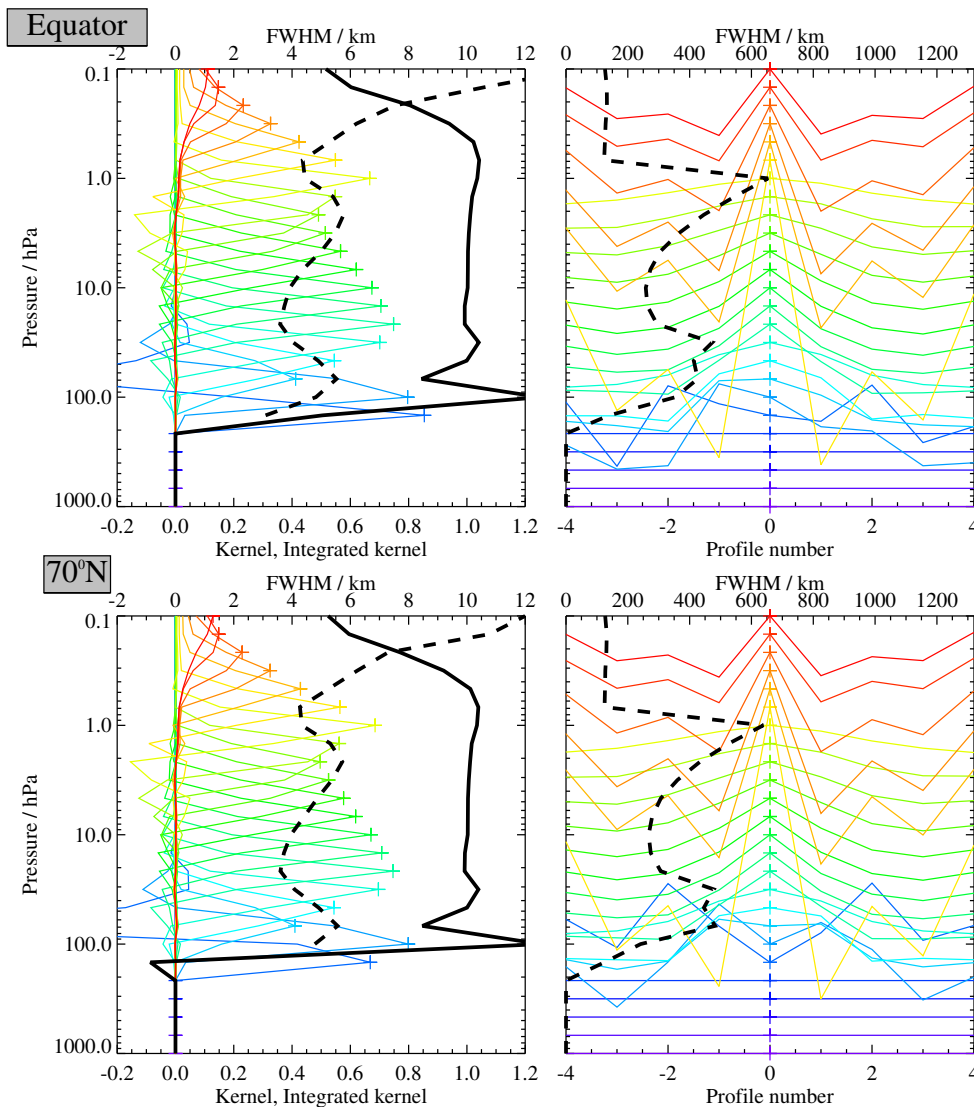


**Figure 3.5.1:** Typical two-dimensional (vertical and horizontal along-track) averaging kernels for the MLS v4.2x CH<sub>3</sub>OH data at the equator (upper) and at 70°N (lower); variation in the averaging kernels is sufficiently small that these are representative of typical profiles. Colored lines show the averaging kernels as a function of MLS retrieval level, indicating the region of the atmosphere from which information is contributing to the measurements on the individual retrieval surfaces, which are denoted by plus signs in corresponding colors. The dashed black line indicates the resolution, determined from the full width at half maximum (FWHM) of the averaging kernels, approximately scaled into kilometers (top axes). (Left) Vertical averaging kernels (integrated in the horizontal dimension for five along-track profiles) and resolution. The solid black line shows the integrated area under each kernel (horizontally and vertically); values near unity imply that the majority of information for that MLS data point has come from the measurements, whereas lower values imply substantial contributions from a priori information. (Right) Horizontal averaging kernels (integrated in the vertical dimension) and resolution. The horizontal averaging kernels are shown scaled such that a unit averaging kernel amplitude is equivalent to a factor of 10 change in pressure.

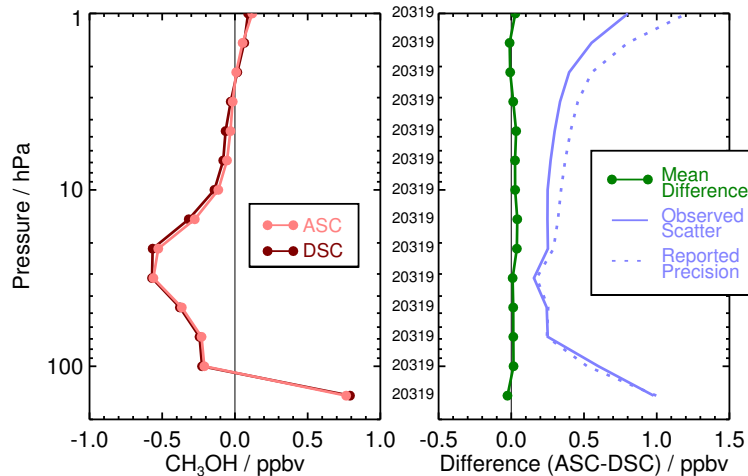


**Figure 3.5.2:** (left) Ensemble mean profiles for ascending (light red) and descending (dark red) orbit matching pairs of MLS v4.2x CH<sub>3</sub>OH profiles averaged over several months of a representative year of data (2005). Symbols indicate MLS retrieval pressure levels. (right) Mean differences (ascending–descending) in pptv (green solid line). Also shown are the standard deviations about the mean differences (light blue solid line) and the root sum square (RSS) of the precisions calculated by the retrieval algorithm for the two sets of profiles (light blue dashed line). The observed scatter about the mean differences and the reported precision values have been scaled by  $1/\sqrt{2}$  (to convert from standard deviations of differences into standard deviations of individual data points); hence the light blue solid line represents the statistical repeatability of the MLS measurements, and the light blue dashed line represents the expected  $1\sigma$  precision for a single profile. The thin black lines mark zero in each panel. The number of crossing pairs of measurements being compared at each pressure level is noted in the space between the panels.

### 3.5.4 Range

CH<sub>3</sub>OH is retrieved (and reported in the L2GP files) over the range 147 to 0.001 hPa. However, zonal mean mixing ratios are negative everywhere at retrieval pressures less than 100 hPa, as well as at middle and high latitudes at 100 hPa. Thus, with rare exceptions (such as during extreme events), the v4 CH<sub>3</sub>OH data are considered potentially useful for scientific studies only at 147 hPa and at low latitudes at 100 hPa.

### 3.5.5 Accuracy

The effects of various sources of systematic uncertainty (e.g., instrumental issues, spectroscopic uncertainty, and approximations in the retrieval formulation and implementation) on the MLS v4.2x CH<sub>3</sub>OH measurements have been quantified through a comprehensive set of retrievals of synthetic radiances. The overall systematic uncertainty, or accuracy, is calculated by combining (RSS) the contributions from both the expected biases and the additional scatter each source of uncertainty may introduce into the data. In aggregate, the factors considered in these simulations are estimated to give rise to total systematic uncertainty of approximately 100–250% in the MLS v4.2x CH<sub>3</sub>OH data (see Table 3.5.1).

### 3.5.6 Review of comparisons with other datasets

Detailed comparisons with correlative data sets have not been undertaken, but preliminary comparisons with version 3 ACE-FTS data suggest that the MLS values may be biased substantially high at 147 hPa (not shown).

### 3.5.7 Data screening

**Do not use:** The v4.2x CH<sub>3</sub>OH data should only be used in consultation with the MLS science team.

### 3.5.8 Artifacts

- A complete assessment of artifacts in the v4.2x CH<sub>3</sub>OH measurements has not been performed, but it is known that zonal mean mixing ratios are negative everywhere at retrieval pressures less than or equal to 68 hPa, as well as at middle and high latitudes at 100 hPa.

### 3.5.9 Desired improvements for future data version(s)

- Specific improvements in the CH<sub>3</sub>OH retrieval remain to be determined.

**Table 3.5.1:** Summary of Aura MLS v4.2x CH<sub>3</sub>OH Characteristics

Pressure / hPa	Resolution V × H <sup>a</sup> / km	Precision <sup>b</sup> / ppbv	Systematic Uncertainty <sup>c</sup> / %	Known Artifacts or Other Comments
68 – 0.001	—	—	—	Unsuitable for scientific use
100	5 × 350	±1	±100	Consult with MLS Science Team
147	3 × 150	±1	±250	Consult with MLS Science Team
1000 – 215	—	—	—	Not retrieved

<sup>a</sup>Vertical and Horizontal resolution in along-track direction.

<sup>b</sup>Precision on individual profiles.

<sup>c</sup>Values should be interpreted as 2- $\sigma$  estimates of the probable magnitude.

Help	
Overview	
Table	
BrO	S T
CH <sub>3</sub> Cl	S T
CH <sub>3</sub> CN	S T
CH <sub>3</sub> OH	S T
<b>ClO</b>	<b>S</b> <b>T</b>
CO	S T
GPH	S T
H <sub>2</sub> O	S T
HCl	S T
HCN	S T
HNO <sub>3</sub>	S T
HO <sub>2</sub>	S T
HOCl	S T
IWC	S T
IWP	S T
N <sub>2</sub> O	S T
O <sub>3</sub>	S T
OH	S T
RHI	S T
SO <sub>2</sub>	S T
	S T

## 3.6 Chlorine Monoxide (ClO)

**Swath name:** ClO

**Useful range:** 147–1.0 hPa

**Contact:** Michelle Santee, **Email:** <Michelle.L.Santee@jpl.nasa.gov>

### 3.6.1 Introduction

The quality and reliability of the version 2 (v2.2) Aura MLS ClO measurements were assessed in detail by Santee *et al.* [2008]. The ClO product was significantly improved in v3.3x and v3.4x [Livesey *et al.*, 2013]; in particular, the substantial (~0.1–0.4 ppbv) negative bias present in the v2.2 ClO values at retrieval levels below (i.e., pressures larger than) 22 hPa was mitigated to a large extent, primarily through retrieval of CH<sub>3</sub>Cl, which was a new MLS product in v3.3x and v3.4x. The ClO retrieval is largely unchanged over much of the profile in v4.2x.

As in previous versions, in v4.2x the standard ClO product is derived from radiances measured by the radiometer centered near 640 GHz. (ClO is also retrieved using radiances from the 190-GHz radiometer, but those data have poorer precision.) The MLS v4.2x ClO data are scientifically useful over the range 147 to 1 hPa. A summary of the estimated precision, resolution (vertical and horizontal), and systematic uncertainty of the v4.2x ClO measurements as a function of altitude is given in Table 3.6.1.

### 3.6.2 Resolution

The resolution of the retrieved data can be described using “averaging kernels” [e.g., Rodgers, 2000]; the two-dimensional nature of the MLS data processing system means that the kernels describe both vertical and horizontal resolution. Smoothing, imposed on the retrieval system in both the vertical and horizontal directions to enhance retrieval stability and precision, degrades the inherent resolution of the measurements. Thus, although ClO measurements are reported at six pressure levels per decade change in pressure (spacing of ~2.7 km), the vertical resolution of the v4.2x ClO data as determined from the full width at half maximum of the rows of the averaging kernel matrix shown in Figure 3.6.1 is ~3–4.5 km throughout the retrieval range (with a mean of ~3.5 km). As in v3.3x and v3.4x, in v4.2x the averaging kernels are sharply peaked at all levels, including 147 hPa. Thus, although some degree of overlap is present, the 147 hPa surface provides independent information in v4.2x. Figure 3.6.1 also shows horizontal averaging kernels, from which the along-track horizontal resolution is determined to be ~250–500 km over most of the vertical range. The cross-track resolution, set by the width of the field of view of the 640-GHz radiometer, is ~3 km. The along-track separation between adjacent retrieved profiles is 1.5° great circle angle (~165 km), whereas the longitudinal separation of MLS measurements, set by the Aura orbit, is 10°–20° over low and middle latitudes, with much finer sampling in the polar regions.

### 3.6.3 Precision

The precision of the MLS ClO measurements is estimated empirically by computing the standard deviation of the descending (i.e., nighttime) profiles in the 20°-wide latitude band centered around the equator. For this region and time of day, natural atmospheric variability should be negligible relative to the measurement noise. As shown in Figure 3.6.2, the observed scatter in the data is essentially unchanged in v4.2x, rising from ~0.1 ppbv over the interval 100 – 3 hPa to ~0.3 ppbv at 1 hPa and 147 hPa. The smoothing of the retrieval is turned off above 1 hPa, and as a consequence the precision rises steeply above this level. The scatter in the data is essentially invariant with time, as seen by comparing the results for the different days shown in Figure 3.6.2.

The single-profile precision estimates cited here are, to first order, independent of latitude and season, but of course the scientific utility of individual MLS profiles (i.e., signal to noise) varies with ClO abundance.



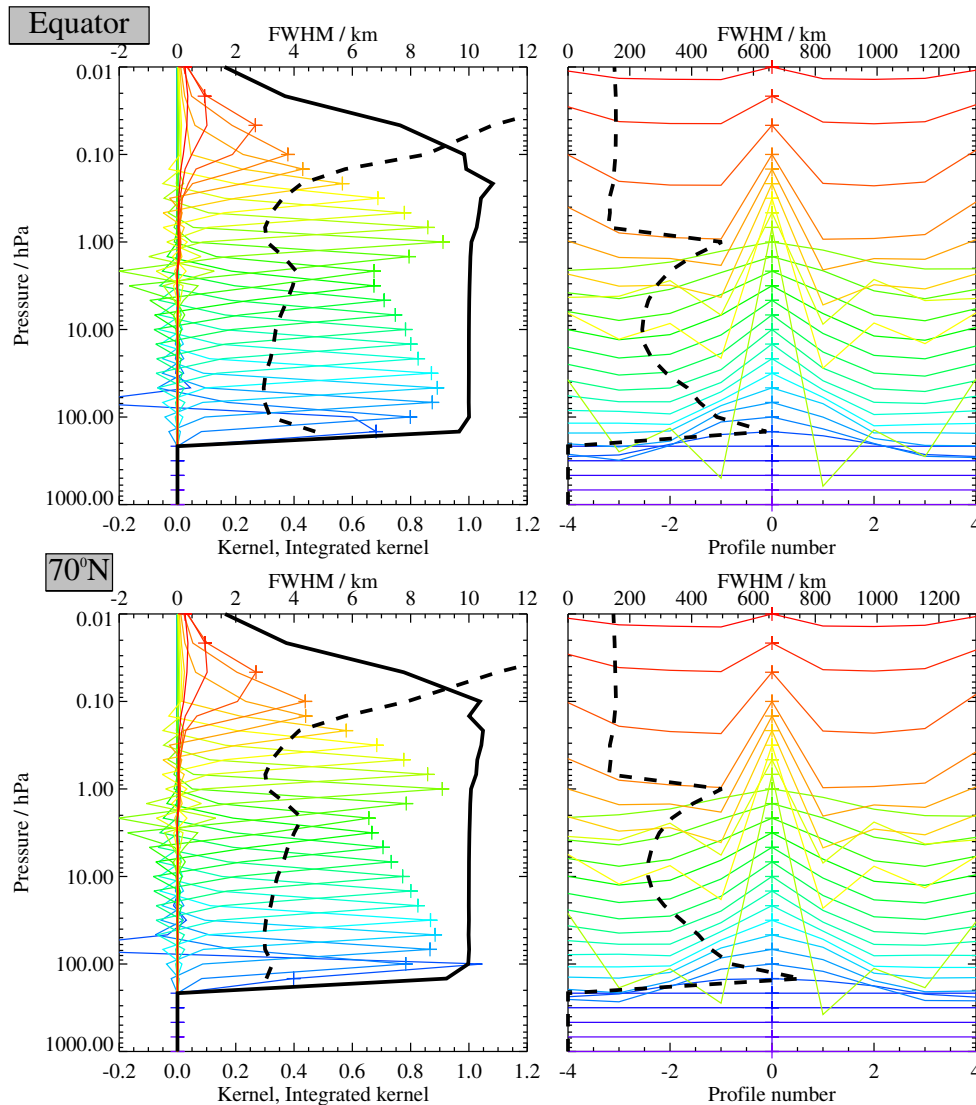


**Figure 3.6.1:** Typical two-dimensional (vertical and horizontal along-track) averaging kernels for the MLS v4.2x ClO data at the equator (upper) and at 70°N (lower); variation in the averaging kernels is sufficiently small that these are representative of typical profiles. Colored lines show the averaging kernels as a function of MLS retrieval level, indicating the region of the atmosphere from which information is contributing to the measurements on the individual retrieval surfaces, which are denoted by plus signs in corresponding colors. The dashed black line indicates the resolution, determined from the full width at half maximum (FWHM) of the averaging kernels, approximately scaled into kilometers (top axes). (Left) Vertical averaging kernels (integrated in the horizontal dimension for five along-track profiles) and resolution. The solid black line shows the integrated area under each kernel (horizontally and vertically); values near unity imply that the majority of information for that MLS data point has come from the measurements, whereas lower values imply substantial contributions from a priori information. (Right) Horizontal averaging kernels (integrated in the vertical dimension) and resolution. The horizontal averaging kernels are shown scaled such that a unit averaging kernel amplitude is equivalent to a factor of 10 change in pressure.

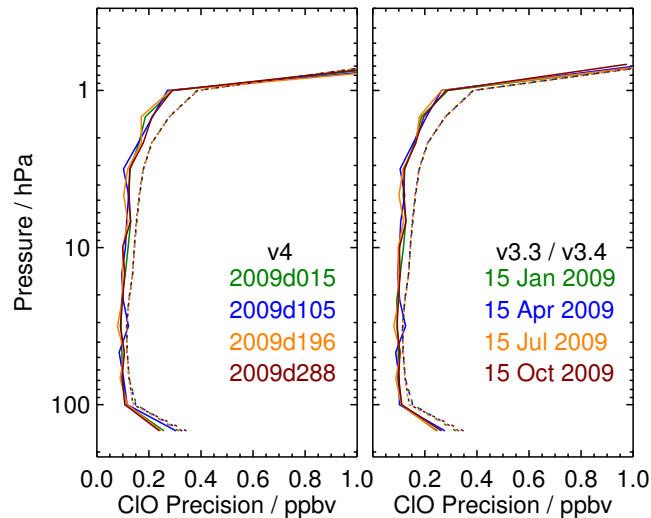


**Figure 3.6.2:** Precision of the (left) v4.2x and (right) v3.3x and v3.4x MLS ClO measurements for four representative days in different seasons (see legend). Solid lines depict the observed scatter in nighttime-only measurements obtained in a narrow equatorial band (see text); dotted lines depict the theoretical precision estimated by the retrieval algorithm.

Outside of the lower stratospheric winter polar vortices, within which ClO is often strongly enhanced, the single-profile precision exceeds typical ClO mixing ratios, necessitating the use of averages for scientific studies. Precision can generally be improved by averaging, with the precision of an average of  $N$  profiles being  $1/\sqrt{N}$  times the precision of an individual profile (although the actual standard error of the mean can in some cases be even smaller [Toohey and von Clarmann, 2013]).

The observational determination of the precision is compared in Figure 3.6.2 to the theoretical precision values reported by the Level 2 data processing algorithms. The predicted precision exceeds the observed scatter, particularly above 15 hPa, indicating that the vertical smoothing (regularization) applied to stabilize the retrieval and improve the precision has a nonnegligible influence on the results at these levels. Because the theoretical precisions take into account occasional variations in instrument performance, the best estimate of the precision of an individual data point is the value quoted for that point in the L2GP files, but it should be borne in mind that this approach slightly overestimates the actual measurement noise.

### 3.6.4 Accuracy

The effects of various sources of systematic uncertainty (e.g., instrumental issues, spectroscopic uncertainty, and approximations in the retrieval formulation and implementation) on the MLS v4.2x ClO measurements have been quantified through a comprehensive set of retrievals of synthetic radiances; see Santee *et al.* [2008] for details of a similar analysis conducted on MLS v2.2 ClO data. The overall systematic uncertainty, or accuracy, is calculated by combining (RSS) the contributions from both the expected biases and the additional scatter each source of uncertainty may introduce into the data. In aggregate, the factors considered in these simulations are estimated to give rise to a total systematic uncertainty ranging from approximately 0.02 to 0.4 ppbv, depending on the level, in the MLS v4.2x ClO data (see Table 3.6.1).

Differences between v4.2x and v3.3x and v3.4x ClO mixing ratios are generally less than 0.04 ppbv (usually considerably so) at and above (i.e., at pressures lower than) 68 hPa, including around the secondary peak in the ClO profile in the upper stratosphere (Figure 3.6.3). Significant differences (as much as 0.1 ppbv) are seen at the lowest retrieval levels, however. Figure 3.6.4 depicts nighttime mixing ratios for a single representative day in Southern Hemisphere late spring / Northern Hemisphere early autumn for which ClO is not enhanced

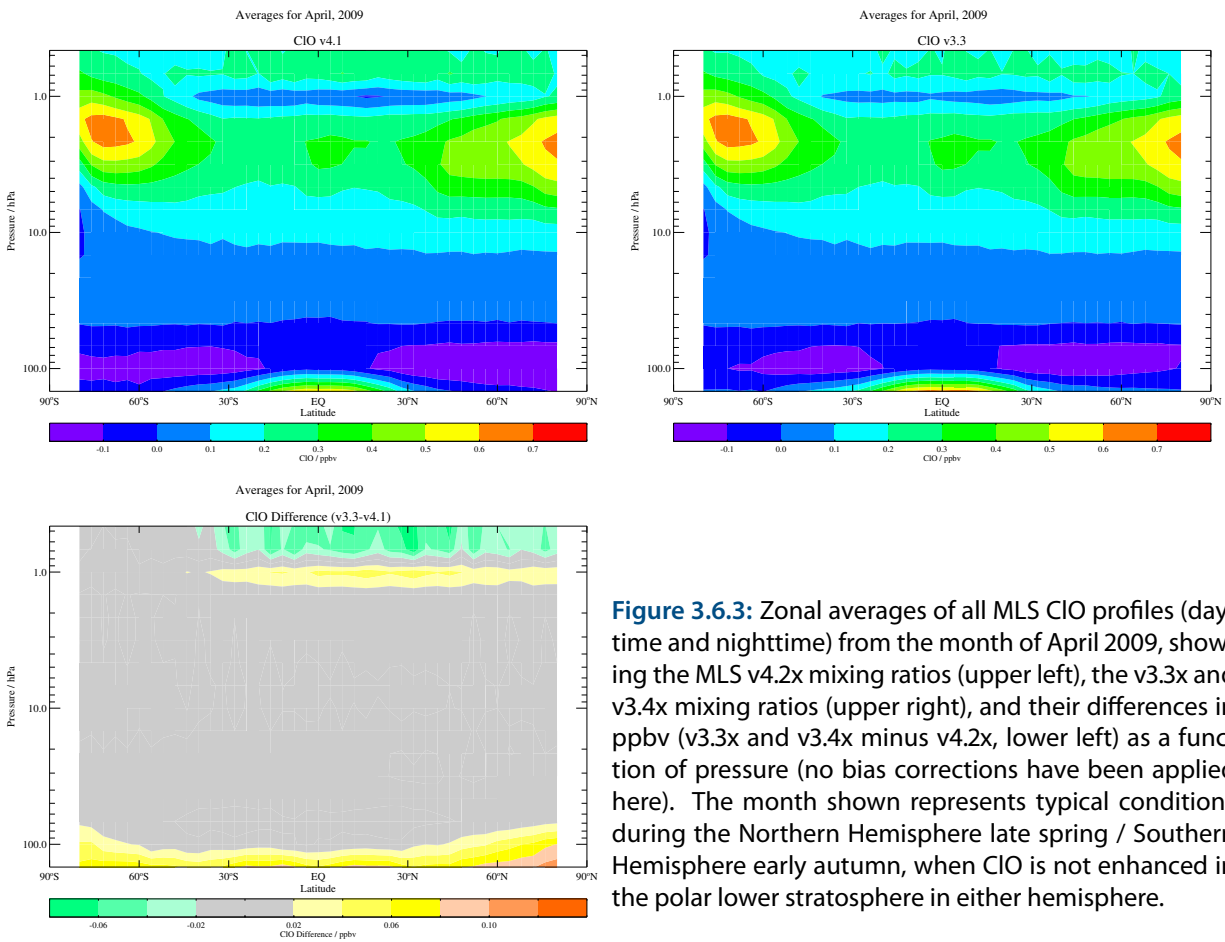


**Figure 3.6.3:** Zonal averages of all MLS ClO profiles (daytime and nighttime) from the month of April 2009, showing the MLS v4.2x mixing ratios (upper left), the v3.3x and v3.4x mixing ratios (upper right), and their differences in ppbv (v3.3x and v3.4x minus v4.2x, lower left) as a function of pressure (no bias corrections have been applied here). The month shown represents typical conditions during the Northern Hemisphere late spring / Southern Hemisphere early autumn, when ClO is not enhanced in the polar lower stratosphere in either hemisphere.

- Help
- Overview
- Table
- BrO
- CH<sub>3</sub>Cl
- CH<sub>3</sub>CN
- CH<sub>3</sub>OH
- ClO**
- CO
- GPH
- H<sub>2</sub>O
- HCl
- HCN
- HNO<sub>3</sub>
- HO<sub>2</sub>
- HOCl
- IWC
- IWP
- N<sub>2</sub>O
- O<sub>3</sub>
- OH
- RHI
- SO<sub>2</sub>

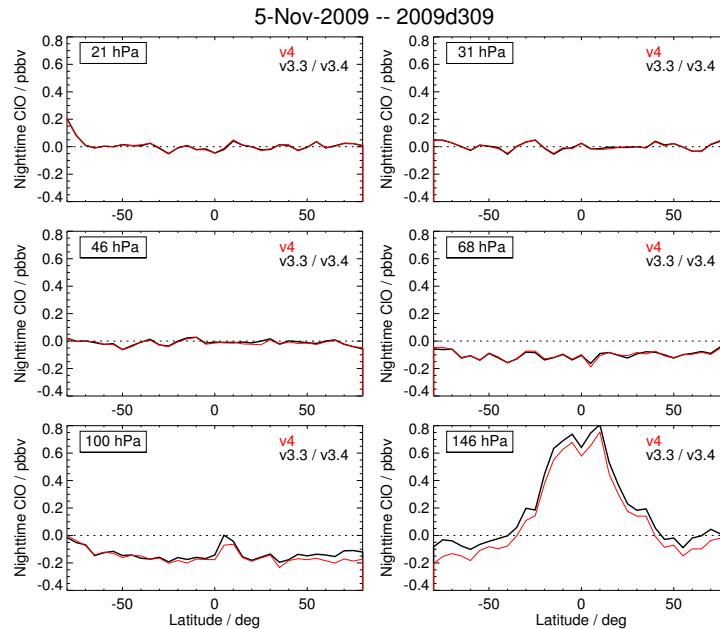


**Figure 3.6.4:** Nighttime v4.2x (red) and v3.3x and v3.4x (black) MLS ClO data as a function of latitude for the six lowest retrieval pressure surfaces (21–147 hPa). The date shown is representative of a typical Southern Hemisphere late spring / Northern Hemisphere early autumn day for which ClO is not enhanced in the polar lower stratosphere in either hemisphere.

in the polar lower stratosphere in either hemisphere; a similar plot for a corresponding day in Northern Hemisphere late spring / Southern Hemisphere early autumn gives very similar results (not shown). This figure demonstrates that a small, somewhat latitude-dependent, negative bias is still evident at 68 and 100 hPa in v4.2x, of approximately the same magnitude as in v3.3x and v3.4x at 68 hPa but a little larger at 100 hPa, especially in the Northern Hemisphere. At 147 hPa, v3.3x and v3.4x ClO displays a strongly latitudinally varying bias that is positive at middle and low latitudes and slightly negative in the polar regions (at least on some days). In v4.2x, ClO mixing ratios at 147 hPa are slightly lower than they were in v3.3x and v3.4x, and consequently the low-latitude positive bias has been reduced, although it remains substantial (exceeding 0.7 ppbv in some cases), and the high-latitude negative bias has been exacerbated.

In many cases the bias can be essentially eliminated by subtracting daily gridded or zonal-mean nighttime values from the individual daytime measurements. This is not a practical approach under conditions of continuous daylight in the summer or continuous darkness in the winter at high latitudes, however. Moreover, under certain circumstances inside the winter polar vortices, chlorine activation leads to nonnegligible ClO abundances even at night. In this case, taking day–night differences considerably reduces the apparent degree of chlorine activation. It is instead recommended that the estimated value of the bias be subtracted from the individual measurements at each affected retrieval level.

To investigate the magnitude of and temporal variations in the bias in the v4.2x MLS ClO data, we show in Figure 3.6.5 monthly zonal means of MLS nighttime ClO measurements for pressure levels 147–46 hPa. Each panel represents a calendar month; data taken during that month over the course of the Aura mission to date (2005–2016) have been binned and averaged in  $5^\circ$ -wide latitude bands between  $\pm 85^\circ$ . Figure 3.6.6 is a similar plot but encompasses all of the MLS nighttime ClO data for pressure levels 147–10 hPa. Although Figure 3.6.5 reveals slight month-to-month variability, it is relatively small (ranging from less than  $\sim 0.04$  ppbv at 147 hPa to less than  $\sim 0.01$  ppbv at 68 hPa) at  $\pm 50^\circ$  (the highest latitudes for which month-to-month variability can be

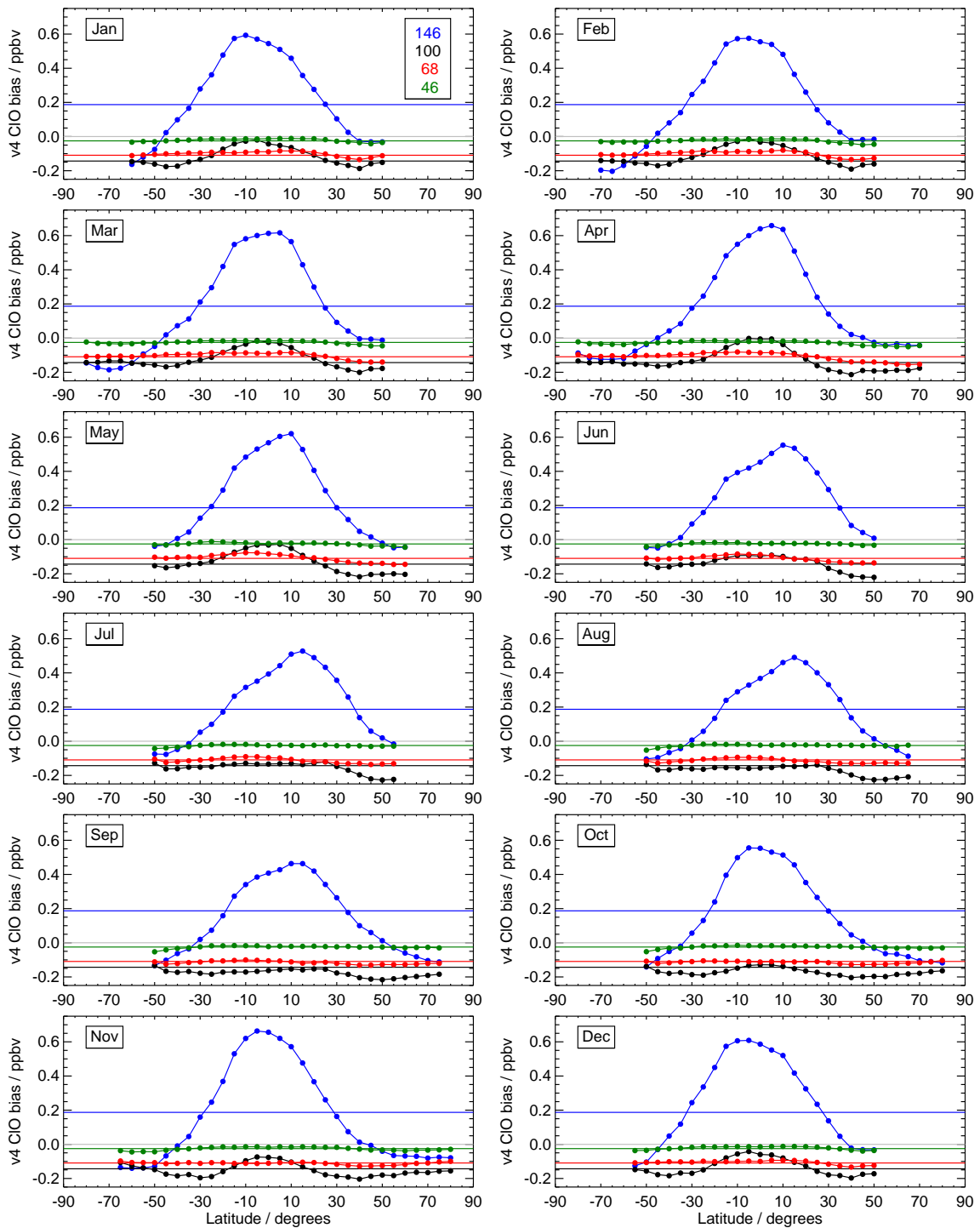


**Figure 3.6.5:** Estimates of the bias in MLS v4.2x ClO data in 5°-wide geographic latitude bands on the 147, 100, 68, and 46 hPa MLS retrieval pressure surfaces (see legend). Each panel shows monthly zonal means of v4.2x MLS nighttime (solar zenith angle (SZA) > 100°) ClO measurements averaged over a 12-yr period (2005–2016, filled circles). The grey line marks the zero level. The colored solid lines denote the global mean bias estimate at each level. To ensure that ClO was not enhanced, consideration was restricted to latitudes equatorward of 50°S for the days between 1 May and 1 November and to latitudes equatorward of 50°N for the days between 1 December and 1 April.

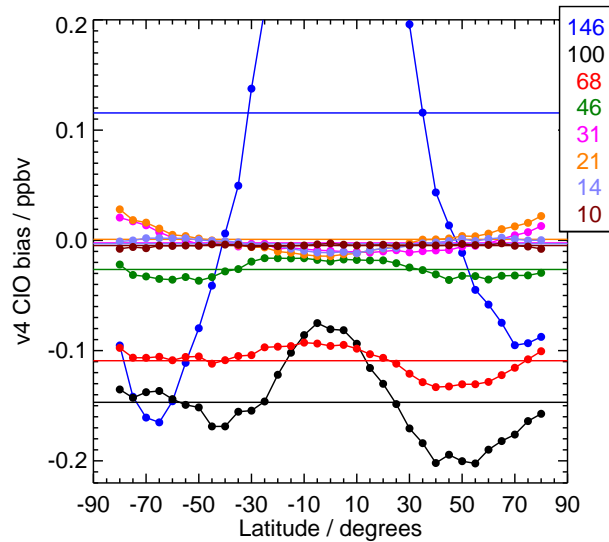


**Figure 3.6.6:** Estimates of the bias in MLS v4.2x ClO data in  $5^\circ$ -wide geographic latitude bands on MLS retrieval pressure surfaces from 147 to 10 hPa (see legend) calculated over a 12-yr period (2005–2016). To ensure that ClO was not enhanced, consideration was restricted to latitudes equatorward of  $50^\circ\text{S}$  for the days between 1 May and 1 November and to latitudes equatorward of  $50^\circ\text{N}$  for the days between 1 December and 1 April. The colored solid lines denote the global mean bias estimate at each level. The large positive bias at low latitudes at 147 hPa is cut off in this figure.

quantified). Moreover, the magnitude of the bias varies little from one year to the next (not shown). Therefore, we compute 12-yr climatological bias estimates. To guide the eye, the global mean climatological bias value is indicated for each level (colored solid lines) in both figures. As discussed above, the magnitude, and at 147 hPa even the sign, of the bias varies with latitude, and Figures 3.6.5 and 3.6.6 underscore the necessity of applying latitudinally and altitudinally varying bias corrections. Given the degree of seasonal variability seen in Figure 3.6.5, monthly varying bias estimates would also be desirable; as noted previously, however, it is not possible to directly quantify the bias in the polar regions during much of the year. Attempts to estimate the bias through approaches other than examination of nighttime ClO measurements (e.g., via correlations with potentially interfering species, which themselves may vary strongly with season) have so far met with only limited success. Consequently, we report time-invariant but altitude- and latitude-dependent v4.2x ClO bias corrections, which are adequate for most studies. An ASCII file containing the estimated bias values is available from the MLS web site.

### 3.6.5 Review of comparisons with other data sets

Extensive comparisons of MLS v2.2 ClO data with a variety of different platforms (ground-based, balloon-borne, aircraft, and satellite instruments) were presented by *Santee et al.* [2008]. A subset of those comparisons with v3.3x and v3.4x ClO data were reported by *Livesey et al.* [2013].

### 3.6.6 Data screening

**Pressure range:** 147 – 1.0 hPa

Values outside this range are not recommended for scientific use.

**Estimated precision:** Only use values for which the estimated precision is a positive number.

Values where the *a priori* information has a strong influence are flagged with negative or zero precision, and should not be used in scientific analyses (see Section 1.5).

**Status flag:** Only use profiles for which the **Status** field is zero.

We recommend that all profiles with nonzero values of **Status** be discarded, because of the potential impact of cloud artifacts at lower levels. Note, however, that rejecting in their entirety all profiles with nonzero **Status** may be unnecessarily severe at and above (i.e., at pressures equal to or smaller than) 46 hPa, where clouds have negligible impact; thus otherwise good-quality profiles with nonzero but even **Status** values may be used without restriction at those levels as long as they are removed at larger pressures. See Section 1.6 for more information on the interpretation of the **Status** field.

**Quality:** Only profiles whose **Quality** field is greater than 1.3 should be used.

This threshold for **Quality** (unchanged from v3.3x and v3.4x) typically excludes less than 1% of ClO profiles on a daily basis; note that it potentially discards some “good” data points while not necessarily identifying all “bad” ones.

**Convergence:** Only profiles whose **Convergence** field is less than 1.05 should be used.

On a typical day this threshold for **Convergence** (unchanged from v3.3x and v3.4x) discards very few (0.3% or less) of the ClO profiles, many (but not all) of which are filtered out by the other quality control measures.

### 3.6.7 Artifacts

- Significant biases are present in both daytime and nighttime v4.2x ClO mixing ratios at and below (i.e., pressures larger than) 68 hPa. The bias should be corrected by subtracting from the individual measurements at each affected retrieval level the altitude- and latitude-dependent bias estimates given in an ASCII file available from the MLS web site.

### 3.6.8 Desired improvements for future data version(s)

- Reduce the biases present at the lowest retrieval levels (147–68 hPa).

**Table 3.6.1:** Summary of Aura MLS v4.2x ClO Characteristics

Pressure / hPa	Resolution $V \times H^a$ / km	Precision <sup>b</sup> / ppbv	Systematic Uncertainty <sup>c</sup> / ppbv	Known Artifacts or Other Comments
0.68–0.001	—	—	—	Unsuitable for scientific use
1.0	$3 \times 500$	$\pm 0.3$	$\pm 0.02$	
15–1.5	$3.5 - 4 \times 250 - 400$	$\pm 0.1$	$\pm 0.02 - 0.03$	
22	$3 \times 300-400$	$\pm 0.1$	$\pm 0.05$	
46–32	$3 \times 300-400$	$\pm 0.1$	$\pm 0.15$	
68	$3 \times 450$	$\pm 0.1$	$\pm 0.2$	Latitude-dependent bias <sup>d</sup>
100	$3 \times 500$	$\pm 0.1$	$\pm 0.25$	Latitude-dependent bias <sup>d</sup>
147	$4.5 \times 600$	$\pm 0.3$	$\pm 0.4$	Latitude-dependent bias <sup>d</sup>
1000–215	—	—	—	Not retrieved

<sup>a</sup>Vertical and Horizontal resolution in along-track direction.

<sup>b</sup>Precision on individual profiles, determined from observed scatter in nighttime (descending) data in a region of minimal atmospheric variability.

<sup>c</sup>Values should be interpreted as 2- $\sigma$  estimates of the probable magnitude and, at the higher pressures, are the uncertainties after subtraction of the known bias.

<sup>d</sup>Correct for the bias by subtracting from the individual measurements at this level the latitude-dependent bias estimates given in the ASCII file available from the MLS website

## 3.7 Carbon monoxide (CO)

**Swath name:** CO

**Useful range:** 215 – 0.0046 hPa

**Contact:** Hugh C. Pumphrey (stratosphere/mesosphere), **Email:** <H.C.Pumphrey@ed.ac.uk>  
 Michael Schwartz (troposphere), **Email:** <Michael.J.Schwartz@jpl.nasa.gov>

### 3.7.1 Introduction

Carbon monoxide is retrieved from radiance measurements of two bands in the MLS 240 GHz radiometer. Full details are given in *Pumphrey et al.* [2007] and *Livesey et al.* [2008].

### 3.7.2 Differences between v4.2x and v03.x

In the upper troposphere (UT), the primary difference between v4.2x CO and v3.3x/v3.4x CO is the reduction in the frequency and severity of artifacts caused by deep convective clouds. This was accomplished through a modification to the manner in which cloud signals are modeled in the retrievals. Screening of data has been simplified, fewer profiles are marked “bad” and fewer profiles that appear to contain cloud artifacts pass through the recommended screening.

A comparison of the two versions in the UTLS for February 2009, shown in Figure 3.7.1, includes non-spurious high values from the plume of the “Black Saturday” fire, that are seen in both versions (so near the black 1:1 line). Scattering from large particles in convective cores produces mostly high outliers in v03.30 CO at 215 hPa, 147 hPa and 100 hPa and low outliers at 68 hPa and 46 hPa that are greatly reduced in v4.2x, resulting in the clouds of points away from the 1:1 line. The “Black Saturday” plume produces UTLS CO values outside of the typically encountered, allowing comparison of non-spurious high values from the two version, unobscured by the v03.30 cloud-induced scatter present at lower v4.2x mixing ratios. At the highest values of the “Black Saturday” tails at 100 hPa and 68 hPa, values from v4.2x are lower than those from v3.3x and v3.4x by ~10%, but fractional differences between the versions are smaller at lower mixing ratios. The screening recommended for v3.3x and v3.4x results in a significant amount of missing data in the tropics, and when the recommended IWC-based component of v3.3x and v3.4x screening is included, a significant fraction of the “Black Saturday” non-spurious high values are screened out.

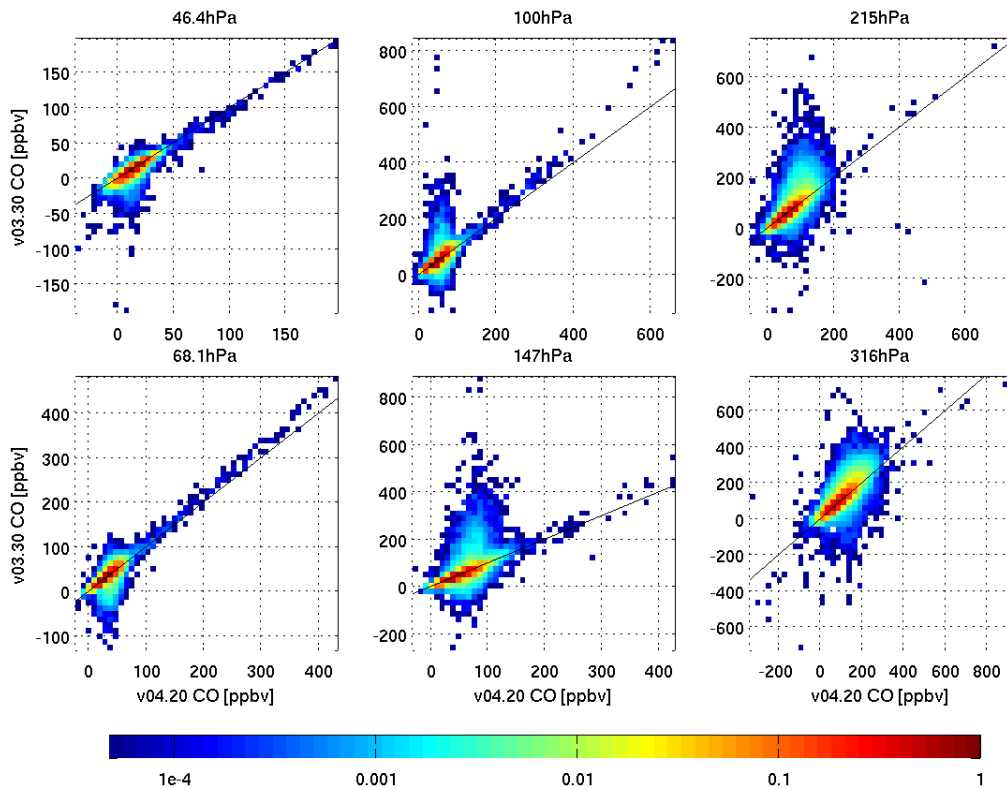
### 3.7.3 Resolution

Figure 3.7.2 shows the horizontal and vertical averaging kernels for v4.2x MLS CO. Vertical and horizontal resolution are essentially unchanged from v3.3x and v3.4x. The vertical resolution is in the range 3.5 – 5 km from the upper troposphere to the lower mesosphere, degrading to 6 – 7 km in the upper mesosphere. Down to the 215 hPa level, the vertical averaging kernels are sharply peaked at the level being retrieved, but while the 316-hPa measurement contains contribution from 316 hPa, it has a larger contribution from 215 hPa and a negative contribution around 100 hPa of similar magnitude to that at 316 hPa. The retrieved value at 316 hPa is thus more an extrapolation of the profile higher in the UTLS than it is an independent measurement at 316 hPa, and it is not recommended for scientific use. The horizontal resolution is about 200 km in the mesosphere, degrading slowly to 300 km with decreasing height in the stratosphere and more rapidly to about 460 km at 100 hPa and 690 km at 215 hPa.

### 3.7.4 Precision

The MLS data are supplied with an estimated precision (the field L2gpPrecision) which is the *a posteriori* precision as returned by the optimal estimation. The precision of the v4.2x CO is very similar to that of v3.3x/v3.4x and is usually smaller (better) than that of v2.2. In all versions, the precision is greater than the





**Figure 3.7.1:** Version v03.30 CO scattered against v04.20 CO for data from February 2009, when the “Black Saturday” fire provided a plume of non-spurious high-CO outliers, unprecedented in the MLS record. This data is unscreened. The 316-hPa retrieval level is shown, but is not recommended for scientific use.

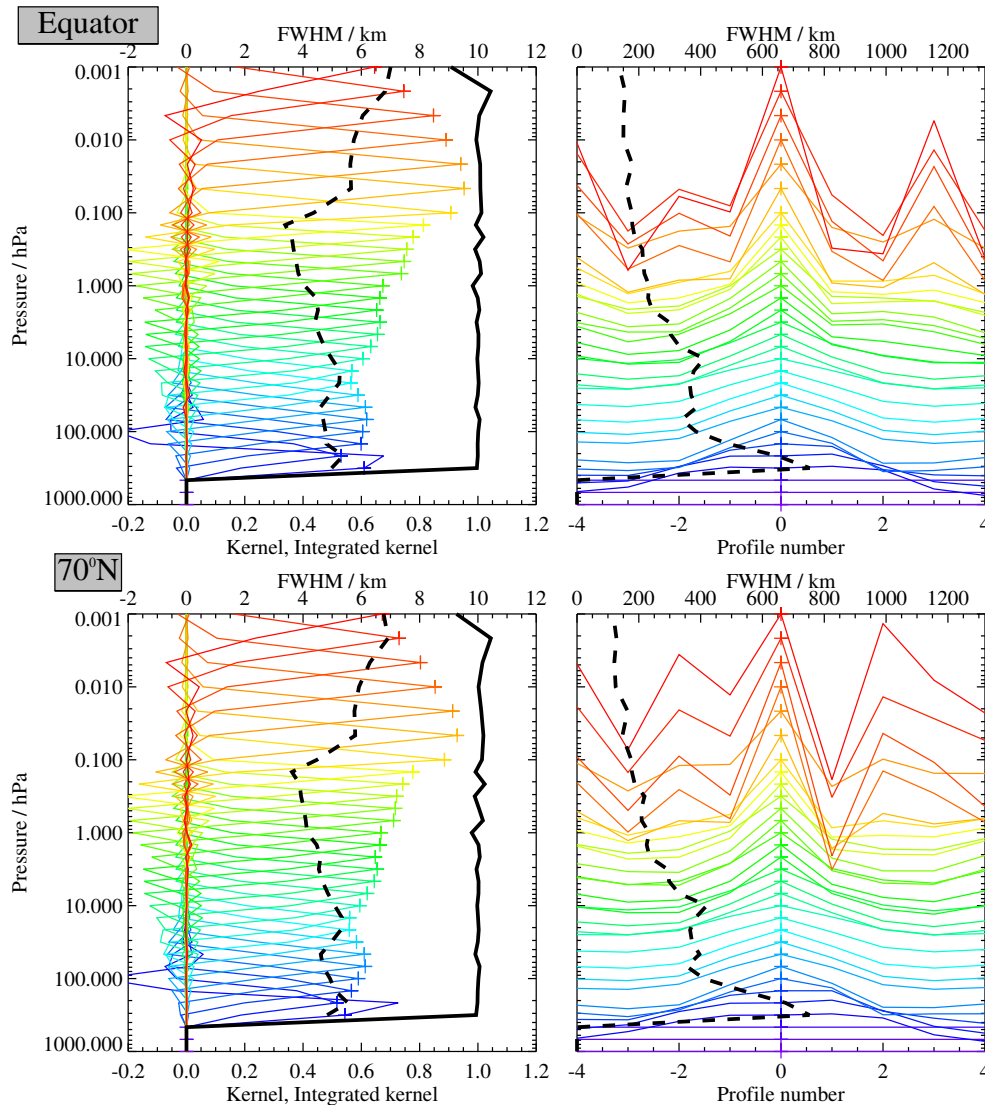


**Figure 3.7.2:** Typical two-dimensional (vertical and horizontal along-track) averaging kernels for the MLS v4.2x CO data at the equator (upper) and at 70°N (lower); variation in the averaging kernels is sufficiently small that these are representative of typical profiles. Colored lines show the averaging kernels as a function of MLS retrieval level, indicating the region of the atmosphere from which information is contributing to the measurements on the individual retrieval surfaces, which are denoted by plus signs in corresponding colors. The dashed black line indicates the resolution, determined from the full width at half maximum (FWHM) of the averaging kernels, approximately scaled into kilometers (top axes). (Left) Vertical averaging kernels (integrated in the horizontal dimension for five along-track profiles) and resolution. The solid black line shows the integrated area under each kernel (horizontally and vertically); values near unity imply that the majority of information for that MLS data point has come from the measurements, whereas lower values imply substantial contributions from a priori information. (Right) Horizontal averaging kernels (integrated in the vertical dimension) and resolution. The horizontal averaging kernels are shown scaled such that a unit averaging kernel amplitude is equivalent to a factor of 10 change in pressure.

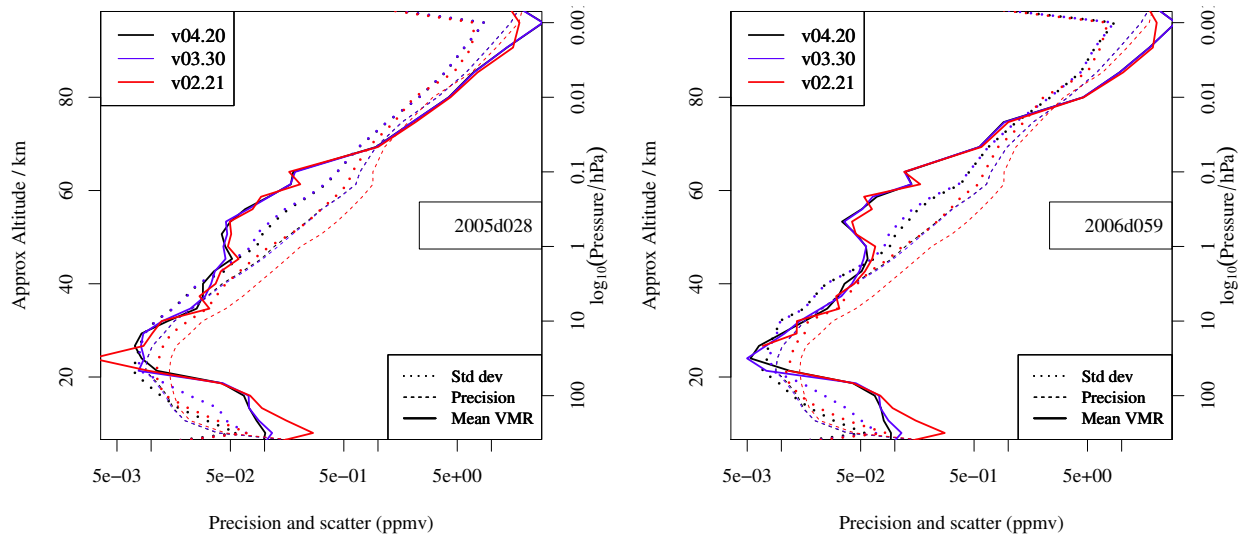


**Figure 3.7.3:** Scatter (standard deviation) and (estimated) precision for MLS v4.2x (black), /prevvShalsh (blue) and v2.2 (red) CO. The statistics shown are generated from all profiles within  $20^\circ$  of the equator on 28 January 2005 and 28 February 2006. Profiles of the mean volume mixing ratio (VMR) are shown for comparison. The vertical co-ordinate is  $16(3 - \log_{10}(\text{Pressure}/\text{hPa}))$  so that 16 km on the axis is exactly 100 hPa.

scatter observed in the data in regions of low natural variability. Where the estimated precision is greater than 50% of the a priori precision the data will be influenced by the a priori to an undesirably large extent. In such cases,  $L2gpPrecision$  is set to be negative (or zero in some cases) to indicate that the data should not be used. Figure 3.7.3 shows both the scatter and estimated precision for CO, with typical profiles for comparison. Note that the random errors are larger than 100% of the mixing ratio for much of the vertical range, meaning that significant averaging (e.g., daily zonal mean or weekly map) is needed to make use of the data.

### 3.7.5 Accuracy

The estimated accuracy is summarized in Table 3.7.1. In the middle atmosphere the accuracies are estimated by comparisons with the ACE-FTS instrument; see *Pumphrey et al.* [2007] for further details. The MLS v2.2 CO data at 215 hPa showed high (factor of  $\sim 2$ ) biases compared to other observations. The morphology, however, was generally realistic [*Livesey et al.*, 2008]. In v4.2x (as in v3.3x/v3.4x) this bias has been essentially eliminated through a change in the approach to modeling the background radiance upon which the CO spectral line sits, and a small reduction in the number of MLS spectral channels considered in the retrieval. Tropospheric (215 – 100 hPa) accuracies in Table 3.7.1 are  $2-\sigma$  estimates obtained by propagating parameter uncertainties through a model of the measurement system.

### 3.7.6 Data screening

**Pressure range:** 215 – 0.0046 hPa.

Values outside this range are not recommended for scientific use.

**Estimated precision:** Only use values for which the estimated precision is a positive number.

Values where the *a priori* information has a strong influence are flagged with negative or zero precision, and should not be used in scientific analyses (see Section 1.5).

**Status flag:** Only use profiles for which the **Status** field is an even number.

Odd values of Status indicate that the profile should not be used in scientific studies. See Section 1.6 for more information on the interpretation of the Status field.

**Clouds:** Clouds have no impact for pressures of 31 hPa or less. v4.2x is much less susceptible to cloud-induced artifacts than was v03.x, so screening of the CO product is considerably simplified, needing only application of the standard Quality and Convergence rules as described below.

**Quality: Only use profiles with Quality greater than 1.5.**

Profiles with Quality less than or equal to 1.5 comprise 0.7% of all data, and ~2% of profiles in the tropics. At 215 hPa in the tropics, the rejected profiles have mixing ratios that are, on average, 7% higher than other tropical values and the occurrence rates of high outliers with mixing ratios greater than 150 ppbv is about twice that of the rest of the tropical ensemble. At 100 hPa there is no significant difference in the means of tropical profiles with Quality less than or greater than 1.5.

**Convergence: Only profiles whose Convergence field is less than 1.03 should be used.**

This Convergence criterion rejects fewer than 0.1% of profiles. Almost all of the retrievals in the phase that produces v4.2x CO converge to their target, so Convergence is of limited use in screening.

### 3.7.7 Artifacts

- Positive systematic error of 20 – 50% throughout the mesosphere.
- Negative systematic error of 50 – 70% near 30 hPa.
- Retrieved profiles are rather jagged, especially between 1 hPa (48 km) and 0.1 hPa (64 km). The greater smoothing applied in v4.2x (and v3.3x/v3.4x) compared to v2.2 has reduced this problem considerably but has not eliminated it entirely.
- There is a tendency for negative values to occur at the level below a large positive value. The most striking examples occur in the polar vortex, where air with high CO mixing ratios descends to the mid-stratosphere. This problem is slightly worse in v4.2x and v3.3x/v3.4x than in v2.2 – this was considered an acceptable trade-off for the less jagged profiles obtained over most of the middle atmosphere.
- Upper-tropospheric v4.2x CO retrieved values still show some anomalous sensitivity to thick clouds associated with deep convection. The screening procedure based upon Quality and Convergence that is described above is generally effective in removing these artifacts.

### 3.7.8 Review of comparisons with other datasets

In the upper troposphere, comparisons with various in situ CO observations (NASA DC-8, WB-57 and the MOZAIC dataset) indicate that the *earlier* MLS v2.2 215 hPa CO product was biased high by a factor of ~2. As in v3.3x and v3.4x, this is largely eliminated in v4.2x.

In the mesosphere, comparisons of the earlier v2.2 MLS CO with ODIN-SMR and ACE-FTS suggest a positive bias: 30% – 50% against ACE-FTS, 50% – 100% against SMR. Near 31 hPa, the MLS values are lower than SMR and ACE-FTS by at least 70%. The MLS values have not changed much between v2.2 and v4.2x in the middle atmosphere, so these comparisons may mostly be considered valid for v4.2x. What change there was between v2.2 and later versions consists of a slight lowering of the MLS values, bringing them slightly towards the ACE-FTS data; 20% is now a better estimate of the MLS-ACE bias in much of the middle atmosphere (compared to 30% with v2.2). The difference between v3.3x/v3.4x and v4.2x in the mesosphere is small.

Table 3.7.1: Data quality summary for MLS v4.2x CO.

Pressure / hPa	Resolution / km Vert × Horiz.	Precision / ppbv	Accuracy	Comment
< 0.001	—	—	—	Not retrieved
0.0022-0.001	—	—	—	Unsuitable for scientific use
0.0046	6.2 × 200	6000	+20% to +50%	
0.01	5.9 × 200	3400	+20% to +50%	
0.046	5.9 × 200	1000	+20% to +50%	
0.14	3.8 × 200	640	+20% to +50%	
1	4.1 × 250	120	+20% to +50%	
10	5.0 × 440	16	±10%	
31	4.9 × 400	9	-70% to -50%	
100	4.9 × 450	14	±19 ppbv and ±30% <sup>a</sup>	
147	5.1 × 570	16	±26 ppbv and ±30%	
215	5.4 × 690	19	±38 ppbv and ±30%	
316	—	—	—	Unsuitable for scientific use
>316	—	—	—	Not retrieved

<sup>a</sup>Estimated 215–100 hPa systematic uncertainty is the RSS of the additive and multiplicative terms.

Help	
Overview	
Table	
BrO	S
CH <sub>3</sub> Cl	S
CH <sub>3</sub> CN	S
CH <sub>3</sub> OH	S
ClO	S
CO	S
GPH	S
H <sub>2</sub> O	S
HCl	S
HCN	S
HNO <sub>3</sub>	S
HO <sub>2</sub>	S
HOCl	S
IWC	S
IWP	S
N <sub>2</sub> O	S
O <sub>3</sub>	S
OH	S
RHI	S
SO <sub>2</sub>	S

## 3.8 Geopotential Height (GPH)

**Swath name:** GPH

**Useful range:** 261 – 0.001 hPa

**Contact:** Michael J. Schwartz, **Email:** <Michael.J.Schwartz@jpl.nasa.gov>

### 3.8.1 Introduction

Geopotential height (GPH) is retrieved, along with temperature and the related assignment of tangent pressures to limb views, primarily from bands near O<sub>2</sub> spectral lines at 118-GHz and 234 GHz. The v4.2x GPH product is generally similar to both the v03.x product and to the v02.2 product that is described in *Schwartz et al.* [2008].

The heights of surfaces of constant geopotential are a property of the Earth’s gravitational field and do not depend upon atmospheric conditions. Geopotential differences between surfaces are equal to the integral with height of the gravitational acceleration,  $g$ . GPH is geopotential difference from the Earth’s surface geopotential to a given location, scaled by the mean-sealevel gravitational acceleration,  $g_0$ , to give units of height.

MLS products, including GPH and temperature, are reported on pressure surfaces, but pressure, temperature and height depend upon one another through assumed hydrostatic balance and the gas law.

$$\frac{1}{g_0} \int g \, dh = \frac{R}{Mg_0} \int T \, dP/P, \quad (3.1)$$

where  $M$  is the molar mass of air and  $R$  is the gas constant.

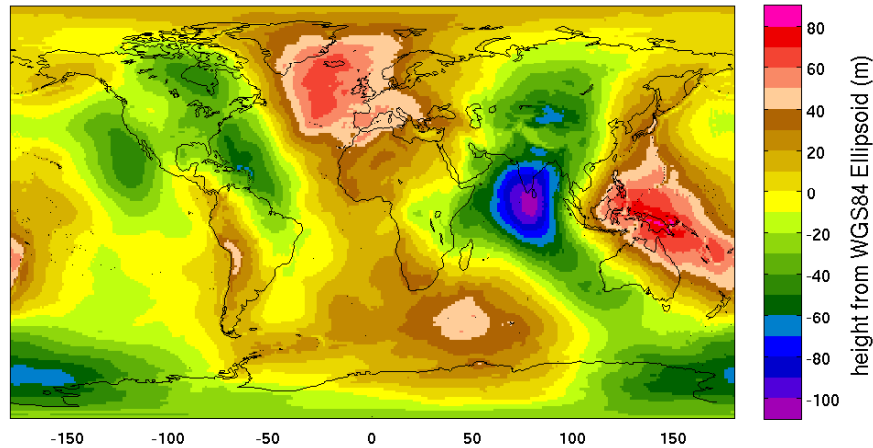
Thus a retrieval of a temperature profile on fixed pressure surfaces also determines GPH differences between those surfaces, and so determines the GPH profile to within an additive constant. Absolute pointing cannot be inferred from radiometric information and must be obtained, for each profile, from the spacecraft orbit/attitude system and the instrument scan model. By convention, this additional degree of freedom is taken to be the height of the 100-hPa reference level, but this choice is arbitrary, as the reference is an additive offset to the entire profile.

Table 3.8.1 summarizes v4.2x measurement precision, modeled accuracy and observed biases. The following sections provide details.

### 3.8.2 Differences between v4.2x and previous versions

The v4.2x GPH product is taken from the CorePlusR3 retrieval phase along with a number of standard products that depend upon radiances of the 240-GHz radiometer. The previously released v02.2x and v03.x GPH products were taken from a preliminary “Core” retrieval phase. Since these GPH profiles are retrieved simultaneously with the CorePlusR3 products and are assumed in the CorePlusR2 and CorePlusR4 retrievals, GPH and the retrieved constituents should be, in some sense, more internally consistent than they were in previous versions.

These previous versions of MLS GPH were referenced to the WGS84 ellipsoid, a simple model of the Earth’s surface but not a surface of constant geopotential. v4.2x uses a surface of constant geopotential, the Earth Gravitational Model 1996 (EGM96) geoid, as its zero GPH surface. The magnitude of the static, latitude/longitude-dependent difference between the geoid and ellipsoid exceeds  $\pm 100$  m in places, as is shown in Figure 3.8.1. This EGM96-WGS84 difference is a bias that should be subtracted from previous versions’ GPH before they are compared to v4.2x GPH. These differences, if not corrected, will result in an erroneous additive contribution to geostrophic winds calculated from v03.x and v02.x GPH at all levels.



**Figure 3.8.1:** The height of the EGM96 geoid from the WGS84 ellipsoid. These values should be subtracted from MLS v03.x and earlier GPH values to give geopotential heights referenced to the Earth's mean sea level geopotential. v4.2x GPH does not include this bias term.

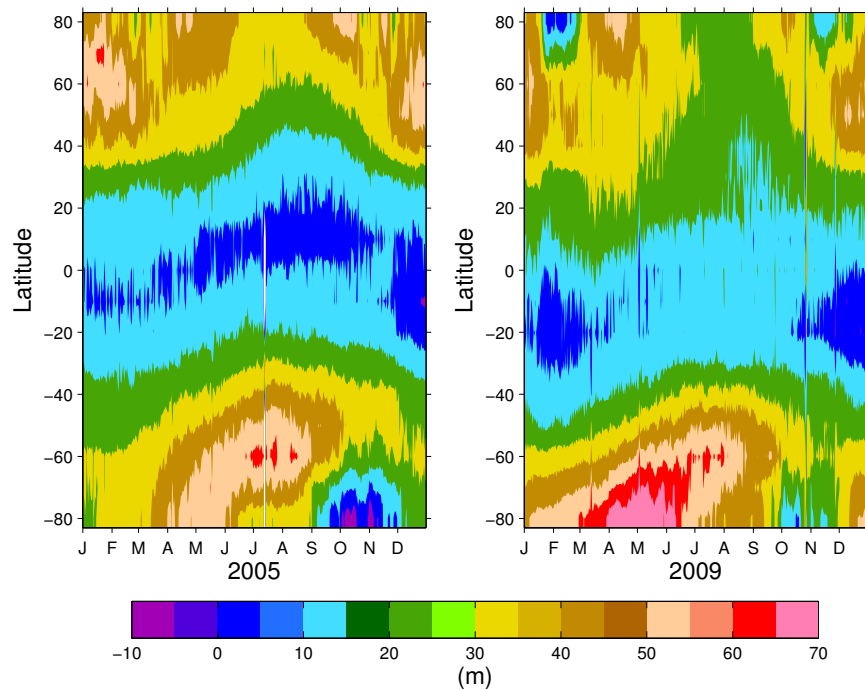


**Figure 3.8.2:** Differences between v4.2x and ellipsoid-referenced v03.30 100-hPa GPH for 2005 and 2009 are shown as functions of latitude and day of year.

After correction of v03.3x for the EGM96-WGS84 bias, v4.2x GPH values are found to be somewhat higher at high latitudes than are those of the v03.3x product, with typical 100-hPa mean differences of 50 m in the high northern latitudes, 30 m in high southern latitudes and close to zero bias in the tropics. Latitudinally and seasonally dependent differences between v4.2x and ellipsoid-referenced v3.3x/v3.4x 100-hPa GPH are shown in Figure 3.8.2 for the years 2005 and 2009. These differences are very similar for ascending and descending parts of the orbits, and the two are averaged in this figure. The details of these differences vary between years, but the morphology is similar.

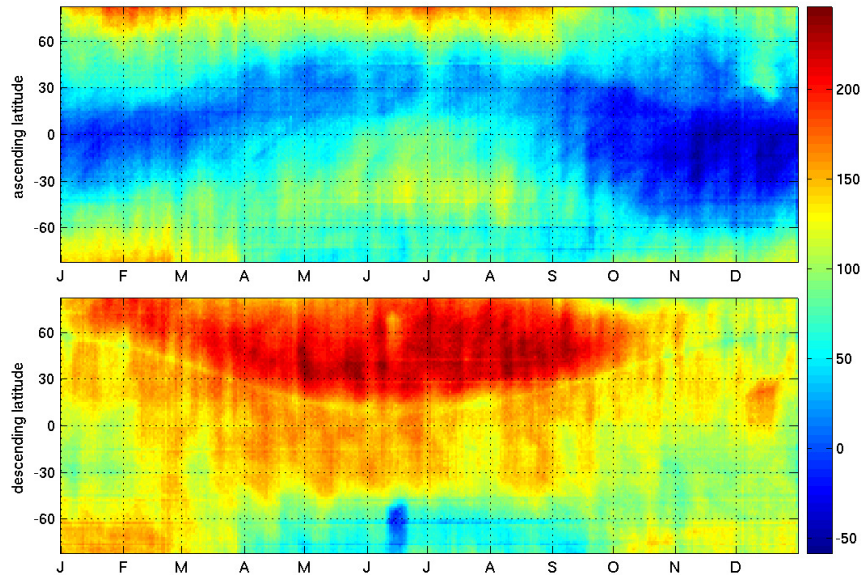


**Figure 3.8.3:** Annually-repeating biases between MLS 100-hPa GPH and GEOS-5.2 100-hPa GPH as functions of ascending and descending latitude and of day of year. These biases were computed based upon data from the years 2005–2012.

### 3.8.3 Comparison to GEOS-5 Analysis

After removal of the geoid correction from v03.3x GPH, there remains a latitudinally and seasonally-varying bias between MLS and GEOS-5 that is also present in v4.2x GPH. Figure 3.8.3 shows this pattern in the difference between geoid-corrected v03.3x and GEOS-5 100-hPa GPH. This pattern is very similar in v4.2x.

Some of this annually-repeating “bias” may result from annually-repeating geophysical information captured by MLS that is not in the GEOS-5 analysis. However, the large ascending-descending differences are almost certainly not primarily diurnal effects. The fidelity with which these patterns annually repeat suggests that they may result from thermal distortions of the spacecraft/instrument that vary annually due to the eccentricity of the Earth’s orbit, or perhaps from orbit/attitude errors from the star trackers that provide the spacecraft-attitude information. The same star fields are viewed each year at the same date and orbit position.

Figure 3.8.4 shows daily-binned differences between v4.2x and GEOS-5.9 100-hPa GPH as functions of orbital position. The patterns are extremely similar in the two years and to the annually repeating v3.3x and v3.4x residual shown in Figure 3.8.3, but 2009 is ~80 m lower than 2005 due to a decreasing trend in MLS v4.2x GPH.

The monthly-averaged differences between MLS v4.2x 100-hPa GPH and GEOS-5.9 100-hPa GPH for 11 years of Januarys are shown in Figure 3.8.5. There is a clear downward trend of ~100 m in the first 4 years of the mission, 2005–2008, with a further ~15 m decrease in 2009–2014. This trend is in the MLS GPH and is not evident in the GEOS-5.9 time series. Analysis of v3.3x and v3.4x GPH, for which the entire MLS record has been processed, shows the same global decreasing trend. It is important to emphasize that MLS radiances do not provide absolute pointing information, but only GPH differences between pointing. Absolute pointing comes from spacecraft ephemeris and attitude data and the instrument scan model. The origins of the trend is a topic of current research, but it is likely not primarily of geophysical origin.

When both the trend and the annually repeating bias are removed from v3.3x and v3.4x, the standard deviation of the residual differences between the bias-corrected MLS and GEOS-5 100-hPa GPH is on the order of 20 m, and a similar result is expected for v4.2x.

The last four profiles of each day show increased rates of outliers relative to GEOS-5 temperature, compared to other profile positions in the day in version 4.20 (fixed in version 4.22). These outliers can be as large



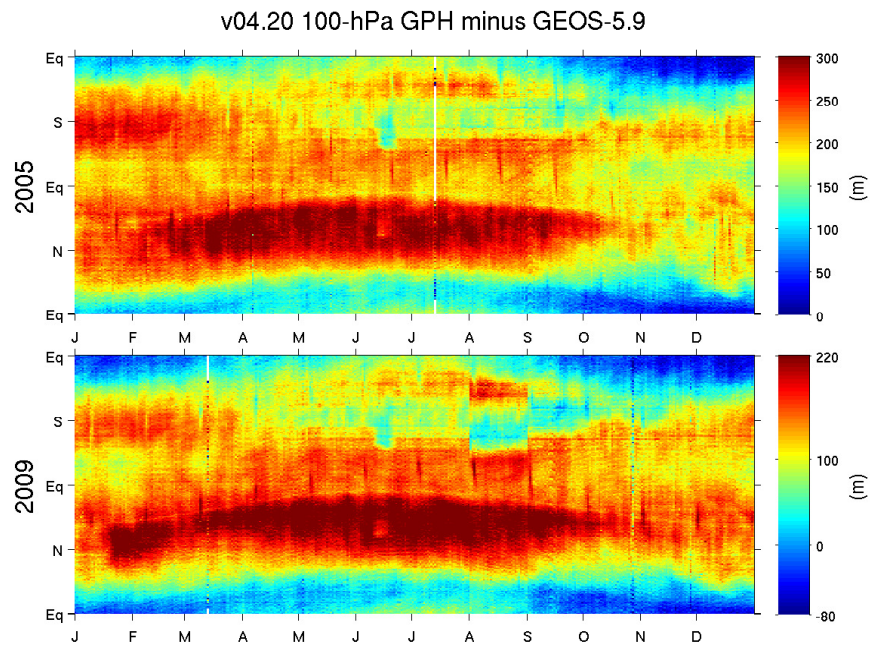


**Figure 3.8.4:** Daily-binned differences between v4.2x and GEOS-5.9 100-hPa GPH as functions of orbital position. Orbital position, from the bottom of each panel, ascends from the equator to the northern terminator, descends through the equator to the southern terminator and then ascends to the equator.

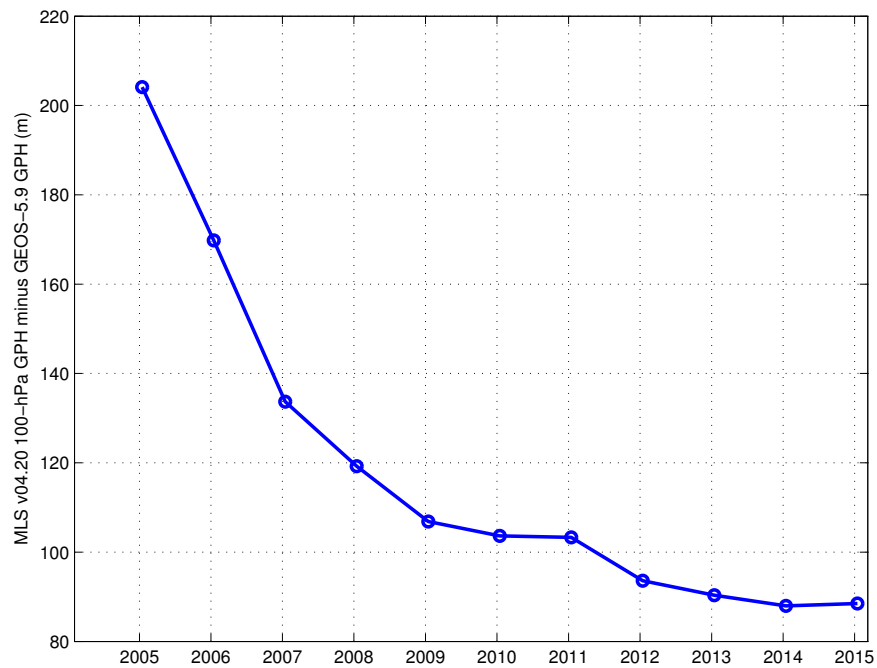


**Figure 3.8.5:** January monthly-binned differences between v4.2x and GEOS-5.9 100-hPa GPH.

- Help
- Overview
- Table
- S
- BrO
- S
- CH<sub>3</sub>Cl
- T
- S
- CH<sub>3</sub>CN
- S
- CH<sub>3</sub>OH
- T
- S
- ClO
- T
- S
- CO
- T
- GPH**
- S
- H<sub>2</sub>O
- T
- S
- HCl
- T
- S
- HCN
- T
- S
- HNO<sub>3</sub>
- T
- S
- HO<sub>2</sub>
- T
- S
- HOCl
- T
- S
- IWC
- T
- S
- IWP
- T
- S
- N<sub>2</sub>O
- T
- S
- O<sub>3</sub>
- T
- S
- OH
- T
- S
- RHI
- T
- S
- SO<sub>2</sub>
- T
- S
- T

as 50 K at at some levels. A recommendation to discard the last 4 profiles of each day for both temperature and GPH (as well as RHI) has been added to recommended screening for v4.20 (not needed for v4.22).

### 3.8.4 Vertical resolution

The GPH profile is vertically-integrated temperature, so its vertical resolution is not well-defined. The vertical resolution of the underlying temperature given in Section 3.22 is repeated in Table 3.8.1.

### 3.8.5 Precision

MLS v4.2x GPH precision is summarized in Table 3.8.1. Precision is the random component of measurements that will average-down if a measurement is repeated. The retrieval algorithms produce an estimate of GPH precision only for the 100 hPa reference level, as this is the only element included in the MLS “state vector.” Precisions reported for this level in the L2GP files are typically less than 8 m, are believed to be optimistically small, and may underestimate the impact of scatter in the absolute pointing information. A precision of 20 m is reported for 100 hPa in Table 3.8.1, column 2. GPH precisions at other standard-product profile levels (summarized in column 2 of Table 3.8.1) are calculated from the GPH precision at the reference level and the profile of temperature precisions, but values in the table are inflated somewhat from those in the L2GP files in the troposphere and stratosphere. Estimated precisions remain at 20 – 25 m up to 1 hPa and degrade to 110 m at 0.01 hPa. Off-diagonal elements of the temperature/GPH error covariance matrix are neglected in this GPH-precision-profile calculation, but resulting errors are believed to be small (~5 m near 100 hPa.)

### 3.8.6 Accuracy

The accuracy of the v2.2 GPH was modeled based upon consideration of a variety of sources of systematic error, as discussed in *Schwartz et al.* [2008]. v4.2x accuracy is believed to be substantially similar and the results of the v2.2 calculations are given in column four of Table 3.8.1. Of the error sources considered, modeled amplifier non-linearity had the largest impact, just as is the case with the calculation for temperature.

The second terms in column four are model-based estimates of the bias magnitude from other sources including uncertainty in pointing/field-of-view, uncertainty in spectroscopic parameters, and retrieval numerics. The combined bias magnitudes due to these sources is 100 – 150 m.

“Observed bias uncertainty” in Table 3.8.1 is an estimate of bias based upon comparisons with analyses and with other previously-validated satellite-based measurements. These comparisons were made using MLS v2.2, but as the biases between v2.2 and v4.2x GPH are generally less than 50 m from 261 – 0.1 hPa and reasonably constant, these results hold for v4.2x as well. The primary sources of correlative data were the Goddard Earth Observing System, Version 5.0.1 data assimilation system (GEOS-5) [*Rienecker et al.*, 2007], used in the troposphere and lower stratosphere, and the Sounding of the Atmosphere using Broadband Radiometry (SABER) [*Mlynczak and Russell*, 1995], used in the upper stratosphere through the mesosphere. MLS has a 150 m high bias relative to analyses (GEOS-5) at 100-hPa that drops to 100 m at 1 hPa. Biases with respect to SABER are small at 0.1 hPa but increasingly negative at higher levels, reaching -600 m at 0.001 hPa, but with significant latitudinal and seasonal variability.

### 3.8.7 Known Artifacts

To maintain its position in the “A-Train” constellation of satellites, the Aura spacecraft periodically executes “inclination adjustment maneuvers” (IAMs) involving large changes in spacecraft yaw and firing of thrusters. There were 39 such maneuvers in the first 10 years of operation. Large systematic errors in spacecraft reported attitude have been found in the first orbit that follows the return to nominally good attitude data after these maneuvers, apparently due to the ringing of a Kalman filter in the attitude measurement system. Since MLS GPH relies on spacecraft attitude for its absolute reference, these attitude errors result in large systematic errors in GPH, typically reaching +3500 m in the first eighth of the orbit and -30 m in the second quarter orbit after the nominal “end of maneuver”. The large positive errors almost always occur on ascending orbits

from near Australia, crossing the Indian Ocean and, at ~3500 m amplitude, are large enough to significantly bias even long-term averages. A file of start and stop times for data to be avoided is maintained on the MLS website: <https://mls.jpl.nasa.gov/cal/issues.txt>.

### 3.8.8 Data screening

GPH should be screened in much the same way as is temperature:

**Pressure range:** 261 – 0.001 hPa.

Values outside this range are not recommended for scientific use.

**Estimated precision:** Only use values for which the estimated precision is a positive number.

Values where the *a priori* information has a strong influence are flagged with negative or zero precision, and should not be used in scientific analyses (see Section 1.5). GPH precision is set negative at and beyond any level in the integration of temperature away from the 100-hPa reference level where temperature has negative precision.

**Status flag:** Only use profiles for which the **Status** field is an even number.

Odd values of Status indicate that the profile should not be used in scientific studies. See Section 1.6 for more information on the interpretation of the Status field.

**Clouds:** Thick clouds are believed have some impact on v4.2x GPH measurements in the upper troposphere (261 – 100 hPa). Tropospheric GPH may be screened using the ice water content (IWC) product, rejecting profiles between 261–100 hPa for which the 215 hPa value of IWC is greater than 0.005 mg/m<sup>3</sup>.

**Quality:** Only use profiles with Quality greater than 0.2 for the 83 hPa level and smaller pressures, and profiles with Quality greater than 0.9 at larger pressures of 100 hPa and larger.

**Convergence:** Only profiles whose **Convergence** field is less than 1.03 should be used.

Use of this threshold typically discards less than 0.1% of profiles and is primarily a safeguard against profiles with extremely poor convergence.

**End of day (v4.20 only):** The last four profiles of each day show greatly increased rates of large temperature departure from *a priori*. Accordingly the last four profiles of the GPH product each day should not be used. Note that this issue was fixed in v4.22.

**IAMs:** Large errors in reported spacecraft attitude have been found following the spacecraft inclination adjustment maneuvers that occur ~4 times per year. A file of times at which GPH should not be used is maintained on the MLS website: <https://mls.jpl.nasa.gov/cal/issues.txt>.

### 3.8.9 Desired improvements for future data version(s)

Reduction of seasonally and latitudinally-repeating systematic errors in GPH that may be the result of errors in the absolute pointing information from the spacecraft attitude and ephemeris data stream is an area of ongoing research. Understanding the decreasing trend in MLS global mean GPH, particularly in the first four years of the mission is an area of active research.

Table 3.8.1: Summary of MLS GPH product.

Region	Resolution Vert. × Horiz. / km	Precision <sup>a</sup> / meters	Observed accuracy / m	Comments
<0.001 hPa	—	—	—	Unsuitable for scientific use
0.001 hPa	10–13 × 220	±160	–450	
0.01 hPa	8–12 × 185	±110	–100	
0.1 hPa	6 × 165	±45	0	
1 hPa	7 × 165	±25	100	
10 hPa	4.3 × 165	±20	100	
100 hPa	5.2 × 165	±20	150	
261 hPa	5.3 × 170	±20	150	
1000 – 316 hPa	—	—	—	Unsuitable for scientific use

<sup>a</sup>Precision on individual profiles

Help	
Overview	
Table	
BrO	S
CH <sub>3</sub> Cl	S
CH <sub>3</sub> CN	T
CH <sub>3</sub> OH	S
ClO	S
CO	T
GPH	S
H <sub>2</sub> O	T
HCl	S
HCN	T
HNO <sub>3</sub>	S
HO <sub>2</sub>	T
HOCl	S
IWC	T
IWP	S
N <sub>2</sub> O	T
O <sub>3</sub>	S
OH	T
RHI	S
SO <sub>2</sub>	T
	S
	T

## 3.9 Water Vapor (H<sub>2</sub>O)

**Swath name:** H2O

**Useful range:** 316 – 0.002 hPa

**Contact:** Alyn Lambert (stratosphere/mesosphere), **Email:** <alyn.lambert@jpl.nasa.gov>  
William Read (troposphere), **Email:** <william.g.read@jpl.nasa.gov>

### 3.9.1 Introduction

The standard water vapor product is taken from the 190-GHz “CorePlusR2” retrieval. The vertical grid for H<sub>2</sub>O is: 12 levels per decade change in pressure (LPD) for 1000 – 1 hPa, 6 LPD for 1.0 – 0.1 hPa, and 3 LPD for 0.1 – 10<sup>-5</sup> hPa. The horizontal grid is every 1.5° along the orbit track. H<sub>2</sub>O is unusual among MLS products in that it is assumed that the logarithm of the mixing ratio, and not mixing ratio itself, varies linearly with log pressure; although, H<sub>2</sub>O, like the other MLS constituents is retrieved in VMR (not log VMR). Vertical and horizontal interpolations of H<sub>2</sub>O should be performed in log(VMR) space.

The MLS v4.2x H<sub>2</sub>O between 1000 and 383 hPa is taken from a retrieval of relative humidity with respect to ice (RHi) product, converted to specific humidity using the Goff-Gratch vapor pressure over ice equation. This RHi retrieval is not vertically resolved, and all levels between 1000 and 383 hPa are assumed to have the same RHi. See Section 3.20 for more information. Validation of MLS v2.2 water vapor is presented in *Read et al.* [2007] and *Lambert et al.* [2007]. This section reiterates the key information from those studies, and updates them for v4.2x. Table 3.9.1 gives a summary of MLS v4.2x H<sub>2</sub>O precision, resolution, and accuracy.

### 3.9.2 Changes from v3.3x and v3.4x

The main H<sub>2</sub>O differences between v4.2x and v3.3x/v3.4x relate to cloud screening and improvements in the “Ini tUTH” initial upper tropospheric and lower stratospheric humidity estimation phase that produces the first guess and sets smoothing constraints on the H<sub>2</sub>O profile retrieved in the final retrieval phase that produces the standard product. There have been no spectroscopy changes either in linewidth or continuum characterization between v4.2x and v3.3x/v3.4x. An improved cloud detection methodology has been developed for v4.2x that does a better job of rejecting cloudy radiances that are likely to cause poor fits and corrupted profiles. The number of erroneous spikes in the upper troposphere has been reduced in v4.2x relative to v3.3x and v3.4x. The Ini tUTH phase retrieves H<sub>2</sub>O on a more coarse 6-LPD grid. The InItUTH H<sub>2</sub>O is used for the initial guess for the final 12-LPD retrieval and sets smoothing constraints for the profile shape instead of smoothing to the shape of a climatological *a priori* profile. The Ini tUTH phase has been expanded to use more channels and better forward model representations to improve its retrieval accuracy. In addition, the retrieval range has been expanded to have its top moved from 100 hPa (in v3.3x and v3.4x) to 10 hPa (in v4.2x), for a more seamless transition from the troposphere to the stratosphere. Simulation studies show that these changes have improved the agreement between the “truth” profiles used to produce the simulated radiances and the retrieved profiles in the 316 – 215-hPa levels.

Figure 3.9.1 compares MLS v4.2x to v3.3x/v3.4x and v2.2. At most levels, the average difference is small – less than 10%. The 316 – 215-hPa levels are 10 – 20% drier in v4.2x than v3.3x and v3.4x. This difference in behavior is replicated in simulation studies where the agreement with truth is better in v4.2x. The extremely low values of the 215-hPa H<sub>2</sub>O at high latitudes seen in previous versions are still present in v4.2x. Unfortunately the high latitude behavior is not replicated in simulation studies and therefore is a systematic error that is not understood.

Humidity data at pressures greater than 316 hPa are derived from a broad layer relative humidity retrieval (using low limb viewing MLS wing channel radiances) similar to that obtained from NOAA operational humidity sounders such as TOVS. As noted in [*Read et al.*, 2007], the v2.2 retrieval at pressures larger than

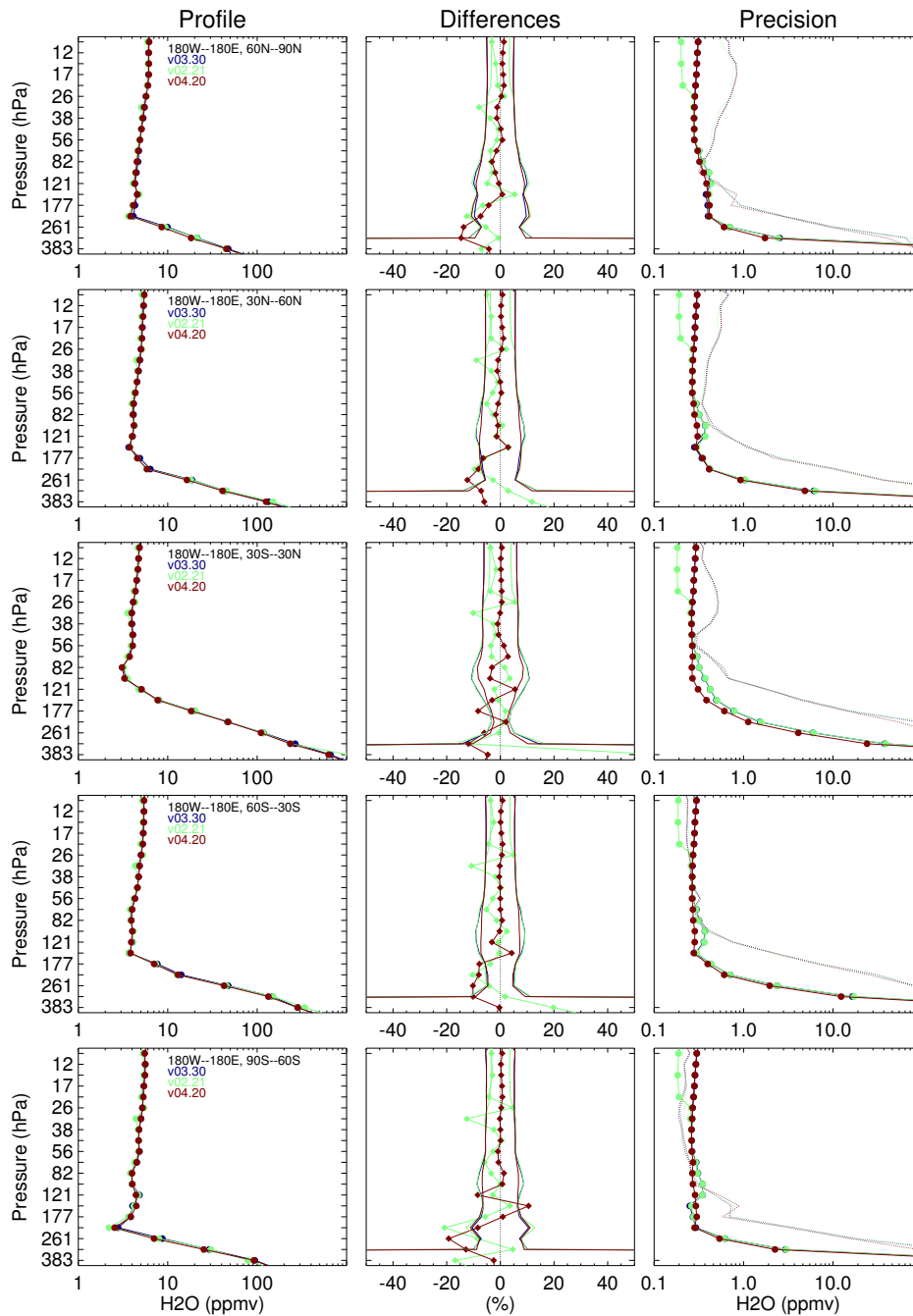


**Figure 3.9.1:** A comparison of v3.3x/v3.4x (blue) to v2.2 (green) and v4.2x (red) water vapor for Jan-Feb-Mar 2005 in 5 latitude bands. Other time periods are similar. The left panel compares mean profiles, the center shows the mean difference (red and green diamonds) surrounded by each version's estimated precision, and the right panel shows the estimated retrieval precision (solid and bullets) and measured variability (dotted) which includes atmospheric variability about the mean profile.

316 hPa was likely to be ~30% too high, based on comparisons with AIRS. The accuracy of this retrieval is highly sensitive to the transmission efficiency of the MLS optics system. In v3.3x and v3.4x the assumed value of the MLS antenna transmission efficiency was adjusted empirically (within the uncertainty range established from MLS calibration) to give better agreement with AIRS in the tropics. In v4.2x the N<sub>2</sub> continuum was adjusted only for this phase to minimize the clear sky cloud induced radiance bias. This retrieval is used as an *a priori* and profile constraint for the humidity profile at pressures greater than 316 hPa, which are not retrieved in the standard H<sub>2</sub>O product retrieval.

The third panel in Figure 3.9.1 shows the mean estimated single profile precision and the measured variability (which includes instrument noise and atmospheric variability). The precisions for v4.2x and v3.3x/v3.4x are nearly identical except for pressures greater than 68 hPa where v4.2x is producing lower values. Version 2 used a more coarse retrieval grid above 22 hPa and a different value of the H<sub>2</sub>O linewidth. Together these account for H<sub>2</sub>O precision differences at these altitudes between v2 and later versions.

Figures 3.9.2 and 3.9.3 show a comparison of H<sub>2</sub>O zonal means from v2, v3, and v4 retrievals for 100 – 2.6 hPa and 2.2 – 0.002-hPa, respectively. Version 4 H<sub>2</sub>O tends to show only minor departures from v3. Version 2 H<sub>2</sub>O shows some vertical oscillatory behavior at some levels that was removed when an improved linewidth was used in v3. The latitude structure tends to be very similar in all cases except at 0.002 hPa for v2.2.

### 3.9.3 Resolution

The spatial resolution is obtained from examination of the averaging kernel matrices shown in Figure 3.9.4. The vertical resolution for H<sub>2</sub>O is in the range 1.3 – 3.6 km from 316 – 0.22 hPa and degrades to 6 – 11 km for pressures lower than 0.22 hPa. The along track horizontal resolution is ~170 – 350 km for pressures greater than 4.6 hPa, and degrades to 400 – 740 km at smaller pressures. The resolutions in Table 3.9.1 are a smoothed average of the equatorial and 70°N values shown in Figure 3.9.4. The horizontal cross-track resolution is 7 km, the width of the MLS 190-GHz field-of-view for all pressures. The longitudinal separation of the MLS measurements is 10° – 20° over middle and lower latitudes, with much finer sampling in polar regions.

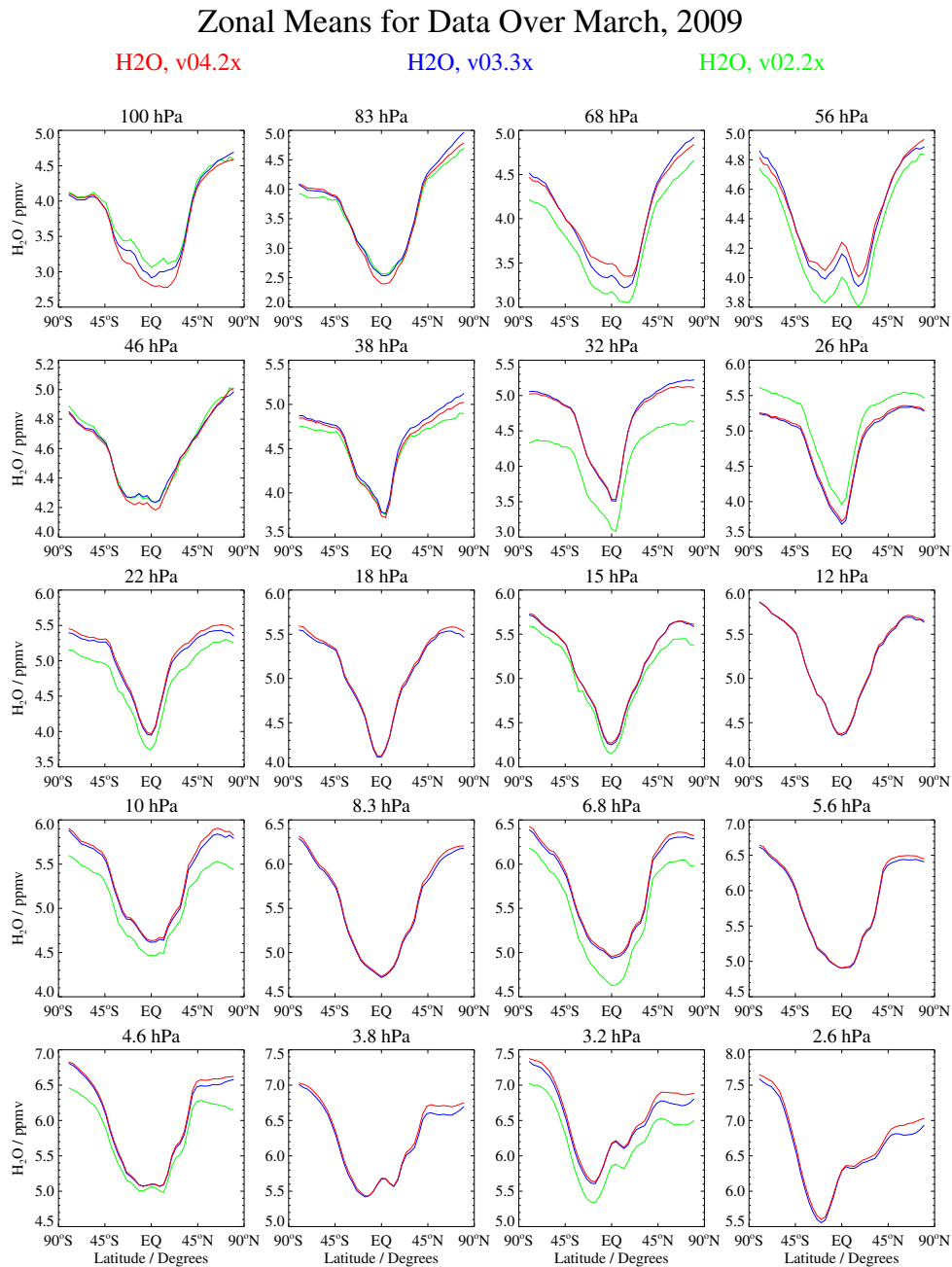
### 3.9.4 Precision

Table 3.9.1 summarizes the estimated precision of the MLS v4.2x H<sub>2</sub>O data. For pressures ≥ 100 hPa, the precisions given are the 1σ scatter about the mean of coincident comparison differences, which are larger than the formal retrieval precisions [Read *et al.*, 2007]. For pressures ≤ 83 hPa the precisions are the 1σ scatter of coincident ascending/descending MLS profile differences [Lambert *et al.*, 2007]. The individual Level 2 precisions are set to negative values or zero in situations when the retrieved precision is larger than 50% of the a priori precision – an indication that the data are biased toward the a priori value.

### 3.9.5 Accuracy

The values for accuracy are based primarily on two sources: comparisons with validated instruments and a full systematic error analysis performed on the MLS measurement system as described (for v2, but the same approach has been used for v4.2x) in Read *et al.* [2007] and Lambert *et al.* [2007]. For pressures between 316 – 178 hPa, comparisons between AIRS v6 and MLS v4.2x show < 20% agreement in the zonal mean (MLS usually drier for low concentrations and wetter for high concentrations) equatorward of 40° with MLS having large dry biases at higher latitudes.

The values in Table 3.9.1 for pressures between 316 and 178 hPa are AIRS validated accuracies which are better than those theoretically possible for the MLS measurement system. For the pressure range 178 – 83 hPa, the quoted values come directly from the systematic error analysis performed on the MLS measurement system. Comparisons between MLS and frost point hygrometers show that, when the tropopause is between 215 and 147 hPa, MLS H<sub>2</sub>O at the tropopause level tends to have a large (20 – 30%) dry biases. Future work to understand this behavior is planned. An estimate of the accuracy between 121 – 83 hPa is also from the



**Figure 3.9.2:** A comparison of v4.2x (red) to v3.3x/v3.4x (blue) and v2.2 (green) water vapor zonal means for March 2009. Each panel represents a pressure as noted above. The pressures shown range from 100 hPa to 2.6 hPa.



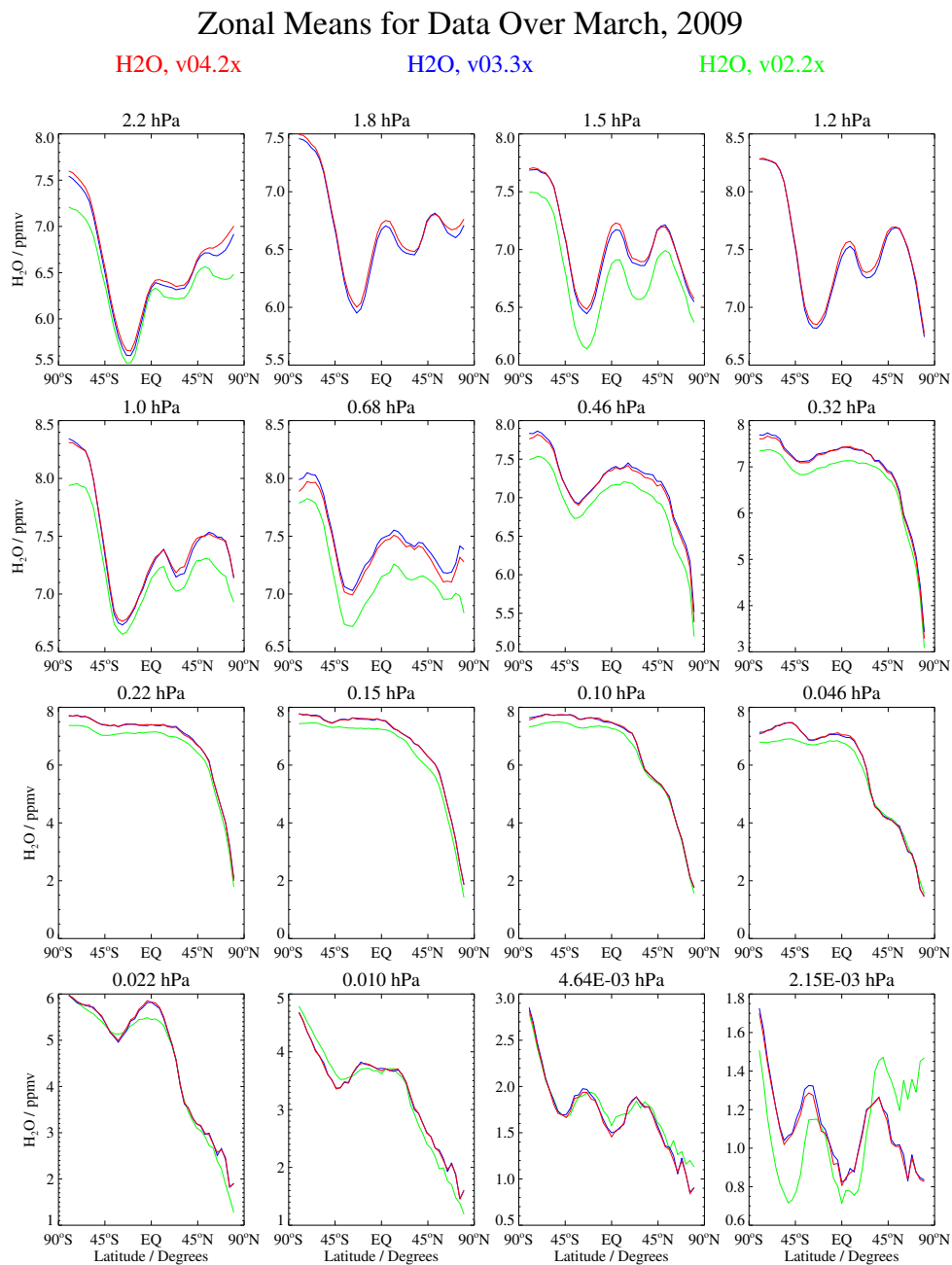


**Figure 3.9.3:** A comparison of v4.2x (red) to v3.3x/v3.4x (blue) and v2.2 (green) water vapor zonal means for March 2009. Each panel represents a pressure as noted above. The pressures shown range from 2.2 hPa to 0.002 hPa.

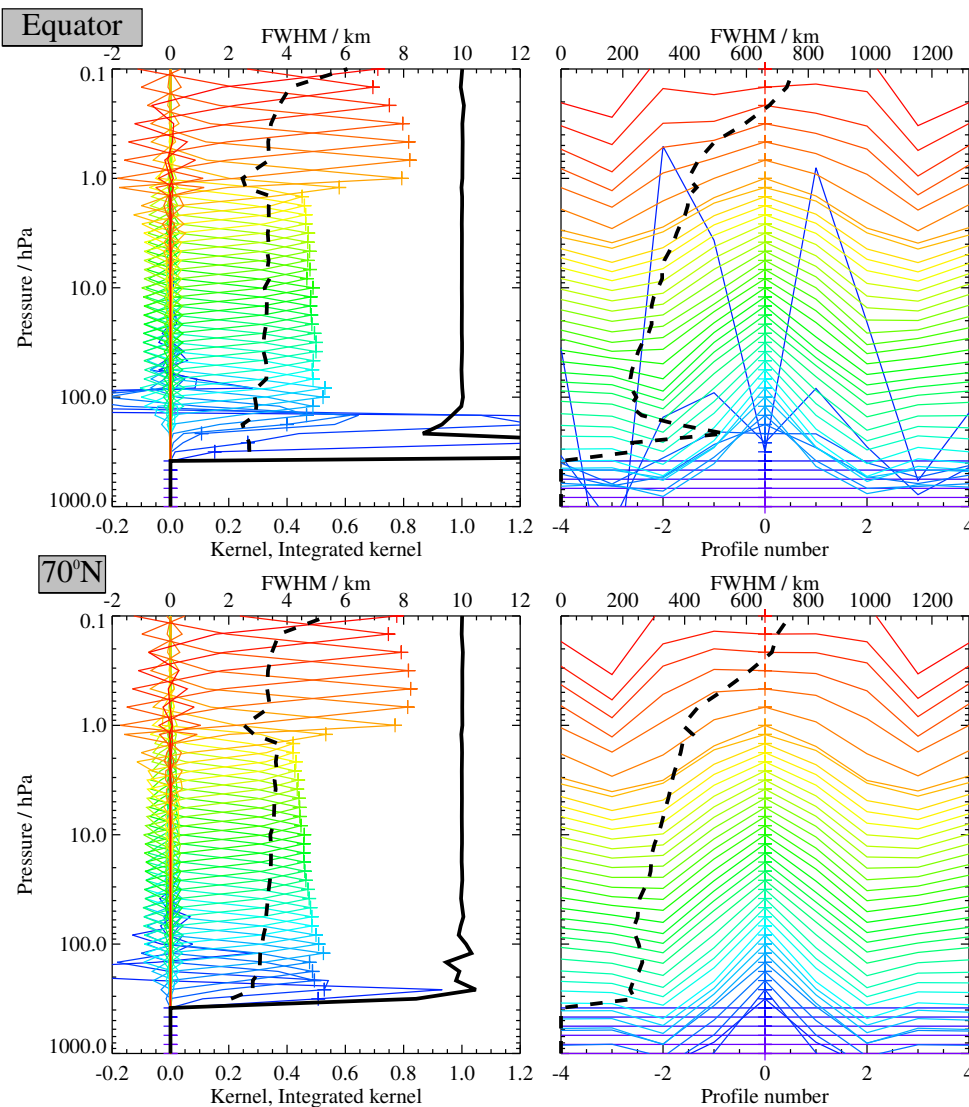


**Figure 3.9.4:** Typical two-dimensional (vertical and horizontal along-track) averaging kernels for the MLS v4.2x H<sub>2</sub>O data at the equator (upper) and at 70°N (lower); variation in the averaging kernels is sufficiently small that these are representative of typical profiles. Colored lines show the averaging kernels as a function of MLS retrieval level, indicating the region of the atmosphere from which information is contributing to the measurements on the individual retrieval surfaces, which are denoted by plus signs in corresponding colors. The dashed black line indicates the resolution, determined from the full width at half maximum (FWHM) of the averaging kernels, approximately scaled into kilometers (top axes). (Left) Vertical averaging kernels (integrated in the horizontal dimension for five along-track profiles) and resolution. The solid black line shows the integrated area under each kernel (horizontally and vertically); values near unity imply that the majority of information for that MLS data point has come from the measurements, whereas lower values imply substantial contributions from a priori information. (Right) Horizontal averaging kernels (integrated in the vertical dimension) and resolution. The horizontal averaging kernels are shown scaled such that a unit averaging kernel amplitude is equivalent to a factor of 10 change in pressure.

systematic error analysis performed on the MLS measurement system. Comparisons among *in situ* sensors on the WB-57 high altitude aircraft and frostpoint hygrometers flown on balloons show 30% disagreements – well in excess of the estimated accuracy of each instrument including MLS – near the tropopause and lower stratosphere. The balloon based frost point hygrometer shows agreement better than indicated in Table 3.9.1. The validation paper describes in detail why a 30% spread is inconsistent with the MLS measurements [Read *et al.*, 2007]. For pressures less than 83 hPa, the accuracy is based on the systematic error analysis.

Please note the discussion of a potential drift in the MLS water vapor measurements discussed below.

### 3.9.6 A note about the water vapor averaging kernels

The averaging kernels are most applicable to linear and moderately non-linear retrieval problems. The MLS H<sub>2</sub>O retrievals are mostly linear, except when the atmosphere approaches opaqueness. This occurs when the limb tangent of the instrument field of view is less than 10 km above the Earth's surface and the atmosphere is moist. In such cases the measurements are very nonlinear and often times the averaging kernel calculations for the lowest retrieved levels are numerically unstable, and unrepresentative of the actual MLS measurement system. This is the case, for example, for the 316-hPa and 262-hPa equatorial kernels shown in Figure 3.9.4. Analysis of simulated MLS observations indicates that application of the averaging kernel provides little benefit to analyses involving the 316-hPa and 262-hPa levels, and accordingly we recommend not applying the (unrepresentative) kernels at those levels.

### 3.9.7 Review of comparisons with other datasets

Figure 3.9.5 shows a latitude-value zonal mean comparison among several satellite data sets. The satellite datasets include MLS v4.2x, AIRS v6, ACE-FTS v3.5, MIPAS IMK v4, HALOE v19, Odin SMR continuum H<sub>2</sub>O, and Odin SMR line resolved H<sub>2</sub>O. ACE-FTS and MLS show the best agreement with each other throughout the full vertical range and over most latitudes. MLS also agrees well with AIRS v6 over the lower latitudes. MLS however does have a significant dry bias at high latitudes which is often a factor of two. MIPAS-IMK at most altitudes and latitudes show similar behavior to MLS except near the cold point tropopause where MLS shows lower values in the tropics whereas MIPAS does not. HALOE is much too dry in the tropics but behaves like MLS for pressures  $\leq 100$  hPa. The Odin SMR continuum product (100–68 hPa) does not agree well with the other satellite based products. The Odin-SMR line resolved product (pressures less than or equal to 46 hPa) usually agrees within 10% of MLS v4 for all heights and latitudes.

One potential improvement in v4.2x is shown in Figures 3.9.6 and 3.9.7 that compare multi-month maps of MLS with AIRS v6. The very moist regions over the tropics in v4 have become a bit drier and in better agreement with AIRS.

Apart from the differences noted above, the MLS v4.2x H<sub>2</sub>O is similar to the MLS v3.3x/v3.4x and MLS v2.2 products, the latter described and validated in Read *et al.* [2007] and Lambert *et al.* [2007]. The H<sub>2</sub>O validation paper used AIRS v4 and MLS v2 humidities and both of them have become more dry in their subsequent versions. A revised validation paper for H<sub>2</sub>O is not planned in the near future and users are encouraged to read Read *et al.* [2007] and Lambert *et al.* [2007] for more information. MLS v4.2x is a part of the second SPARC Water Vapor Assessment (WAVAS-II) activity.

### 3.9.8 Potential drift in lower stratospheric water vapor

Hurst *et al.* [2016] discuss how comparisons between MLS lower stratospheric water vapor observations and those from balloon-borne CFH and FPH<sup>1</sup> instruments from 2004 to 2015 reveal signs of a potential drift between the two sets of measurements, with MLS water vapor increasing at a rate of around 0.03 – 0.07 ppmv yr<sup>-1</sup> relative to the frostpoint sondes (roughly 0.6 to 1.5% per year), starting around 2009. Comparisons with the ACE-FTS instrument, and with measurements of upper stratospheric water vapor from ground-based microwave sensors, provide evidence for a smaller (~+0.2% per year) drift. Investigations by the MLS team have

<sup>1</sup>Cryogenic Frostpoint Hygrometer (CFH) and Frost Point Hygrometer (FPH)

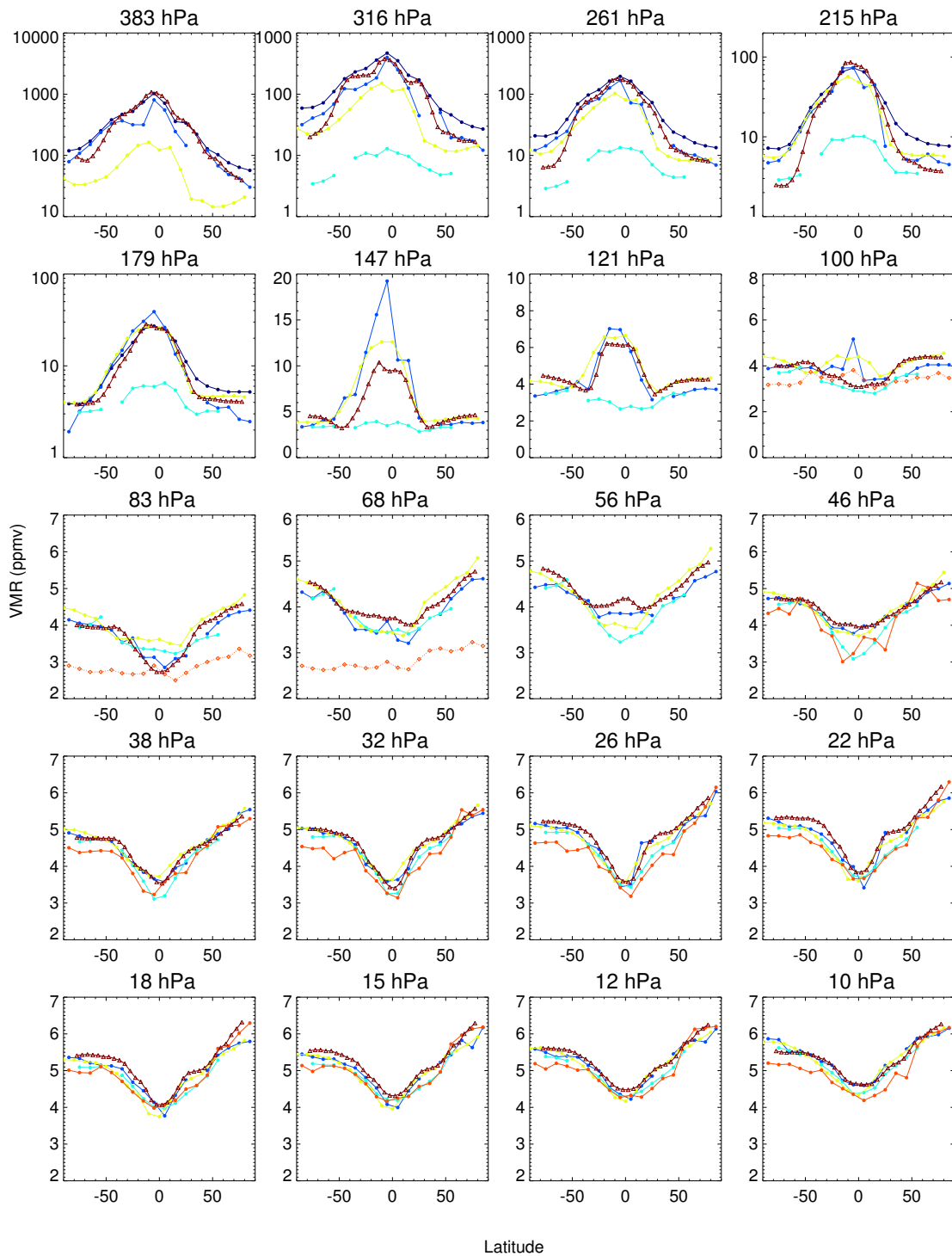


**Figure 3.9.5:** A comparison of MLS v4.2x (red) water vapor for Jan-Feb-Mar 2005 with other satellite observations shown as latitude-value zonal means. Each panel represents a pressure surface. The satellites are: AIRS v6 (dark blue), ACE-FTS v3.5 (light blue), MIPAS IMK v4 (yellow-green), HALOE v19 (cyan), Odin SMR 544 GHz continuum product (orange open diamonds), and Odin SMR line resolved product (orange solid bullets).

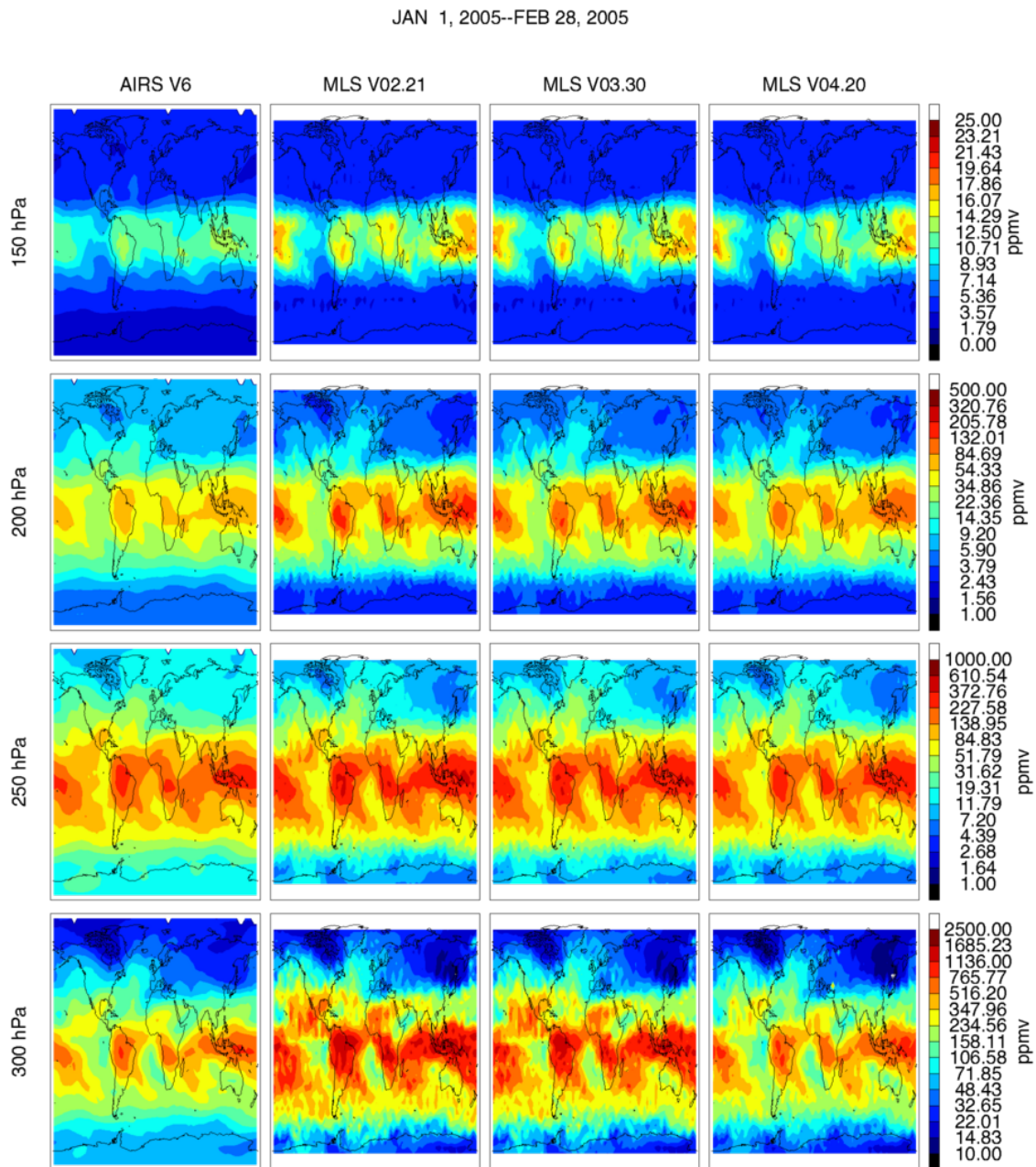


**Figure 3.9.6:** Mapped fields from AIRS v6 (left), MLS v2.2 (center-left), MLS v3.3x/v3.4x (center-right), and MLS v4.2x (right) pressures between 300–150 hPa for January and February 2005. Note that the AIRS measurement is mostly suitable for H<sub>2</sub>O greater than 10 ppmv.

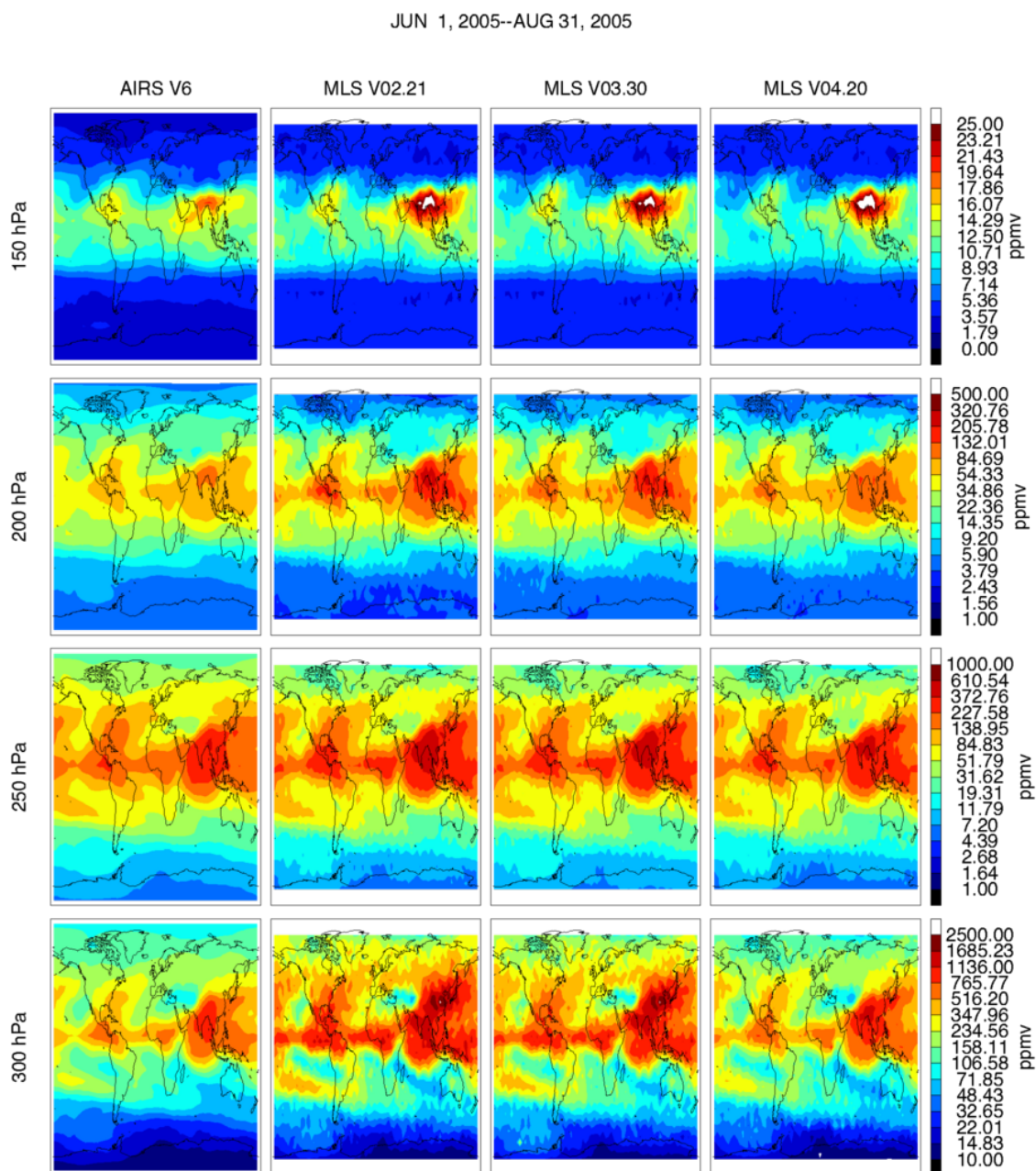


**Figure 3.9.7:** Mapped fields from AIRS v6 (left), MLS v2.2 (center-left), MLS v3.3x/v3.4x (center-right), and MLS v4.2x (right) pressures between 300 – 150 hPa for June through August 2005. Note that the AIRS measurement is mostly suitable for H<sub>2</sub>O greater than 10 ppmv.

indicated that this latter, smaller, drift is consistent with observed changes in instrument performance (correction of which is a goal for future versions of the MLS data processing software). However, these observed instrument changes cannot (at least in our current understanding) account for the larger drift reported by *Hurst et al.*. These issues are under active investigation by the MLS team.

### 3.9.9 Data screening

**Pressure range:** 316 – 0.002 hPa.

Values outside this range are not recommended for scientific use.

**Estimated precision:** Only use values for which the estimated precision is a positive number.

Values where the *a priori* information has a strong influence are flagged with negative or zero precision, and should not be used in scientific analyses (see Section 1.5).

**Status flag:** Only use profiles for which the **Status** field is an even number.

Odd values of Status indicate that the profile should not be used in scientific studies. See Section 1.6 for more information on the interpretation of the Status field.

**Clouds:** Ignore status bit 16 (high cloud) or bit 32 (low cloud) set indicating the presence of clouds. See artifacts for more details.

**Quality field:** Only profiles with a value of the **Quality** greater than 0.7 should be used in scientific studies.

Note that this is a change from the value originally recommended for v4.2x, as described at the end of this subsection. Also, note the “additional screening” information given below.

**Convergence field:** Only profiles with a value of the **Convergence** less than 2.0 should be used in scientific studies.

**Additional screening to avoid outliers:** Even after application of the Status, Quality, and Convergence screening described above, there remain some unphysical profiles in the MLS v4.2x H<sub>2</sub>O dataset. These are characterized by unrealistically low water vapor mixing ratios in the upper troposphere and stratosphere. These should be excluded from analyses by simply neglecting any H<sub>2</sub>O profile where the mixing ratio at any pressure at or larger than 1 hPa (i.e., altitudes below that pressure level) is less than 0.101 ppmv. Note that this additional screening is an additional step beyond those originally recommended for v4.2x H<sub>2</sub>O.

#### Updated Quality screening recommendation

A byproduct of the aging in MLS that gives rise to the drift in the water vapor product and 190-GHz N<sub>2</sub>O (see section 3.17) is that the **Quality** metric for the H<sub>2</sub>O product exhibits a decreasing trend (most notable in the years following ~2009). This decrease is not correlated with any actual decline in the accuracy of the MLS H<sub>2</sub>O product, which appears largely unchanged (drift issues aside). However, application of the previously recommended 1.45 **Quality** threshold leads to rejection of an unreasonably large fraction of the H<sub>2</sub>O profiles in the more recent years of the Aura mission, particularly during southern winter. The revised 0.7 **Quality** threshold restores these profiles without erroneously identifying any obviously poor profiles as acceptable. Figure 3.9.8 compares the amounts of H<sub>2</sub>O observations flagged as acceptable according to the “old” and “new” screening methods over the life of the Aura mission to date. The new screening method rejects fewer H<sub>2</sub>O profiles than the old one. In addition the old method rejects more profiles in the later part of the mission than in the earlier years, a behavior the new method avoids.

### 3.9.10 Artifacts

There is a minimum concentration where MLS H<sub>2</sub>O measurements become unreliable. This is given in Table 3.9.1 under the “Min. H<sub>2</sub>O” column. The lowest allowable H<sub>2</sub>O value is 0.1 ppmv. Differences between

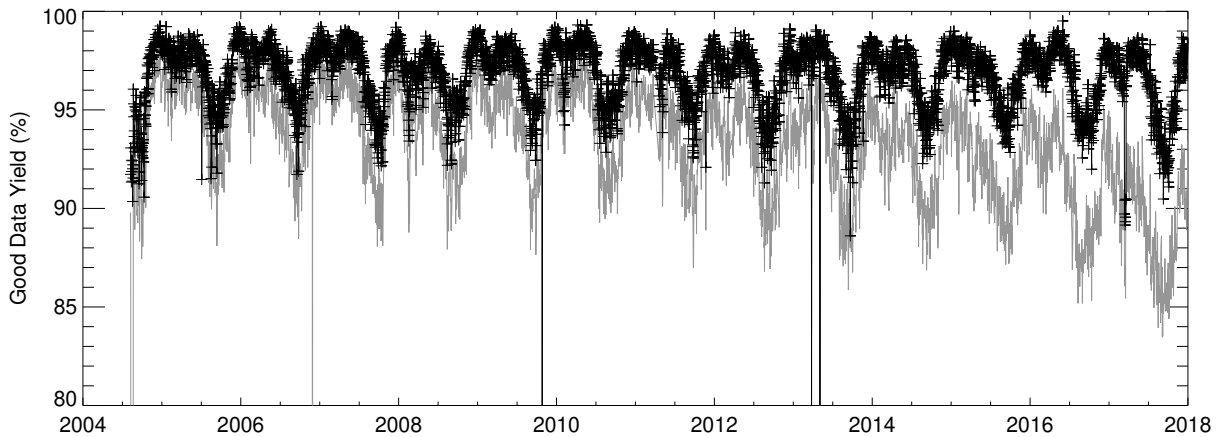


**Figure 3.9.8:** A time series of daily good data yields using the previous data quality screening for v04.2x (grey) and the current revised quality and profile value screening method (black).

the retrieved middle tropospheric H<sub>2</sub>O constraint and the true atmospheric state can cause errors at 316 and 261 hPa. The error manifests either as dry (<1 ppmv) or moist spikes in an orbital time series. Such data are often accompanied with good quality and status.

Clouds in the field of view degrade the data in unpredictable ways. Many instances of quality <1.45 occur in the presence of clouds where the cloud screening has not rejected the radiances. Cloud radiative scattering distorts the spectral lineshape causing poor fits and low quality values. However, not all MLS signals are obviously affected. Coincident comparisons of MLS cloud flagged H<sub>2</sub>O (status bit 16 or 32 set between 316 – 215 hPa) with good quality AIRS show a small mean bias of 10% but exhibit a 50% increase in variability for the individual differences. Therefore users should be aware that, although the overall biases for measurements inside clouds are similar to that for clear sky, individual profiles will exhibit greater variability about the true atmospheric humidity.

Note the discussion of the drift in MLS stratospheric water vapor above.

### 3.9.11 Desired improvements for future data version(s)

We want to improve high latitude performance of 261 and 215 hPa H<sub>2</sub>O in future work. Possibly a vertically resolved H<sub>2</sub>O product for pressure > 316 hPa at high latitudes during dry conditions.



**Table 3.9.1:** Summary of MLS v4.2x H<sub>2</sub>O product.

Pressure / hPa	Resolution V×H / km	Precision <sup>a</sup> / %	Accuracy / %	Min. / ppmv <sup>b</sup>	Comments
≤0.001	—	—	—	—	Unsuitable for scientific use
0.002	10.3 × 350	152	40	0.1	
0.004	10.8 × 585	81	23	0.1	
0.010	8.8 × 725	55	17	0.1	
0.021	8.0 × 745	41	19	0.1	
0.046	7.4 × 540	35	17	0.1	
0.10	5.8 × 745	24	14	0.1	
0.21	3.6 × 670	19	11	0.1	
0.46	3.3 × 505	12	8	0.1	
1.0	2.5 × 400	6	7	0.1	
2.2	3.5 × 385	4	7	0.1	
4.6	3.4 × 350	4	5	0.1	
10	2.8 × 290	6	19	0.1	
22	3.2 × 265	5	5	0.1	
46	3.2 × 230	5	4	0.1	
68	3.1 × 190	5	9	0.1	
83	3.1 × 190	7	9	0.1	
100	3.0 × 198	15	8	0.1	
121	2.6 × 193	20	12	0.1	
147	2.3 × 188	20	15	0.1	
178	1.7 × 183	25	20	3	
215	1.6 × 178	40	25	3	Large low bias for latitudes > 60°
261	1.4 × 173	35	20	4	Large low bias for latitudes > 60°
316	1.3 × 168	65	15	7	Occasionally erroneous low value < 1 ppmv and high value fliers are retrieved in the tropics, usually in clouds.
> 316	—	—	—	—	Unsuitable for scientific use

<sup>a</sup>Precision for a single MLS profile<sup>b</sup>Minimum H<sub>2</sub>O is an estimate of the minimum H<sub>2</sub>O concentration measurable by v4.2x MLS.

## 3.10 Hydrogen Chloride (HCl)

**Swath name:** HCl

**Useful range:** 100 – 0.32 hPa

**Contact:** Lucien Froidevaux, **Email:** <Lucien.Froidevaux@jpl.nasa.gov>

### 3.10.1 Introduction

There has been very little change in the v4.2 HCl retrieval results, in comparison to v3.3/v3.4. We provide below sample mean HCl distributions for the two data versions, and their differences. Otherwise, previous information regarding this species remains largely unchanged; the main points are mentioned here mainly for new data users.

The MLS v3.3/v3.4 retrievals of the HCl standard product (from the 640 GHz radiometer) use channels from band 14, as a result of the deterioration observed since early 2006 in nearby band 13, originally targeted (with narrower channels than band 14) at the main HCl emission line center. Full measurement days with band 13 on after February 15, 2006, are as follows: March 15, 2006 (2006d074), April 14, 2006 (2006d104), January 6 through 8, 2009 (2009d006 through 2009d008), and January 24 through 27, 2010 (2010d024 through 2010d027). For days prior to February 16, 2006 and for the few days (as listed above) when band 13 gets turned on thereafter, the MLS Level 2 software also produces a separate HCl-640-B13 product (stored in the L2GP-DGG file), using the band 13 radiances. This product has slightly better precision and vertical resolution in the upper stratosphere than the standard HCl product. The MLS team plans to turn band 13 on very infrequently (possibly only one more time), as its lifetime is estimated at a few days to a few weeks at most, based on the channel counts and channel noise characteristics observed during the 3-day turn-on period in late January, 2010; band 13 should provide useful trend information for upper stratospheric data, given its narrower channels. Upper stratospheric trends from the (uninterrupted from 2004 to present) band 14 retrievals are not reliable enough and are too small, compared to band 13 data and expectations, as well as versus ACE-FTS HCl data. Scientific usage of the MLS standard HCl (band 14) dataset should therefore be restricted to the lower stratosphere; in this region, studies of tendencies and longer-term trends are justified (e.g., see the HCl comparisons discussed by *Mahieu et al.* [2014]).

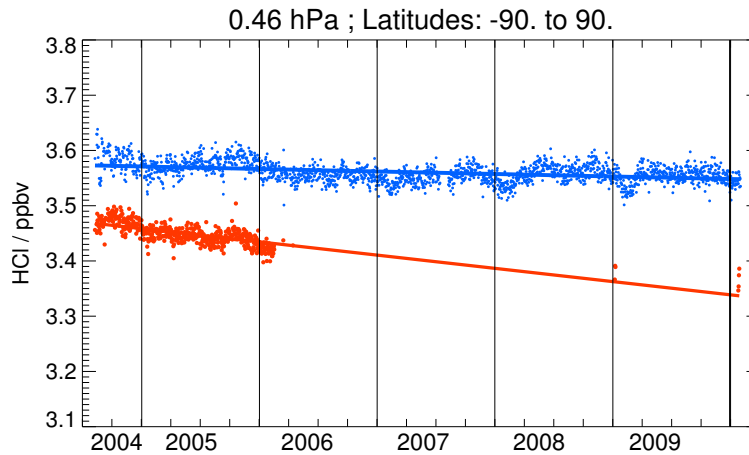
See Figure 3.10.1 for an illustration of the trend differences between these two MLS band measurements of HCl. In the lower stratosphere, however, variations in the two HCl products are closer together, although there is also more seasonal variability; we believe that the band 14 retrievals are quite appropriate to use in studies of seasonal (and latitudinal) changes (e.g., during polar winter/spring), as well as for longer-term trend studies in the lower stratosphere.

Table 3.10.1 summarizes the MLS HCl resolution, precision, and accuracy estimates as a function of pressure. More discussion and data screening recommendations for the MLS HCl v4.2 data are provided below (but this is unchanged from the v3.3/v3.4 recommendations). Analyses describing detailed validation of the MLS (v2.2) product and comparisons with other data sets are described in *Froidevaux et al.* [2008a]. Based on the fairly small overall changes in v3.3/v3.4 and v4.2 HCl data versus v2.2, the conclusions of the latter reference should remain essentially unchanged.

### 3.10.2 Changes from v3.3/v3.4

There were no large algorithmic changes relating to HCl for the v4.2 retrievals. Small differences in HCl abundances (see below) have occurred mainly near 147 hPa, most likely mainly as a result of changes in water vapor in the UTLS.

The background observed in the 640-GHz radiances includes emissions from N<sub>2</sub>, O<sub>2</sub>, and H<sub>2</sub>O. There are laboratory-based and ground-based models for the continuum absorptions that are the basis for the MLS



**Figure 3.10.1:** Daily zonal averages for MLS HCl at 0.46 hPa, from mid-August, 2004, through January, 2010, for the originally-targeted band 13 measurements (red points), now available only on occasion (to preserve lifetime), and the band 14 data (blue points). The lines are simple linear fits through the daily data points; trend differences are apparent in this region of the atmosphere, where the information obtained from band 14 HCl data is not reliable enough.

absorption model [*Pardo, 2001*, and references therein]. These models were tested against MLS extinction measurements from the wing channels in the 640-GHz radiometer. The latitude dependence of this extinction was found to agree better with the expected most plus dry continuum extinction values if the dry and moist continuum functions were scaled by factors close to 20%; however, this is not a change from the v3.3/v3.4 retrievals.

A comparison plot showing zonal average HCl contours and differences between the two data versions for a typical month (March, 2009) is provided in Figure 3.10.2. For pressures larger than or equal to 0.22 hPa, the average differences between the two data versions are typically within 0.1 ppbv (or 1 – 2%). The average changes are easily within the estimated accuracy values (see Table 3.10.1). The largest percentage changes in HCl occur for very small mixing ratio values, close to 100 and (mainly) 147 hPa; v4.2 values are usually smaller than the v3.3/v3.4 values by 10 to 15% in the lower stratosphere at low latitudes or during winter at polar latitudes. There is still, however, an unrealistic high bias in HCl at 147 hPa in the tropics, so values at this pressure are not recommended (reliable in absolute value) within the 40°S to 40°N latitude range. The precisions estimated in the Level 2 files are essentially unchanged from v3.3/v3.4.

### 3.10.3 Resolution

Typical (rounded off) values for resolution are provided in Table 3.10.1. Based on the width of the averaging kernels shown in Figure 3.10.3, the vertical resolution for the standard HCl stratospheric product is ~3 km (2.7 km at best in the lower stratosphere), or about double the 640-GHz radiometer vertical field of view width at half-maximum; the vertical resolution degrades to 4–6 km in the lower mesosphere. The along-track resolution is ~200 to 350 km for pressures of 2 hPa or more, and ~500 km in the lower mesosphere. The cross-track resolution is set by the 3 km width of the MLS 640-GHz field of view. The longitudinal separation of MLS measurements, set by the Aura orbit, is 10° – 20° over middle and lower latitudes, with much finer sampling in polar regions.

### 3.10.4 Precision

The estimated single-profile precision reported by the Level 2 software varies from ~0.2 to 0.6 ppbv in the stratosphere (see Table 3.10.1), with poorer precision obtained in the lower mesosphere. These precision values have not changed significantly for v4.2x data. The Level 2 precision values are often only slightly lower than

Help
Overview
Table
S
BrO
S
CH <sub>3</sub> Cl
T
S
CH <sub>3</sub> CN
T
S
CH <sub>3</sub> OH
T
S
ClO
T
S
CO
T
S
GPH
T
S
H <sub>2</sub> O
T
S
HCl
T
S
HCN
T
S
HNO <sub>3</sub>
T
S
HO <sub>2</sub>
T
S
HOCl
T
S
IWC
T
S
IWP
T
S
N <sub>2</sub> O
T
S
O <sub>3</sub>
T
S
OH
T
S
RHI
T
S
SO <sub>2</sub>
T
S
T

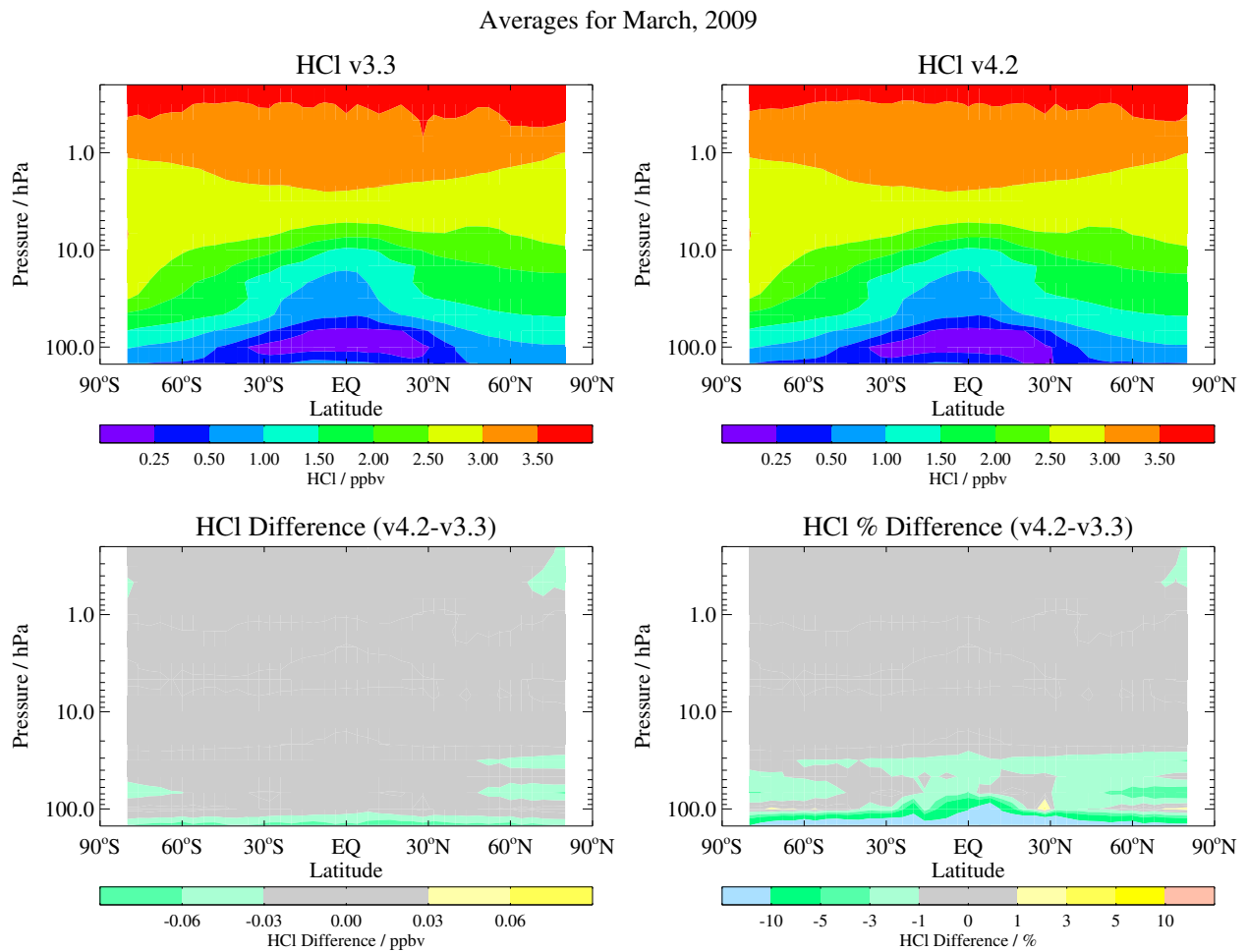


**Figure 3.10.2:** Zonal averages for MLS HCl profiles during March, 2009, showing the MLS v3.3 HCl mixing ratio contours (top left panel), the v4.2 contours (top right panel), and their differences in ppbv (v4.2 minus v3.3, bottom left panel) and percent (v4.2 minus v3.3 versus v3.3, bottom right panel).

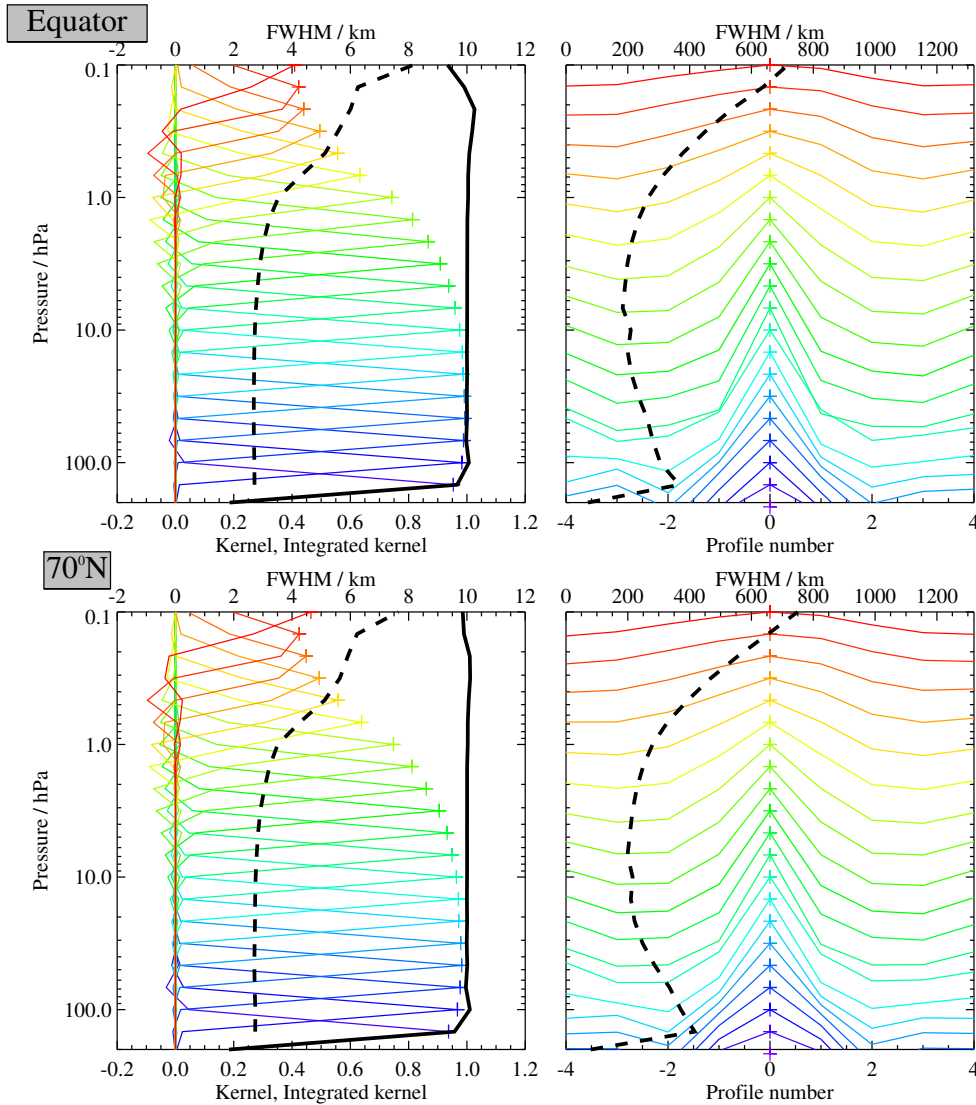


**Figure 3.10.3:** Typical two-dimensional (vertical and horizontal along-track) averaging kernels for the MLS v4.2x HCl data at the equator (upper) and at 70°N (lower); variation in the averaging kernels is sufficiently small that these are representative of typical profiles. Colored lines show the averaging kernels as a function of MLS retrieval level, indicating the region of the atmosphere from which information is contributing to the measurements on the individual retrieval surfaces, which are denoted by plus signs in corresponding colors. The dashed black line indicates the resolution, determined from the full width at half maximum (FWHM) of the averaging kernels, approximately scaled into kilometers (top axes). (Left) Vertical averaging kernels (integrated in the horizontal dimension for five along-track profiles) and resolution. The solid black line shows the integrated area under each kernel (horizontally and vertically); values near unity imply that the majority of information for that MLS data point has come from the measurements, whereas lower values imply substantial contributions from a priori information. (Right) Horizontal averaging kernels (integrated in the vertical dimension) and resolution. The horizontal averaging kernels are shown scaled such that a unit averaging kernel amplitude is equivalent to a factor of 10 change in pressure.

the observed scatter in the data, as evaluated from a narrow latitude band centered around the equator where atmospheric variability is often smaller than elsewhere, or as obtained from a comparison between ascending and descending coincident MLS profiles. The scatter in MLS data and in simulated MLS retrievals (using noise-free radiances) becomes smaller than the theoretical precision (given in the Level 2 files) in the upper stratosphere and mesosphere, where there is a larger impact of *a priori* and smoothing constraints. The HCl precision values increase rapidly at pressures less than 0.2 hPa, and are generally flagged negative (or zero) at pressures less than 0.1 hPa; this indicates an increasing influence from the *a priori* (with poorer measurement sensitivity and reliability).

### 3.10.5 Accuracy

The accuracy estimates in the Table came from a quantification of the combined effects of possible systematic errors in MLS calibration, spectroscopy, etc. on the HCl retrievals; there are several error sources (mostly from radiometric calibration components) that contribute significantly to the total error. These values are intended to represent  $2\sigma$  estimates of accuracy. For more details, see the MLS validation paper by *Froidevaux et al.* [2008a]. For v4.2x (as for v3.3x and v3.4x), given the trend issues affecting the (band 14) standard HCl product in the upper stratosphere and lower mesosphere, we have recommended an accuracy estimate of no better than 10% in this region (or about 0.3 ppbv). For the lower stratosphere, given the agreement between the two bands' retrievals as well as some trend studies (for the standard product), we use the more formal accuracy estimates (see Table 3.10.1).

### 3.10.6 Data screening

**Pressure range: 100 – 0.32 hPa**

Values outside this range are not recommended for scientific use. We note that the MLS values at 147 hPa are biased high, at least at low to mid-latitudes – and these values are not recommended (particularly equatorward of about 40°). Also, although the vertical range at the top end is recommended up to 0.32 hPa, users should note the significant issues relating to HCl trend estimates in the upper stratosphere and lower mesosphere; average profiles in this region can be used for studies not involving trends (or accuracy requirements not as tight as 10%).

**Estimated precision: Only use values for which the estimated precision is a positive number.**

Values where the *a priori* information has a strong influence are flagged with negative or zero precision, and should not be used in scientific analyses (see Section 1.5).

**Status flag: Only use profiles for which the Status field is an even number.**

Odd values of Status indicate that the profile should not be used in scientific studies. See Section 1.6 for more information on the interpretation of the Status field.

**Quality field: Only profiles with a value of the Quality field greater than 1.2 should be used.**

This criterion removes profiles with the poorest radiance fits, typically less than 0.1% of the daily profiles. For HCl (and for other 640 GHz MLS products), this screening correlates well with the poorly converged sets of profiles (see below); we recommend the use of both the Quality and Convergence fields for data screening.

**Convergence field: Only profiles with a value of the Convergence field less than 1.05 should be used.**

For the vast majority of profiles (99% or more for most days), this field is less than 1.05. Nevertheless, on occasion, sets of profiles (typically one or more groups of ten profiles, retrieved as a “chunk”) have this Convergence field set to larger values, and should be discarded.

**Clouds:** Thick clouds can add significant artifacts (mainly in the tropics, statistically), with total systematic errors potentially as large as 0.5 ppbv at 100 hPa and even larger at 147 hPa. Studies in this region could

**Table 3.10.1:** Summary for MLS hydrogen chloride

Pressure hPa	Precision <sup>a</sup>		Resolution V × H km	Accuracy <sup>b</sup>		Comments
	ppbv	%		ppbv	%	
0.22 – 0.001	—	—	—	—	—	Unsuitable for scientific use
0.32	0.8	25	5 × 450	0.3	10	Unsuitable for trend studies
0.5	0.7	20	5 × 400	0.3	10	Unsuitable for trend studies
1	0.5	15	4 × 300	0.3	10	Unsuitable for trend studies
2	0.4	15	3 × 250	0.3	10	Unsuitable for trend studies
5	0.3	10	3 × 200	0.3	10	Unsuitable for trend studies
10	0.2	10	3 × 200	0.2	10	
20	0.2	15	3 × 200	0.15	10	
46	0.2	10 to > 40	3 × 250	0.2	20	
68	0.2	15 to > 80	3 × 300	0.2	25	
100	0.3	30 to > 100	3 × 350	0.2	40	
147	0.4	50 to > 100	3 × 400	0.3	50 to > 100	High bias at low lats. (use with caution elsewhere)
1000 – 215	—	—	—	—	—	Unsuitable for scientific use

<sup>a</sup>Precision ( $1\sigma$ ) for individual profiles; note that % values tend to vary strongly with latitude in the lower stratosphere.

<sup>b</sup> $2\sigma$  estimate from systematic uncertainty characterization tests (but see text for estimates at pressures lower than 10 hPa); note that percent values tend to vary strongly with latitude and season in the lower stratosphere, due to the variability in HCl.

benefit from additional screening that correlates any outliers in the data with the occurrence of thick clouds (using some subset of the profiles with set cloud status flags, namely status bits 16 and 32, or using the MLS retrievals of ice water content). However, the large positive HCl bias at 147 hPa for low latitudes likely arises in part from unknown or improperly modeled systematic error sources, and not just from clouds. At other pressures, the potential impact on HCl from clouds is small or negligible.

### 3.10.7 Review of comparisons with other datasets

*Froidevaux et al.* [2008a] provided results of generally good comparisons between MLS HCl and other satellite, balloon, and aircraft measurements. Both MLS and ACE-FTS HCl values are generally larger (by about 10 – 15%) than the HCl values from HALOE, especially at upper stratospheric altitudes; this feature has not changed, overall, with the new data version(s) from both MLS and ACE-FTS. MLS HCl at 147 hPa is biased high versus WB-57 aircraft in-situ (CIMS) measurements (low to mid-latitudes); while this is still true for v4 data, MLS data at this pressure level are potentially useful and accurate enough at high latitudes.

### 3.10.8 Artifacts

- We do not recommend the use of the MLS HCl standard product in the upper stratosphere and lower mesosphere, especially in terms of trend studies, for reasons mentioned above.
- The HCl values at 147 hPa are biased high and generally not usable (except possibly at high latitudes). Please consult with the MLS team for further information.
- Users should screen out the non-converged and poorest quality HCl profiles, as such profiles (typically less than 0.1% of the data) tend to behave unlike the majority of the other MLS retrievals. See the criteria listed above.

## 3.11 Hydrogen Cyanide (HCN)

**Swath name:** HCN

**Useful range:** 21 – 0.1 hPa

**Contact:** Hugh C. Pumphrey, **Email:** <Hugh.Pumphrey@ed.ac.uk>

### 3.11.1 Introduction

HCN is retrieved from bands encompassing, in the lower sideband, the 177.26 GHz spectral line of HCN. Although the target line is in an uncluttered part of the spectrum, the upper sideband contains many interfering lines of O<sub>3</sub> and HNO<sub>3</sub>. As a result, the v4.2x HCN product is not recommended for general use in the lower stratosphere. In the recommended range it is usable, but has rather poor precision and resolution.

It is possible to retrieve weekly zonal means of HCN over a greater vertical range by first averaging the radiances. Results of this process and further information on the HCN measurement may be found in *Pumphrey et al.* [2006].

### 3.11.2 Differences between v3.x and v4.2x

No changes specific to the HCN retrieval were made between v2.x and v3.x. For v4.2x a new phase was introduced in which HCN is retrieved using only bands 6 and 27, rather than all of R2. The v4.2x HCN still has obvious biases in the lower stratosphere, but they are less severe than in previous versions. As a result, the lowest recommended level is now 21 hPa rather than the 10 hPa recommended for earlier versions.

Figure 3.11.2 shows that the precisions in v4.2x are essentially unchanged from earlier versions. The retrieved mixing ratios change very little in the region where use was recommended for earlier versions. Mixing ratios are considerably different between all three versions in the lower stratosphere where the data are not recommended for general use. However, the values in v4.2x appear less unrealistic than in either v2.x or v3.x.

### 3.11.3 Vertical resolution

The HCN signal is rather small, so a rather strong smoothing constraint has to be applied to ensure that the retrieval is at all useful. As Figure 3.11.1 shows, the vertical resolution is about 8 km at 10 hPa, degrading to 12 km at 0.1 hPa. The horizontal resolution along the measurement track is between 2 and 4 profile spacings.

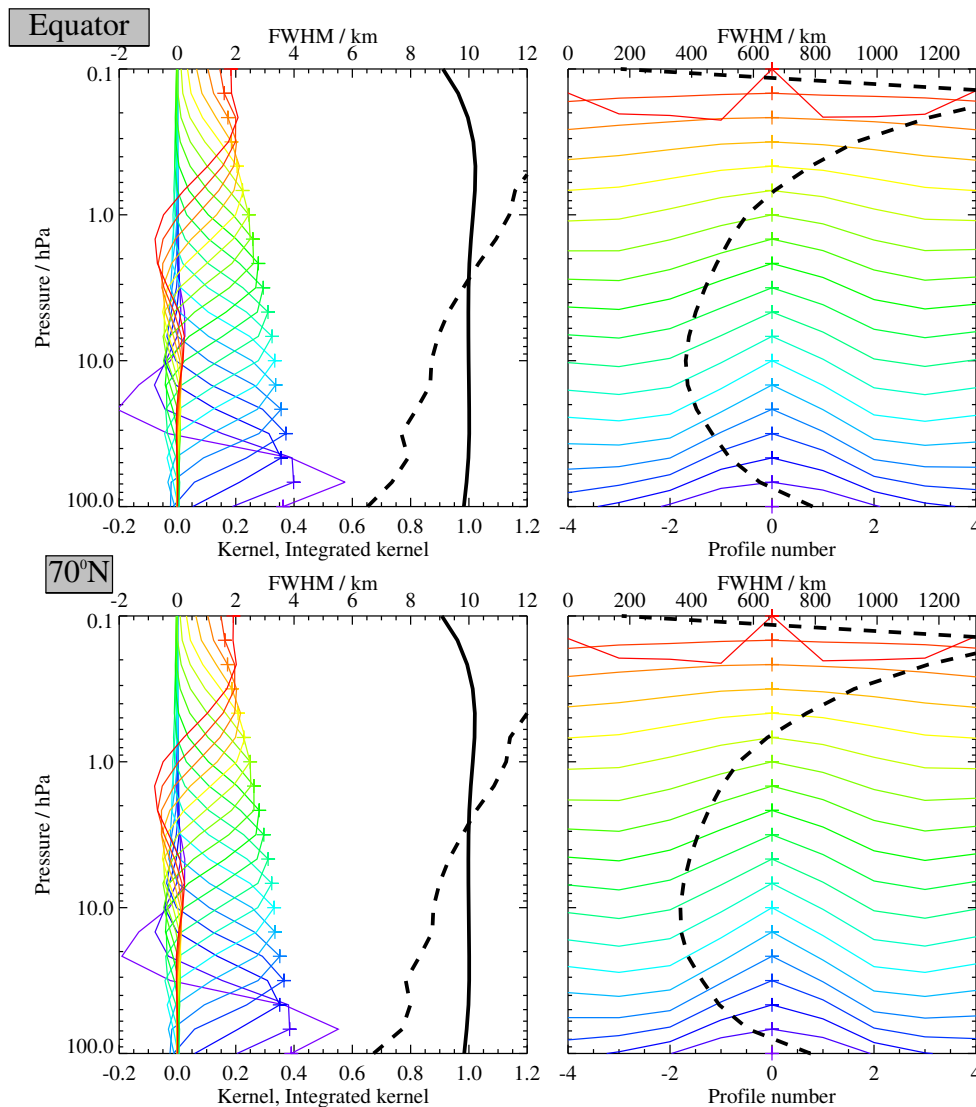
### 3.11.4 Precision

Figure 3.11.2 shows the estimated precision (values of the field L2gpPrecision), together with the observed standard deviation in an equatorial latitude band where the natural variability of the atmosphere is small. The observed scatter is smaller than the estimated precision due to the effects of retrieval smoothing.

### 3.11.5 Accuracy

The accuracy of the HCN product has not been assessed in detail because a cursory inspection revealed that previous versions of the product had extremely large systematic errors in the lower stratosphere. These errors are smaller in v4.2x, but remain present and un-quantified. For this reason the data are not considered to be useful at pressures greater than 21 hPa (altitudes below ~27 km). In the upper stratosphere the values are in line with current understanding of the chemistry of HCN. Comparison to historical values suggests an accuracy of no worse than 50%. The precision, resolution and accuracy of the HCN data are summarized in table 3.11.1.





**Figure 3.11.1:** Typical two-dimensional (vertical and horizontal along-track) averaging kernels for the MLS v4.2x HCN data at the equator (upper) and at 70°N (lower); variation in the averaging kernels is sufficiently small that these are representative of typical profiles. Colored lines show the averaging kernels as a function of MLS retrieval level, indicating the region of the atmosphere from which information is contributing to the measurements on the individual retrieval surfaces, which are denoted by plus signs in corresponding colors. The dashed black line indicates the resolution, determined from the full width at half maximum (FWHM) of the averaging kernels, approximately scaled into kilometers (top axes). (Left) Vertical averaging kernels (integrated in the horizontal dimension for five along-track profiles) and resolution. The solid black line shows the integrated area under each kernel (horizontally and vertically); values near unity imply that the majority of information for that MLS data point has come from the measurements, whereas lower values imply substantial contributions from a priori information. (Right) Horizontal averaging kernels (integrated in the vertical dimension) and resolution. The horizontal averaging kernels are shown scaled such that a unit averaging kernel amplitude is equivalent to a factor of 10 change in pressure.

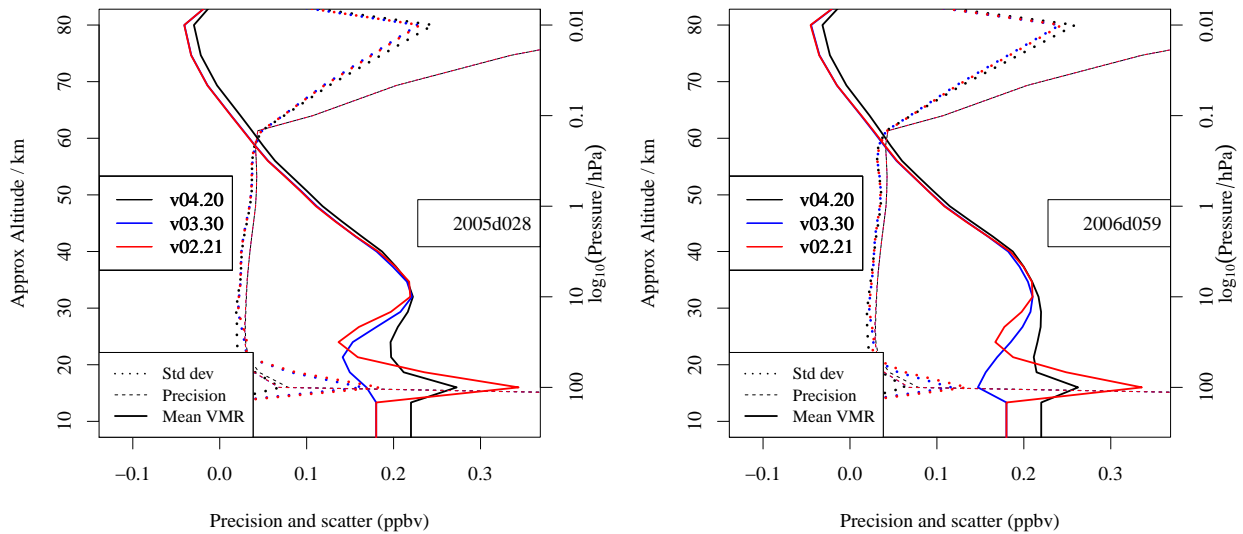


**Figure 3.11.2:** Estimated precision L2gpPrecision and observed standard deviation for MLS v4.2x (black), v3.x (blue) and v2.x (red) HCN. The data shown are all profiles within  $20^\circ$  of the equator for 28 January, 2005 and 28 February 2006. Mean mixing ratio (VMR) profiles are shown for comparison. Note that these are essentially the same in v2.x, v3.x and v4.2x for the region recommended for use in all three versions (10 hPa - 0.1 hPa).

**Table 3.11.1:** Summary of data quality for MLS v4.2x HCN. The precision shown is the estimated precision (L2gpPrecision); the observed scatter is about 80% of this value.

Pressure	Resolution V × H / km	Precision / pptv	Accuracy / %	Comments
< 0.1 hPa	—	—	—	Unsuitable for scientific use
1 – 0.1 hPa	12 × 500	50	50	
21 – 1 hPa	10 × 300	30	50	
100 – 21 hPa	10 × 300	50	Very poor	Unsuitable for scientific use
> 100 hPa				Not Retrieved

### 3.11.6 Data screening

**Pressure range:** 21 – 0.1 hPa

Values outside this range are not recommended for scientific use.

**Estimated precision:** Only use values for which the estimated precision is a positive number.

Values where the *a priori* information has a strong influence are flagged with negative or zero precision, and should not be used in scientific analyses (see Section 1.5).

**Status flag:** Only use profiles for which the **Status** field is an even number.

Odd values of Status indicate that the profile should not be used in scientific studies. See Section 1.6 for more information on the interpretation of the Status field.

**Clouds:** Clouds have no impact, profiles with non-zero even values of **Status** are suitable for use.

As HCN is only useable in the upper stratosphere, profiles which have either, both or neither of the cloud flags set may be used.

**Quality:** Only profiles whose **Quality** field is greater than 0.2 should be used.

Values of Quality are usually near 1.5; occasional lower values do not seem correlated with unusual profiles, but we suggest as a precaution that only profiles with Quality > 0.2 be used. Typically this will eliminate only 1-2% of profiles.

**Convergence:** Only profiles whose **Convergence** field is less than 2.0 should be used.

This should eliminate any chunks which have obviously failed to converge – typically this is only 1-2% of the total.

### 3.11.7 Artifacts

There are no obvious artifacts within the recommended altitude range

### 3.11.8 Desired improvements for future data version(s)

Hopefully it will prove possible to retrieve HCN in the lower stratosphere.

Help
Overview
Table
BrO
CH <sub>3</sub> Cl
CH <sub>3</sub> CN
CH <sub>3</sub> OH
ClO
CO
GPH
H <sub>2</sub> O
HCl
HCN
<b>HNO<sub>3</sub></b>
HO <sub>2</sub>
HOCl
IWC
IWP
N <sub>2</sub> O
O <sub>3</sub>
OH
RHI
SO <sub>2</sub>

## 3.12 Nitric Acid (HNO<sub>3</sub>)

**Swath name:** HNO3

**Useful range:** 215 – 1.5 hPa (1.0 hPa under enhanced conditions)

**Contact:** Gloria Manney, **Email:** <manney@nwra.com>

### 3.12.1 Introduction

The standard HNO<sub>3</sub> product is derived from the 240-GHz retrievals at pressures equal to or greater than 22 hPa and from the 190-GHz retrievals for lesser pressures. The quality and reliability of the Aura MLS v2.2 HNO<sub>3</sub> measurements were assessed in detail by *Santee et al.* [2007]. V3.3 HNO<sub>3</sub> was greatly improved over that in version v2.2, especially in that a low bias through much of the stratosphere (especially evident at levels with pressure greater than or equal to 100 hPa) was largely eliminated. However, v3.3 240-GHz HNO<sub>3</sub> was adversely impacted by clouds [*Livesey et al.*, 2013], leading to a noisy HNO<sub>3</sub> product in the UTLS. The adverse cloud impacts have been substantially mitigated in v4.2x (see 1.4). Figure 3.12.1 shows an example of typical differences between v3.3x/v3.4x and v4.2x HNO<sub>3</sub>. When each version is screened as recommended [see below and *Livesey et al.*, 2013], v4.2x is slightly lower than v3.3x and v3.4x at pressures greater than or equal to 215 hPa in middle to high latitudes, and shows an oscillatory pattern of differences in the tropical UTLS, such that v4.2x values are slightly higher than those in v3.3x and v3.4x at 147 hPa and slightly lower at 100 hPa. A summary of the estimated precision, resolution (vertical and horizontal), and systematic uncertainty of the v4.2x HNO<sub>3</sub> measurements as a function of altitude is given in Table 3.12.1.

### 3.12.2 Resolution

The resolution of the retrieved data can be described using “averaging kernels” [e.g., *Rodgers*, 2000]; the two-dimensional nature of the MLS data processing system means that the kernels describe both vertical and horizontal resolution. Smoothing, imposed on the retrieval system in both the vertical and horizontal directions to enhance retrieval stability and precision, reduces the inherent resolution of the measurements. Consequently, the vertical resolution of the v4.2x HNO<sub>3</sub> data, as determined from the full width at half maximum of the rows of the averaging kernel matrix shown in Figure 3.12.2, is 3 – 4 km through most of the useful range, degrading to ~4.5 km at 22 hPa and some levels in the upper stratosphere (see Table 3.12.1). Note that the averaging kernels for the 215 and 316-hPa retrieval surfaces overlap over most of their depth, indicating that the 316-hPa retrieval provides little independent information. Figure 3.12.2 also shows horizontal averaging kernels, from which the along-track horizontal resolution is determined to be 400 – 500 km over most of the vertical range, improving to 250 – 300 km between 15 and 4.6 hPa, and degrading to 600 – 700 km at 1.5 and 1 hPa. The cross-track resolution, set by the widths of the fields of view of the 190-GHz and 240-GHz radiometers, is ~10 km. The along-track separation between adjacent retrieved profiles is 1.5° great circle angle (~165 km), whereas the longitudinal separation of MLS measurements, set by the Aura orbit, is 10° – 20° over low and middle latitudes, with much finer sampling in the polar regions.

### 3.12.3 Precision

The precision of the MLS HNO<sub>3</sub> measurements is estimated empirically by computing the standard deviation of the profiles in the 20°-wide latitude band centered around the equator, where natural atmospheric variability should be small relative to the measurement noise. Because meteorological variation is never completely negligible, however, this procedure produces an upper limit on the precision-related variability. As shown in Figure 3.12.3, the observed scatter in the v4.2x data is ~0.5 – 0.6 ppbv throughout the range from 215 to 3.2 hPa, and increases sharply at lower pressures. The scatter is essentially invariant with time, as seen by comparing the results for the different days shown in Figure 3.12.3. An alternative method using the difference between ascending and descending values at orbit crossings yields very similar estimates.

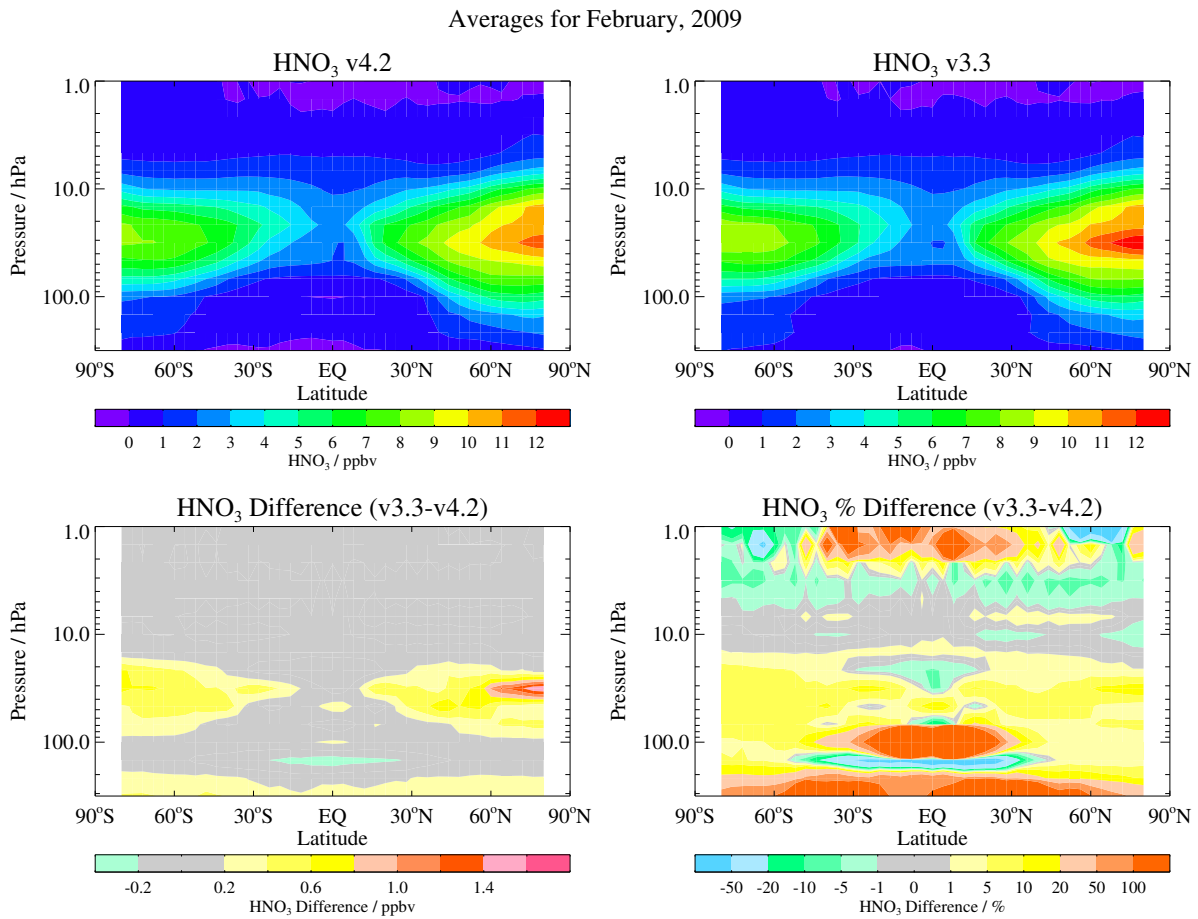


**Figure 3.12.1:** V3.3 (top left) and v4.1 (top right) zonal mean HNO<sub>3</sub> for February 2009, and differences (v3.3 – v4.1) expressed in ppbv (bottom left) and percent (bottom right). Each version is screened with the recommended criteria.

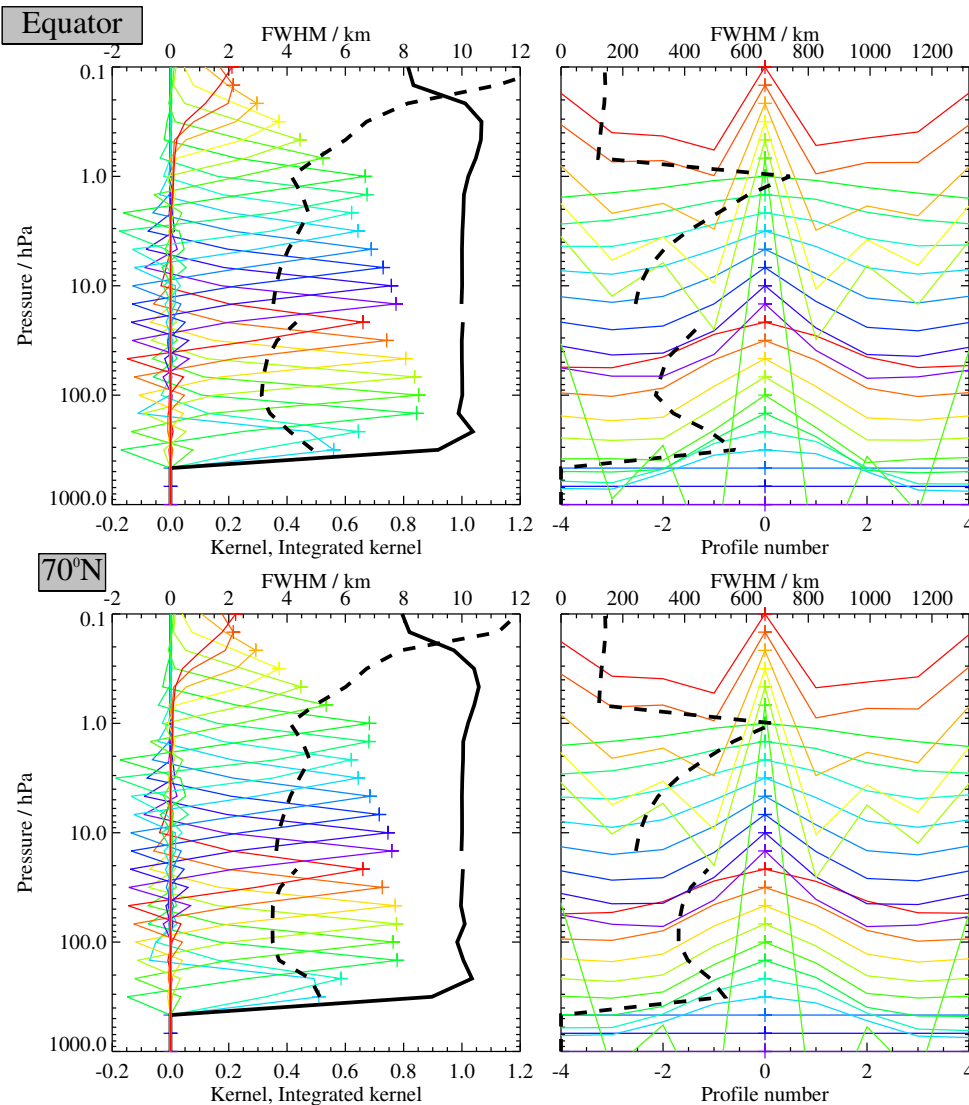


**Figure 3.12.2:** Typical two-dimensional (vertical and horizontal along-track) averaging kernels for the MLS v4.2x HNO<sub>3</sub> data at the equator (upper) and at 70°N (lower); variation in the averaging kernels is sufficiently small that these are representative of typical profiles. Colored lines show the averaging kernels as a function of MLS retrieval level, indicating the region of the atmosphere from which information is contributing to the measurements on the individual retrieval surfaces, which are denoted by plus signs in corresponding colors. The dashed black line indicates the resolution, determined from the full width at half maximum (FWHM) of the averaging kernels, approximately scaled into kilometers (top axes). (Left) Vertical averaging kernels (integrated in the horizontal dimension for five along-track profiles) and resolution. The solid black line shows the integrated area under each kernel (horizontally and vertically); values near unity imply that the majority of information for that MLS data point has come from the measurements, whereas lower values imply substantial contributions from a priori information. (Right) Horizontal averaging kernels (integrated in the vertical dimension) and resolution. The horizontal averaging kernels are shown scaled such that a unit averaging kernel amplitude is equivalent to a factor of 10 change in pressure.

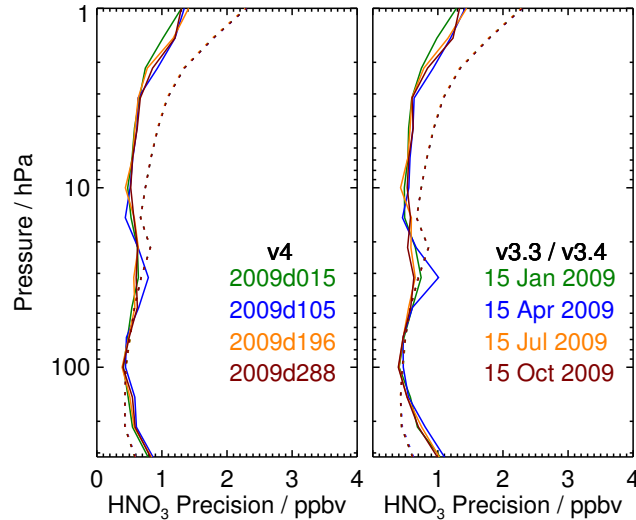


**Figure 3.12.3:** Precision of the (left) v3.3 and (right) v2.2 MLS HNO<sub>3</sub> measurements for four representative days (see legend). Solid lines depict the observed scatter in a narrow equatorial band (see text); dotted lines depict the theoretical precision estimated by the retrieval algorithm.

The single-profile precision estimates cited here are, to first order, independent of latitude and season, but it should be borne in mind that the large geographic variations in HNO<sub>3</sub> abundances gives rise to a wide range of signal to noise ratios. At some latitudes and altitudes and in some seasons, HNO<sub>3</sub> abundances are smaller than the single-profile precision, necessitating the use of averages for scientific studies. In most cases, precision can be improved by averaging, with the precision of an average of  $N$  profiles being  $1/\sqrt{N}$  times the precision of an individual profile (note that this is not the case for averages of successive along-track profiles, which are not completely independent because of horizontal smearing).

The observational determination of the precision is compared in Figure 3.12.3 to the theoretical precision values reported by the Level 2 data processing algorithms. Although the two estimates compare very well between 215 and 15 hPa, at pressures smaller than 10 hPa the predicted precision substantially exceeds the observed scatter. This indicates that the a priori information and the vertical smoothing applied to stabilize the retrieval are influencing the results at the higher retrieval levels. Because the theoretical precisions take into account occasional variations in instrument performance, the best estimate of the precision of an individual data point is the value quoted for that point in the L2GP files, but it should be borne in mind that this approach overestimates the actual measurement noise at pressures less than 10 hPa. Conversely, the observed scatter at pressures higher than 100 hPa is somewhat larger than the theoretical precision in v4.2x and much larger than the theoretical precision in v3.3. This is related to the spikes and increased noise in the UTLS in v3.3, and can be seen to be much improved in v4.2x. Nevertheless, some outliers in this region persist in v4.2x. Procedures for screening outliers in the UTLS are discussed below.

### 3.12.4 Accuracy

The effects of various sources of systematic uncertainty (e.g., instrumental issues, spectroscopic uncertainty, and approximations in the retrieval formulation and implementation) on the MLS v4.2x HNO<sub>3</sub> measurements have been quantified through a comprehensive set of retrievals of synthetic radiances; see *Santee et al.* [2007] for details of a similar analysis conducted on MLS v2.2 HNO<sub>3</sub> data. The overall systematic uncertainty, or accuracy, is calculated by combining (RSS) the contributions from both the expected biases and the additional scatter each source of uncertainty may introduce into the data. In aggregate, the factors considered in these simulations are estimated to give rise to a total systematic uncertainty ranging from approximately 0.1

to 2.4 ppbv, depending on the level, in the MLS v4.2x HNO<sub>3</sub> data (see Table 3.12.1).

### 3.12.5 Comparisons with other datasets

v4.2x HNO<sub>3</sub> profiles generally show only small differences in magnitude from v3.3 when each data version is screened according to the criteria above. Therefore, the comparisons with correlative data are expected to be very similar to those described for v3.3 by *Livesey et al.* [2013].

### 3.12.6 Data screening – all data

**Pressure range:** 215 – 1.5 hPa

Values outside this range are not recommended for scientific use.

**Estimated precision:** Only use values for which the estimated precision is a positive number.

Values where the *a priori* information has a strong influence are flagged with negative or zero precision, and should not be used in scientific analyses (see Section 1.5).

**Status flag:** Only use profiles for which the **Status** field is an even number.

Odd values of Status indicate that the profile should not be used in scientific studies. See Section 1.6 for more information on the interpretation of the Status field.

### 3.12.7 Data screening – upper troposphere, lower stratosphere (pressures of 22 hPa or greater)

The **Quality** and **Convergence** fields included in the HNO<sub>3</sub> swath in the standard L2GP-HNO<sub>3</sub> files are appropriate for use in screening at levels at and below (that is, pressures greater than) 22 hPa. For those levels:

**Quality:** Only profiles whose **Quality** field is greater than 0.8 should be used.

This threshold for **Quality** typically excludes ~1 – 3% of HNO<sub>3</sub> profiles on a daily basis; it is a conservative value that potentially discards a significant fraction of “good” data points while not necessarily identifying all “bad” ones. A significant fraction of the HNO<sub>3</sub> profiles in v4.2x show a “notch”, with unexpectedly low (often negative in the tropics) values at 100 hPa and high values at 147 hPa; many such profiles are removed by using this **Quality** threshold.

**Convergence:** Only profiles whose **Convergence** field is less than 1.03 should be used.

On a typical day this threshold for **Convergence** discards a very small fraction of the data, rarely eliminating more than 0.1% of the HNO<sub>3</sub> profiles. Some such profiles show unphysical behavior.

**Clouds:** Clouds impact HNO<sub>3</sub> data in the UTLS, see discussion below and the discussion on “outliers” that follows.

Nonzero but even values of **Status** indicate that the profile has been marked as questionable, typically because the measurements may have been affected by the presence of thick clouds. Globally ~1 – 2% of profiles are identified in this manner, with the fraction of profiles possibly impacted by clouds rising to ~5% on average in the tropics. Clouds generally have little influence on the stratospheric HNO<sub>3</sub> data. In the lowermost stratosphere and upper troposphere, however, thick clouds can lead to spikes in the HNO<sub>3</sub> mixing ratios in the equatorial regions.

Therefore, it is recommended that at and below 68 hPa, in addition to performing the “outlier screening” described below, all profiles with nonzero values of **Status** be discarded because of the potential for cloud contamination. While this will reject some profiles that are probably not significantly impacted by cloud effects, and the number of profiles rejected that are not flagged by other criteria is small (~0.5 to 1% of total profiles), it does eliminate some unphysical profiles that are not flagged by the outlier screening.



**Outliers: Alternative screening approaches in the UTLS remove outliers while reducing “false positives”**

While the number, and particularly the extreme values of, outliers in v4.2x HNO<sub>3</sub> at levels between 316 and 100 (sometimes to 68) hPa is greatly reduced over that in v3.3, such outliers are still present. These typically appear as highly negative mixing ratios at the lowest several retrieval levels, often as part of oscillatory profiles with unrealistically high values at higher altitudes. A simple procedure is recommended to screen such profiles based on eliminating all profiles with large negative mixing ratios at pressure levels between 316 and 68 hPa. Through extensive examination of data screened in this way, flagging profiles that have either HNO<sub>3</sub> vmr less than  $-2.0$  ppbv at 316 hPa or less than  $-1.6$  ppbv at any level between 215 and 68 hPa eliminates most of the troublesome outliers, including those with positive vmr spikes overlying the negative ones that are directly flagged by these criteria. This screening procedure is recommended for any studies focusing on the UTLS. A detailed description of the testing procedure for this screening is given by *Livesey et al.* [2013], and this testing has demonstrated that it effectively removes most of the suspect profiles that are not eliminated by requiring Status to be zero.

Figure 3.12.4 shows an example of the results of screening profiles by each of the Quality, Convergence and the recommended outlier flagging on a typical ‘bad’ day (i.e., one with a relatively large number of outliers) in v4.2x versus v3.3. The Quality screening removes many of the profiles that are strongly negative at the bottom, as well as many (but not all) with the “notch” structure between 147 and 100 hPa. Most or all of the remainder of the profiles that are strongly negative at the bottom are flagged by the outlier screening; many of these profiles are oscillatory, so this screening also removes most or all of the strong positive outliers (typically at 147 hPa). Most of the profiles flagged by any of the criteria are in the tropics, as expected; low HNO<sub>3</sub> values in Antarctic winter resulting from denitrification are rarely, if ever, affected by this outlier screening. It is clear from this example that the outliers in v4.2x are less frequent and much less extreme than those in v3.3

**3.12.8 Data screening – upper stratosphere (pressures of 15 hPa or less)**

The above screening criteria *should not be used* for 15 hPa and higher altitudes, as they result in filtering profiles for which all quality indicators are good when the Quality and Convergence values are properly taken from the 190-GHz HNO<sub>3</sub> information, and not filtering ones with indications of poor quality. The HNO<sub>3</sub>-190 swath has been included in the standard HNO<sub>3</sub> files for v4.2x, and the appropriate Quality and Convergence values for the 190-GHz HNO<sub>3</sub> from that swath must be used to apply the following screening criteria:

**Clouds:** Profiles where the Status field for HNO<sub>3</sub>-190 has a non-zero even number can be used without restriction.

Clouds generally have little influence on the stratospheric HNO<sub>3</sub> data at these altitudes.

**Quality:** Only profiles with a value of the Quality field for HNO<sub>3</sub>-190 (see section 1.6) *greater than 0.8* should be used in scientific study.

This threshold for Quality typically excludes  $\sim 1 - 3\%$  of HNO<sub>3</sub> profiles on a daily basis; it is a conservative value that potentially discards some “good” data points while not necessarily identifying all “bad” ones.

**Convergence:** Only profiles with a value of the Convergence field (see section 1.6) for the HNO<sub>3</sub>-190 product *less than 1.4* should be used in investigations.

On a typical day this threshold for Convergence discards  $\sim 0.5 - 1.5\%$  of the HNO<sub>3</sub> profiles. Many of the profiles thus flagged show some unphysical behavior, especially at the highest altitudes in the recommended range.

**Outliers:** For levels at and above (pressures less than) 4.6 hPa, especially at 2.2 hPa and above, some profiles show vertically oscillatory behavior in conditions where HNO<sub>3</sub> is very low. The Quality and



**Table 3.12.1:** Summary of Aura MLS v4.2x HNO<sub>3</sub> Characteristics

Pressure / hPa	Resolution V × H <sup>a</sup> / km	Precision <sup>b</sup> / ppbv	Systematic Uncertainty <sup>c</sup> / ppbv	Comments
0.68 – 0.001	—	—	—	Unsuitable for scientific use
1.5 – 1.0	4.5 × 550 – 750	±1.2	±0.3	Caution, averaging recommended
2.1	5 × 450 – 500	±0.8	±0.5	
3.2	4.5 × 400	±0.6	±0.1	
15 – 4.6	3 – 4 × 250 – 350	±0.6	±0.5	
22	4.5 × 500	±0.6	±2.4	
32	4 × 400	±0.6	±1.5	
147 – 46	3 – 4 × 350 – 400	±0.6	±1.0	
215	4 – 4.5 × 450	±0.6	±1.1	
316	—	—	—	Unsuitable for scientific use
1000 – 464	—	—	—	Not retrieved

<sup>a</sup>Horizontal resolution in along-track direction.

<sup>b</sup>Precision on individual profiles, determined from observed scatter in the data in a region of minimal atmospheric variability.

<sup>c</sup>Values should be interpreted as 2- $\sigma$  estimates of the probable magnitude.

Help	S
Overview	S
Table	S
BrO	T
CH <sub>3</sub> Cl	S
CH <sub>3</sub> CN	T
CH <sub>3</sub> OH	S
ClO	T
CO	S
GPH	T
H <sub>2</sub> O	S
HCl	T
HCN	S
HNO <sub>3</sub>	T
HO <sub>2</sub>	S
HOCl	T
IWC	S
IWP	T
N <sub>2</sub> O	S
O <sub>3</sub>	T
OH	S
RHI	T
SO <sub>2</sub>	S
	T

### 3.13 Peroxy Radical (HO<sub>2</sub>)

**Swath name:** HO2

**Useful range:** 22 – 0.046 hPa

**Contact:** Luis Millan, **Email:** <Luis.F.Millan@jpl.nasa.gov> and Shuhui Wang, **Email:** <shw@gps.caltech.edu>

#### 3.13.1 Introduction

A description of HO<sub>2</sub> data quality, precision, systematic errors, and validation for an earlier version, v2.2, is given in *Pickett et al.* [2006b]. An early validation using v1.5 software is also described in *Pickett et al.* [2006b]. The estimated uncertainties, precisions, and resolution for v4.2x HO<sub>2</sub> are summarized below in Table 3.13.1.

An algorithm to retrieve daily zonal means of HO<sub>2</sub> over an extended vertical range by first averaging the radiances has been developed by the MLS team [*Millán et al.*, 2015]. This alternative dataset is the first long-term daytime and nighttime HO<sub>2</sub> satellite record covering the stratosphere and the mesosphere. In the near future, this dataset will be available at the GFSC DISC, in the meantime, those interested in using it are advised to contact the MLS team.

#### 3.13.2 Resolution

Figure 3.13.1 shows the HO<sub>2</sub> averaging kernel for daytime at 70°N and the Equator. The latitudinal variation in the averaging kernel is very small. The vertical resolution for pressures greater than 0.1 hPa is generally about 5 km.

#### 3.13.3 Precision

A typical HO<sub>2</sub> profile and the associated precisions (for both v3.3x and v3.4x and v4.2x) are shown in Figure 3.13.2. The profile is shown in both volume mixing ratio (vmr) and density units. All MLS data are reported in vmr for consistency with the other retrieved molecules. However, use of density units (10<sup>6</sup> cm<sup>-3</sup>) reduces the apparent steep gradient of HO<sub>2</sub> vertical profile, allowing one to see the profile with more detail. The night HO<sub>2</sub> profile is expected to exhibit a narrow layer near the altitudes of the nighttime OH layer at ~82 km [*Pickett et al.*, 2006a], which is not shown in Figure 3.13.2 since MLS HO<sub>2</sub> data is not recommended for altitudes above 0.046 hPa (~70 km). Precisions are such that an HO<sub>2</sub> zonal average within a 10° latitude bin can be determined with better than 10% relative precision with 20 days of data (~2000 samples) for most pressure levels over 22 – 0.046 hPa.

#### 3.13.4 Accuracy

Table 3.13.1 summarizes the accuracy expected for HO<sub>2</sub>. The effect of each identified source of systematic error on MLS measurements of radiance has been quantified and modeled [*Read et al.*, 2007]. These quantified effects correspond to either 2σ estimates of uncertainties in each MLS product, or an estimate of the maximum reasonable uncertainty based on instrument knowledge and/or design requirements. These accuracy calculations were performed with more realistic HO<sub>2</sub> atmospheric profiles than for v3.3x and v3.4x estimates. The HO<sub>2</sub> bias can be eliminated by taking day-night differences over the entire recommended pressure range. The overall uncertainty is the square root of the sum of squares of the precision and accuracy.

#### 3.13.5 Data screening

It is recommended that HO<sub>2</sub> data values be used in scientific investigations if all the following tests are successful:

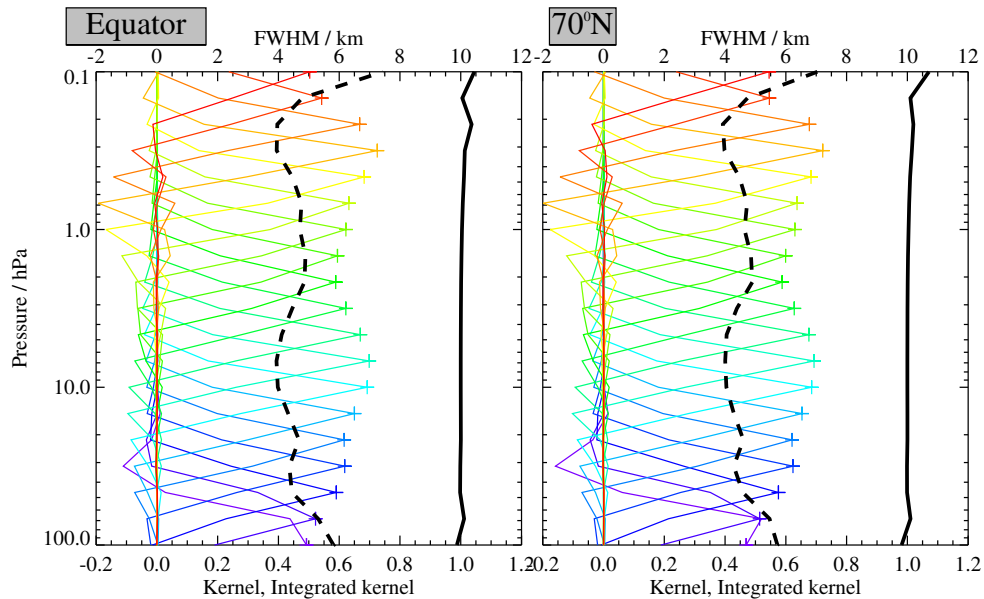


**Figure 3.13.1:** Typical vertical averaging kernels for the MLS v4.2x HO<sub>2</sub> data at the equator (left) and at 70°N (right); variation in the averaging kernels is sufficiently small that these are representative of typical profiles. Colored lines show the averaging kernels as a function of MLS retrieval level, indicating the region of the atmosphere from which information is contributing to the measurements on the individual retrieval surfaces, which are denoted by plus signs in corresponding colors. The dashed black line indicates the vertical resolution, determined from the full width at half maximum (FWHM) of the averaging kernels, approximately scaled into kilometers (top axes). The solid black line shows the integrated area under each kernel; values near unity imply that the majority of information for that MLS data point has come from the measurements, whereas lower values imply substantial contributions from a priori information. The low signal to noise for this product necessitates the use of significant averaging (e.g., monthly zonal mean), making horizontal averaging kernels largely irrelevant.

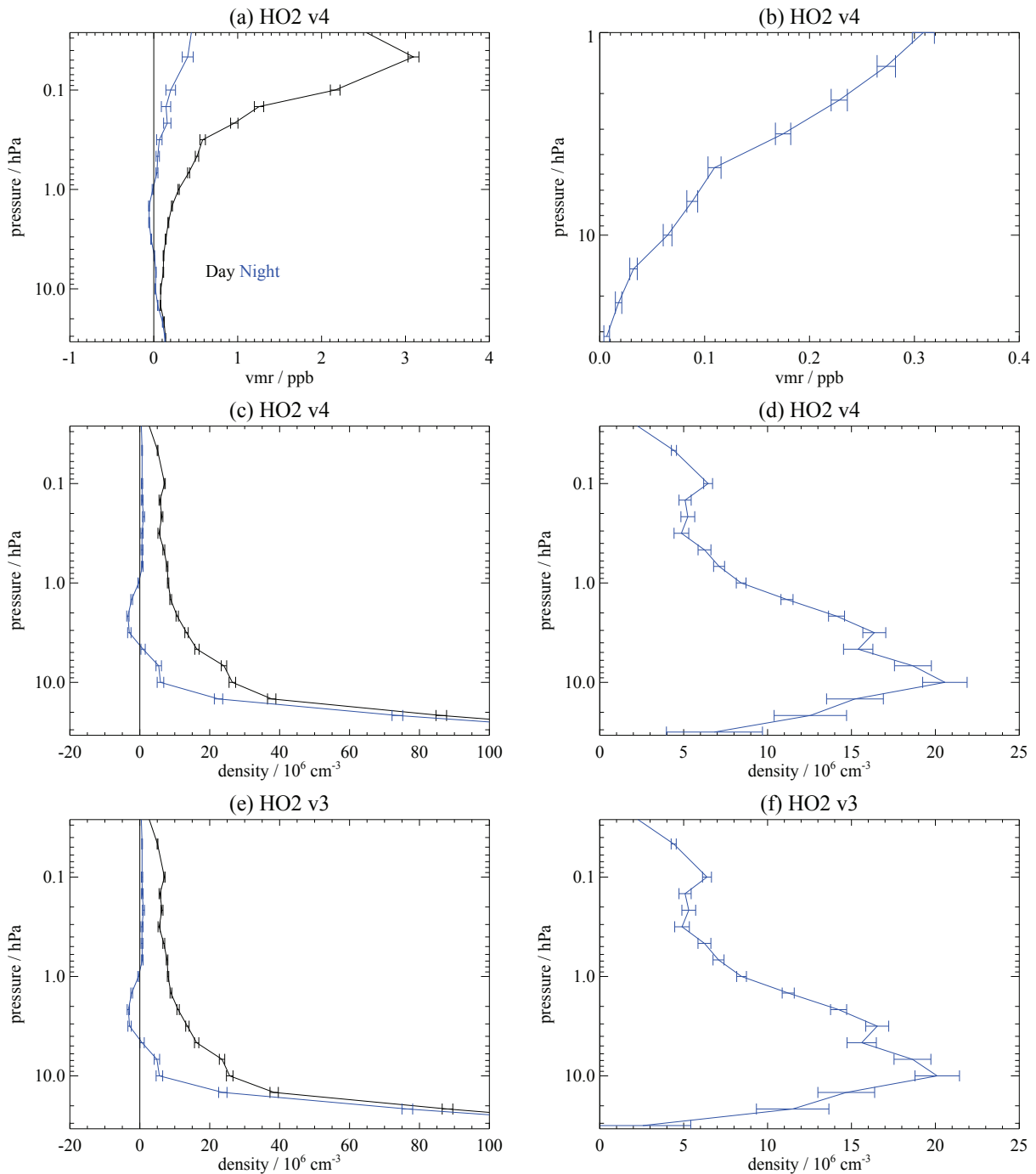


**Figure 3.13.2:** Monthly zonal mean of retrieved HO<sub>2</sub> and its estimated precision (horizontal error bars) for September, 2005 averaged over 29°N to 39°N. Panel (a) shows v4.2x HO<sub>2</sub> vmr vs. pressure for day (black) and night (blue). Panel (b) shows the same data plotted for the stratosphere as a day-night difference (note that a day-night difference is required for HO<sub>2</sub> for all pressure levels). Panel (c) shows the same data in (a) converted into density units. Panel (d) shows the day-night differences for the data in panel (c). Panels (e) and (f) are equivalent to (c) and (d) but using v3.3x and v3.4x data. The average in panels (a) – (d) using v4.2x data includes 3052 profiles, while the average in panels (e) – (f) using v3.3x and v3.4x data includes 2695 profiles.

**Table 3.13.1:** Summary of precisions, resolution, and uncertainties for the MLS v4.2x HO<sub>2</sub> product

Pressure / hPa	Vertical resolution km	Precision <sup>a</sup> / 10 <sup>6</sup> cm <sup>-3</sup>	Day-night accuracy / 10 <sup>6</sup> cm <sup>-3</sup>	Comments
< 0.03 hPa	—	—	—	Unsuitable for scientific use
0.046 hPa	10	6	0.01	Use day-night difference
0.10 hPa	7	10	0.2	Use day-night difference
1.0 hPa	5	11	0.2	Use day-night difference
10 hPa	4	50	14	Use day-night difference
> 22 hPa	—	—	—	Unsuitable for scientific use

<sup>a</sup>Precision for a single profile

**Pressure range: 22 – 0.046 hPa**

Values outside this range are not recommended for scientific use.

**Estimated precision: Only use values for which the estimated precision is a positive number.**

Values where the *a priori* information has a strong influence are flagged with negative or zero precision, and should not be used in scientific analyses (see Section 1.5).

**Status flag: Only use profiles for which the Status field is an even number.**

Odd values of Status indicate that the profile should not be used in scientific studies. See Section 1.6 for more information on the interpretation of the Status field.

**Quality: MLS v4.2x HO<sub>2</sub> data can be used irrespective of the value of the Quality field.**

**Convergence: Only profiles whose Convergence field is less than 1.1 should be used.**

In version v2.2 this test often fails for 100 out of 3500 profiles in a day. In the current version, v4.2x, there are often zero or very few non-converged profiles.

### 3.13.6 Artifacts

Currently there are no known artifacts in the HO<sub>2</sub> product. The primary limitation is the precision and the altitude range.

### 3.13.7 Review of comparisons with other datasets

HO<sub>2</sub> data from MLS v2.2 software have been validated with two balloon-borne remote-sensing instruments. Details of the comparison are given in *Pickett et al.* [2006b]. Differences between v2.2 and v4.2x show no differences large enough to alter results of previous validation studies.

Help	
Overview	
Table	
BrO	S
CH <sub>3</sub> Cl	S
CH <sub>3</sub> CN	T
CH <sub>3</sub> OH	S
ClO	T
CO	S
GPH	T
H <sub>2</sub> O	S
HCl	T
HCN	S
HNO <sub>3</sub>	T
HO <sub>2</sub>	S
HOCl	T
IWC	S
IWP	T
N <sub>2</sub> O	S
O <sub>3</sub>	T
OH	S
RHI	T
SO <sub>2</sub>	S
	T

## 3.14 Hypochlorous Acid (HOCl)

**Swath name:** HOCl

**Useful range:** 10 – 2.2 hPa

**Contact:** Lucien Froidevaux, **Email:** <Lucien.Froidevaux@jpl.nasa.gov>

### 3.14.1 Introduction

There has been little change in the v4.2 HOCl retrieval results, in comparison to v3.3/v3.4. We provide below sample mean HOCl distributions for the two data versions, and their differences. Otherwise, previous information regarding this species remains largely unchanged; the main points are mentioned here mainly for new data users.

The HOCl retrieval is quite noisy for individual profiles and HOCl data require some averaging (e.g., in 10° zonal means for one or more weeks) to get useful precision of better than 10 pptv, in comparison to typical upper stratospheric HOCl abundances of 100 – 150 pptv. Table 3.14.1 summarizes the MLS HOCl resolution, precision, and accuracy estimates for the upper stratosphere. More discussion and a brief validation summary are given in the following sections, along with data screening recommendations, which should be of particular interest to MLS data users.

### 3.14.2 Changes from v3.3/v3.4

There were no algorithmic changes relating to HOCl for the v4.2 retrievals. Small differences in HOCl abundances (see below) are likely related mainly to small changes in tangent pressure and/or temperature.

The background observed in the 640-GHz radiances includes emissions from N<sub>2</sub>, O<sub>2</sub>, and H<sub>2</sub>O. There are laboratory-based and ground-based models for the continuum absorptions that are the basis for the MLS absorption model [*Pardo et al.*, 2001, and references therein]. These models were tested against MLS extinction measurements from the wing channels in the 640-GHz radiometer. The latitude dependence of this extinction was found to agree better with the expected most plus dry continuum extinction values if the dry and moist continuum functions were scaled by factors close to 20%; however, this is not a change from the v3.3/v3.4 retrievals.

A comparison plot showing zonal average upper stratospheric HOCl contours (from 10 to 2 hPa) and differences between the two data versions for a typical month (March, 2009) is provided in Figure 3.14.1. The v4.2 HOCl abundances are mostly slightly larger than the v3.3 retrievals, typically by only a few pptv (a few percent). The estimated precision values are essentially unchanged from v3.3.

### 3.14.3 Resolution

Based on the width of the averaging kernels shown in Figure 3.14.2, the vertical resolution for upper stratospheric HOCl is ~6 km (significantly worse than the 640-GHz radiometer vertical field of view width of 1.4 km). This reflects the choice of smoothing constraints for HOCl which favor precision over vertical resolution.

### 3.14.4 Precision

The estimated single-profile precision reported by the Level 2 software is about 300 to 400 pptv in the upper stratosphere. A more useful number of 10 pptv is quoted in Table 3.14.1 for the typical precision of a 10° weekly zonal means for this product.



Averages for March, 2009

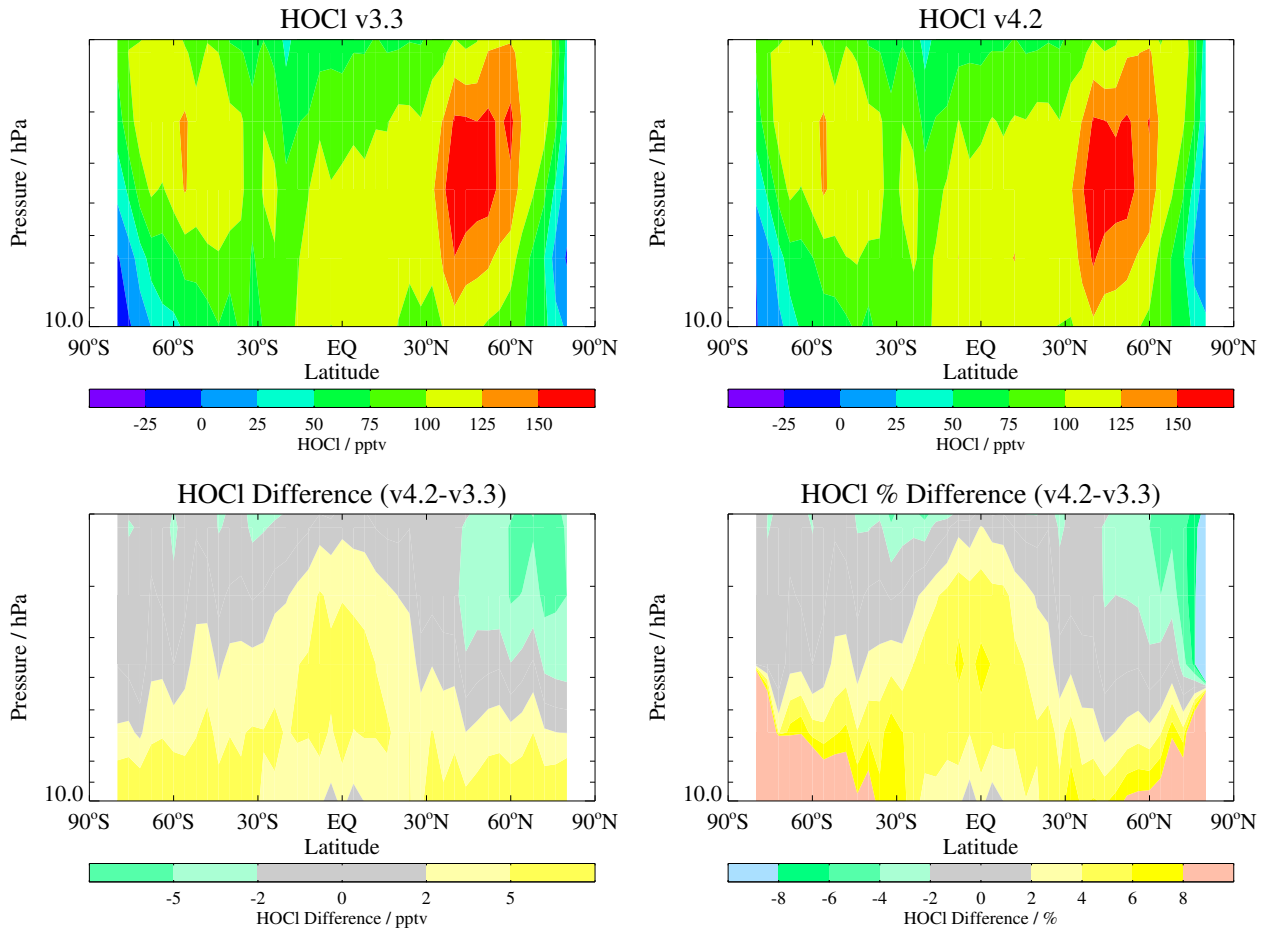


**Figure 3.14.1:** Zonal averages for upper stratospheric MLS HOCl profiles during March, 2009, showing the MLS v3.3 HOCl mixing ratio contours (top left panel), the v4.2 contours (top right panel), and their differences in pptv (v4.2 minus v3.3, bottom left panel) and percent (v4.2 minus v3.3 versus v3.3, bottom right panel).

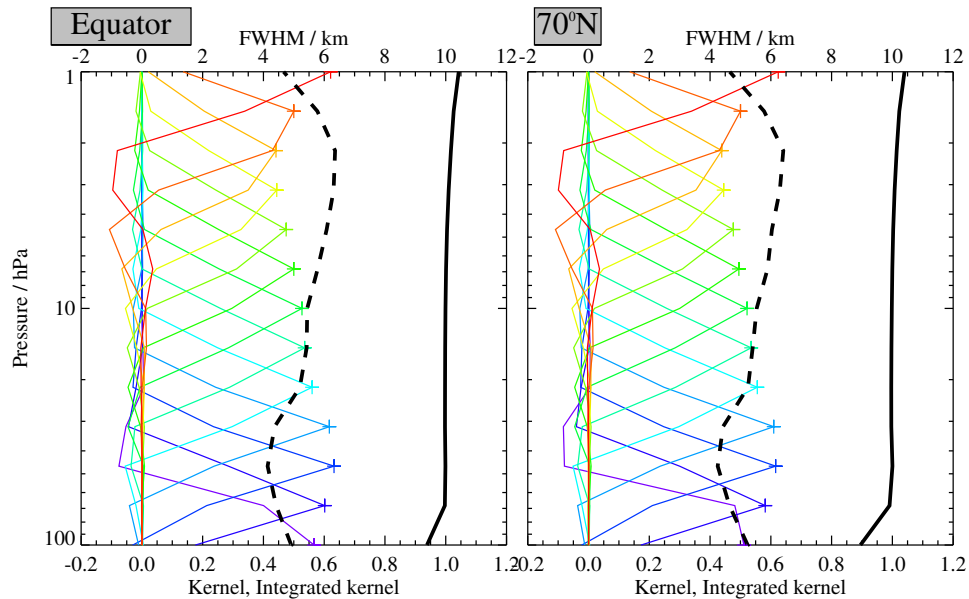


**Figure 3.14.2:** Typical vertical averaging kernels for the MLS v4.2x HOCl data at the equator (left) and at 70°N (right); variation in the averaging kernels is sufficiently small that these are representative of typical profiles. Colored lines show the averaging kernels as a function of MLS retrieval level, indicating the region of the atmosphere from which information is contributing to the measurements on the individual retrieval surfaces, which are denoted by plus signs in corresponding colors. The dashed black line indicates the vertical resolution, determined from the full width at half maximum (FWHM) of the averaging kernels, approximately scaled into kilometers (top axes). The solid black line shows the integrated area under each kernel; values near unity imply that the majority of information for that MLS data point has come from the measurements, whereas lower values imply substantial contributions from a priori information. The low signal to noise for this product necessitates the use of significant averaging (e.g., monthly zonal mean), making horizontal averaging kernels largely irrelevant.

### 3.14.5 Accuracy

The accuracy estimates shown in Table 3.14.1 come from a formal quantification of the combined effects of possible systematic errors in MLS calibration, spectroscopy, etc. on the HOCl retrievals [Read *et al.*, 2007]. These (updated) values are intended to represent  $2\sigma$  estimates of accuracy. The largest contributors to possible errors for HOCl are contaminant species, gain compression, and sideband ratio uncertainties. The Table gives a range of error estimates (for the range of pressures). The average changes for upper stratospheric HOCl between v3.3 and v4.2 are well within the quoted accuracy estimates (which may be somewhat conservative). The HOCl signal becomes too small compared to the systematic uncertainties to allow for reliable retrievals at pressures larger than 10 hPa.

### 3.14.6 Data screening

**Pressure range: 10 – 2.2 hPa**

Values outside this range are not recommended for scientific use. Artifacts (negative averages) for pressures larger than about 10 hPa make this product unsuitable for use in the lower stratosphere. Regarding the topmost altitude range, the sensitivity to *a priori* increases rapidly at pressures of 1 hPa or less; we continue to recommend the use of (average) HOCl values only up to 2.2 hPa.

**Estimated precision: Only use values for which the estimated precision is a positive number.**

Values where the *a priori* information has a strong influence are flagged with negative or zero precision, and should not be used in scientific analyses (see Section 1.5).

**Status flag: Only use profiles for which the Status field is an even number.**

Odd values of Status indicate that the profile should not be used in scientific studies. See Section 1.6 for more information on the interpretation of the Status field.

**Quality field: Only profiles with a value of the Quality field greater than 1.2 should be used.**

This criterion removes profiles with the poorest radiance fits, typically less than 0.1% of the daily profiles. For HOCl (and for other 640-GHz MLS products), this screening correlates well with the poorly converged sets of profiles (see below); we recommend the use of both the Quality and Convergence fields for data screening.

**Convergence field: Only profiles with a value of the Convergence field less than 1.05 should be used.**

For the vast majority of profiles (99% or more for most days), this field is less than 1.05. Nevertheless, on occasion, sets of profiles (typically one or more groups of ten profiles, retrieved as a ‘chunk’) have this Convergence field set to larger values, and should be discarded.

**Clouds: Profiles identified as being affected by clouds can be used with no restriction.**

### 3.14.7 Review of comparisons with other datasets

The MLS HOCl retrievals exhibit the expected morphology in monthly mean latitude / pressure contour plots; for example, such plots for September months from MLS compare favorably, to first-order, with results produced by the Michelson Interferometer for Passive Atmospheric Sounding (MIPAS) for September, 2002 [von Clarmann *et al.*, 2006]. MLS HOCl averages at midlatitudes are close to the results from balloon-borne infrared measurements. Generally favorable comparisons (within the error bars) have been made of the diurnal changes in upper stratospheric HOCl between Aura MLS (v3.3), other satellite datasets, and a 1-D photochemical model [Khosravi *et al.*, 2013].

### 3.14.8 Artifacts

- The 640-GHz radiometer bands 10 (for ClO) and 29 (for HOCl) were turned off for a few time periods in 2006 to investigate degradation issues that might affect these channels in the future. These bands

**Table 3.14.1:** Summary for MLS hypochlorous acid

Pressure hPa	Precision <sup>a</sup>		Vertical Resolution km km	Accuracy <sup>b</sup>		Comments
	pptv	%		pptv	%	
1.5 or less	—	—	—	—	—	Unsuitable for scientific use
2.2 to 10	10	10	6	40 – 80	~150	Some averaging required
15 or more	—	—	—	—	—	Unsuitable for scientific use

<sup>a</sup>Precision ( $1\sigma$ ) for 1 week/10 degrees zonal means or 2 weeks/5 degrees zonal means

<sup>b</sup> $2\sigma$  estimate from systematic uncertainty characterization tests

were off on April 8,9, and 10, 2006, and also for April 17, 2006 (after 19:52 UT) through May 17, 2006. There are essentially no useful HOCl (or ClO) data for these time periods. The v4.2 (as for the v3.3/v3.4) software correctly flags these incidents with poor (odd) Status values (which should be screened out).

- There are significant artifacts in the mean values (large negative values) for HOCl in the lower stratosphere, where the use of this product is not recommended.
- Users should screen out the non-converged and poorest quality HOCl profiles, as such profiles (typically a very small number per day) tend to behave unlike the majority of the other MLS retrievals. See the criteria listed above.

## 3.15 Cloud Ice Water Content (IWC)

**Swath name:** IWC

**Units:** g/m<sup>3</sup>

**Useful range:** 215 – 83 hPa

**Contact:** Alyn Lambert, **Email:** <Alyn.Lambert@jpl.nasa.gov>

### 3.15.1 Introduction

The MLS IWC is retrieved from cloud-induced radiances ( $T_{\text{cir}}$ ) of the 240-GHz window channel in a separate processing step after the atmospheric state (Temperature and tangent pressure) and important gaseous species (H<sub>2</sub>O, O<sub>3</sub>, HNO<sub>3</sub>) have been finalized in the retrieval processing. The derived  $T_{\text{cir}}$  are binned onto the standard horizontal (1.5° along track) and vertical (12 surfaces per decade change in pressure) grids, and converted to IWC using the modeled  $T_{\text{cir}}$  – IWC relations [Wu *et al.*, 2006]. The standard IWC profile has a useful vertical range between 215 – 83 hPa although the validation has been conducted for a subset of the range of IWC values. IWC measurements beyond the value ranges specified in Table 3.15.1 are to be regarded currently as giving only qualitative information on cloud ice. They require further validation for quantitative interpretation.

### 3.15.2 Resolution

In the IWC ranges specified in Table 3.15.1, each MLS measurement can be quantitatively interpreted as the average IWC for the volume sampled. This volume has a vertical extent of ~3 km, with ~300 km and 7 km along and cross track respectively.

### 3.15.3 Precision

The precision values quoted in the IWC files do not represent the true precision of the data. The precision for a particular measurement must be evaluated on a daily basis using the method described in the screening section below. The precision listed in Table 3.15.1 reflects typical values obtained from the method described below.

### 3.15.4 Accuracy

The IWC accuracy values listed in Table 3.15.1 are estimates from comparisons of the earlier v2.2 MLS data product with CloudSat and detailed analyses on the v2.2 error budget can be found in Wu *et al.* [2008].

### 3.15.5 Data screening

**Pressure range (215 – 83 hPa):** Values outside this range are not recommended for scientific use. The maximum detectable IWC is ~100 mg/m<sup>3</sup>.

**Use Temperature Status, Quality and Convergence:** The user is recommended to screen the IWC data using the Status field in the collocated temperature profile to exclude bad retrievals [Schwartz *et al.*, 2008]. In other words, only IWC profiles for which temperature Status is an even number should be used. Similarly, the users should only use IWC profiles where the corresponding Temperature profiles have Quality of 0.9 or larger and Convergence less than 1.03.

**Other screening:** The IWC product derives from differences between measured radiances and those predicted assuming cloud free conditions. Spectroscopic and calibration uncertainties give rise to temporally and geographically varying biases in this difference, and hence the IWC product. These biases must be iteratively identified and removed, using a “2σ – 3σ” screening method, as described below.

1. Uncertainties in spectroscopy and atmospheric composition are manifested as residual biases in the IWC fields which should be identified and removed as follows. IWC data should be averaged in a  $10^\circ$  latitude bins and outliers rejected iteratively by excluding measurements greater than  $2\sigma$  standard deviation about the mean ( $\mu$ ) of the bin. Repeat the  $\sigma$  and  $\mu$  calculations after every new set of rejections. Convergence is usually reached within 5 – 10 iterations, and the final  $\sigma$  is the estimated precision for the IWC measurements.
2. Interpolate the final  $\sigma$  and  $\mu$  to the latitude of each measurement, and subtract  $\mu$  from IWC for each measurement.
3. Finally, apply the  $3\sigma$  threshold to determine if an IWC measurement is statistically significant. In other words, it must have  $IWC > \mu + 3\sigma$  in order to be considered as a significant cloud hit. The  $3\sigma$  threshold is needed for cloud detection since a small percentage of clear-sky residual noise can result in a large percentage of “false alarms” in cloud detection.

### 3.15.6 Artifacts

At wintertime mid-to-high latitudes, strong stratospheric gravity waves may induce large fluctuations in the retrieved tangent pressure, and cause false cloud detection with the  $2\sigma - 3\sigma$  screening method. The false cloud detection seems to affect the 100 hPa pressure level most, as expected for such impact coming from the lower stratosphere.

### 3.15.7 Comparisons with other datasets

Compared to v2.2 IWC the v4.2x IWC values are within 5% over the pressure range 215 – 100 hPa and generally the random noise in v4.2x IWC is larger than in v2.2 (see Figure 3.15.1 and Table 3.15.1). Apart from the differences noted above, the MLS v4.2x IWC is similar to the MLS v2.2 product described and validated in *Wu et al.* [2008]. A revised validation paper for IWC is not planned in the near future and users are encouraged to read *Wu et al.* [2008] for more information.

Comparisons between v2.2 MLS and CloudSat IWC showed good agreement with PDF differences <50% for the IWC ranges specified in Table 3.15.1. Comparisons with AIRS, OMI and MODIS suggest that MLS cloud tops are slightly higher by ~1 km than the correlative data in general.

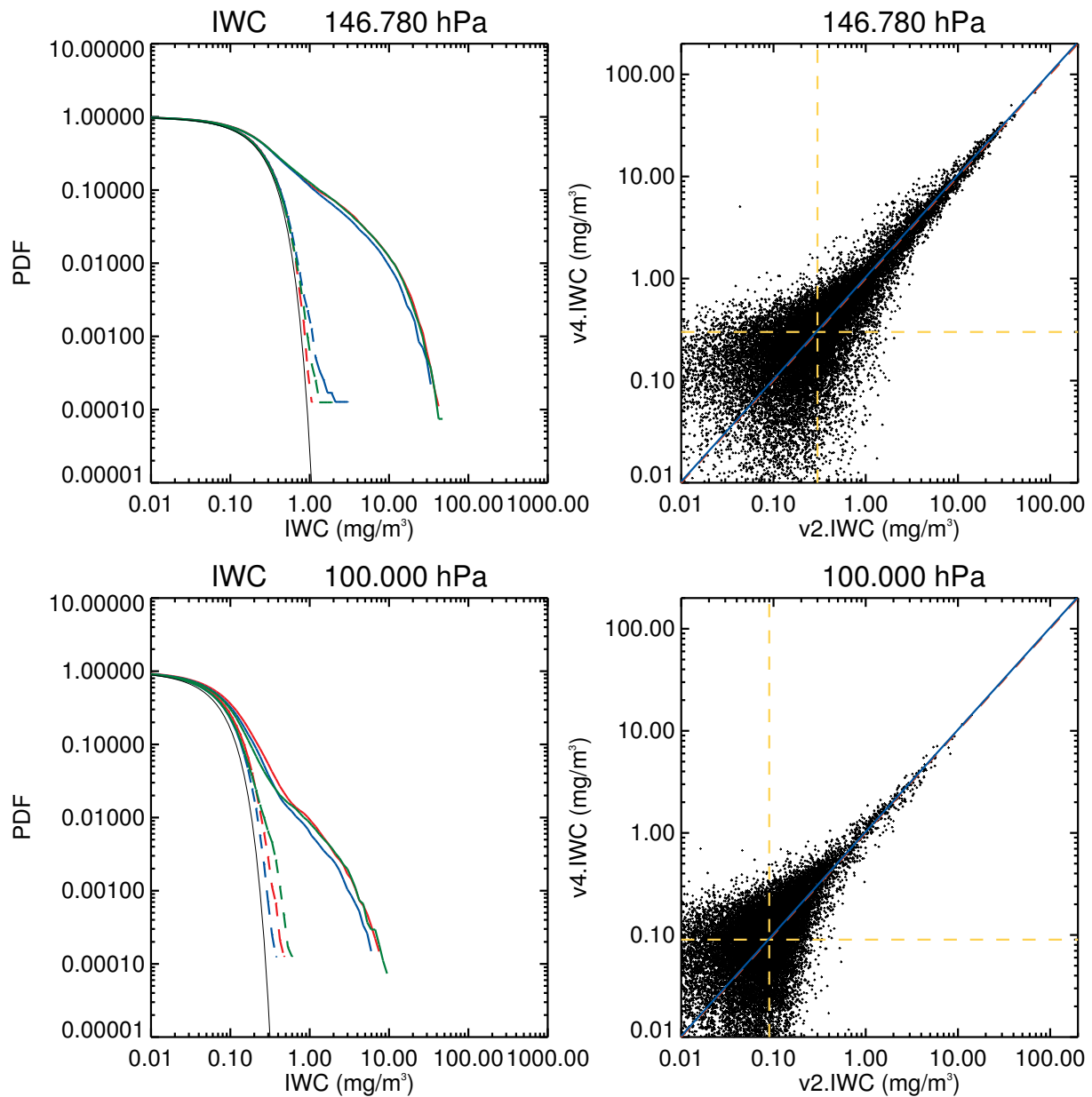


**Figure 3.15.1:** MLS v4, v3 and v2 IWC comparisons for July 2009 at 146 hPa and 100 hPa. (a) Left: Probability density functions (PDF) (v4, red; v3, blue; and v2, green) with dashed lines showing the corresponding noise levels (obtained by folding the negative IWC values about the origin) and the thin black lines representing the gaussian error function. (b) Right: Scatter plots of IWC v4 vs. v2 (black points) with dashed red lines indicating the 1:1 line, dashed yellow lines the  $1\sigma$  uncertainties and the blue lines are linear fits to the data.

**Table 3.15.1:** Summary of MLS v4.2x IWC precision, accuracy, and resolution.

Pressure / hPa	Resolution <sup>a</sup> / km	Typical precision <sup>b</sup> / mg/m <sup>3</sup>	Accuracy <sup>c</sup> / mg/m <sup>3</sup>		Valid IWC range <sup>d</sup> / mg/m <sup>3</sup>
			<10 mg/m <sup>3</sup>	>10 mg/m <sup>3</sup>	
p<70		Unsuitable for scientific use			
83	200×7×5	0.07	100%	—	0.02 – 50
100	200×7×5	0.10	100%	150%	0.02 – 50
121	250×7×4	0.15	100%	100%	0.04 – 50
147	300×7×4	0.25 – 0.35	100%	100%	0.1 – 50
177	300×7×4	0.5 – 1.0	150%	100%	0.3 – 50
215	300×7×4	1.2 – 2.1	300%	100%	0.6 – 50
p>260		Unsuitable for scientific use			

<sup>a</sup>The along-track, cross-track and vertical extent, respectively of the atmospheric volume sampled by an individual MLS measurement.

<sup>b</sup>These are typical  $1\sigma$  precisions where the better values are for the extratropics and the poorer values for the tropics. The precision for a particular measurement must be evaluated on a daily basis using the method described in the text.

<sup>c</sup>Estimated from comparisons with CloudSat.

<sup>d</sup>This is the range where the stated precision, accuracy and resolution are applied. In this range MLS measurements can be quantitatively interpreted as the average IWC for the volume sampled. IWC values above this range, currently giving qualitative information on cloud ice, require further validation for quantitative interpretation.



### 3.16 Cloud Ice Water Path (IWP)

**Swath name:** IWP (stored as an additional swath in the L2GP-IWC file).

**Units:** g/m<sup>2</sup>

**Useful range:** MLS IWP is the ice water column above ~6 km

**Contact:** Alyn Lambert, **Email:** <Alyn.Lambert@jpl.nasa.gov>

#### 3.16.1 Introduction

MLS standard IWP is retrieved from cloud-induced radiances ( $T_{\text{cir}}$ ) of the 240-GHz window channel at 650 hPa tangent pressure (see Figure 3.16.1). It represents a partial column above ~6 km, and is stored in the v4.2x L2GP IWC file as a separate swath. For the IWP retrieval,  $T_{\text{cir}}$  is first converted to a near horizontal slant path (with a ~3° elevation angle) IWP “hIWP”, using the modeled  $T_{\text{cir}}$  – hIWP relation. The hIWP is then converted to the nadir IWP at the tangent point location, and interpolated to the MLS standard horizontal grid.

#### 3.16.2 Resolution

In the IWP ranges specified in the summary at the end of this section, each MLS measurement can be quantitatively interpreted as the average IWP for the volume sampled. The MLS IWP volume is a vertical column above ~6 km, with 60 km and 7 km along and cross track extent respectively.

#### 3.16.3 Precision

The precision values quoted in the IWP swaths do not represent the true precision of the data. The precision for a particular measurement must be evaluated on a daily basis using the method described in the screening section below. The 3 g/m<sup>2</sup> precision given the summary at the end of this section reflects *typical values* for MLS IWP measurements.

#### 3.16.4 Accuracy

The IWP accuracy is ~50%, as estimated from comparisons of the earlier v2.2 MLS data product with CloudSat and detailed analyses on the v2.2 error budget can be found in *Wu et al.* [2009].

#### 3.16.5 Data screening

**Sensitivity:** The standard IWP product has a useful sensitivity up to 200 g/m<sup>2</sup> where MLS measurements can be quantitatively interpreted as the average IWP for the volume sampled.

**Use Temperature Status, Quality and Convergence:** The user is recommended to screen the IWP data using the Status field in the collocated temperature profile to exclude bad retrievals [*Schwartz et al.*, 2008]. In other words, only IWP values for which temperature Status is an even number should be used. Similarly, the users should only use IWP values where the corresponding Temperature profiles have *Quality* of 0.9 or larger and *Convergence* less than 1.03.

**Other screening:** the user is also recommended to screen the IWP data for significant cloud hits on a daily basis using the “2σ – 3σ” method described in the IWC section (3.15). The 3σ threshold is needed for cloud detection since a small percentage of clear-sky residual noise can result in a large percentage of false alarm in cloud detection.

### 3.16.6 Artifacts

High-latitude high-land surface can be mistakenly detected as a cloud when the atmosphere is very dry, allowing MLS 240-GHz radiances to penetrate down to the surface. Surface emission/scattering can then reduce brightness temperature. Surface effects (e.g., over the highland over Antarctica) may introduce artificial IWP values as large as  $10 \text{ g/m}^2$ . In addition, the geographical location of MLS IWP is currently registered at the tangent point, which is  $\sim 2$  profiles away from the actual location of the IWP column as shown in Figure 3.16.1. The user needs to correct this offset by replacing the IWP location with the one at 2 profiles earlier.

### 3.16.7 Comparisons with other datasets

Compared to v2.2 IWP the v4.2x IWP values are systematically larger by  $\sim 2\%$  and the random noise is slightly smaller than in v2.2 (see Figure 3.16.2). Apart from the differences noted above, the MLS v4.2x IWP is similar to the MLS v2.2 product described and validated in *Wu et al.* [2009]. A revised validation paper for IWP is not planned in the near future and users are advised to read *Wu et al.* [2009] for more information.

Comparisons between v2.2 MLS and CloudSat IWP showed good agreement with PDF differences  $< 50\%$  for the IWP range specified in the summary at the end of this section.

### 3.16.8 Desired improvements for future data version(s)

The IWP retrieval in v4.2x is a simple first-order conversion, applied independently to each  $T_{\text{cir}}$  measurement. Plans for future versions include development of 2-D cloudy-sky radiative transfer model. This will allow IWP to be retrieved jointly with the  $T_{\text{cir}}$  measurements from adjacent scans.

### 3.16.9 Summary for IWP

**IWP Column Bottom:** 6 km (estimated from MLS radiative transfer model calculations).

The calculation of the bottom height of the IWP column depends on the tropospheric water vapor loading and on the IWP itself and is discussed in *Wu et al.* [2009].

**Typical precision:**  $3 \text{ g/m}^2$  is the typical  $1\sigma$  precision.

The precision for a particular measurement must be evaluated on a daily basis using the method described in the text.

**Accuracy:** 50% (estimated from comparisons with CloudSat)

**Resolution:** 60 km along track, 7 km across track (the volume of air sampled by MLS)

**Valid IWP range:**  $\leq 200 \text{ g/m}^2$

This is the range where the stated precision, accuracy and resolution are applied. In this range MLS measurements can be quantitatively interpreted as the average IWP for the volume sampled. IWP values above this range, currently giving qualitative information on cloud ice, require further validation for quantitative interpretation.

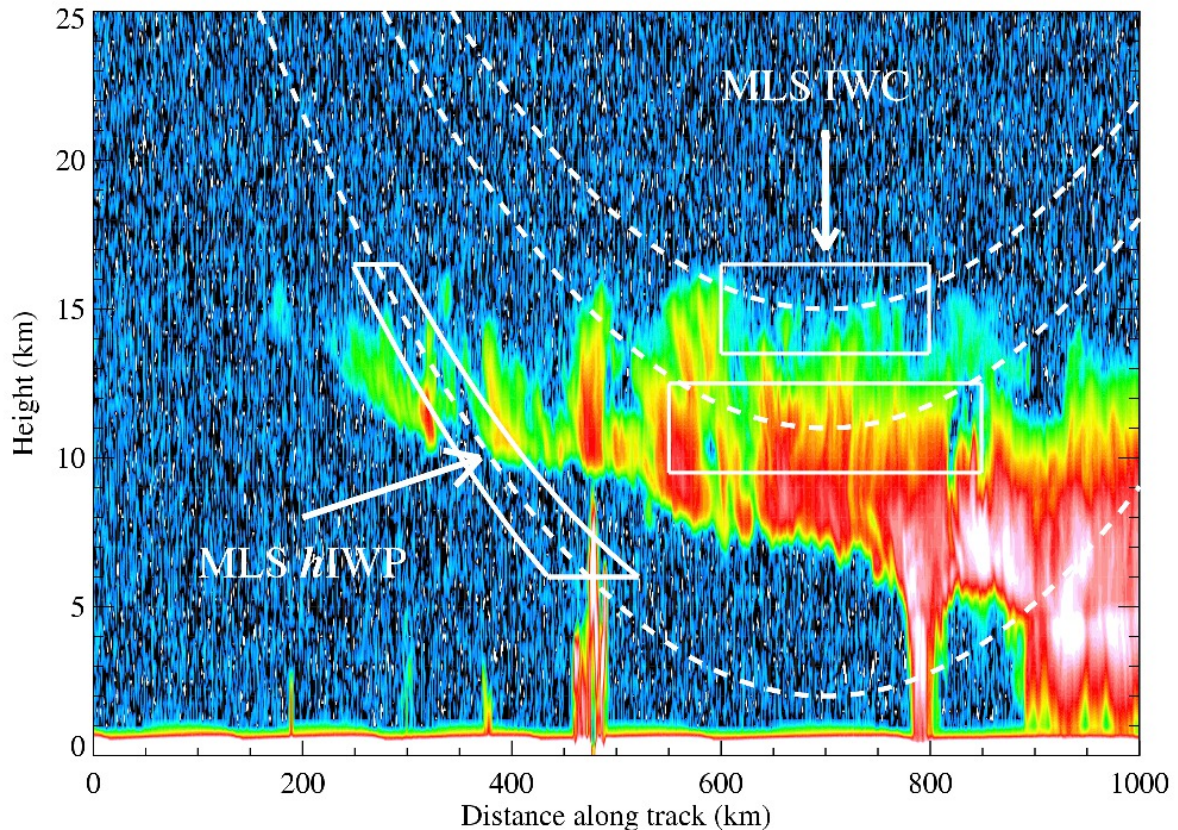


**Figure 3.16.1:** Diagram to illustrate the MLS IWC and IWP measurement. The dashed lines are the MLS tangential beams. At high tangent heights, the beams penetrate through the limb and become sensitive to a volume-averaged IWC, whereas at low tangent heights the MLS beams cannot penetrate through the limb due to strong gaseous absorption and become only sensitive to a partial slant column of IWP, with a shallow ( $\sim 3^\circ$ ) angle, “hIWP”. Note that the actual volume of the air represented by hIWP is centered  $\sim 300$  km away from the tangent point, or  $\sim 2$  profiles from the location of the nominal profile.

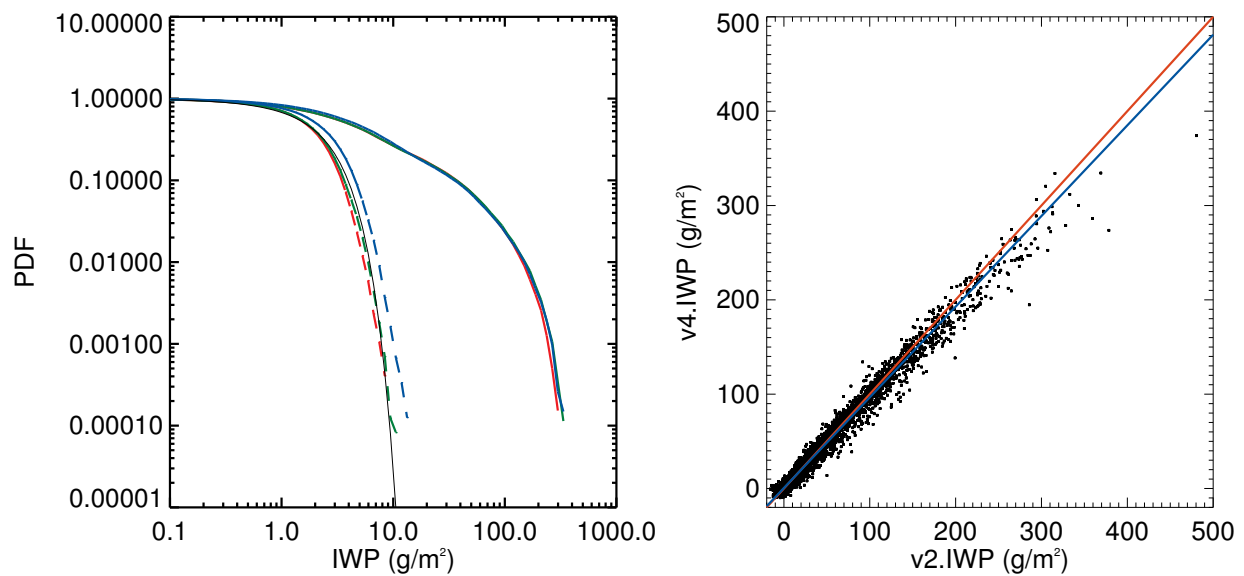


**Figure 3.16.2:** MLS v4, v3 and v2 IWP comparisons for July 2009. (a) Left: Probability density functions (PDF) (v4 (red), v3 (blue) and v2 (green)) with dashed lines showing the corresponding noise levels (obtained by folding the negative IWP values about the origin) and the thin black lines representing the gaussian error function. (b) Right: Scatter plot of IWP v4 vs v2 (black points) with a dashed red lined indicating the 1:1 line and a linear fit to the data shown as a blue line.

## 3.17 Nitrous Oxide (N<sub>2</sub>O)

**Swath name:** N2O

**Useful range:** 68 – 0.46 hPa

**Contact:** Alyn Lambert, **Email:** <Alyn.Lambert@jpl.nasa.gov>

### 3.17.1 Introduction

#### Redefinition of the N<sub>2</sub>O standard product for v4.2x to use band 3 (190-GHz) signals

The standard product for v4.2x N<sub>2</sub>O is taken from the 190-GHz (“Core+R2”) retrieval (N20-190) instead of the 640-GHz (“Core+R4B”) retrieval (N20-640) as used in previous versions.

Aging of the MLS “band 12” (640-GHz) signals was revealed by analysis of housekeeping data during June-August 2013 which showed declining output in counts, increasing radiance noise (variance) and also increasing correlation between the band 12 radiance channels. As the 640 GHz N<sub>2</sub>O product began to show further deterioration in quality a decision was made to turn off band 12 on August 6, 2013. Prior to that, the level-2 processing stream for the N<sub>2</sub>O standard product in v3.x was switched to output the “band 3” (190-GHz, N20-190) retrieval on 7 June 2013 and later data for N20-640 are not recommended for scientific use.

The 190-GHz N<sub>2</sub>O data show slightly worse precision and resolution compared to the 640-GHz retrievals. Data from N20-190 and N20-640 have been compared from launch until the end of band 12 operations. There is a persistent high bias in N20-190 of > 30% at 100 hPa (although some seasonal variations are evident) and we recommend that at this particular pressure level N20-190 only be used in consultation with the MLS science team. A smaller bias of 5–10% at 68 hPa in N20-190 is seen compared to N20-640. From 46 to 3.2 hPa the biases are less than 5% (see Figure 3.17.1).

Other significant differences between the v4.2x N20-190 and N20-640 data such as the resolution, precision, recommended pressure levels, quality and convergence criteria are noted below.

The secondary v4.2x N<sub>2</sub>O 640-GHz product is available for the period from launch until June 6, 2013 and stored in the L2GP-DGG files in the N20-640 swath. Details of the retrieval method and validation results are presented in [*Lambert et al., 2007*].

### 3.17.2 Resolution

The spatial resolution reported by the averaging kernel matrices is shown in Figures 3.17.2 for the 190 GHz measurements and 3.17.3 for the 640 GHz measurements (available in the L2GP-DGG files for data prior to June 6, 2013). For N20-190, the vertical resolution is 4 – 8 km and the horizontal along-track resolution is 300 – 600 km. For N20-640, the vertical resolution is 4 – 6 km and the horizontal along-track resolution is 300 – 600 km over most of the useful range of the retrievals.

The horizontal cross-track resolution is set by the 7 km width of the MLS 190-GHz field-of-view for all pressures. Note that the higher frequency MLS 640-GHz measurements have a narrower 3 km field-of-view. The longitudinal separation of the MLS measurements is 10° – 20° over middle and lower latitudes, with much finer sampling in polar regions.

### 3.17.3 Precision

Precision as defined here is the 1σ uncertainty in the retrieved value calculated by the Level 2 algorithms and has been validated against the scatter about the mean of coincident ascending/descending MLS profile differences. The estimated precision on a single retrieved profile given in Tables 3.17.1 and 3.17.2 varies with height from ~15 – 20 ppbv for N20-190 and ~12 – 25 ppbv for N20-640.

The N<sub>2</sub>O values at the 147 hPa pressure level have a large a priori influence and practically all precisions are flagged negative at this level.

## Zonal Means for Data Over March, 2009

N2O-190, v04.2x

N2O-640, v04.2x

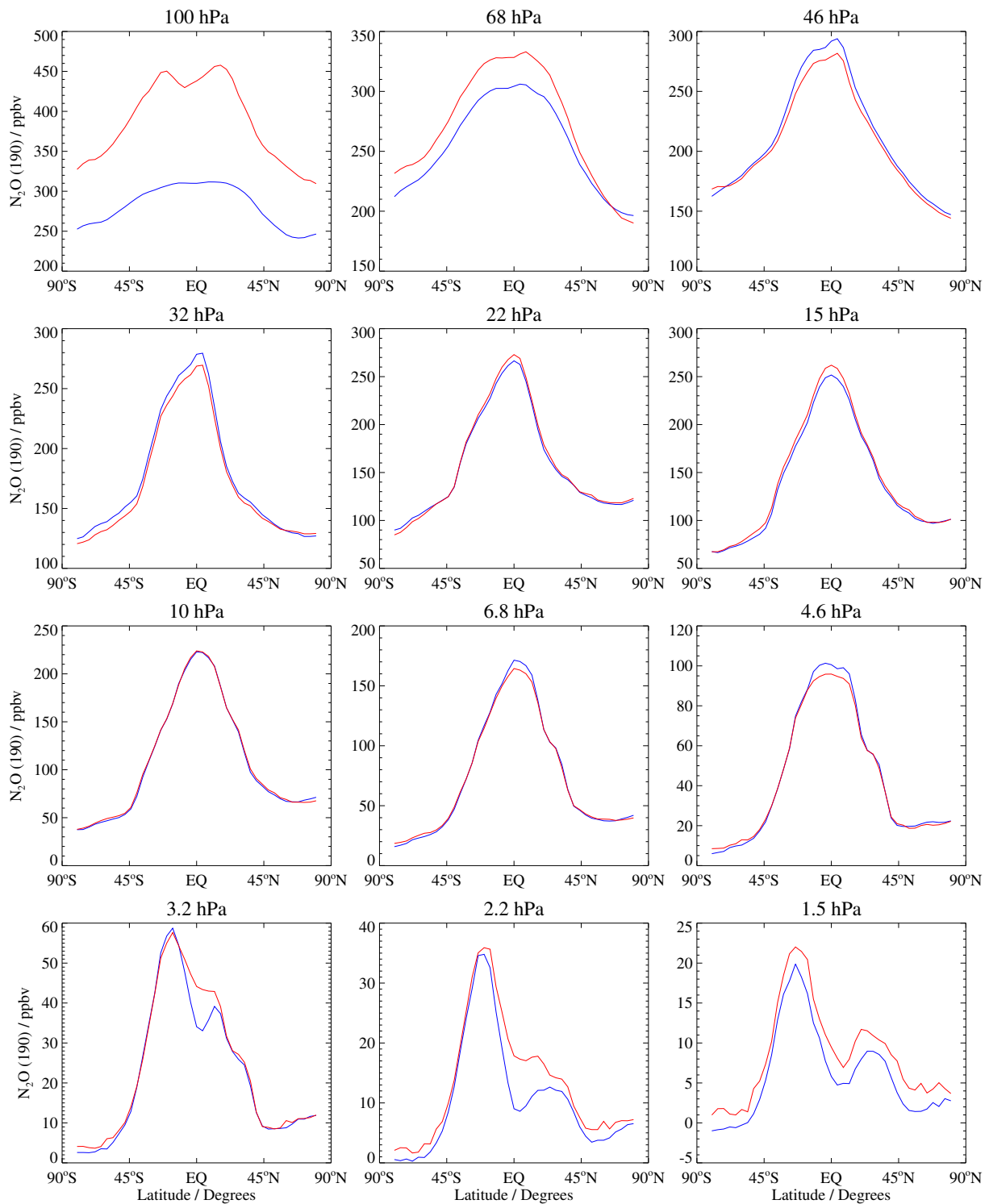
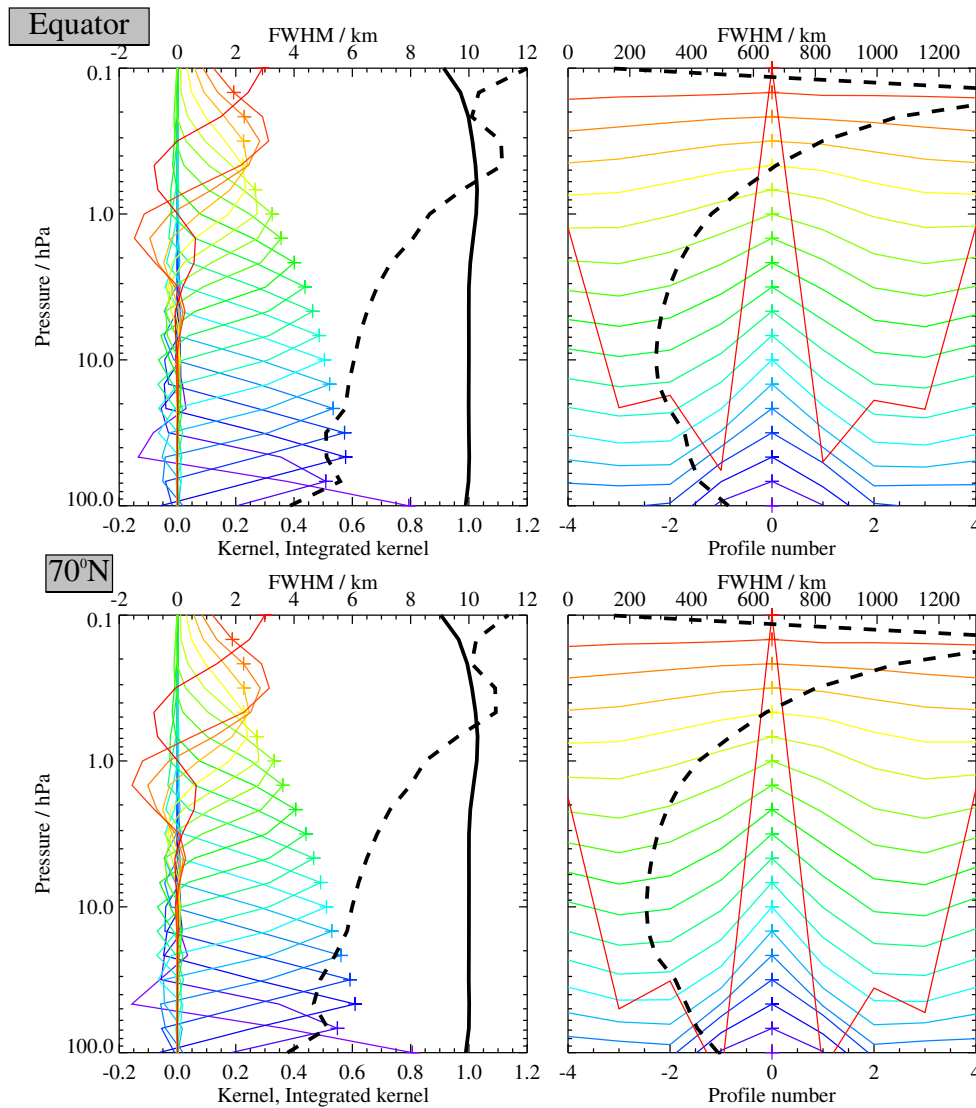
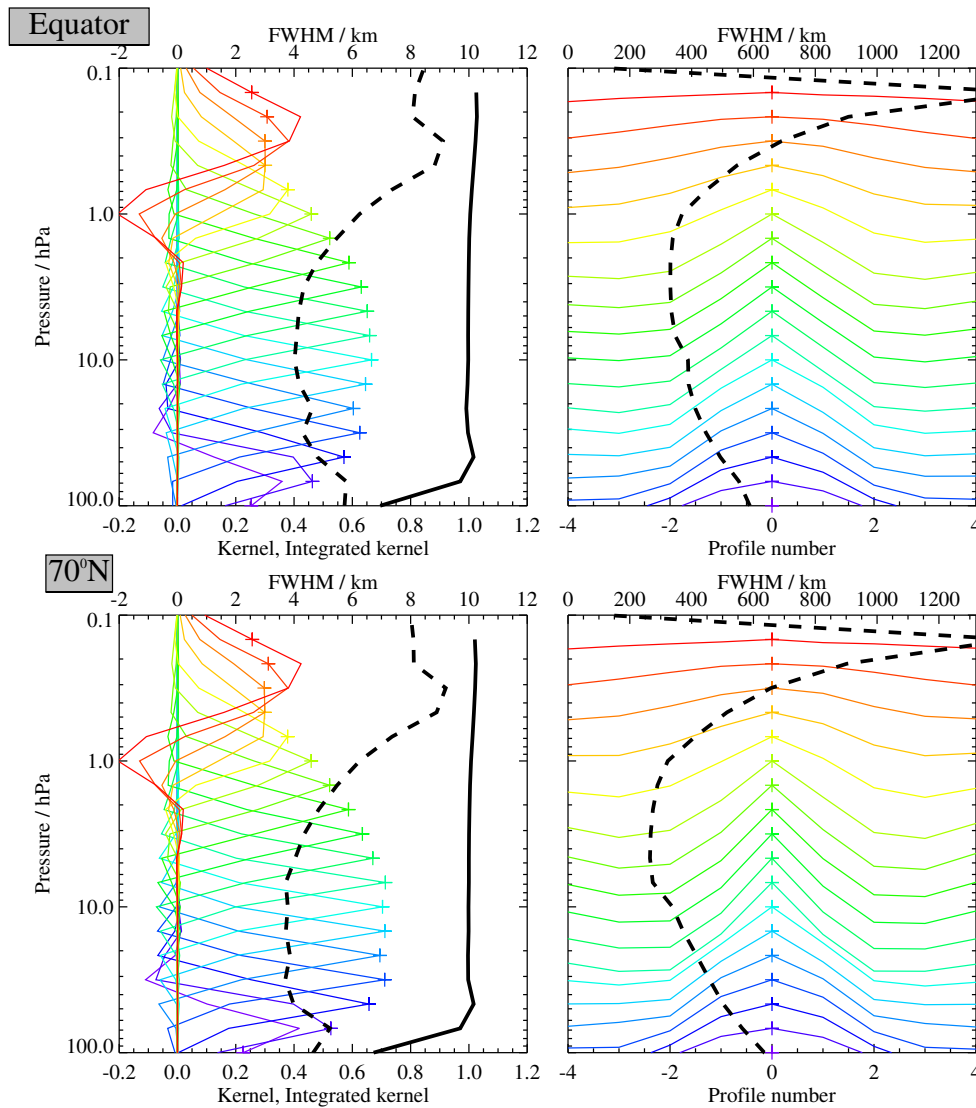


Figure 3.17.1: MLS v4.2x N2O-190 and N2O-640 comparison for March 2009



**Figure 3.17.2:** Typical two-dimensional (vertical and horizontal along-track) averaging kernels for the MLS v4.2x 190 GHz N<sub>2</sub>O data at the equator (upper) and at 70°N (lower); variation in the averaging kernels is sufficiently small that these are representative of typical profiles. Colored lines show the averaging kernels as a function of MLS retrieval level, indicating the region of the atmosphere from which information is contributing to the measurements on the individual retrieval surfaces, which are denoted by plus signs in corresponding colors. The dashed black line indicates the resolution, determined from the full width at half maximum (FWHM) of the averaging kernels, approximately scaled into kilometers (top axes). (Left) Vertical averaging kernels (integrated in the horizontal dimension for five along-track profiles) and resolution. The solid black line shows the integrated area under each kernel (horizontally and vertically); values near unity imply that the majority of information for that MLS data point has come from the measurements, whereas lower values imply substantial contributions from a priori information. (Right) Horizontal averaging kernels (integrated in the vertical dimension) and resolution. The horizontal averaging kernels are shown scaled such that a unit averaging kernel amplitude is equivalent to a factor of 10 change in pressure.



**Figure 3.17.3:** Typical two-dimensional (vertical and horizontal along-track) averaging kernels for the MLS v4.2x 640 GHz N<sub>2</sub>O data at the equator (upper) and at 70°N (lower); variation in the averaging kernels is sufficiently small that these are representative of typical profiles. Colored lines show the averaging kernels as a function of MLS retrieval level, indicating the region of the atmosphere from which information is contributing to the measurements on the individual retrieval surfaces, which are denoted by plus signs in corresponding colors. The dashed black line indicates the resolution, determined from the full width at half maximum (FWHM) of the averaging kernels, approximately scaled into kilometers (top axes). (Left) Vertical averaging kernels (integrated in the horizontal dimension for five along-track profiles) and resolution. The solid black line shows the integrated area under each kernel (horizontally and vertically); values near unity imply that the majority of information for that MLS data point has come from the measurements, whereas lower values imply substantial contributions from a priori information. (Right) Horizontal averaging kernels (integrated in the vertical dimension) and resolution. The horizontal averaging kernels are shown scaled such that a unit averaging kernel amplitude is equivalent to a factor of 10 change in pressure.



### 3.17.4 Accuracy

The accuracy values given in Table 3.17.2 were obtained for both v4 N<sub>2</sub>O products using the same detailed analyses presented for MLS N20–640 v2.2 data in *Lambert et al.* [2007] to quantify the systematic uncertainties associated with the MLS instrument calibration, spectroscopic uncertainty and approximations in the retrieval formulation and implementation.

### 3.17.5 Data screening

**Pressure range (N20–190): 68 – 0.46 hPa**

**Pressure range (N20–640): 100 – 0.46 hPa**

Values outside this range are not recommended for scientific use. In the upper stratosphere and lower mesosphere v4.2x N<sub>2</sub>O requires significant averaging for useful signals, but see the note under “Artifacts” for issues at pressures below 0.1 hPa.

**Estimated precision: Only use values for which the estimated precision is a positive number.**

Values where the *a priori* information has a strong influence are flagged with negative or zero precision, and should not be used in scientific analyses (see Section 1.5).

**Status flag: Only use profiles for which the Status field is an even number.**

Odd values of Status indicate that the profile should not be used in scientific studies. See Section 1.6 for more information on the interpretation of the Status field.

**Quality (N20–190): Only profiles whose Quality field is greater than 1.0 should be used.**

Note that this is a change from the threshold originally suggested for v4.2x. See the discussion of this topic below.

**Convergence (N20–190): Only profiles whose Convergence field is less than 2.0 should be used.**

A fraction of the N20–190 data (typically less than 0.5%) at this level will be discarded via this screening.

**Quality (N20–640): Only profiles whose Quality field is greater than 1.4 should be used.**

A small fraction of N20–640 profiles (typically less than 0.5%) will be discarded via this screening.

**Convergence (N20–640): Only profiles whose Convergence field is less than 1.01 should be used.**

A fraction of the N20–640 data (typically less than 0.5%) at this level will be discarded via this screening.

**Clouds: Clouds have little impact on the N<sub>2</sub>O products at the recommended pressure levels. Ignore status bit 16 (high cloud) or bit 32 (low cloud) indicating the presence of clouds. See artifacts for more details.**

#### Updated Quality screening recommendation

A byproduct of the aging in MLS that gives rise to the drift in the water vapor product (see section 3.9.8) and 190-GHz N<sub>2</sub>O (see below) is that the Quality metric for the 190-GHz N<sub>2</sub>O product exhibits a decreasing trend (most notable in the years following ~2009). This decrease is not correlated with any actual decline in the accuracy of the MLS N<sub>2</sub>O product, which appears largely unchanged (drift issues aside). However, application of the previously recommended 1.3 Quality threshold leads to rejection of an unreasonably large fraction of the N<sub>2</sub>O profiles in the more recent years of the Aura mission, particularly during southern winter. The revised 1.0 Quality threshold restores these profiles without erroneously identifying any obviously poor profiles as acceptable.

### 3.17.6 Artifacts

In addition to the large bias of the 190-GHz N<sub>2</sub>O at 100 hPa (not removed by screening), there are occasional outliers at the highest pressure levels in N20–190 and N20–640 products. Very thick clouds in the tropics

produce a low rate of artifacts in the v4.2x N<sub>2</sub>O products since improvements in the handling of radiances affected by clouds have reduced the frequency of outliers compared to previous versions. The cloud bits of the Status field are too blunt a tool to identify these rare cases, needlessly discarding reasonable data. Screening using the convergence and quality fields (see above) is recommended to remove the majority of these data points.

The retrieval restricts N<sub>2</sub>O values to be greater than -40 ppbv (approximately three times the retrieval noise level in the recommended pressure range) in order to prevent problems in the minimization search process. The low bound is applied at all levels, but it is only evident in the data for pressures less than 0.1 hPa, where the vertical smoothing is relaxed and the retrieval noise becomes comparable to the magnitude of the low bound value. Accordingly, statistical averaging of the data (zonal means or longer time periods) cannot be applied successfully for pressures at and less than 0.1 hPa as the -40 ppbv hard limit introduces a positive bias in any average.

A long-term trend of about -0.5% per year has been observed in the MLS N20-190 data product, through analysis of the mean values in the equatorial lower stratosphere in the years following 2009. Since the long term secular increase in tropospheric N<sub>2</sub>O observed by ground-based instruments is about +0.25%/year, the anomalous MLS N20-190 drift giving rise to the observed N20-190 trend is probably around -0.75%/year. The cause of this small but statistically significant drift is under investigation.

### 3.17.7 Review of comparisons between MLS N<sub>2</sub>O versions and other datasets

Average values for v4.2x 190-GHz N<sub>2</sub>O are up to 10% smaller than in v2.2 for the 100 and 68 hPa pressure levels, and within a few percent for pressures greater than 46 hPa (see Figure 3.17.4). Differences between v4.2x 190-GHz N<sub>2</sub>O and v3.3 are less than a few percent at all levels.

Average values for v4.2x 640-GHz N<sub>2</sub>O are 20% larger than in v2.2 for the 100 hPa pressure level, up to 10% smaller at the 46 – 32 hPa levels, and within 5% for pressures greater than 22 hPa (see Figure 3.17.5). Differences between v4.2x 640-GHz N<sub>2</sub>O and v3.3 are less than a few percent at all levels. Unlike the N20-190 product, the N20-640 product is recommended for scientific use at 100 hPa.

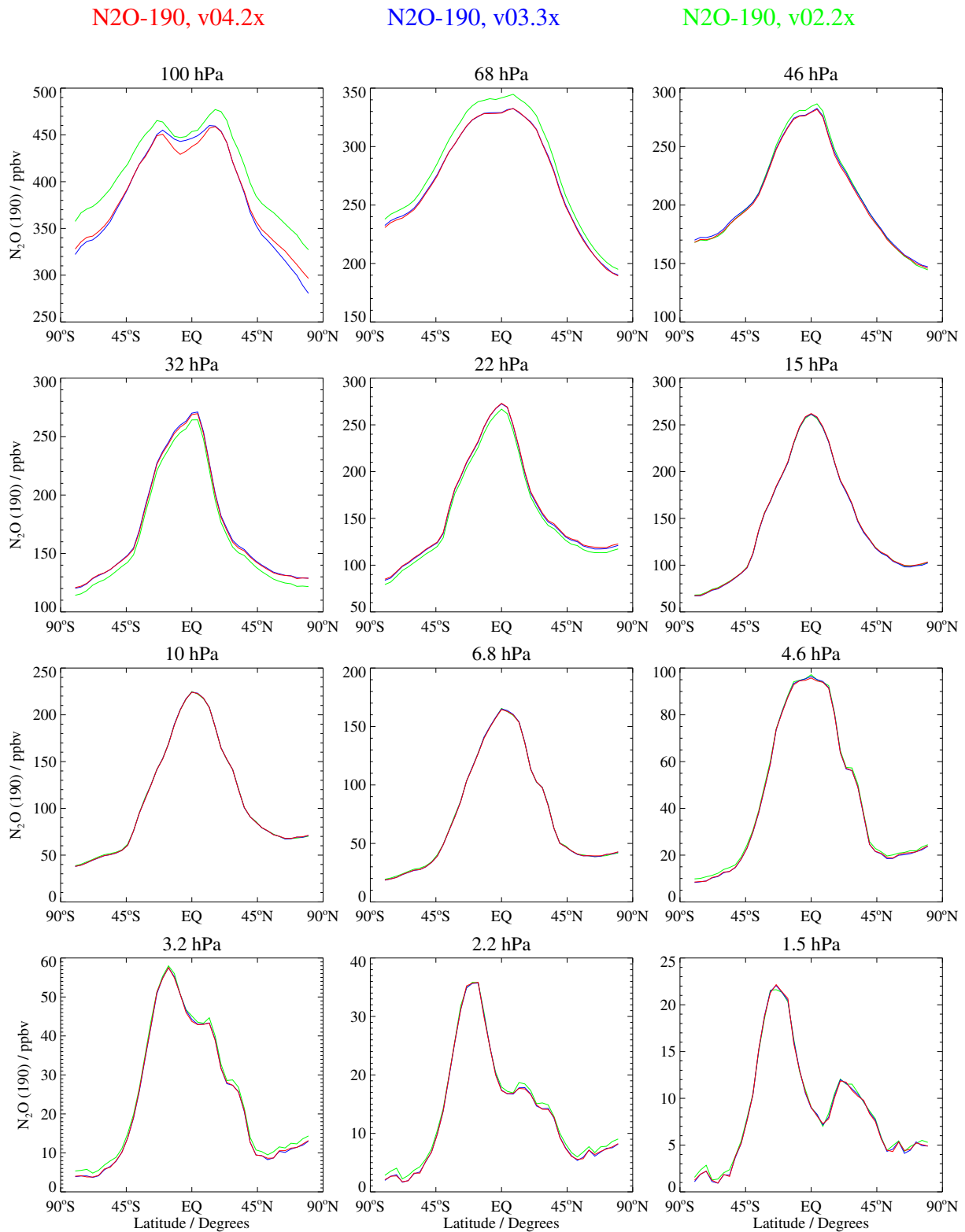
Apart from the differences noted above, the MLS v4.2x 640 GHz N<sub>2</sub>O is similar to the MLS v2.2 product described and validated in *Lambert et al.* [2007]. Comparisons of v2.2 640 GHz N<sub>2</sub>O with coincident measurements by ACE-FTS, Odin/SMR, and Envisat/MIPAS and balloon borne observations are shown in *Lambert et al.* [2007]. A revised validation paper for N<sub>2</sub>O is not planned in the near future and users are encouraged to read *Lambert et al.* [2007] for more information.

### 3.17.8 Desired improvements for future data version(s)

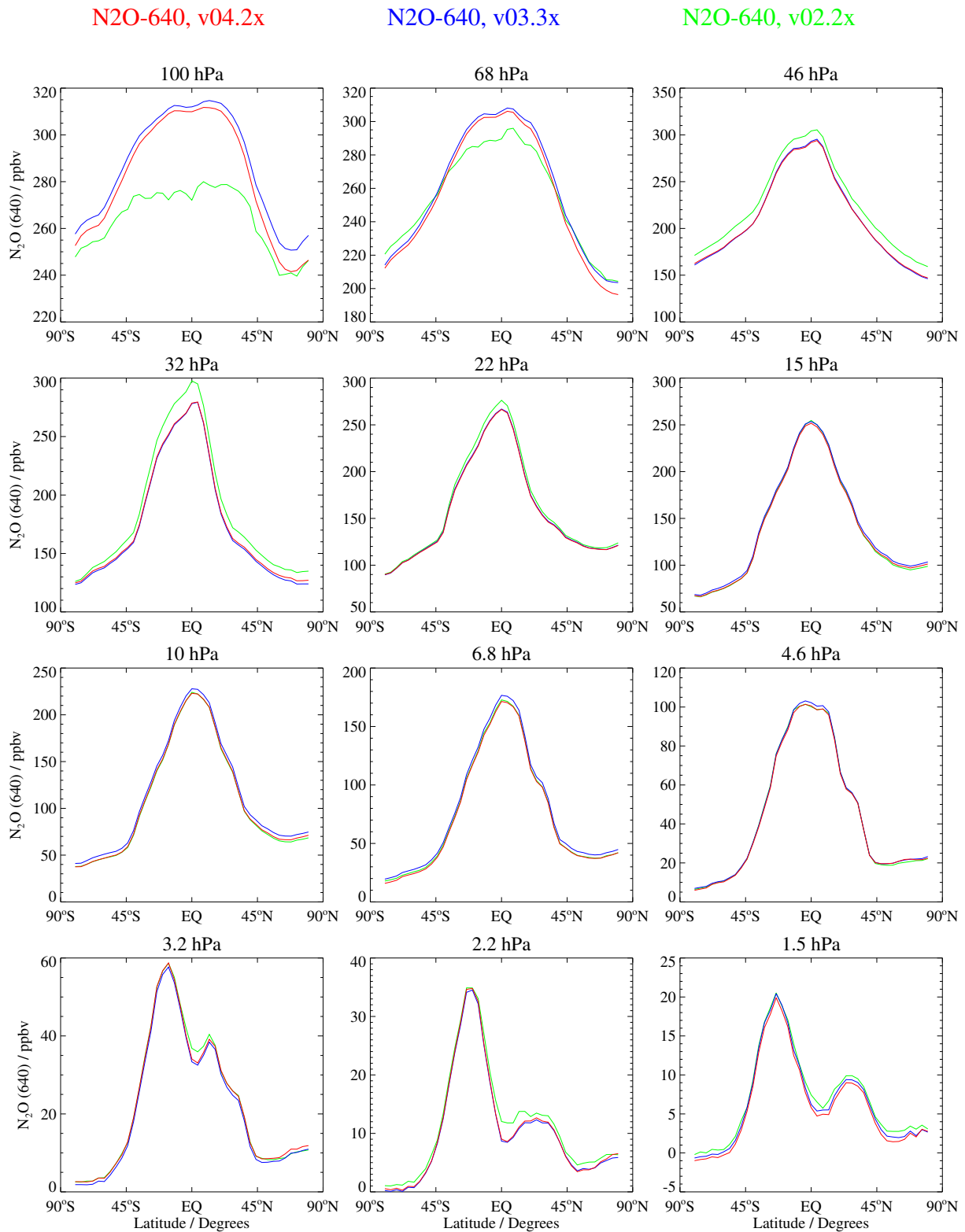
Retrievals of N<sub>2</sub>O to pressures greater than 100 hPa *may* be possible in later versions from the 190-GHz observations.

S  
TS  
TS  
TS  
TS  
TS  
TS  
TS  
TS  
TS  
TS  
TS  
TS  
TS  
TS  
TS  
TS  
TS  
TS  
TS  
TS  
TS  
TS  
TS  
TS  
TS  
TS  
TS  
TS  
TS  
TS  
TS  
TS  
TS  
TS  
TS  
TS  
TS  
T

## Zonal Means for Data Over March, 2009

Figure 3.17.4: MLS v4.2 190-GHz N<sub>2</sub>O compared to v2.2 and v3.3 for March 2009

## Zonal Means for Data Over March, 2009

Figure 3.17.5: MLS v4.2 640 GHz N<sub>2</sub>O compared to v2.2 and v3.3 for March 2009

**Table 3.17.1:** Summary of MLS v4.2x N<sub>2</sub>O (N20–190) product.

Region hPa	Resolution Vert. × Horiz. km	Precision <sup>a</sup>		Accuracy		Comments
		ppbv	%	ppbv	%	
≤0.33	—	—	—	—	—	Unsuitable for scientific use
0.46	11.0 × 655	15	>100	2	>100	
0.68	9.7 × 540	17	>100	2	89	
1.0	8.6 × 440	18	>100	2	50	
2.2	7.3 × 340	19	64	4	36	
4.6	6.5 × 285	17	23	5	11	
10	6.0 × 265	16	12	7	7	
22	5.6 × 305	15	9	10	6	
46	4.9 × 385	14	7	30	10	
68	5.4 × 420	16	6	55	22	
100	3.8 × 500	20	7	124	44	Consult with MLS science team
147	—	—	—	—	—	Unsuitable for scientific use
≥215	—	—	—	—	—	Not retrieved

<sup>a</sup>Precision on individual profiles**Table 3.17.2:** Summary of MLS v4.2x N<sub>2</sub>O (N20–640) product.

Region hPa	Resolution Vert. × Horiz. km	Precision <sup>a</sup>		Accuracy		Comments
		ppbv	%	ppbv	%	
≤0.33	—	—	—	—	—	Unsuitable for scientific use
0.46	8.9 × 530	12	>100	1	88	
0.68	7.4 × 430	13	>100	2	89	
1.0	6.2 × 345	14	>100	2	50	
2.2	4.8 × 300	15	49	3	27	
4.6	4.1 × 295	14	18	6	14	
10	3.9 × 360	13	10	12	11	
22	4.2 × 410	14	8	22	14	
46	4.4 × 495	16	7	40	19	
68	5.5 × 555	20	8	70	28	
100	5.2 × 610	25	9	51	18	
147	—	—	—	—	—	Unsuitable for scientific use
≥215	—	—	—	—	—	Not retrieved

<sup>a</sup>Precision on individual profiles

### 3.18 Ozone (O<sub>3</sub>)

Swath name: O3

Useful range: 261 – 0.02 hPa

Contact: Lucien Froidevaux (stratosphere/mesosphere),

Email: <Lucien.Froidevaux@jpl.nasa.gov>

Michael Schwartz (upper troposphere), Email: <Michael.J.Schwartz@jpl.nasa.gov>

#### 3.18.1 Introduction

As is the case with previous versions, the v4.2x standard O<sub>3</sub> product is taken from a retrieval using 240-GHz radiances, providing sensitivity from the upper troposphere into the mesosphere. In v4.2x, an optimized retrieval phase for production of the O<sub>3</sub> standard product has been added prior to the phase that uses 240-GHz radiances to produce the standard carbon monoxide and nitric acid products. Table 3.18.1 summarizes typical O<sub>3</sub> resolution, precision, and systematic uncertainty estimates as a function of pressure. Papers describing detailed validation of the MLS v2.2 product and comparisons with other data sets were published in a special Aura validation issue of the *Journal of Geophysical Research*, see [Froidevaux et al., 2008b; Jiang et al., 2007; Livesey et al., 2008]. In the stratosphere and above, v4.2x ozone profiles are very similar to the v2.2 and v3.3x/v3.4x profiles, so the stratospheric results from the above references will generally hold for the product. Initial documentation of changes, improvements, and issues with v4.2x data are discussed here, including data screening criteria. Recommended screening is less complex than it was for v3.3x/v3.4x data and is again primarily based on thresholds for Quality, and Convergence, as was the case for v2.2. Ozone profile behavior has been improved, with reduction of vertical oscillations in the low-latitude UTLS and reduction of sensitivity to thick clouds, through changes in the spectral form used to model cloud impacts on the MLS radiances, through tightening of vertical smoothing at pressures greater than or equal to 68 hPa (leading to an increase in averaging kernel FWHM by a factor of ~1.15) and through retrieval of an independent, spectrally-flat baseline over the ozone band for each limb view to better account for cloud inhomogeneity.

In addition to the swath O3, which is the O<sub>3</sub> profile on 55 pressure surfaces, the L2GP-O3 files contain a swath, O3 column, which is the integrated stratospheric column down to the thermal tropopause (WMO definition) calculated from MLS temperature. The MLS temperature profiles from which the WMO tropopause is determined are not screened per the instructions of section 3.22 and users may wish to reject columns for which standard screening rejects the corresponding temperature profile.

#### 3.18.2 Comparison of v4.2x with past data versions

The vertical retrieval grid has not changed from v3.3x/v3.4x; between 316 hPa and 1 hPa, v4.2x ozone profiles are retrieved on 12 surfaces per decade, a grid twice as fine as the 6-level-per-decade grid used in v2.2 Tightened vertical smoothing has degraded vertical resolution in v4.2x from the upper troposphere to 68 hPa by ~15%. Table 3.18.1 summarizes resolution, precision, and accuracy estimates.

Figures 3.18.1 and 3.18.2 show zonally-averaged stratospheric and mesospheric field comparisons between data versions for the (full) month of March, 2009, for properly screened profiles only; mean differences (ppmv and percent) are also shown. Similar plots focusing on the UTLS are provided in Figures 3.18.3 and 3.18.4. Average ozone mixing ratio values (e.g., for monthly means) have typically not changed by more than 1 to 2% for pressures less than 100 hPa. In the tropical UTLS (most notably), the new dataset is improved. Specifically, we show average UTLS profiles during March, 2009 from three data versions for 0° – 10°N in Figure 3.18.5. The new version shows less oscillatory behavior in the mean profiles, in comparison to the previous version (v3.3 on the same retrieval grid), although small oscillations are still present; certain months and latitude regions exhibited larger effects (in the previous data version) than those shown in the above figure.

Averages for March, 2009

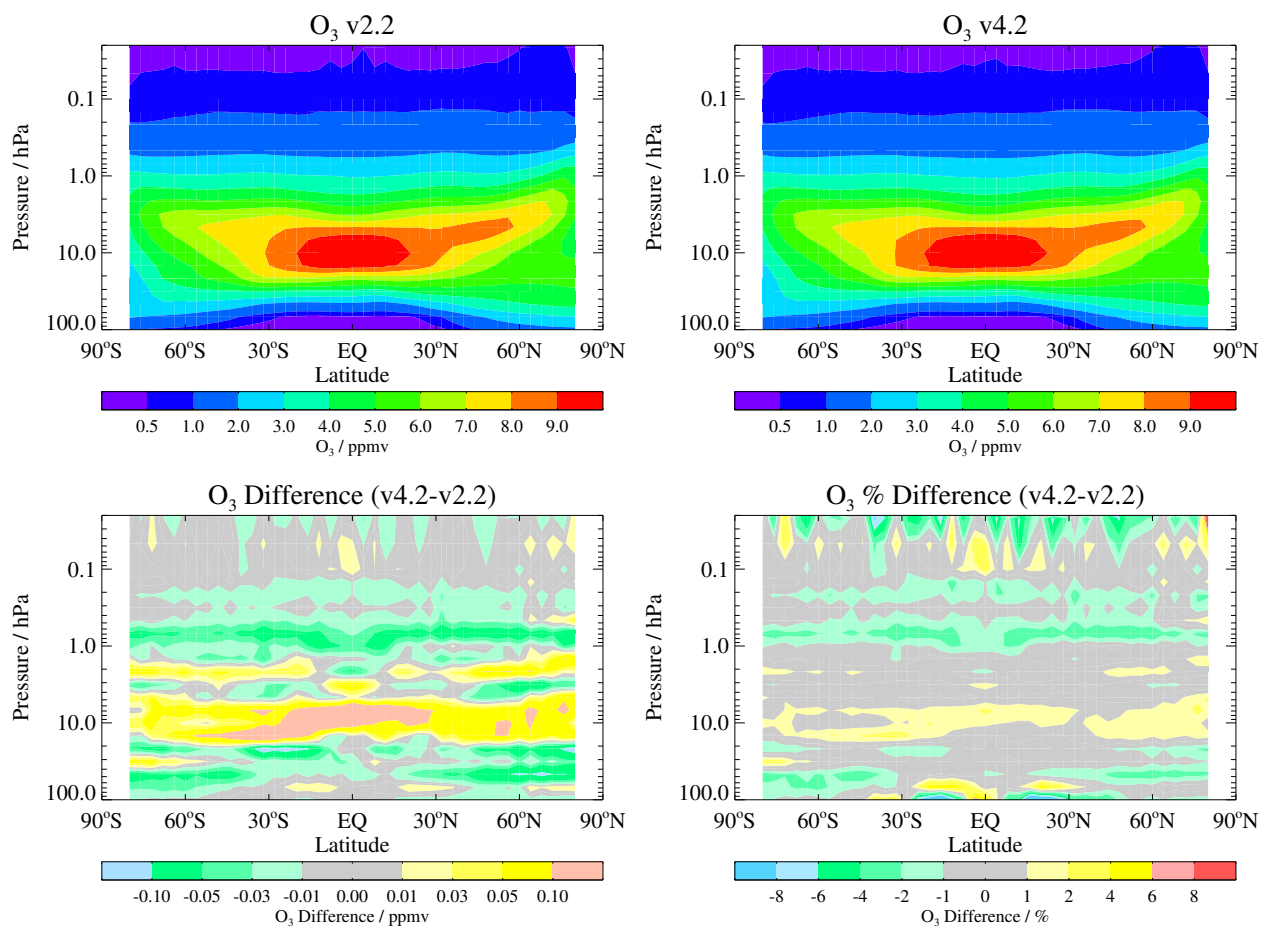


**Figure 3.18.1:** Zonal averages for stratospheric and mesospheric MLS ozone profiles during March, 2009, showing the MLS v2.2 ozone mixing ratio contours (top left panel), the v4.2x contours (top right panel), and their differences in ppmv (v4.2x minus v2.2, bottom left panel) and percent (v4.2x minus v2.2 versus v2.2, bottom right panel).

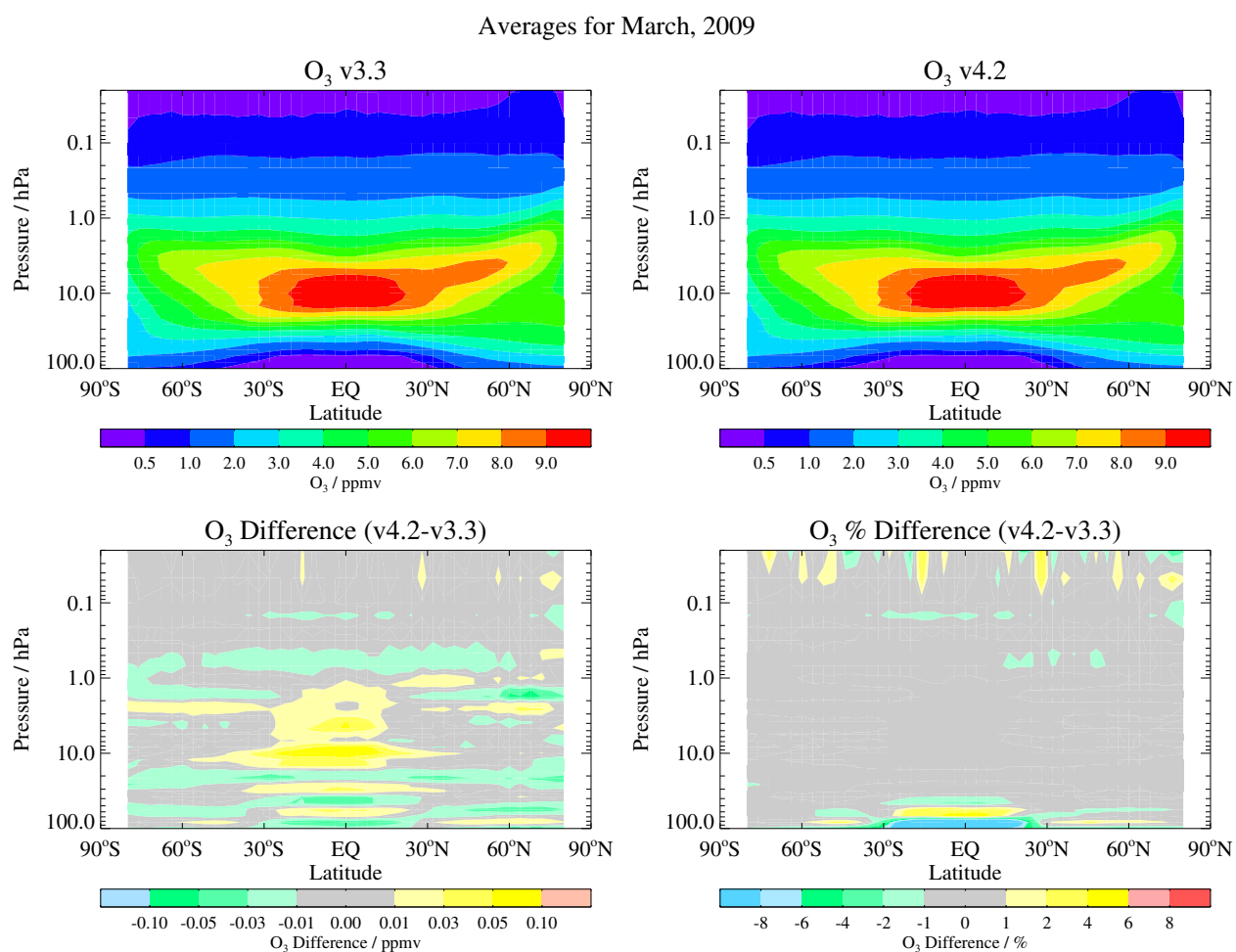


**Figure 3.18.2:** Zonal averages for stratospheric and mesospheric MLS ozone profiles during March, 2009, showing the MLS v3.3 ozone mixing ratio contours (top left panel), the v4.2x contours (top right panel), and their differences in ppmv (v4.2x minus v3.3, bottom left panel) and percent (v4.2x minus v3.3 versus v3.3, bottom right panel).



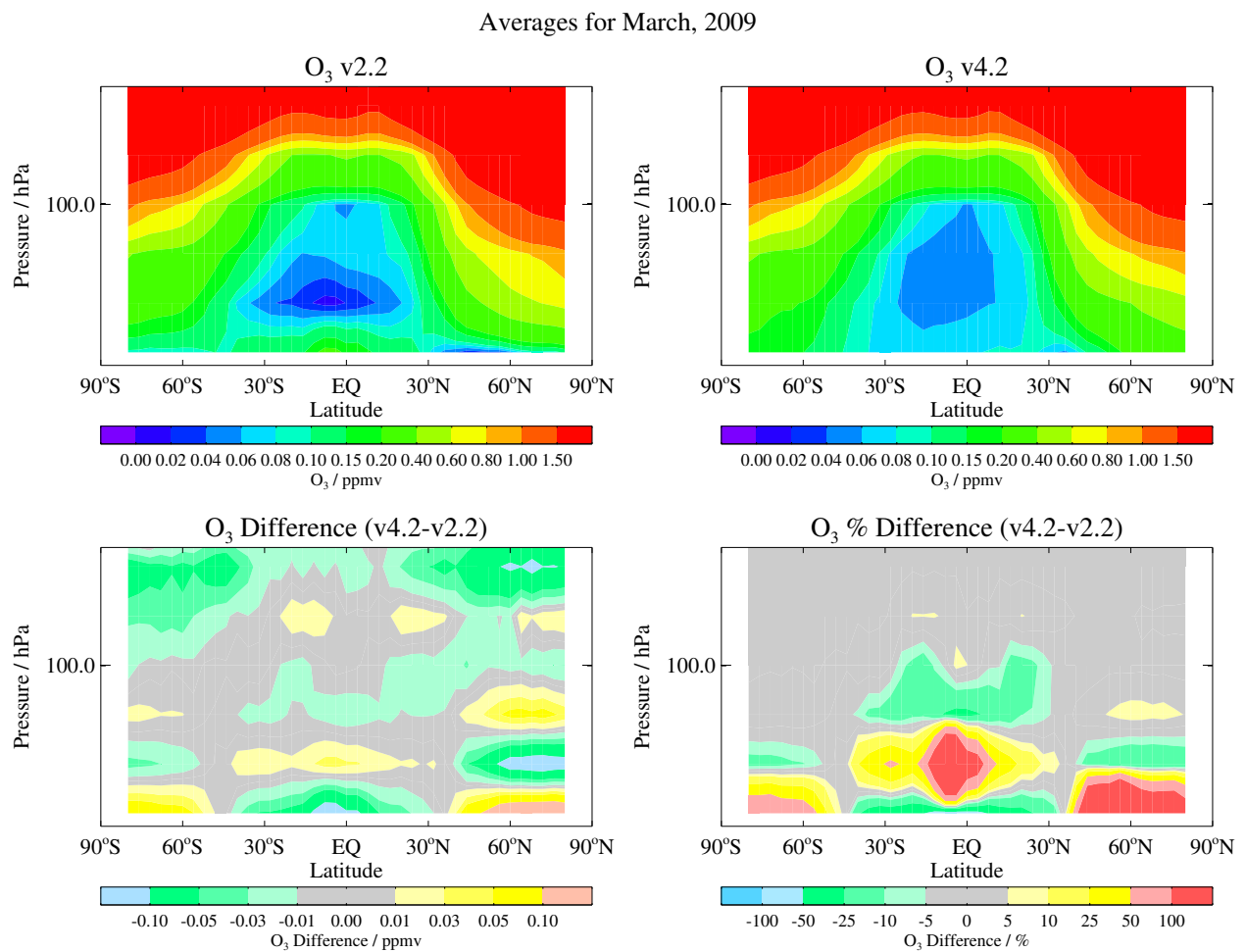


**Figure 3.18.3:** Zonal averages for UTLS MLS ozone profiles during March, 2009, showing the MLS v2.2 ozone mixing ratio contours (top left panel), the v4.2x contours (top right panel), and their differences in ppmv (v4.2x minus v2.2, bottom left panel) and percent (v4.2x minus v2.2 versus v2.2, bottom right panel).

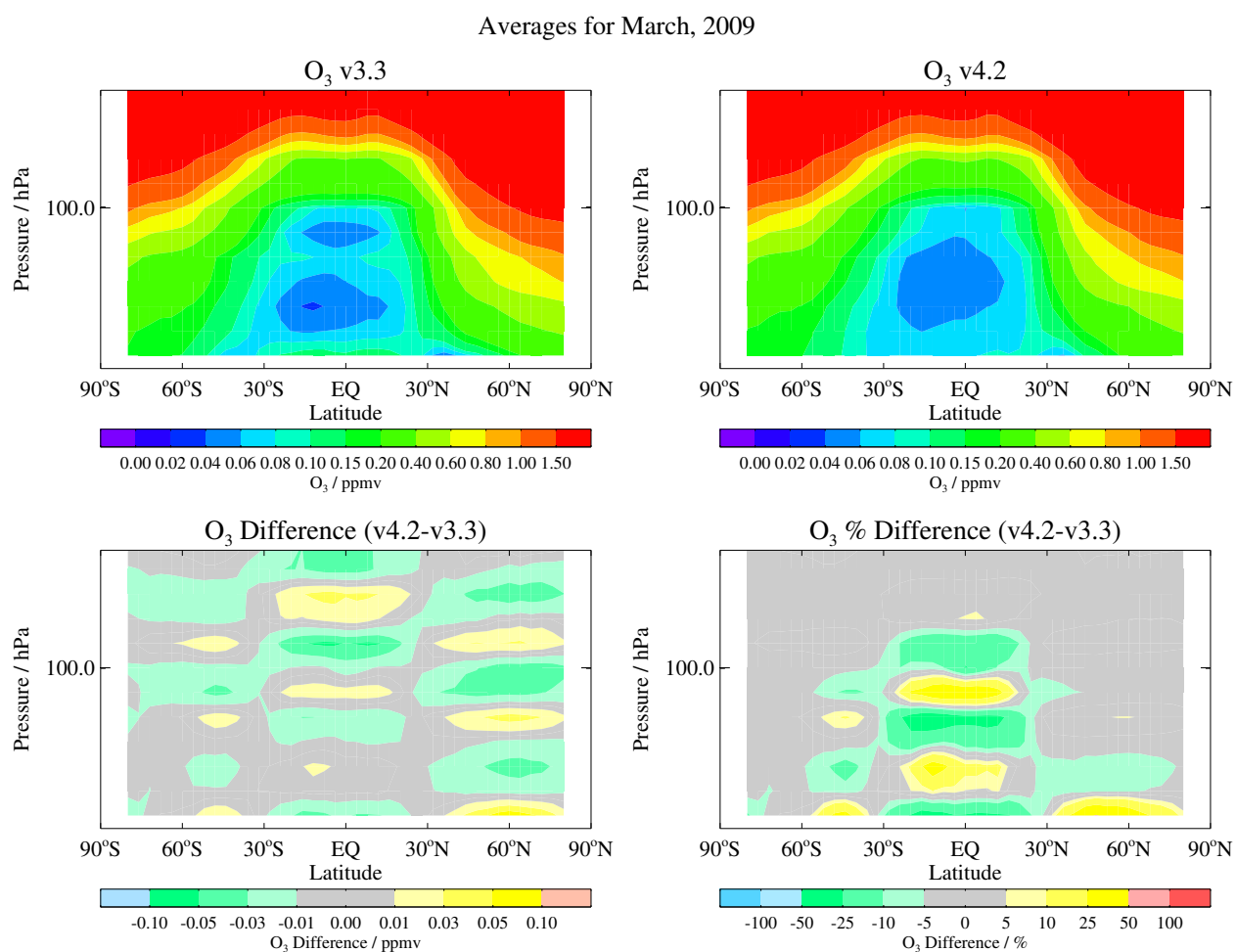


**Figure 3.18.4:** Zonal averages for UTLS MLS ozone profiles during March, 2009, showing the MLS v3.3 ozone mixing ratio contours (top left panel), the v4.2x contours (top right panel), and their differences in ppmv (v4.2x minus v3.3, bottom left panel) and percent (v4.2x minus v3.3 versus v3.3, bottom right panel).

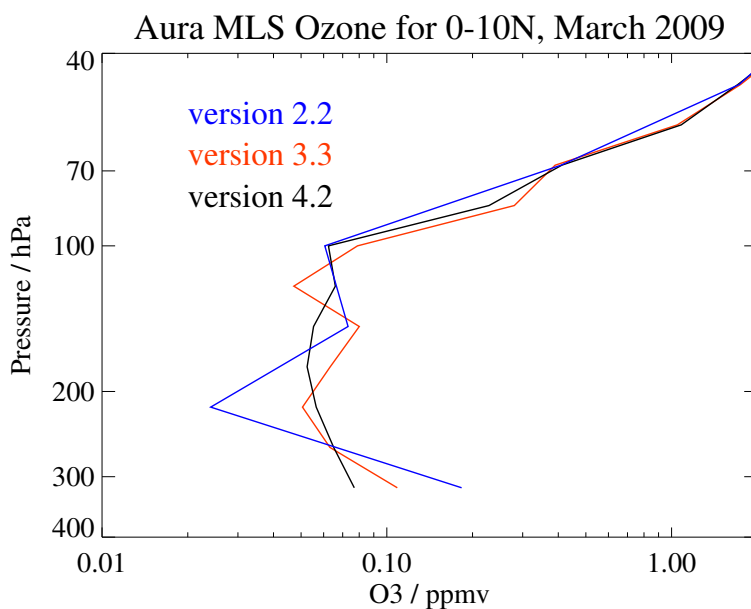


**Figure 3.18.5:** Zonal means from equator to 10°N during March, 2009, showing the average behavior of ozone profiles for MLS v2.2, v3.3, and v4.2x, as indicated by the color-coded legend.

Figure 3.18.6 shows histograms of tropical UTLS v04.20 and v03.30 ozone for all of 2005. V04.20 ozone unscreened (blue) and screened (green) histograms are quite similar to one another, with only small reductions in scatter in the screened case. V3.3 has significantly broader distributions in the troposphere than v04.20, both in the widths of the central peaks and in the tails of the distributions. While screened v3.3 (cyan) has reduced tails of cloud-impacted outliers compared to unscreened (red), these tails are clearly reduced in v4.2x even before screening. The reduced tropical vertical oscillation seen in Figures 3.18.4 and 3.18.5 is reflected in the shifts of the histogram peaks between versions, with higher v4.2x values at 121 hPa and lower values at 82, 100, 147, 178 and 316 hPa. The 316-hPa level of v4.2x, though not currently recommended for general scientific use, is under evaluation.

### Ozone Columns

Changes in the MLS stratospheric ozone columns between v3.3x/v3.4x and v4.2x are quite small; typical daily zonal averages are within one percent, with a tendency towards slightly lower values (but within about 1%) in the new data version. Only one stratospheric column swath, using a tropopause derived from MLS temperature, is calculated by the v4.2x O<sub>3</sub> retrieval. The column based upon the GEOS-5 tropopause is no longer routinely produced.

### 3.18.3 Resolution

Typical resolution values are provided in the summary Table 3.18.1. The cross-track resolution is set by the 6 km width of the MLS 240 GHz field of view. Daily longitudinal separation of MLS measurements, set by the Aura orbit, is 10° – 20° over middle and lower latitudes, with much finer sampling at the highest latitudes sampled in each hemisphere.

### 3.18.4 Precision

As found previously, the Level 2 precision values are often slightly lower than the scatter observed in a narrow latitude band centered around the equator (where atmospheric variability is expected to be small) or obtained from a comparison between ascending and descending coincident MLS profiles.

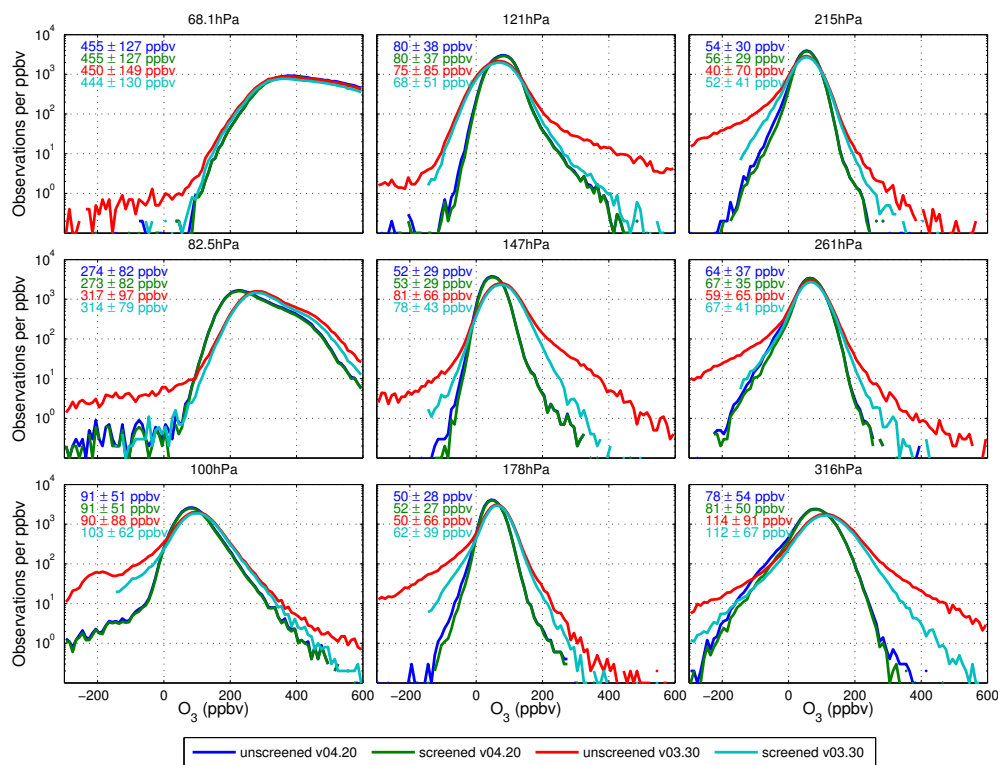


**Figure 3.18.6:** Histograms of screened and unscreened v04.20 and v03.30 ozone for the 2005 tropical average (20° S–20° N).

Negative precision values for ozone occur for almost every data point at pressures smaller than 0.01 hPa, indicating increasing influence from the *a priori*, although some MLS information exists (e.g., regarding average day/night differences) into the uppermost mesosphere and lower thermosphere. Generally, however, we recommend that scientific studies be restricted to pressures of 0.02 hPa or larger.

### Column values

The estimated precisions for the v4.2x MLS column ozone abundances down to pressures of 100 to 215 hPa are 2% or less. The typical empirical precision in the columns based on (1- $\sigma$ ) variability in the tropics is 2 to 3%.

### 3.18.5 Accuracy

The accuracy estimates shown in Table 3.18.1 are from an analysis which propagated estimated systematic errors in MLS calibration, spectroscopy, etc., through the (v4.2x) measurement system. The values shown here are intended to represent 2 $\sigma$  estimates of accuracy. Comparison of MLS O<sub>3</sub> with well-established data sets shows no evidence of significant biases overall, although the oscillations in the UTLS at low latitudes lead to some systematic effects which can reach 20–40%, depending on the pressure level. For more details, see the MLS validation papers by *Froidevaux et al.* [2008b], *Jiang et al.* [2007], and *Livesey et al.* [2008], as well as references therein; some more recent references relevant to MLS ozone are available on the MLS website under “Publications”. In particular, see the comprehensive work by *Hubert et al.* [2016] (more related information further below). In recent years, validation studies have focused more on longer-term changes or drifts (with good stability being observed versus other reliable measurements) and on the UTLS region.

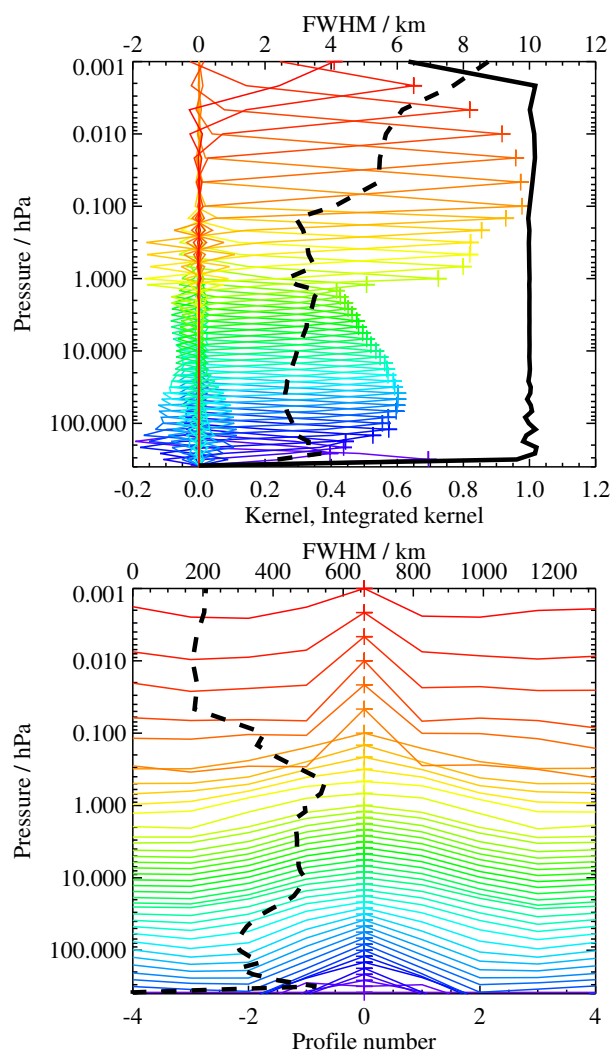


**Figure 3.18.7:** Typical two-dimensional (vertical and horizontal along-track) averaging kernels for the MLS v4.2x O<sub>3</sub> at 35° N; variation in the averaging kernels is sufficiently small that these are representative of typical profiles. Colored lines show the averaging kernels as a function of MLS retrieval level, indicating the region of the atmosphere from which information is contributing to the measurements on the individual retrieval surfaces, which are denoted by plus signs in corresponding colors. The dashed black line indicates the resolution, determined from the full width at half maximum (FWHM) of the averaging kernels, approximately scaled into kilometers (top axes). (Upper) Vertical averaging kernels (integrated in the horizontal dimension for five along-track profiles) and resolution. The solid black line shows the integrated area under each kernel (horizontally and vertically); values near unity imply that the majority of information for that MLS data point has come from the measurements, whereas lower values imply substantial contributions from a priori information. (Lower) Horizontal averaging kernels (integrated in the vertical dimension) and resolution. The averaging kernels are scaled such that a unit change is equivalent to one decade in pressure.

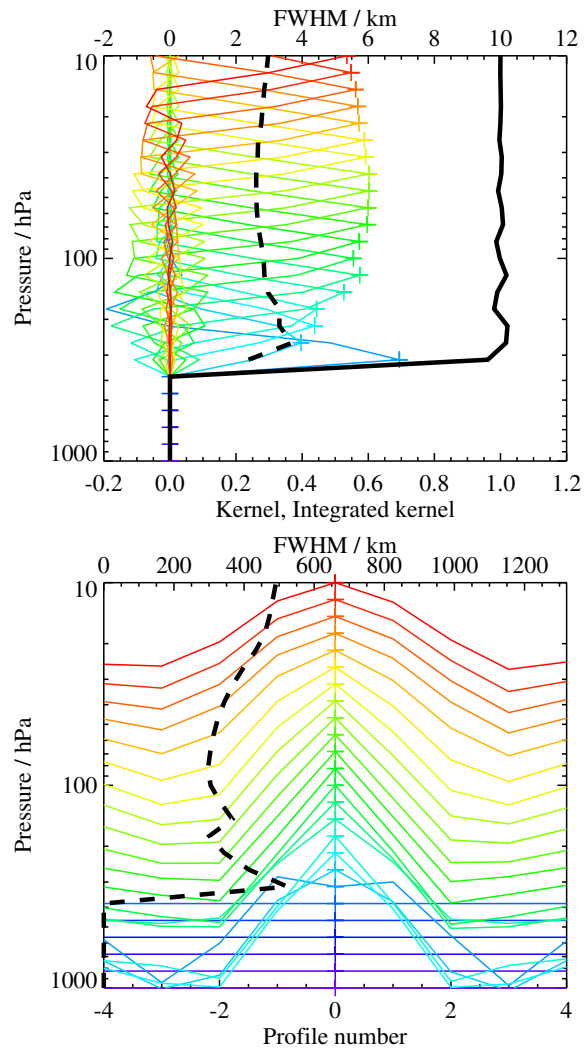


**Figure 3.18.8:** As for 3.18.7 but zooming in on the upper troposphere and lower stratosphere region.

Help	S
Overview	T
Table	S
BrO	S
CH <sub>3</sub> Cl	T
CH <sub>3</sub> CN	S
CH <sub>3</sub> OH	T
ClO	S
CO	T
GPH	S
H <sub>2</sub> O	T
HCl	S
HCN	T
HNO <sub>3</sub>	S
HO <sub>2</sub>	T
HOCl	S
IWC	T
IWP	S
N <sub>2</sub> O	T
O <sub>3</sub>	S
OH	T
RHI	S
SO <sub>2</sub>	T
	S
	T

### Column values

Sensitivity tests using systematic changes in various parameters that could affect the accuracy of the MLS retrievals lead to possible biases ( $2\sigma$  estimates) of about 4%, as an estimated accuracy for the MLS column values (from integrated MLS ozone profiles down to 100, 147, and 215 hPa). See also the (v2.2) validation papers (and subsequent ozone-related publications, e.g., available from the MLS website) for results on column ozone comparisons versus satellite, sonde, and lidar data.

#### 3.18.6 Data screening

**Pressure range:** 261 – 0.02 hPa.

Values outside this range are not recommended for scientific use.

**Estimated precision:** Only use values for which the estimated precision is a positive number.

Values where the *a priori* information has a strong influence are flagged with negative or zero precision, and should not be used in scientific analyses (see Section 1.5).

**Status flag:** Only use profiles for which the **Status** field is an even number.

Odd values of Status indicate that the profile should not be used in scientific studies. See Section 1.6 for more information on the interpretation of the Status field.

**Quality:** Only profiles whose **Quality** field is greater than 1.0 should be used.

**Convergence:** Only profiles whose **Convergence** field is less than 1.03 should be used.

**Clouds:** Scattering from thick clouds can lead to more systematic effects in the UTLS.

Most of the affected profiles are removed by the **Quality** and **Convergence** screening recommendations (although **Convergence** issues occur only rarely).

One should *reject* profiles with odd Status *or* even Status profiles with **Convergence** above the convergence threshold *or* **Quality** below the quality threshold. Conversely, one should *keep* profile values with even status *and* good **Convergence** *and* good **Quality**. These criteria typically remove 1 to 2 % of global daily data, with tropical latitudes showing somewhat larger data removal fractions of about 5%. This screening generally maintains sufficient coverage for a near-complete daily map (for any given day), even in the UTLS.

Compared to data screening recommendations for past data versions, the screening of v4.2x data generally removes somewhat fewer ozone profiles on a typical day.

#### 3.18.7 Review of comparisons with other datasets

O<sub>3</sub> comparisons have indicated general agreement at the 5 – 10 % level with stratospheric profiles from a number of comparisons using satellite, balloon, aircraft, and ground-based data. A high MLS v2.2 bias at 215 hPa had been observed in some comparisons versus certain ozonesonde and satellite datasets. Such high biases were reduced in versions v3.3x and v3.4x, with additional smaller reductions in the ozone values in v4.2x. We have found that latitudinal and temporal changes observed in various correlative datasets are well reproduced by the MLS ozone product. Intercomparisons of a large variety of ozone measurements by satellite instruments have been documented by *Tegtmeier et al.* [2013], as part of the analyses produced by the SPARC Data Initiative; the Aura MLS ozone values compare quite favorably to the multi-instrument mean values as well as to SAGE II ozone. The temporal stability of the Aura MLS ozone dataset has been shown to be very good, in comparison to lidar datasets (*Nair et al.* [2012]). The more recent work by *Hubert et al.* [2016] includes both the lidar network and the ozonesonde network as references for a comprehensive satellite data intercomparison study. The latter authors show that average biases between MLS and latitudinally-binned data from lidar and ozonesonde sites across the globe is typically within 5% or better, with poorer behavior (known vertical oscillations) at low latitudes in the UTLS. In terms of drifts, the Aura MLS ozone dataset is shown (in the

Table 3.18.1: Summary for MLS ozone

Pressure / hPa	Resolution Vert. × Horiz.	Precision <sup>a</sup>		Accuracy <sup>b</sup>		Comments
		ppmv	%	ppmv	%	
≤ 0.01	—	—	—	—	—	Unsuitable for scientific use
0.02	5.5 × 200	1.2	300	0.2	50	
0.05	5.5 × 200	0.8	150	0.2	30	
0.1	4 × 400	0.5	60	0.2	20	
0.2	3 × 450	0.4	30	0.15	10	
0.5	3.5 × 550	0.3	20	0.2	10	
1	3 × 500	0.2	7	0.3	10	
2	3.5 × 450	0.15	3	0.3	7	
5	3 × 450	0.15	2	0.4	7	
10	3 × 500	0.1	2	0.4	6	
22	2.5 × 400	0.1	2	0.25	5	
46	2.5 × 350	0.06	3	0.2	8	
68	2.5 × 350	0.04	4	0.1	7	
100	3 × 300	0.03	15–25	[+0.005 + 7%]		
150	3 × 400	0.02	5–70	[+0.005 + 7%]		
215	3.5 × 350	0.02	5–100	[+0.01 + 10%]		
261	3.5 × 400	0.03	5–100	[+0.02 + 10%]		See note <sup>c</sup>
316	2.5 × 550	0.03	—	—	—	Not recommended
1000 – 464	—	—	—	—	—	Not retrieved

<sup>a</sup>Precision on individual profiles

<sup>b</sup>Primarily as estimated from systematic uncertainty characterization tests. Stratospheric values are expressed in ppmv with a typical *equivalent* percentage value quoted. 261 – 100 hPa accuracies are the sum of the ppmv *and* *percentage* uncertainties; the ppmv terms arise from observed average positive biases in the MLS values relative to tropical sonde data (from 2005 through 2015).

<sup>c</sup>Positive bias in the UT, but the mean annual variation is nevertheless well behaved versus tropical sonde data.

above work) to be very stable, a term also applied only to the SAGE II dataset; MLS exhibits drifts with respect to the ground-based networks that fall within 1.5 to 2% per decade, with zero drift encompassed by the error bars (i.e. non-significant drifts), at least in the middle stratosphere. The Aura MLS data, in combination with older datasets, provides a critical tool for the study of global O<sub>3</sub> in a changing climate and into the expected O<sub>3</sub> recovery period, as anthropogenic ozone depleting substances decline in concentration.

### 3.18.8 Artifacts

**Oscillations in tropical UTLS ozone:** There has been some improvement in the v4.2x profiles (especially at low latitudes), in terms of reducing (but not eliminating) systematic vertical oscillations. Further characterization of MLS tropical UTLS data, in particular, is warranted in order to more fully understand any data limitations in this region.



## 3.19 Hydroxyl Radical (OH)

**Swath name:** OH ite

**Useful range:** 32 – 0.0032 hPa

**Contact:** Luis Millan, **Email:** <Luis.F.Millan@jpl.nasa.gov> and Shuhui Wang,  
**Email:** <shw@gps.caltech.edu>

### 3.19.1 Introduction

The MLS THz radiometer is dedicated to measuring OH in the 2.5 THz spectral region. A description of OH data quality, precision and systematic errors for an earlier version, v2.2, is given in *Pickett et al.* [2006b]. The validation studies are described in *Pickett et al.* [2008] and *Wang et al.* [2008]. While the OH data quality is generally similar between v2.2 and v3.3x and v3.4x, there are significant improvements in the current version v4.2x. In previous versions, OH data near the mesospheric density peak, ~0.032 hPa, often show considerable amount of data flagged with negative precision, indicating strong influence of *a priori* information, particularly in the summer hemisphere (or tropics when near the equinox) and sometimes causes gaps in zonal mean time series. The v4.2x software resolves this issue by fixing the overly tight *a priori* constraints. The resulting mesospheric OH data are less noisy and generally have somewhat larger values than previous versions for the problematic seasons/latitudes. Another improvement is the smaller bias at 10 – 15 hPa. Therefore, the day-night correction for bias is only required for pressure levels at 21 and 32 hPa. Note that users may notice more zig-zags in v4.2x nighttime mesospheric OH vertical profiles. This is a side effect of fixing the possible positive bias introduced by tight lower limits set in previous version retrievals.

The estimated uncertainties, precisions, and resolution for v4.2x OH are summarized in Table 3.19.1.

### 3.19.2 Resolution

Figure 3.19.1 shows the OH averaging kernel for daytime and nighttime at 35°N. The reason to separate daytime and nighttime is that the largest natural variability in OH is diurnal. The vertical resolution is slightly different between day and night. The nighttime resolution is sufficient to allow the study of (for example) the “nighttime OH layer” around 82 km. The vertical width of the averaging kernel for pressures greater than 0.01 hPa is 2.5 km. The horizontal width of the averaging kernel is equivalent to a width of 1.5° (165 km distance) along the orbit. The changes in vertical resolution above 0.01 hPa are due mainly to use of a faster instrument vertical scan rate for tangent heights above 70 km. The horizontal resolution across track is 2.5 km. The averaging kernel and resolution for high and low latitudes are very similar to Figure 3.19.1 for most pressure levels. At the topmost two pressure levels, 0.0046 hPa and 0.0032 hPa, the vertical resolution is slightly better at the equator than at 70°N.

### 3.19.3 Precision

A typical OH profile and the associated precisions (for both v3.3x and v3.4x and v4.2x) are shown in Figure 3.19.2. The profile is shown in both volume mixing ratio (vmr) and density units. All MLS data are reported in vmr for consistency with the other retrieved molecules. However, use of density units ( $10^6 \text{ cm}^{-3}$ ) reduces the apparent steep gradient of OH vertical profile, allowing one to see the profile with more detail, especially in the stratosphere where most atmospheric OH is present. Additionally, at THz frequencies the collisional line-width is approximately equal to the Doppler width at 1 hPa. Above 1 hPa, Doppler broadening is dominant and the peak intensity of OH spectral absorption is proportional to density, while below 1 hPa the peak intensity is proportional to vmr. The daytime OH density profile shows two peaks at ~45 km and ~75 km. The night OH profile exhibits the narrow layer at ~82 km [*Pickett et al.*, 2006a]. Precisions are such that an OH zonal average within a 10° latitude bin can be determined with better than 10% relative precision with one day of data (~100 samples) over 21 – 0.01 hPa. With 4 days of data, the 10% precision limits can be extended to 32 – 0.0046 hPa.

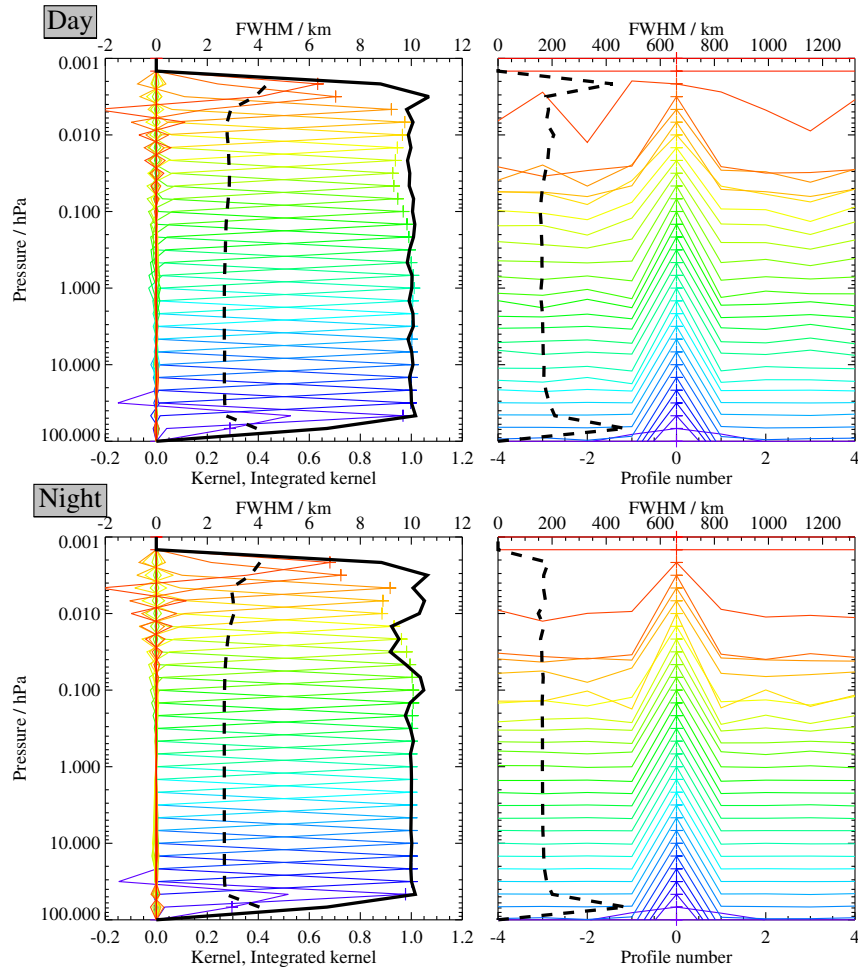


**Figure 3.19.1:** Typical two-dimensional (vertical and horizontal along-track) averaging kernels for the MLS v4.2x OH data at 35°N for daytime (upper) and nighttime (lower); variation in the averaging kernels is sufficiently small that these are representative of typical profiles. Colored lines show the averaging kernels as a function of MLS retrieval level, indicating the region of the atmosphere from which information is contributing to the measurements on the individual retrieval surfaces, which are denoted by plus signs in corresponding colors. The dashed black line indicates the resolution, determined from the full width at half maximum (FWHM) of the averaging kernels, approximately scaled into kilometers (top axes). (Left) Vertical averaging kernels (integrated in the horizontal dimension for five along-track profiles) and resolution. The solid black line shows the integrated area under each kernel (horizontally and vertically); values near unity imply that the majority of information for that MLS data point has come from the measurements, whereas lower values imply substantial contributions from a priori information. (Right) Horizontal averaging kernels (integrated in the vertical dimension) and resolution. The averaging kernels are scaled such that a unit change is equivalent to one decade in pressure.

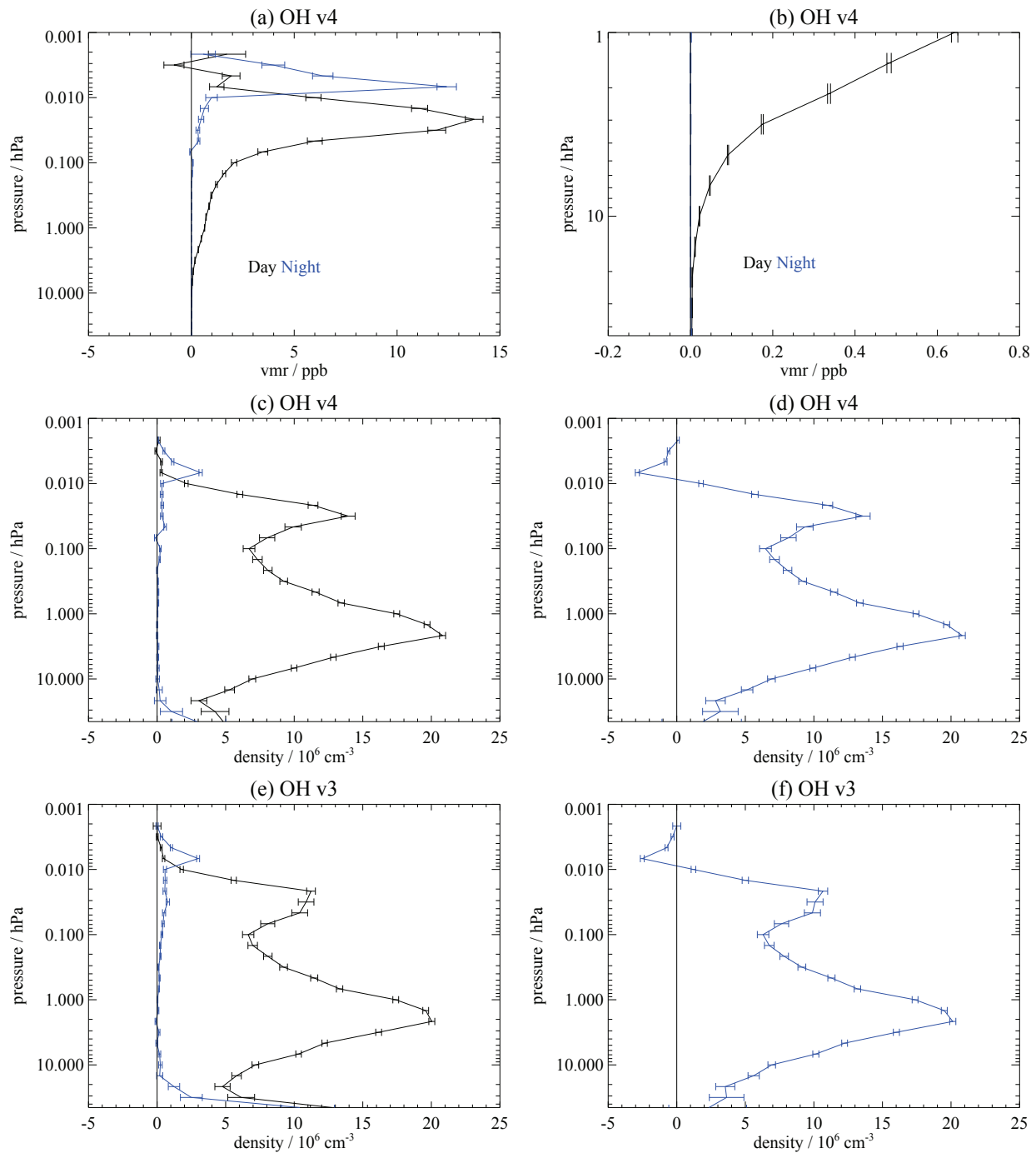


**Figure 3.19.2:** Zonal mean of retrieved OH and its estimated precision (horizontal error bars) for September 20, 2005 averaged over 29°N to 39°N. The average includes 98 profiles. Panel (a) shows v4.2x OH vmr vs. pressure for day (black) and night (blue). Panel (b) shows the same data plotted for the stratosphere. The retrieved night OH concentration is near zero for altitudes below 1 hPa. Panel (c) shows the same data in (a) converted into density units. Panel (d) shows the day-night differences for the data in panel (c). Note that the day-night difference is required for altitudes below 20 hPa. Panels (e) and (f) are equivalent to (c) and (d) but using v3.3x and v3.4x OH data.

### 3.19.4 Accuracy

Table 3.19.1 summarizes the accuracy expected for OH. The effect of each identified source of systematic error on MLS measurements of radiance has been quantified and modeled [Read *et al.*, 2007]. These quantified effects correspond to either  $2\sigma$  estimates of uncertainties in each MLS product, or an estimate of the maximum reasonable uncertainty based on instrument knowledge and/or design requirements. These accuracy calculations were performed with more realistic OH atmospheric profiles than for v3.3x and v3.4x estimates. Biases can be eliminated by taking day-night differences from 32 – 21 hPa. For 15 – 0.1 hPa, the observed night OH concentration is small and day-night differencing is not ordinarily needed. The overall uncertainty is the square root of the sum of squares of the precision and accuracy.

### 3.19.5 Data screening

It is recommended that OH data values be used in scientific investigations if all the following tests are successful:

**Pressure range:** 32 – 0.0032 hPa.

Values outside this range are not recommended for scientific use.

**Estimated precision:** Only use values for which the estimated precision is a positive number.

Values where the *a priori* information has a strong influence are flagged with negative or zero precision, and should not be used in scientific analyses (see Section 1.5).

**Status flag:** Only use profiles for which the **Status** field is an even number.

Odd values of Status indicate that the profile should not be used in scientific studies. See Section 1.6 for more information on the interpretation of the Status field.

**Quality:** MLS v4.2x OH data can be used irrespective of the value of the **Quality** field.

**Convergence:** Only profiles whose **Convergence** field is less than 1.1 should be used.

### 3.19.6 Artifacts

For some seasons, the Gas Laser Local Oscillator (GLLO) for the THz receiver is automatically “relocked” as many as 5 times during a day, leading to data gaps. In these cases the Status flag is set to 257 and the profile is ignored. This can present a problem when compiling maps, because the missing data may appear at the same latitude and longitude on successive days.

### 3.19.7 Review of comparisons with other datasets

Data from MLS v2.2 software have been validated with two balloon-borne remote-sensing instruments and with ground-based column measurements. Details of the comparison are given in Pickett *et al.* [2008] and Wang *et al.* [2008]. The comparison among v2.2, v3.3x and v3.4x, and v4.2x show no significant differences except for the mesosphere where v4.2x OH daytime values are somewhat larger and less noisy in the summer hemisphere (or tropics when near equinox).

**Table 3.19.1:** Summary of precisions, resolution, and uncertainties for the MLS OH product

Pressure	Resolution V × H /km	Precision <sup>a</sup> (day/night) / 10 <sup>6</sup> cm <sup>-3</sup>	Accuracy / 10 <sup>6</sup> cm <sup>-3</sup>	Comments
<0.003 hPa	—	—	—	Unsuitable for scientific use
0.003 hPa	5.0 × 220	0.5 / 0.5	0.5	
0.01 hPa	2.5 × 180	1.1 / 1.1	2	
0.1 hPa	2.5 × 165	3.3 / 0.6	1.0	
1.0 hPa	2.5 × 165	1.9 / 0.4	1.0	
10 hPa	2.5 × 165	2.3 / 1.4	0.9	
32 – 14 hPa	2.5 × 165	6 – 10 / 4 – 8	1.3	Use day–night difference
>32 hPa	—	—	—	Unsuitable for scientific use

<sup>a</sup>Precision on an individual profile

## 3.20 Relative Humidity with respect to Ice (RHI)

**Swath name:** RHI

**Useful range:** UTRHI, mean layer value for  $P \leq 383$  hPa, Profile from 316 – 0.002 hPa.

**Contact:** William Read, **Email:** <william.g.read@jpl.nasa.gov>

### 3.20.1 Introduction

RHI is relative humidity with respect to ice. The vertical grid for RHI is 12 levels per decade change in pressure for 1000 – 1.0 hPa thinning to 6 levels per decade for 1.0 – 0.1 hPa and finally 3 levels per decade for 0.1 –  $10^{-5}$  hPa. The RHI product is a fusion of information from two separate retrievals. From 1000 – 383 hPa, RHI is retrieved directly from optically thick radiances using measurement and retrieval principles similar to nadir sounding humidity receivers (e.g., TOVS). All grid levels between 1000 – 383 hPa are filled with a uniform “UTRHI” (upper tropospheric relative humidity with respect to ice) value representing the mean value of a broad layer (~4 – 6 km) that peaks between ~350 hPa (in the moist tropics) and ~650 hPa (typical for dry high latitudes). This humidity is used as a lower altitude constraint and *a priori* for the vertically resolved humidity product that begins at 316 hPa. From 316 – 0.002 hPa, RHI is derived from the standard products of water and temperature using the Goff-Gratch ice humidity saturation formula. RHI validation is presented in *Read et al.* [2007]. Table 3.20.1 is summary of precision, resolution, and accuracy.

### 3.20.2 Changes from v3

The main differences between v4.2 and v3.3 relate to cloud screening and improvements in the Initial UTRHI initial upper tropospheric and lower stratospheric humidity estimation phase that produces the first guess and sets smoothing constraints on the H<sub>2</sub>O profile retrieved in the final retrieval phase that produces the standard product. There have been no spectroscopy changes either in linewidth or continuum characterization between v4 and v3. An improved cloud detection methodology has been developed for v4 that does a better job of rejecting cloudy radiances that are likely to cause poor fits and corrupted profiles. The number of erroneous spikes in the upper troposphere has been reduced in v4 relative to v3. The Initial UTRHI phase retrieves H<sub>2</sub>O on a more coarse 6 levels per decade grid. The Initial UTRHI H<sub>2</sub>O is used for the initial guess for the final 12 levels per decade retrieval and sets smoothing constraints for the profile shape instead of smoothing to the shape of a climatological *a priori* profile. The Initial UTRHI phase has been expanded to use more channels and better forward model representations to improve its retrieval accuracy. In addition, the retrieval range has been expanded to have its top moved from 100 hPa (in v3) to 10 hPa (in v4). This change makes a more seamless transition from the troposphere to the stratosphere. Simulation studies show that these changes have improved the agreement between the “truth” profiles used to produce the simulated radiances and the retrieved profiles in the 316 – 215 hPa levels.

Figure 3.20.1 compares MLS v4.2 to v3.3. RHI shows bigger differences than that for H<sub>2</sub>O because it also includes changes between the two versions for temperature. The differences sometimes exceed 20% and can be either a low or high bias.

Relative humidity data at pressures greater than 316 hPa are derived from a broad layer relative humidity retrieval (using low limb viewing MLS wing channel radiances) similar to that obtained from NOAA operational humidity sounders such as TOVS. As noted in [*Read et al.*, 2007], the v2.2 retrieval at these pressures was likely to be ~30% too high based on comparisons with AIRS. The accuracy of this retrieval is highly sensitive to the transmission efficiency of the MLS optics system. In v3.3 this was adjusted empirically (within the uncertainty range established from MLS calibration) to give better agreement with AIRS in the tropics. In v4 the N<sub>2</sub> continuum was adjusted only for this phase to minimize the clear sky cloud induced radiance bias. This retrieval is used as an *a priori* and profile constraint for the humidity profile at pressures greater than 316 hPa which are not retrieved in the standard H<sub>2</sub>O product retrieval.

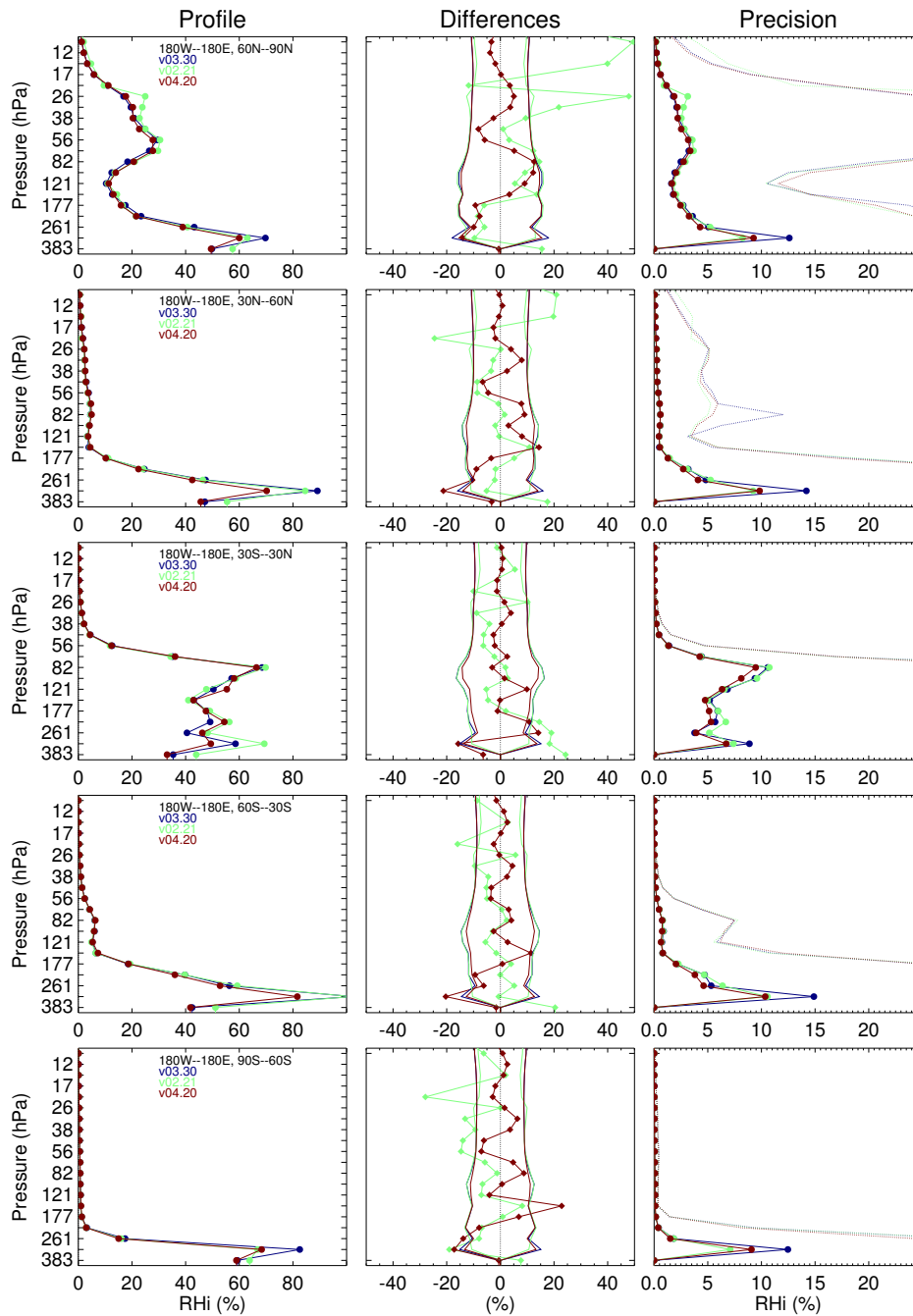


**Figure 3.20.1:** A comparison of v3.3 (blue), v2.2 (green), and v4.2 (red) rhi for Jan-Feb-Mar 2005 in 5 latitude bands. Other time periods are similar. The left panel compares mean profiles, the center shows the mean difference (red and green diamonds) surrounded by each versions' estimated precision, and the right panel shows the estimated retrieval precision (solid and bullets) and measured variability (dotted) which includes atmospheric variability about the mean profile.

The third panel in Figure 3.20.1 shows the mean estimated single profile precision and the measured variability (which includes instrument noise and atmospheric variability). The precisions for the two versions are nearly identical except for pressures greater than 68 hPa, where v4 produces lower values.

### 3.20.3 Resolution

RHi for pressures of 316 hPa and smaller is a derived product and therefore a retrieval averaging kernel is not directly available. An estimate for the spatial resolution (vertical  $X$  along track) of this product is a convolution of the temperature and H<sub>2</sub>O resolutions. Since temperature has lower spatial resolution than H<sub>2</sub>O in the troposphere and lower stratosphere it is assumed that the spatial resolution of temperature shown in Figure 3.22.4 best represents the resolution of the RHi product. The cross track resolution is probably 12 km, the larger of temperature and H<sub>2</sub>O cross track resolutions. These resolutions are only true in the limit that the mean log( H<sub>2</sub>O) doesn't change appreciably over the broader temperature measurement volume. The longitudinal separation of the MLS measurements, set by the Aura orbit, is 10°–20° over middle and lower latitudes, with much finer sampling in polar regions.

The RHi for pressures greater than 316 hPa, represents a mean value in a broad layer (4–6 km) whose sensitivity peaks between ~350 hPa (in the moist tropics) and ~650 hPa (typical for dry high latitudes).

### 3.20.4 Precision

The values for precision are the root sum square (RSS) precisions for H<sub>2</sub>O and temperature propagated through the Goff-Gratch relationship, see sections 3.9 and 3.22 for more details. The precisions are set to negative values (or zero in some cases) in situations when the retrieved precision is larger than 50% of the a priori precision for either temperature or H<sub>2</sub>O — an indication that the data is biased toward the a priori value.

### 3.20.5 Accuracy

The values for accuracy are the RSS accuracies for H<sub>2</sub>O and temperature scaled into % RHi units. see sections 3.9 and 3.22 for more details.

### 3.20.6 Data screening

**Pressure range: Profile from 316 – 0.002 hPa, larger pressures represent mid/upper troposphere column.**

Values outside this range are not recommended for scientific use.

**Estimated precision: Only use values for which the estimated precision is a positive number.**

Values where the *a priori* information has a strong influence are flagged with negative or zero precision, and should not be used in scientific analyses (see Section 1.5).

**Status flag: Only use profiles for which the Status field is an even number.**

Odd values of Status indicate that the profile should not be used in scientific studies. See Section 1.6 for more information on the interpretation of the Status field.

**Clouds:** Ignore status bits 16 (high clouds) or 32 (low clouds) set indicating the presence of clouds. See artifacts for more details.

**Quality field: The Quality fields for both the L2GP-RHI and L2GP-Temperature swaths need to be considered, as described below:**

**For pressures of 83 hPa and smaller:** Use only profiles with RHi Quality *greater* than 1.45 and Temperature Quality *greater* than 0.2

**For pressures of 100 hPa and larger:** Use only profiles with RHi Quality *greater* than 1.45 and Temperature Quality *greater* than 0.9.



**Convergence field:** Only profiles with a value of the RHi Convergence *less than 2.0* and Temperature Convergence *less than 1.03* should be used in scientific studies.

**Temperature precision:** The L2gpPrecision field in the L2GP-Temperature file can be used to further eliminate outliers that are believed to be the result of thick clouds, primarily in the tropics. If careful screening of the troposphere is required, levels 261 – 178 hPa should be avoided if any of the following criteria are met:

At 316 hPa: L2gpPrecision > 1.1 K and latitude > -60°

At 261 hPa: L2gpPrecision > 0.7 K

At 215 hPa: L2gpPrecision > 0.825 K

**End of day (v4.20 only):** The last four profiles of each day show greatly increased rates of large temperature departure from *a priori*. Accordingly the last four profiles of the RHI product each day should not be used in v4.20. The issue is fixed in v4.22.

### 3.20.7 Artifacts

See sections 3.9 for H<sub>2</sub>O and 3.22 for temperature for specific issues related to these parent products. Effects of MLS temperature precision (~1 – 2 K) must be considered if one wishes to use MLS RHi to study supersaturation. In simulation studies, systematic errors (such as tangent pressure retrieval and errors), in addition to introducing biases, also increase variability in differences with respect to a “truth” data set particularly for pressures greater than 200 hPa. This will add to the frequency of supersaturation in the tail of MLS RHi distribution functions. Therefore, MLS RHi is not recommended for studying statistics of supersaturation at pressures greater than 178 hPa. For smaller pressures, one must remove the contribution from temperature noise as part of the analysis. Measurements taken in the presence of clouds significantly degrade the precision, that is increases the scatter about the mean, but the mean bias as compared to AIRS changes by less than 10%.

The last four temperature profiles of each day show increased rates of outliers relative to GEOS-5 temperature, compared to other profile positions in the day. These outliers can be as large as 50 K at some levels. Attempts to address this end of day boundary problem by creating daily overlap periods that can be discarded have not yet satisfactorily addressed this problem and the magnitude of the outliers has increased somewhat in v4.2x. A recommendation to discard the last 4 profiles of each day for temperature, GPH, and RHI has been added to recommended screening.

Also, users should note the possibility of a potential drift in the MLS lower stratospheric water vapor product, discussed in section 3.9.8. Such a drift will also impact the RHi product.

### 3.20.8 Review of comparisons with other datasets

Figures 3.20.2 and 3.20.3 show comparisons between AIRS v6 and MLS v2, 3, and 4. Mapped features tend to agree well but MLS produces higher relative humidities in the moist regions of the tropics relative to AIRS. Version 4 at 300 hPa in high northern latitudes during January and February show marked improvement over the earlier versions by comparison to AIRS. Except as noted previously, the three MLS versions show little change amongst themselves.

### 3.20.9 Desired improvements

We are aiming to improve high latitude performance of 261 and 215 hPa H<sub>2</sub>O in future work.

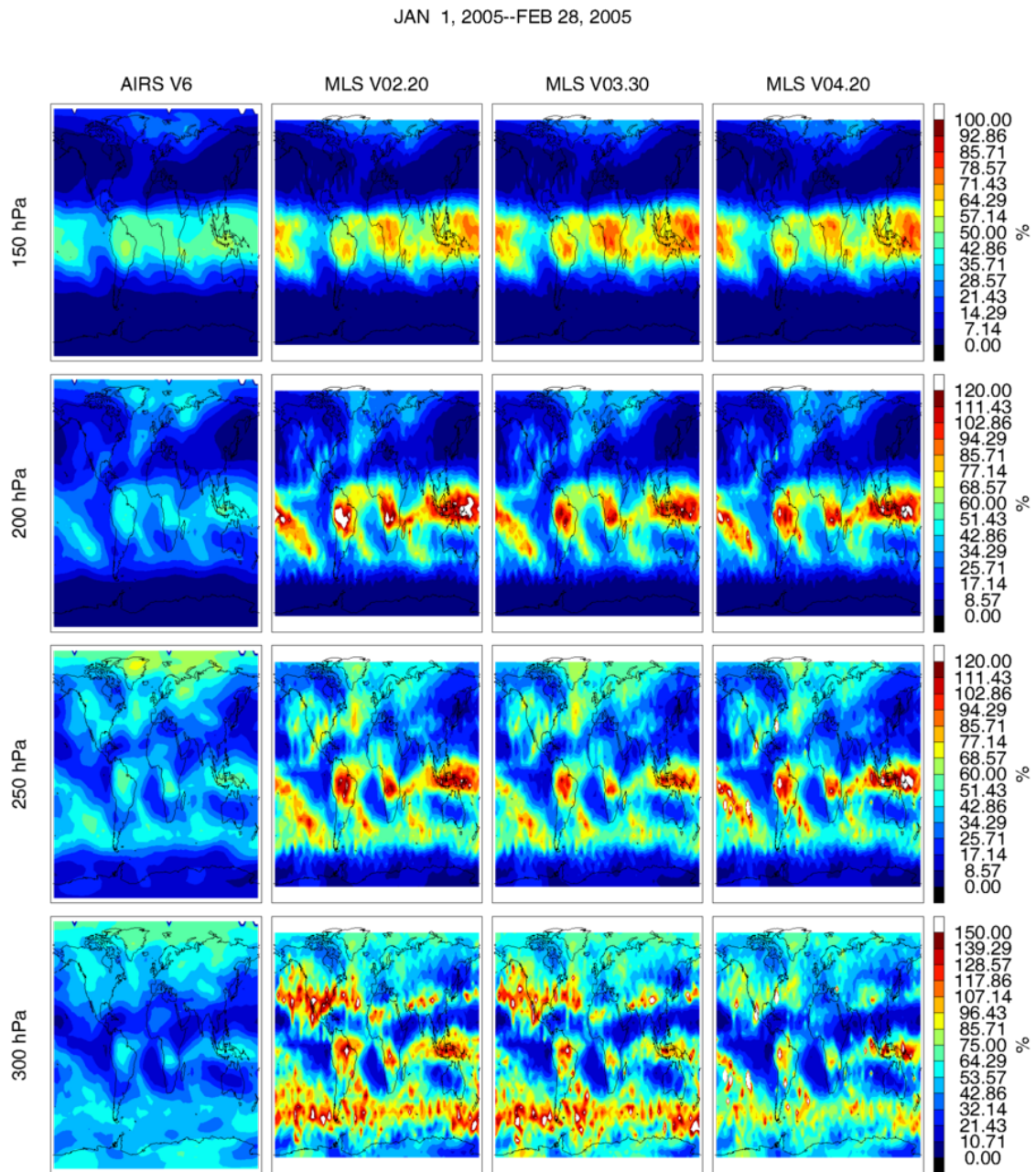


**Figure 3.20.2:** Mapped fields from AIRS v6 (left), MLS v2.2 (center-left), MLS v3.3 (center-right), and MLS v4.2 (right) pressures between 300–150 hPa for January and February 2005.

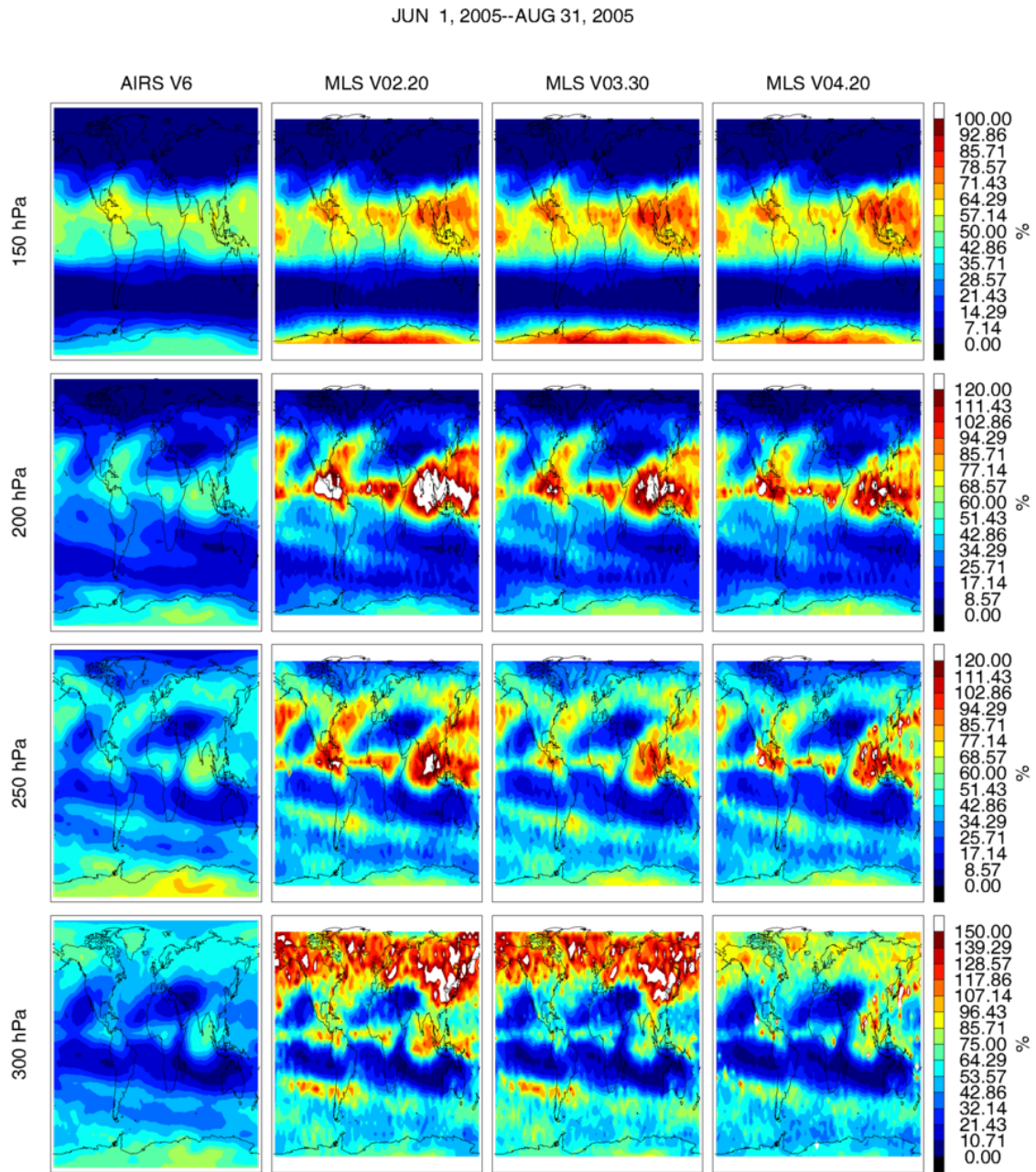


**Figure 3.20.3:** Mapped fields from AIRS v6 (left), MLS v2.2 (center-left), MLS v3.3 (center-right), and MLS v4.2 (right) pressures between 300–150 hPa for June–August 2005.

Table 3.20.1: Summary of MLS v3.3 UTLS RHI product.

Pressure / hPa	Resolution V × H km	Single profile precision <sup>a</sup> / %	Accuracy <sup>b</sup> / %	Comments
0.001	—	—	—	Unsuitable for scientific use
0.002	13 × 230	190	100	
0.004	13 × 260	100	100	
0.010	12 × 590	50	100	
0.022	12 × 750	40	100	
0.046	16 × 400	30	100	
0.10	14 × 420	30	100	
0.22	8 × 370	20	90	
0.46	8 × 320	15	75	
1.00	8 × 280	15	60	
2.15	8 × 250	15	35	
4.64	6 × 220	15	15	
10	4 × 210	15	15	
22	4 × 210	15	20	
46	4 × 210	15	25	
68	4 × 200	15	25	
83	4 × 200	20	25	
100	4 × 200	20	20	
121	4 × 200	25	20	
147	4 × 200	25	20	
178	4 × 200	35	30	
215	4 × 200	45	35	see Table 3.9.1
261	4 × 200	45	30	see Table 3.9.1
316	6 × 200	70	20	see Table 3.9.1
UTRHI, >316	6 × 150	40(est)	10(est)	measurement height depends on atmospheric humidity

<sup>a</sup> Absolute error in percent<sup>b</sup> Fractional error ( [error in RHi] / RHi) in percent

## 3.21 Sulfur Dioxide (SO<sub>2</sub>)

**Swath name:** S02

**Useful range:** 215 – 10.0 hPa

**Contact:** William Read, **Email:** <william.g.read@jpl.nasa.gov>

### 3.21.1 Introduction

The standard SO<sub>2</sub> product is taken from the 240-GHz retrieval (CorePlusR3). MLS can only measure significantly enhanced concentrations above nominal background such as that from volcanic injections. Validation of SO<sub>2</sub> is published in *Pumphrey et al.* [2015].

### 3.21.2 Changes from v3

The v4 SO<sub>2</sub> retrieval has two significant changes from v3. The first is a different method of modeling the background radiance signal from unknown or unaccountable sources. The method is specifically designed to be more immune to clouds. The other change is an improved cloud detection and radiance rejection algorithm. These changes have significantly improved the convergence and quality performance of the retrieval system and eliminated much of the poor in-cloud behavior present in v3. There have been no changes to the spectroscopic characterization of the major species in the 240 GHz bands used to retrieve SO<sub>2</sub>.

Figure 3.21.1 compares MLS v4.2 and v3.3. The atmosphere typically has ~0.1 ppbv SO<sub>2</sub>, which is far smaller than the MLS SO<sub>2</sub> accuracy estimate. Both versions (erroneously) report typical abundance of order of a few ppbv, due to systematic errors in the MLS measurement system. The -20 ppbv reported at 215 hPa is also a systematic artifact.

### 3.21.3 Resolution

Based on Figure 3.21.2, the vertical resolution for SO<sub>2</sub> is ~3 km and the horizontal resolution is 170 km. The horizontal resolution perpendicular to the orbit track is 6 km, the full width at half maximum of the MLS antenna, for all pressures.

### 3.21.4 Precision

The estimated precision for SO<sub>2</sub> is ~4 ppbv for all heights between 215 – 10 hPa. The precisions are set to negative values (or zero in some cases) in situations when the retrieved precision is larger than 50% of the a priori precision – an indication that the data is biased toward the a priori value.

### 3.21.5 Accuracy

Accuracy is estimated to be 10 – 15 ppbv for pressures less than 147 hPa increasing to ~20 ppbv at 215 hPa. These may be different for the v4 SO<sub>2</sub> product.

### 3.21.6 Data screening

**Pressure range:** 215 – 10.0 hPa

Values outside this range are not recommended for scientific use.

**Estimated Precision:** Values with negative precision can be used, though with caution.

Although it is generally recommended to not use values where precision is flagged negative, SO<sub>2</sub> is an exception and it is appropriate to use values with negatively flagged precision (provided that the entire profile is not so flagged). High retrieved values of SO<sub>2</sub> at the larger pressures (e.g., 215 and 147 hPa) will also have larger (i.e., poorer) precision values which are sometimes large enough to trigger the “too

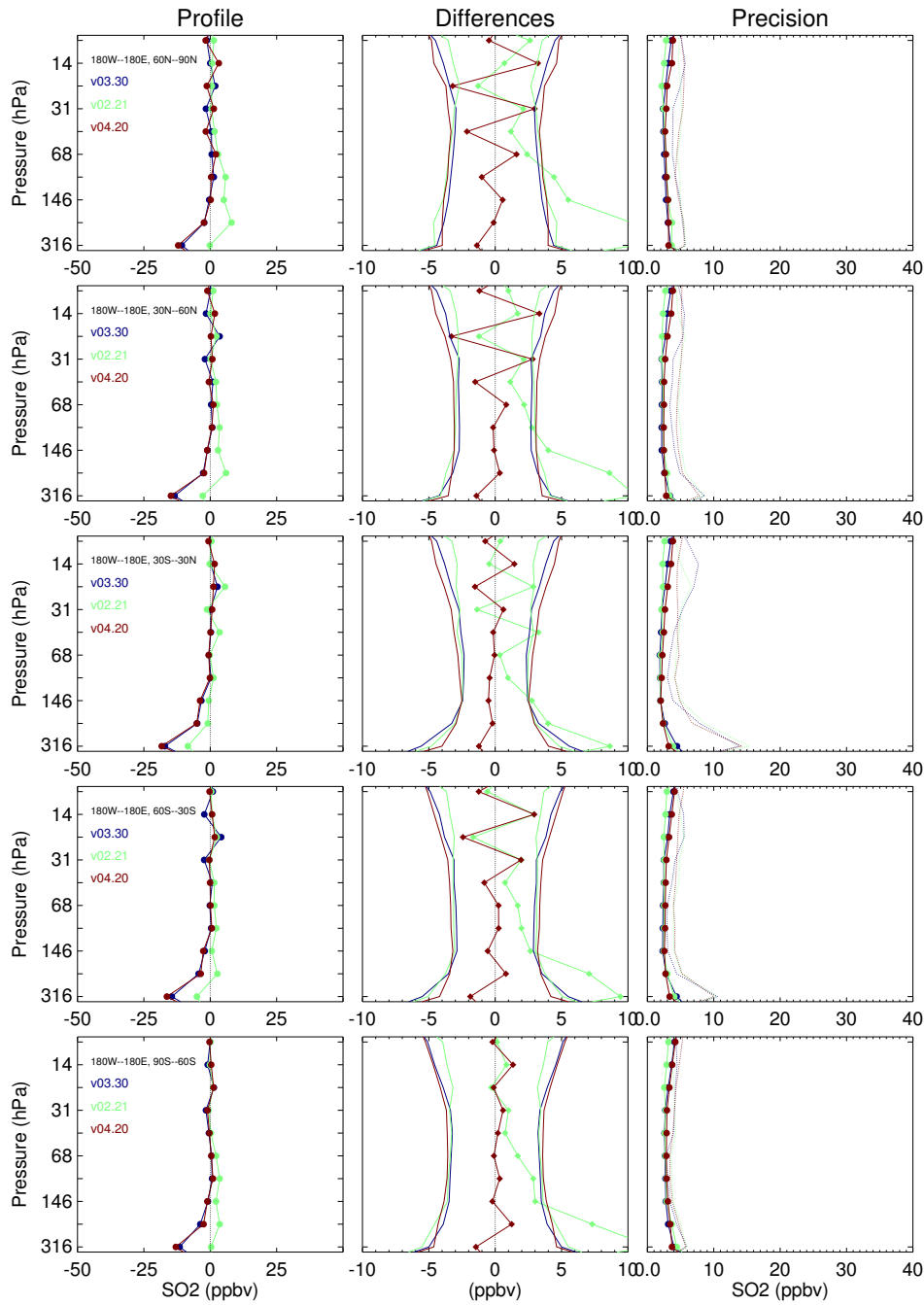


**Figure 3.21.1:** A comparison of v3.3 (blue) and v4.2 (red) SO<sub>2</sub> for Jan-Feb-Mar 2005 in 5 latitude bands. Other time periods are similar. The left panel compares mean profiles, the center shows the mean difference (red diamonds) surrounded by each versions' estimated precision, and the right panel shows the estimated retrieval precision (solid and bullets) and measured variability (dotted) which includes atmospheric variability about the mean profile.

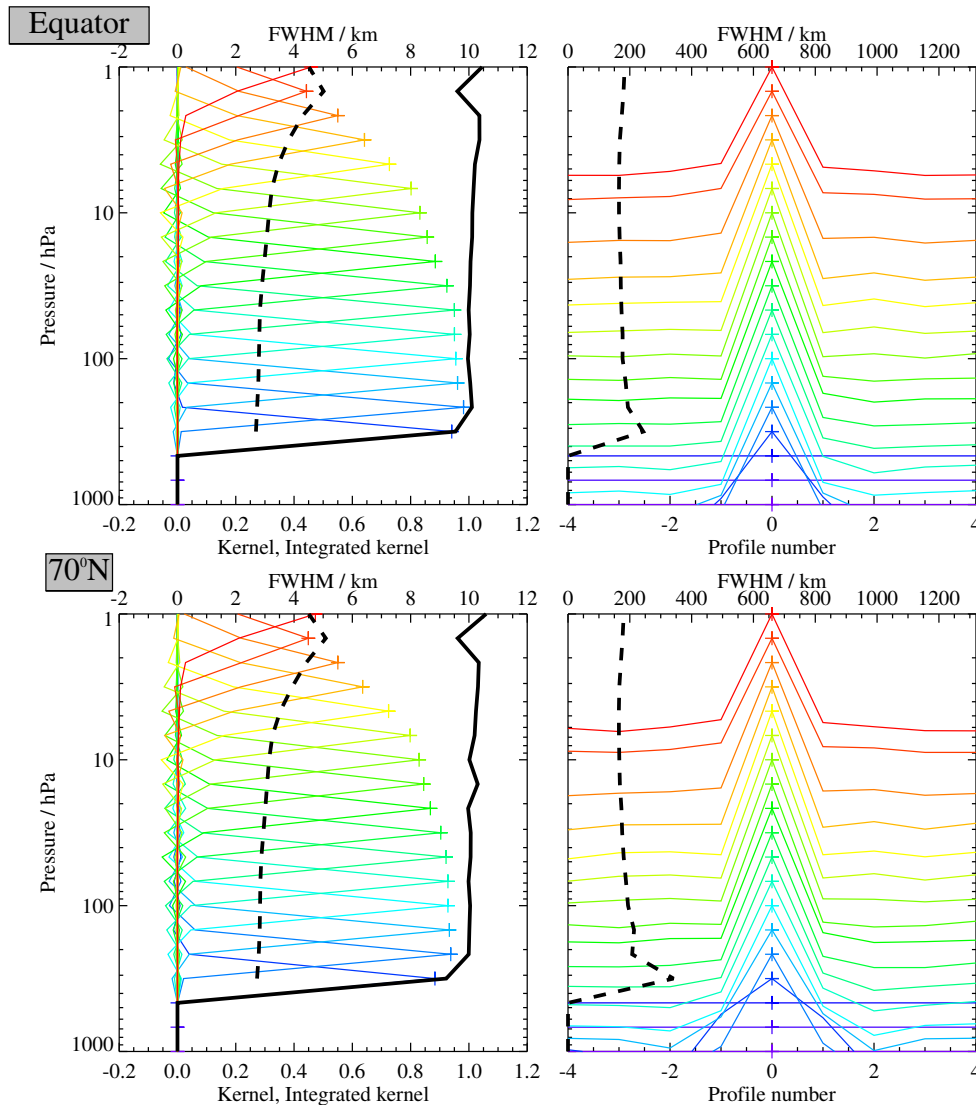


**Figure 3.21.2:** Typical two-dimensional (vertical and horizontal along-track) averaging kernels for the MLS v4.2x SO<sub>2</sub> data at the equator (upper) and at 70°N (lower); variation in the averaging kernels is sufficiently small that these are representative of typical profiles. Colored lines show the averaging kernels as a function of MLS retrieval level, indicating the region of the atmosphere from which information is contributing to the measurements on the individual retrieval surfaces, which are denoted by plus signs in corresponding colors. The dashed black line indicates the resolution, determined from the full width at half maximum (FWHM) of the averaging kernels, approximately scaled into kilometers (top axes). (Left) Vertical averaging kernels (integrated in the horizontal dimension for five along-track profiles) and resolution. The solid black line shows the integrated area under each kernel (horizontally and vertically); values near unity imply that the majority of information for that MLS data point has come from the measurements, whereas lower values imply substantial contributions from a priori information. (Right) Horizontal averaging kernels (integrated in the vertical dimension) and resolution. The horizontal averaging kernels are shown scaled such that a unit averaging kernel amplitude is equivalent to a factor of 10 change in pressure.

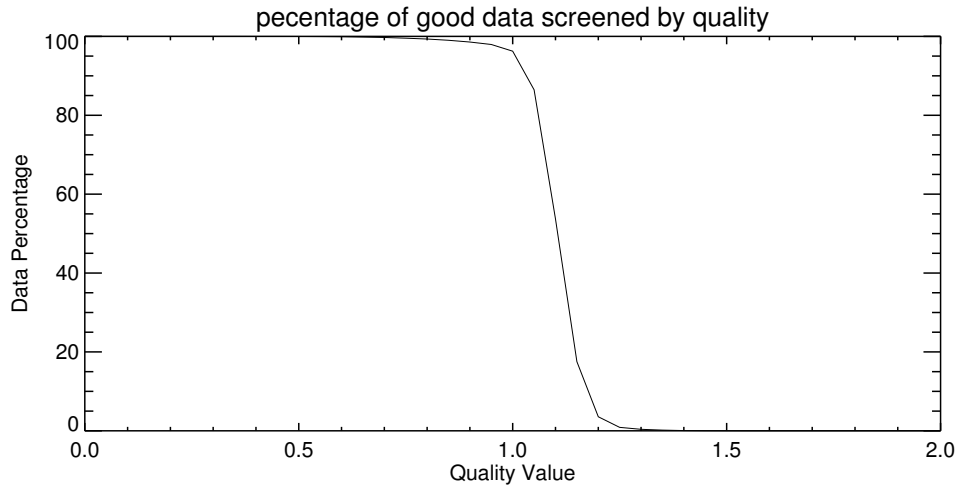


**Figure 3.21.3:** Percentage of data having a quality greater than that indicated on the x-axis for v4.2 data processed for June–August 2005.

much *a priori* influence” negative-precision flag. In these cases, there will be an *a priori* influence, and the retrieved value will probably be smaller than reality because the retrieval is being pulled towards the *a priori* value of zero ppbv. Nonetheless, this does not detract from the fact that greatly enhanced SO<sub>2</sub> is being observed, reflecting the detection of a plume. Profiles where the precision is set to zero, however, should be omitted from analyses.

**Status flag:** Only use profiles for which the **Status** field is an even number.

Odd values of Status indicate that the profile should not be used in scientific studies. See Section 1.6 for more information on the interpretation of the Status field.

**Quality field:** Only profiles having **Quality** greater than 0.95 should be used.

As with water vapor, this value represents where the quality versus yield sharply drops indicating the transition from well fit profiles toward more poorly fit ones as shown in figure 3.21.3

**Convergence field:** Only profiles having **Convergence** less than 1.03 should be used.

### 3.21.7 Artifacts

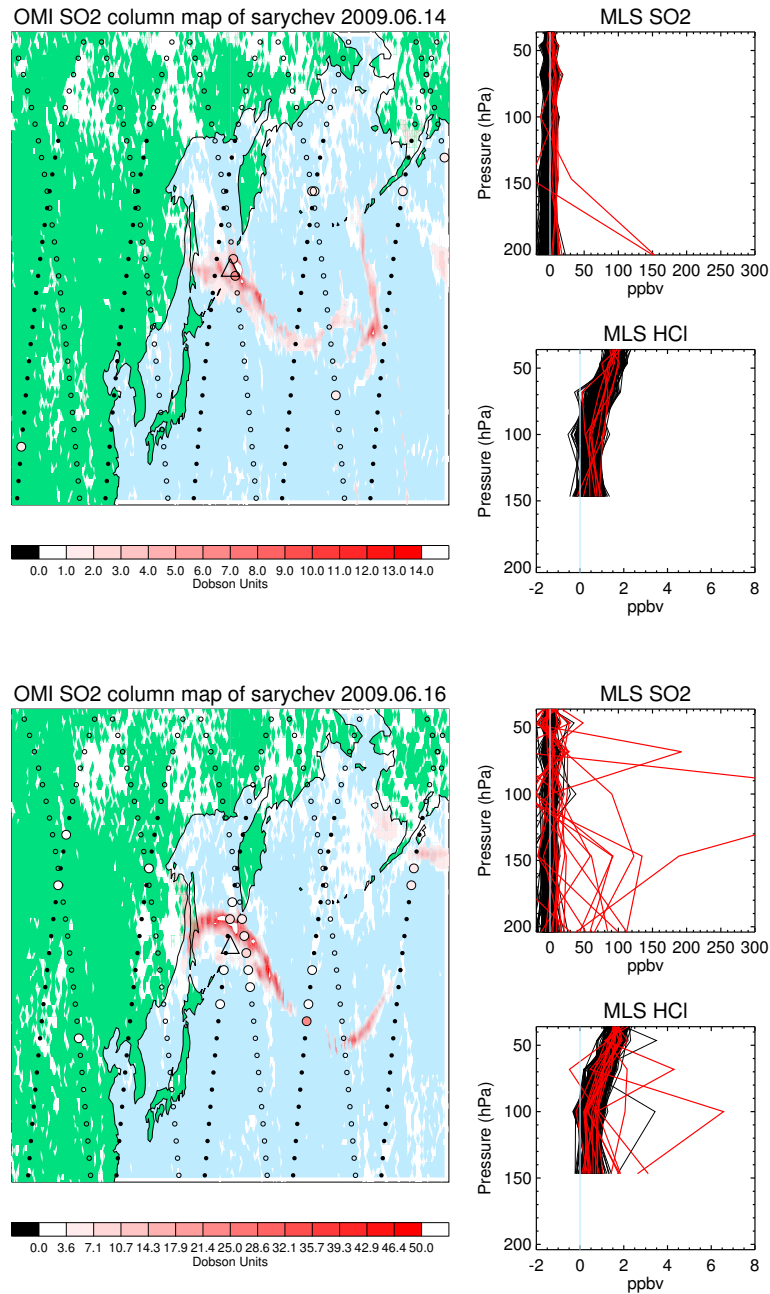
High values of SO<sub>2</sub> accompanied with negative errors are likely to be underestimated due to a priori influence which biases the value toward zero. The atmospheric background SO<sub>2</sub> (~0.1 ppbv) cannot be measured by MLS even with extensive data averaging because there are systematic errors producing biases of a few ppbv. The 215-hPa SO<sub>2</sub> has a background bias of ~ -20 ppbv.

### 3.21.8 Review of comparisons with other datasets

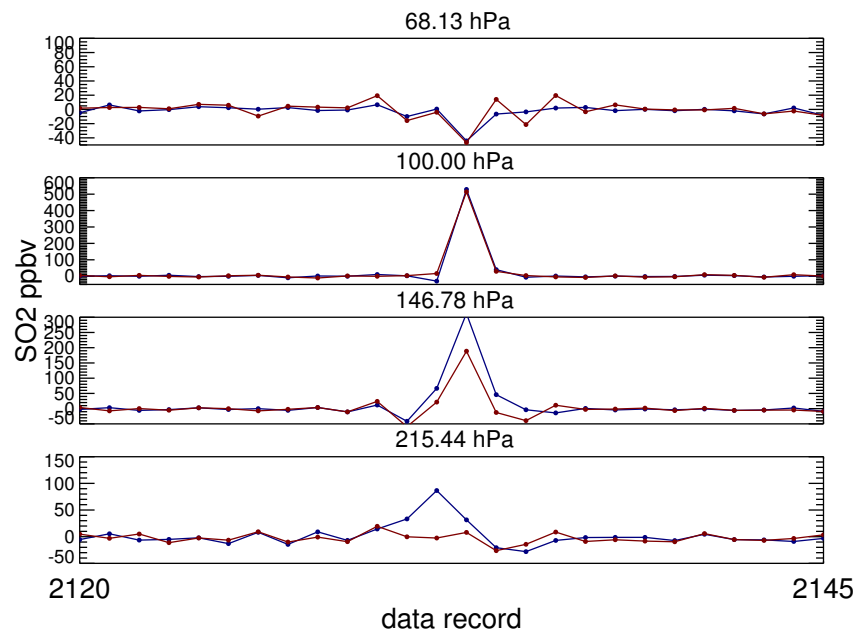
MLS has successfully detected SO<sub>2</sub> from 23 eruptions since launch. These include Manam (Papua, New Guinea – 3 events), Anatahan (Mariana Islands), Sierra Negra (Galapagos Island), Soufriere Hills (Montserrat, West Indies – 2 events), Tunguraua (Ecuador), Rabaul (Papua New Guinea), Piton de la Fournaise (Reunion Island), Jebel al-Tair (Yemen), Okmok (Alaska), Kasatochi (Alaska), Dalaffilla (Ethiopia), Redoubt (Alaska), Sarychev (Kuril Islands, Russia), Pacaya (Guatemala), and Merapi (Indonesia), Grimsvotn (Iceland), Puyehue-Cordon Caulle, (Chile), Nabro (Eritrea), Paluweh (Indonesia), Sangeang Api (Indonesia).

Figure 3.21.4 shows an overlay comparison of column SO<sub>2</sub> measured by OMI and the same calculated by MLS for two days following the Sarychev eruption. It is clear that MLS detects the main plume dispersal fea-





**Figure 3.21.4:** An overlay of MLS measurement tracks on an OMI SO<sub>2</sub> measurement on 14 and 16 June 2009 (separate maps) showing the dispersal of SO<sub>2</sub> from the Sarychev eruption (13 June 2009, black triangle). The color scale indicates the SO<sub>2</sub> column measured by OMI. The daytime MLS tracks are small open circles and the nighttime tracks are filled black. When the calculated column from MLS exceeds 1 DU, that measurement is indicated by a larger open circle filled with the color of the column measurement as indicated by the color scale below (same as for OMI). The panels at right show all the measured profiles covering the area shown in the maps for SO<sub>2</sub> and HCl. Profiles where the MLS column calculation exceeds 1 DU are highlighted in red.



**Figure 3.21.5:** Time series overlay where MLS measures more than 500 ppbv at 100 hPa for the Sarychev eruption. Blue is version 3, and red is version 4.

tures. It also appears that MLS columns are often smaller than those from OMI. Interpreting the significance of this is not straightforward given that OMI has to make assumptions regarding the profile shape and can observe SO<sub>2</sub> down to the boundary layer. The MLS column begins at 215 hPa and integrates upward neglecting the tropospheric contributions. Another limitation is that OMI can only make measurements during the day whereas MLS can make them day and night. Since the plume is moving relatively quickly over the 12-hour measurement separation time, MLS nighttime measurements often miss and/or detect plume features differently than OMI.

Figure 3.21.5 shows a comparison between v4 and v3 for a track showing the maximum SO<sub>2</sub> measured on 16 June 2009. Although both versions detect large amounts of SO<sub>2</sub> at 100 hPa, v4 shows this being more concentrated in the 100-hPa layer than v3, as the newer version shows less SO<sub>2</sub> at 147 hPa and none at 215 hPa compared to v3. Neither version shows any SO<sub>2</sub> at 68 hPa.

**Table 3.21.1:** Summary of MLS v3.3 SO<sub>2</sub> product.

Pressure / hPa	Resolution V × H km	Single profile precision ppbv	Accuracy / ppbv	Comments
< 10	—	—	—	Unsuitable for scientific use
10	3.1 × 165	4.3	16	
15	3.1 × 171	4.3	12	
22	3.1 × 171	3.9	17	
32	3.0 × 176	3.4	14	
46	2.9 × 176	3.2	12	
68	2.9 × 183	3.2	10	
100	2.8 × 180	3.1	10	
147	2.8 × 180	3.2	10	
215	3.5 × 186	3.8	20	
>215	—	—	—	Unsuitable for scientific use

## 3.22 Temperature (T)

**Swath name:** Temperature

**Useful range:** 261 – 0.001 hPa

**Contact:** Michael J. Schwartz, **Email:** <Michael.J.Schwartz@jpl.nasa.gov>

### 3.22.1 Introduction

The MLS v4.2x temperature product is similar to both the v3.3 product and to the v2.2 product that is described in *Schwartz et al.* [2008]. MLS temperature is retrieved primarily from bands near O<sub>2</sub> spectral lines at 118 GHz and 239 GHz that are measured with MLS radiometers R1A/B and R3, respectively. The isotopic 239-GHz line is the primary source of temperature information in the troposphere, while the 118-GHz line is the primary source of temperature in the stratosphere and above. MLS v4.2x temperature has a ~-1 K bias with respect to correlative measurements in the troposphere and stratosphere, with 2 – 3 K peak-to-peak additional systematic vertical structure. Table 3.22.1 summarizes the measurement precision, resolution, and modeled and observed biases. The following sections provide details.

### 3.22.2 Differences between v4.2x and v3.3x/v3.4x

Mean differences between v4.2x temperature and v3.3x/v3.4x temperature are typically less than 0.5 K and exceed 1 K only in the tropical troposphere and, in some instances, at the highest retrieval levels, 0.01–0.001 hPa (see Figure 3.22.1). In the tropics, a cold bias in unscreened v4.2x relative to v3.3x and v3.4x reaches 2 K, and is reduced to 1.5 K by the recommended screening, discussed below.

Versions v3.x and v2.x take the standard temperature product from FinalPtan, a preliminary “phase” of the MLS retrieval that uses only the O<sub>2</sub> bands and that focuses on retrieval of temperature and tangent-point pressure. The standard v4.2x temperature product is taken from the CorePlusR3 phase, which adds radiances from the 240-GHz radiometer and which simultaneously retrieves standard products for a number of atmospheric constituents. The CorePlusR3 temperature and GPH along with the accompanying tangent-point pressures, are used for all subsequent constituent retrievals, so they are more internally consistent with the suite of constituent retrievals than were the standard temperature and GPH products of previous versions.

MLS is generally insensitive to the presence of thin clouds, but scattering in the cores of convective storms can produce significant perturbations in MLS retrieved quantities. Temperature is particularly susceptible to “significant” perturbations, because *a priori* knowledge from analysis is generally good enough in much of the lower and middle atmosphere that perturbations of a few percent (a level negligible for trace-gas constituent retrievals) are considered “significant” for temperature. In the troposphere where *a priori* knowledge may be on the order of 1–2 K, large differences between MLS and GEOS-5 are believed to typically result from problems in the MLS measurements. Plotting differences between the MLS retrieved temperatures and the GEOS-5 temperatures (the retrieval *a priori* in the UT and stratosphere) is often useful in identification of retrieval artifacts. Cloud-induced perturbations generally occur in the tropics and mid-latitudes (where convective storms occur) in both the v3 and v4 retrieval versions, but perturbations of retrieved temperature and the recommended screening for their removal have changed between v3.3x/v3.4x and v4.2x. In unscreened data at retrieval levels 316 – 178 hPa, clouds produce primarily positive outliers in v4.2x and negative perturbations in v03.30. The top panels of Figure 3.22.2 show this behavior at 215 hPa. Conversely, at 121 hPa, outliers are primarily negative in v03.x and positive in v4.2x.

Unscreened and screened histograms of tropical (20°S–20°N) v03.30 and v04.20 temperature from 2005 are shown in Figure 3.22.3. Tails of low, unscreened v04.20 outliers (dark red) are particularly evident from 316–147 hPa, but are greatly reduced by recommended screening (magenta). Changes at 316 – 215 hPa between v03.30 and v4.2x in mean tropical temperature differences from GEOS-5.9, given numerically in the upper left

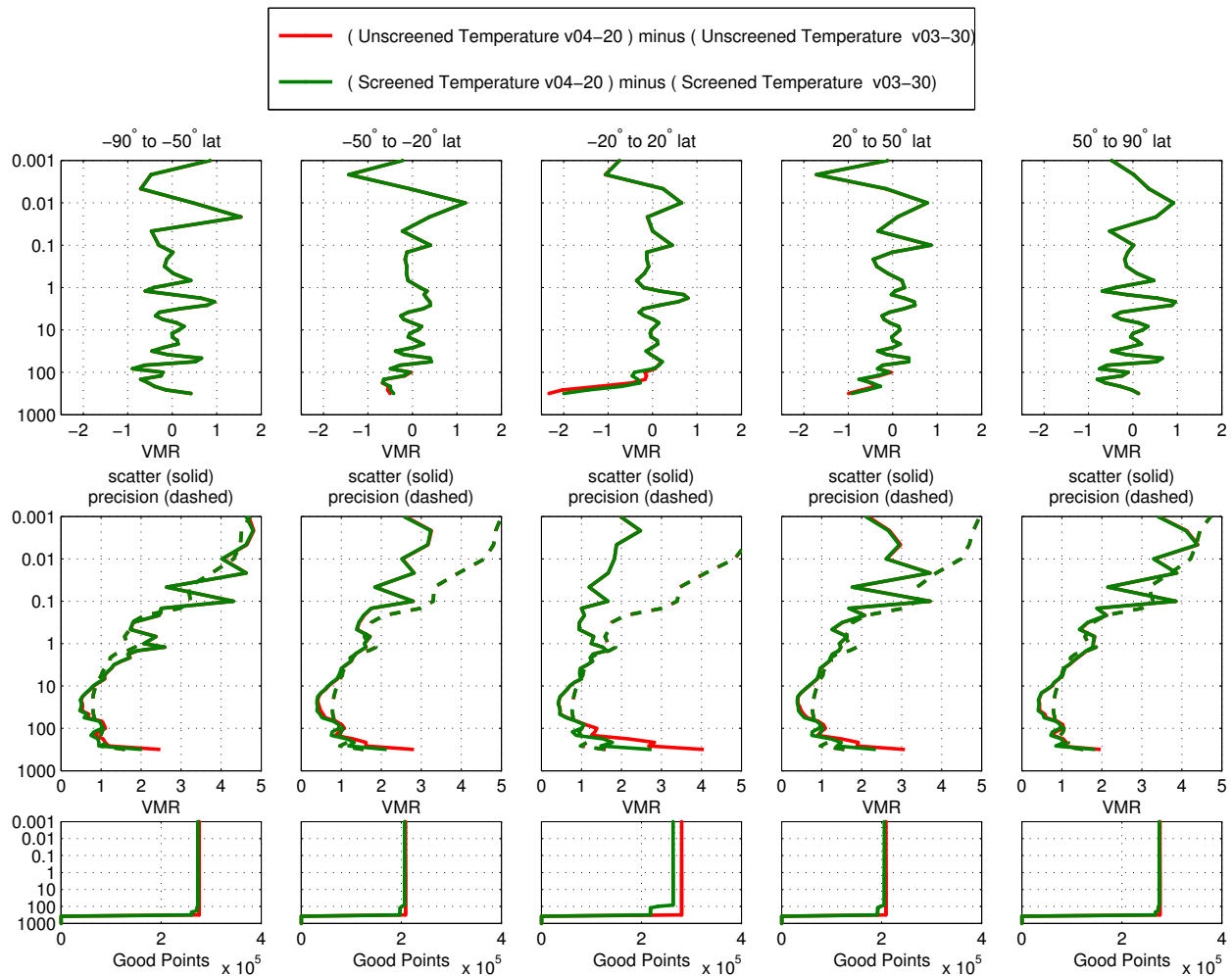


**Figure 3.22.1:** Temperature differences between v4.2x and v03.30 standard products, screened per recommendations of this document (green) and unscreened (red). 2005 data are shown. Top row is mean difference between versions, binned by latitude. Screening has a significant impact on mean values only at low latitudes in the troposphere. The middle panel show considerably more scatter in unscreened data at the bottom of the retrieval, particularly at low latitudes. Bottom panels' difference between red and green lines is the number of points that are screened out

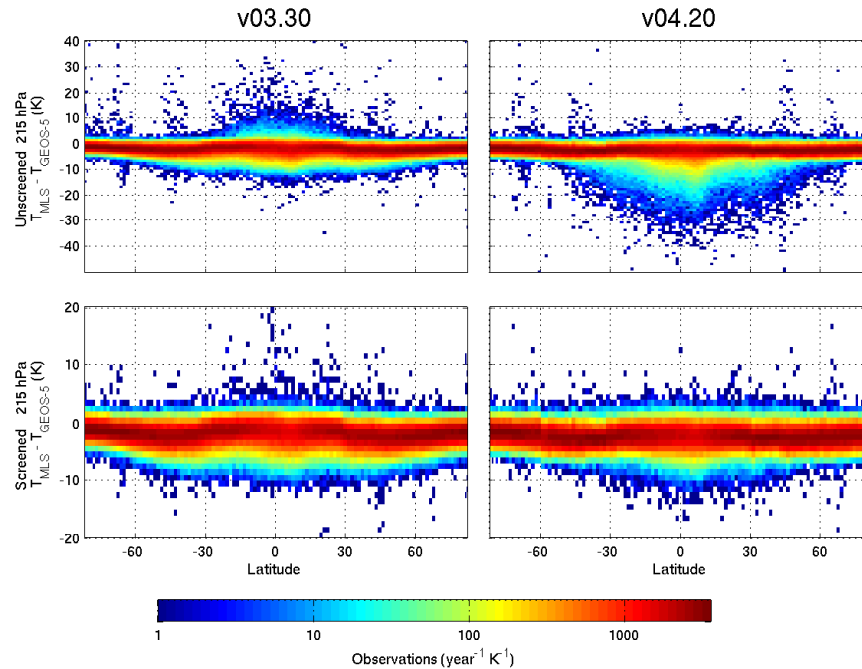


**Figure 3.22.2:** The top row shows histograms of unscreened 215-hPa v03.30 (left) and v04.20 (right) temperature differences from GEOS-5.9 temperature from 2005 data. The horizontal bin spacing is  $\sim 1.5^\circ$  latitudinal spacing of the repeating MLS scan pattern. The bottom panels show histograms of analogous screened differences on a finer vertical scale. Outliers beyond  $\pm 20$  K have been almost completely eliminated and are not shown.

corners of the panels, can be seen to reflect shifts in the peaks of the distributions as well as the contributions of the outlier tails.

The tropospheric and stratospheric *a priori* temperature profiles used in v4.2x are from GEOS-5.9, but are quite similar to the GEOS-5.7 and GEOS-5.2 profiles used in previous version, departing most significantly near the stratopause. This change in *a priori* temperature is believed to have only minimal impact on retrievals.

### 3.22.3 Resolution

The vertical and horizontal resolution of the MLS temperature measurement is shown by averaging kernels in Figure 3.22.4. Vertical resolution, shown on the left panel, is  $\sim 4.5$  km from 261 hPa to 100 hPa, improves to 3.6 km at 31.6 hPa and then degrades to 4.3 km at 10 hPa, 5.5 km at 3.16 hPa, 6 km at 0.01 hPa, and 8 – 10 m at 0.01 hPa. Along track resolution is  $\sim 165$  km from 261 hPa to 0.1 hPa and degrades to 280 km at 0.001 hPa. The cross-track resolution is set by the 6-km width of the MLS 240-GHz field of view in the troposphere and by the 12-km width of the MLS 118-GHz field of view in the stratosphere and above. The longitudinal separation of MLS measurements from a given day, which is determined by the Aura orbit, is  $10^\circ - 20^\circ$  over middle and low latitudes, and finer in polar regions.

### 3.22.4 Precision

The precision of the MLS v4.2x temperature measurement is summarized in Table 3.22.1. Precision is the random component of measurements which would average down if the measurement were repeated. The retrieval software returns an estimate of precision based upon the propagation of radiometric noise and *a priori* uncertainties through the measurement system. These values, which range from 0.5 K in the lower stratosphere to  $\sim 2.5$  K in the mesosphere, are given, for selected levels, in column 2. Column 3 gives the rms of differences of values from successive orbits (divided by the square-root of two as we are looking at the difference of two noisy signals) for latitudes and seasons where longitudinal variability is small and/or is a function

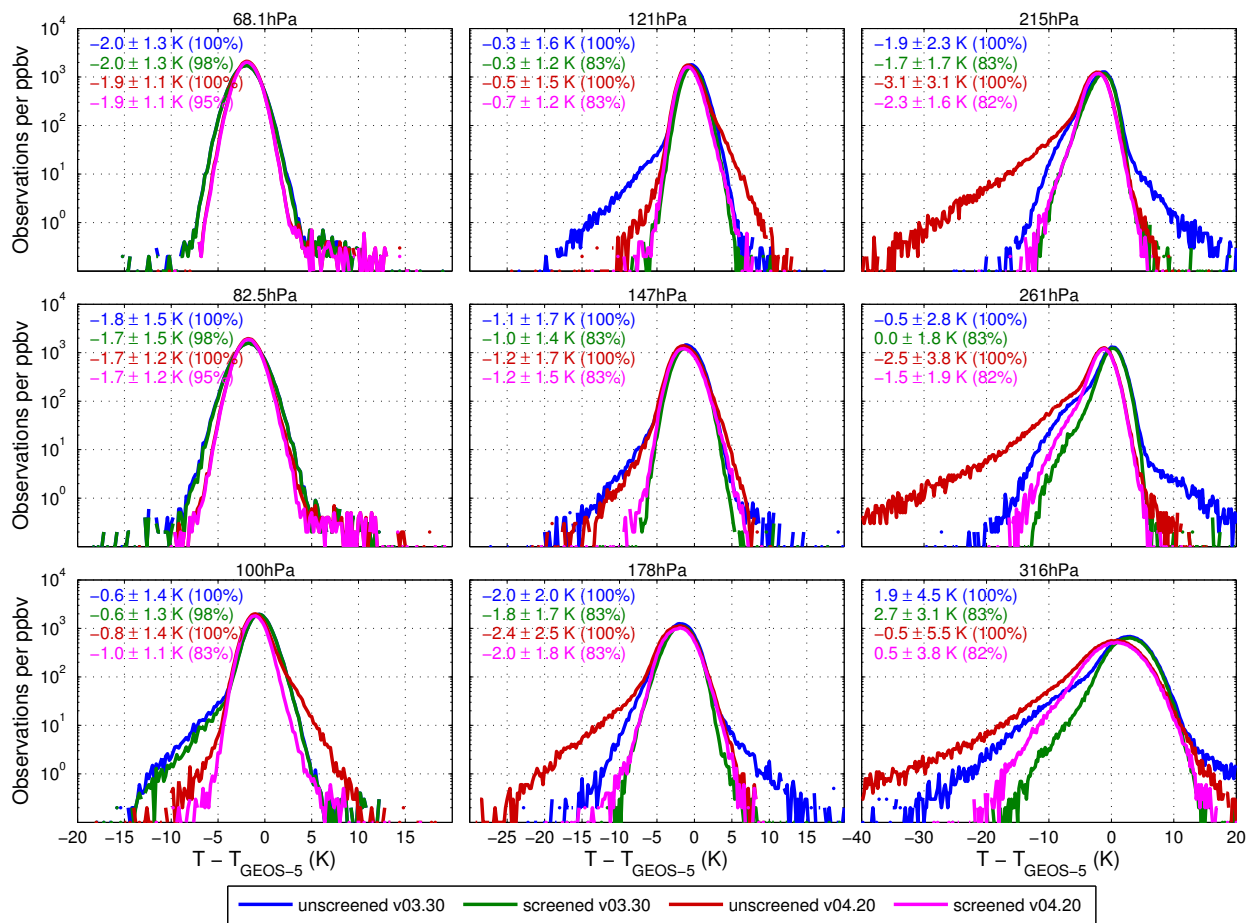


**Figure 3.22.3:** Panels show histograms of tropical ( $20^{\circ}\text{S}$ – $20^{\circ}\text{N}$ ) differences between MLS retrieved temperatures and GEOS-5.9 temperature for all of 2005. Blue and green lines are unscreened and screened v03.30, respectively. Red and magenta are unscreened and screened v04.20, respectively. Distribution means and standard deviations are given in the upper left of each panel along with the percentage of points included after screening. The 316-hPa level is shown for reference although this level is not recommended to be used for scientific work.

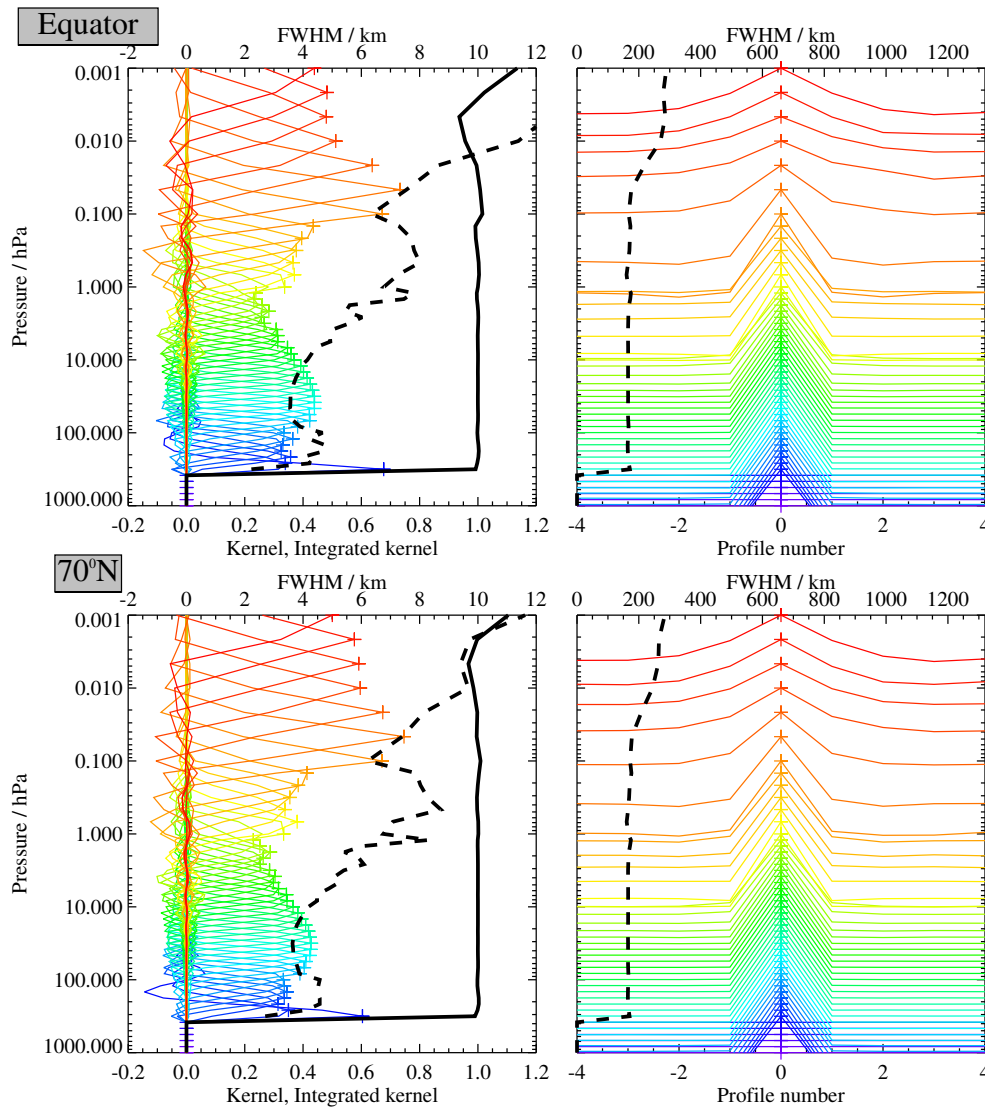


**Figure 3.22.4:** Typical two-dimensional (vertical and horizontal along-track) averaging kernels for the MLS v4.2x Temperature data at the equator (upper) and at 70°N (lower); variation in the averaging kernels is sufficiently small that these are representative of typical profiles. Colored lines show the averaging kernels as a function of MLS retrieval level, indicating the region of the atmosphere from which information is contributing to the measurements on the individual retrieval surfaces, which are denoted by plus signs in corresponding colors. The dashed black line indicates the resolution, determined from the full width at half maximum (FWHM) of the averaging kernels, approximately scaled into kilometers (top axes). (Left) Vertical averaging kernels (integrated in the horizontal dimension for five along-track profiles) and resolution. The solid black line shows the integrated area under each kernel (horizontally and vertically); values near unity imply that the majority of information for that MLS data point has come from the measurements, whereas lower values imply substantial contributions from a priori information. (Right) Horizontal averaging kernels (integrated in the vertical dimension) and resolution. The horizontal averaging kernels are shown scaled such that a unit averaging kernel amplitude is equivalent to a factor of 10 change in pressure.



only of local solar time. The smallest values found, which are in the tropics in the troposphere and in high-latitude summer in the stratosphere and mesosphere, are taken to be those least impacted by atmospheric variability and are what is reported in column 3. These values are 0.5–0.8 K larger than those estimated by the measurement system in the troposphere and lower stratosphere, and a factor of ~1.4 larger from the middle stratosphere through the mesosphere.

### 3.22.5 Accuracy

A substantial study has been made of sources of systematic error in MLS v4.2x measurements, similar to that which was done as a part of the validation of v2.2. The accuracy of the v4.2x temperature measurements is estimated both by modeling the impact of uncertainties in measurement and retrieval parameters that could lead to systematic errors, and through comparisons with correlative data sets. Column 5 of Table 3.22.1 gives estimates from the propagation of parameter uncertainties, as discussed in *Schwartz et al.* [2008]. This estimate is broken into two pieces. The first term was modeled as amplifier non-linearity, referred to as “gain compression,” and was believed to have a known sign, as gain is known to drop at high background signal levels. Correction of these nonlinearities was a goal of v4.2x, but closer examination of the simple non-linearity model found that it did not close forward model and measured radiances as expected. It had been hoped that better radiance closure would permit the use of more radiances in the middle of the 118-GHz O<sub>2</sub> band, giving better resolution, precision and accuracy in the upper stratosphere and better accuracy everywhere. This work is still ongoing, and it is hoped that advances will manifest in improvements in a future version.

The second term of column 5 combines  $2\sigma$  estimates of other sources of systematic uncertainty, such as spectroscopic parameters, retrieval numerics and pointing, for which the sign of resulting bias is unknown. Gain compression terms range from –1.5 K to +4.5 K, and predicted vertical structure is similar to observed biases relative to correlative data in the troposphere and lower stratosphere. The terms of unknown sign are of ~2 K magnitude over most of the retrieval range, increasing to 5 K at 261 hPa and to 3 K at 0.001 hPa.

Column 6 contains estimates of bias based upon comparisons with analyses and with other previously-validated satellite-based measurements. In the troposphere and lower stratosphere, the observed biases between MLS and most correlative data sets are consistent to within ~1.5 K, and have vertical oscillation with an amplitude of 2 – 3 K and a vertical frequency of about 1.5 cycles per decade of pressure. A global average of correlative measurements is shown in Figure 3.22.5.

### 3.22.6 Data screening

**Pressure range:** 261 – 0.001 hPa

Values outside this range are not recommended for scientific use.

**Estimated precision:** Only use values for which the estimated precision is a positive number.

Values where the *a priori* information has a strong influence are flagged with negative or zero precision, and should not be used in scientific analyses (see Section 1.5).

**Status flag:** Only use profiles for which the **Status** field is an even number.

Odd values of Status indicate that the profile should not be used in scientific studies. See Section 1.6 for more information on the interpretation of the Status field.

**Quality:** Only use profiles with Quality greater than 0.2 for the 83 hPa level and smaller pressures, and profiles with Quality greater than 0.9 at larger pressures of 100 hPa and larger.

Profiles with Quality less than or equal to 0.9 comprise 1.4% of all data, and 4.8% of profiles in the tropics.

**Convergence:** Only profiles whose **Convergence** field is less than 1.03 should be used.

This Convergence criterion rejects < 0.1% of profiles and chunks with convergence slightly over this target do not contain manifestly pathological profiles. The primary purpose of this criterion is to reject

profiles with extremely poor convergence that may be expected to reflect poor retrieval behavior.

**Cloud Screening:** The “low cloud” bit of the temperature Status field does not contain useful information in v4.2x, so it cannot be used to screen temperature as it was in previous versions. However, cloud impacts can largely be removed using the ice water content (IWC) product, rejecting profiles between 261 – 100 hPa for which the 215 hPa value of IWC is greater than  $0.005 \text{ g/m}^3$ . Implementation of this criteria requires the loading of the v4.2x IWC swath, but is responsible for most of the rejection of cloud-induced outliers seen in Figure 3.22.3. This criteria removes 4.7% of UT profiles globally and 15% of profiles in the tropics ( $20^\circ \text{ N}$ – $20^\circ \text{ S}$ ).

**Precision:** The L2gpPrecision field can be used to further eliminate outliers that are believed to be the result of thick clouds, primarily in the tropics. If careful screening of the troposphere is required, levels 261 – 178 hPa should be avoided if any of the following criteria are met:

At 316 hPa: L2gpPrecision > 1.1 K and latitude >  $-60^\circ$

At 261 hPa: L2gpPrecision > 0.7 K

At 215 hPa: L2gpPrecision > 0.825 K

**End of day (v4.20 only):** The last four profiles of each day show greatly increased rates of large departure from *a priori* and should not be used. This issue was fixed in v4.22.

### 3.22.7 Artifacts

MLS temperature has persistent, vertically oscillating biases with respect to analysis and correlative measurements in the troposphere and stratosphere that are an area of continued research. The impact of clouds is generally limited to tropospheric levels and to the tropics and, to a lesser extent, mid-latitudes. Cloud impacts in unscreened data at the lowest retrieved levels are larger in v4.2x than they were in v3.3x and v3.4x and are harder to screen due to the lack of a useful “low cloud” status bit. However, after recommended screening, tropical negative departures from *a priori* of greater than 10 K (believed almost always to cloud-induced artifacts) are seen in only 0.2% of tropical profiles. Flagging of clouds is discussed above. Further discussion of artifacts may be found in *Schwartz et al.* [2008].

The last four profiles of each day show increased rates of outliers relative to GEOS-5 temperature, compared to other profile positions in the day in version 4.20 (the problem is fixed in version 4.22). These outliers can be as large as 50 K at some levels. A recommendation to discard the last 4 profiles of each day has been added to recommended screening for v4.20 (not needed for v4.22 and later versions).

### 3.22.8 Review of comparisons with other datasets

*Schwartz et al.* [2008] describes detailed comparisons of MLS v2.2 temperature with products from the Goddard Earth Observing System, version 5 [*Rienecker et al.*, 2007] (GEOS-5), the European Center for Medium-Range Weather Forecast [e.g., *Simmons et al.*, 2005] (ECMWF), the CHALLENGING Minisatellite Payload (CHAMP) [*Wickert et al.*, 2001], the combined Atmospheric Infrared Sounder / Advanced Microwave Sounding Unit (AIRS/AMSU), the Sounding of the Atmosphere using Broadband Radiometry (SABER) [*Mlynzczak and Russell*, 1995], the Halogen Occultation Experiment [*Hervig et al.*, 1996] (HALOE) and the Atmospheric Chemistry Experiment [*Bernath et al.*, 2004] (ACE), as well as to radiosondes from the global network. From 261 hPa to ~10 hPa there is generally agreement to ~1 K between the assimilations (ECMWF and GEOS-5) and AIRS, radiosondes and CHAMP, with SABER and ACE having generally warm biases of ~2 K relative to this group. Figure 3.22.5 shows the global mean biases in the left panel and the  $1\sigma$  scatter about the mean in the right panel for these eight comparisons. Between 1 hPa and 0.001 hPa, MLS has biases with respect to SABER of +1 K to –5 K between 1 hPa and 0.1 hPa, of 0 K to –3 K between 0.1 K and 0.01 K and increasing in magnitude to –10 K at 0.001 hPa. Estimates of systematic error in the MLS temperature are shown in black,

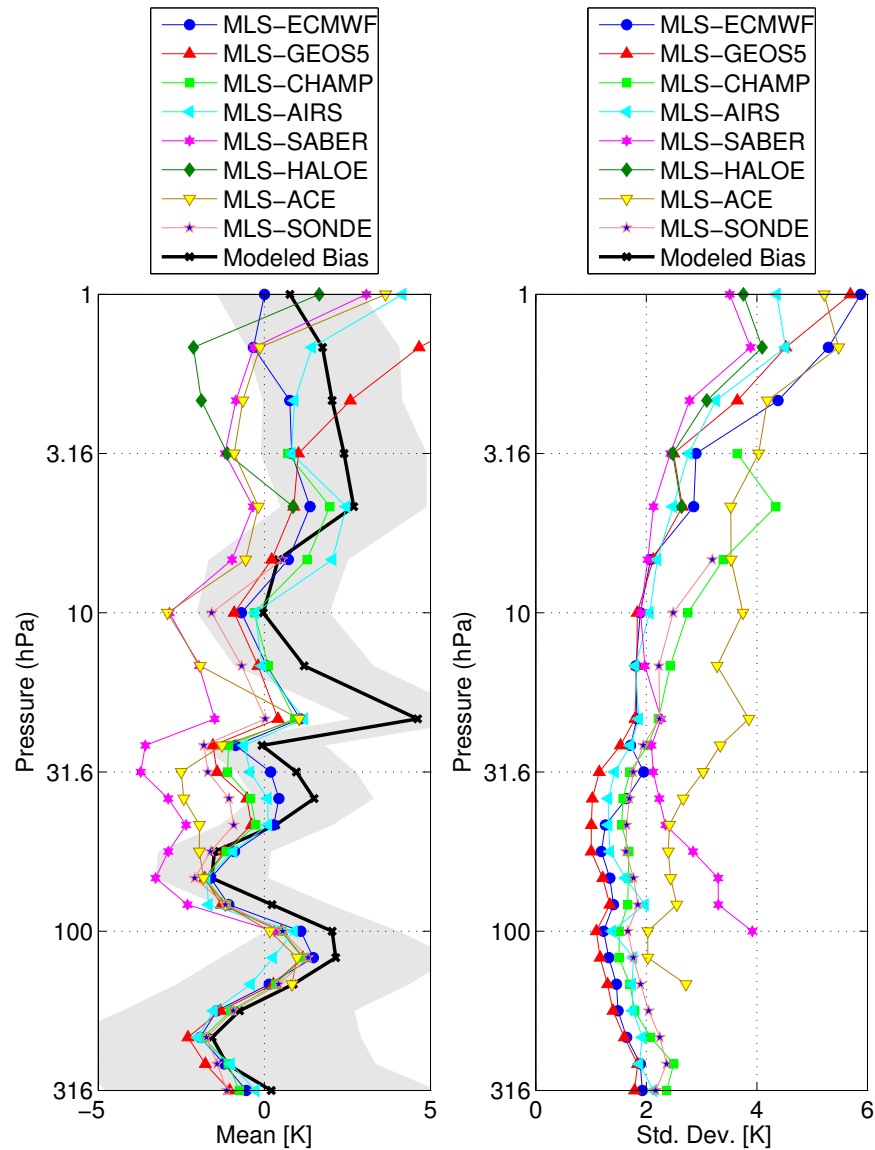


**Figure 3.22.5:** The left panel shows globally-averaged mean differences between MLS temperature and eight correlative data sets. Criteria for coincidences are described in detail in Schwartz et al. [2008]. The right panel shows the global standard deviations about the means.

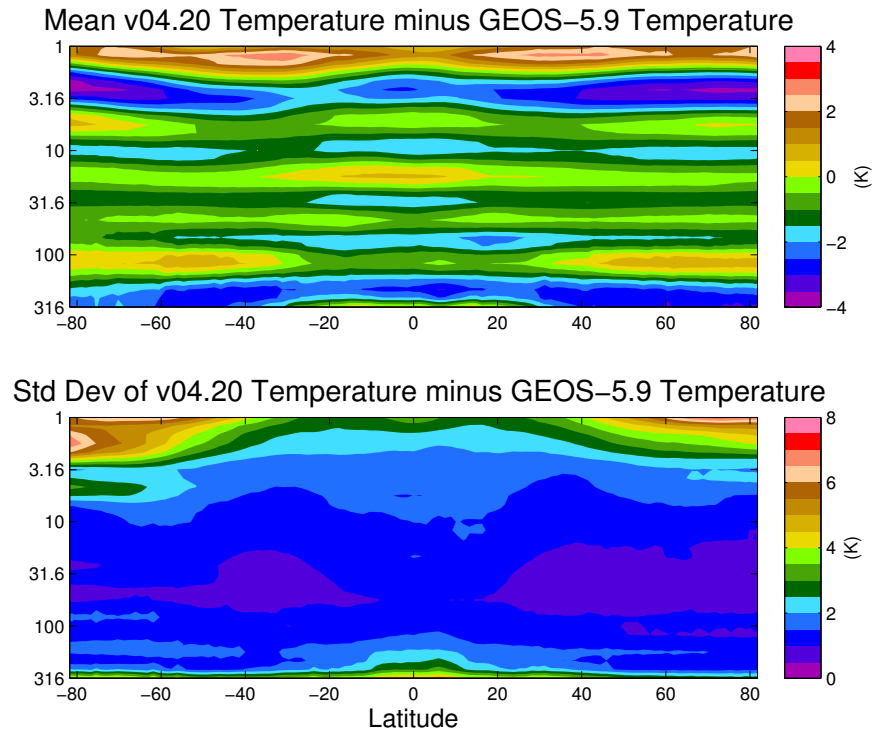


**Figure 3.22.6:** Zonal mean of the difference between MLS v4.2x temperature and GEOS-5.9 temperature (upper), and variability about that mean (lower), averaged for 2005.

with  $2\sigma$  uncertainty shown with gray shading. The black line is the modeled contribution of “gain compression,” which was hoped would explain much of the vertical structure of MLS biases in the upper troposphere and lower stratosphere. As discussed above, the gain-compression model used in this study does not adequately close the retrieval’s radiance residuals, so further study is needed to understand the forward-model inadequacies.

The upper panel of Figure 3.22.6 shows zonal-mean differences between v4.2x temperature and GEOS-5.9 temperature, averaged over 2005; the lower panel is the  $1\sigma$  variability about that mean. Persistent vertical structure in the troposphere and lower stratosphere is evident, with the oscillations somewhat stronger at the equator and poles than at mid-latitudes. In the upper stratosphere, MLS has a general warm bias relative to GEOS-5 at mid and high latitude that increases to more than 10 K in the poles at 1 hPa. The bias at 1 hPa is much smaller in polar summer, but persists in polar winter.

Table 3.22.1: Summary of MLS Temperature product

Pressure	Precision <sup>a</sup> / K	Observed Scatter <sup>b</sup> / K	Resolution V × H / km	Modeled accuracy / K	Observed accuracy / K	Comments
<0.001 hPa	—	—	—	—	—	Unsuitable for scientific use
0.001 hPa	±3.6	±3.5	13–14 × 290	+2 ± 1	–9	
0.01 hPa	±3.3	±3	10–11 × 260	+2 ± 1	–2 to 0	
0.1 hPa	±2.4	±2.7	6 × 170	+3 ± 1.2	–8 to 0	
0.316 hPa	±1.3	±1.5	8 × 170	+2 ± 0.8	–7 to –4	
1 hPa	±1.2	±1.3	6.8 × 165	+1 ± 0.5	0 to +5	
3.16 hPa	±0.8	±0.8	5.5 × 165	+2 ± 1.2	+1	
10 hPa	±0.6	±0.7	4.1 × 165	–1 ± 0.5	–1 to 0	
14.7 hPa	±0.6	±0.7	3.9 × 165	+2.7 ± 0.9	0 to +1	
31.6 hPa	±0.6	±0.6	3.6 × 165	+0.7 ± 0.7	–2 to 0	
56.2 hPa	±0.6	±0.7	3.7 × 165	–1.5 ± 0.8	–2 to 0	
100 hPa	±0.7	±1.0	4.7 × 165	+1.8 ± 1.2	0 to +1	
215 hPa	±0.8	±1.2	4.2 × 165	–0.8 ± 1.4	–2.5 to –1.5	
261 hPa	±0.7	±1.5	4.2 × 167	0.4 ± 2.4	–2 to 0	
1000 – 316 hPa	—	—	—	—	—	Unsuitable for scientific use

<sup>a</sup>Precision on individual profiles<sup>b</sup>Precision inferred from differences of individual profiles from successive orbits (v2.2 results shown)

## Chapter 4

### MLS Level 3 datasets

#### 4.1 Introduction

The other chapters of this guide describe MLS “Level 2” data – geophysical products along the instrument observing track. This chapter describes MLS “Level 3” data – geophysical products binned onto regular grids. There is a wide array of techniques for transforming along-track observations into regular grids, including “kriging” approaches [e.g., *Cressie*, 2015], Fourier-series-based approaches [*Salby*, 1982], approaches using various windowing functions such as Hamming windows, and simple binning approaches. All methods have strengths and weaknesses, and the choice of which one to use is best made by the individual data user, based on the nature of the specific scientific question to be tackled. For this reason, until 2020, the MLS team had not produced any “official” Level 3 data products.

However, in order to facilitate certain studies by MLS data users, the MLS team is now producing and distributing a select set of Level 3 products derived using a simple “binning” approach (i.e., simply reporting the mean measured value within a given spatial/temporal “box”). As part of the generation of these data products, all the data screening rules described in chapters 1 and 3 are applied (along with the ClO bias correction, see section 3.6), providing a significant additional simplification to data users. Level 3 data are supplied for most MLS standard products. BrO and HO<sub>2</sub> are excluded, as they have a different Level 3 product available (see sections 3.2 and 3.13). We also exclude CH<sub>3</sub>CN and CH<sub>3</sub>OH in light of the narrow range over which these products are recommended for scientific use.

Three sets of Level 3 products are provided:

**Daily Binned Files:** These are stored as one product per day of MLS data per file. The daily binned files contain the following datasets:

- Geodetic latitude and longitude maps on a pressure vertical coordinate (i.e., “3D” fields).
- Geodetic latitude and longitude maps on a potential-temperature vertical coordinate (i.e., “3D” fields).
- Geodetic latitude zonal means on a pressure vertical coordinate (“2D”).
- Geodetic latitude zonal means on a potential-temperature vertical coordinate (“2D”).
- Equivalent latitude<sup>1</sup> “zonal means” on a potential-temperature vertical coordinate (“2D”).
- Vortex averages on a potential-temperature vertical coordinate (“1D”).

**Monthly Binned Files:** These are stored as one product per year of MLS data per file. The monthly binned files contain the same datasets as the daily binned files, except with twelve monthly entries in each dataset instead of one daily one.

**Zonal Mean Binned Files:** These files contain “roll-ups” of all the datasets in the daily binned files, excluding the “3D” maps. These are provided with fields having 365 or 366 entries per dataset in each file.

For species with non-negligible diurnal variations over all or part of their vertical range (ClO, OH, HOCl, and O<sub>3</sub>), the datasets described above are further subdivided into five different datasets containing:

<sup>1</sup>Equivalent latitude is the geographical latitude that encloses the same area as an isoline of potential vorticity, giving a polar vortex-centered latitude [*Butchart and Remsberg*, 1986].

- All valid profiles (as for all the non-diurnal products).
- All profiles measured on the ascending side of the orbit (mainly daytime observations, except in polar regions).
- All profiles measured on the descending side of the orbit (mainly nighttime observations, except in polar regions).
- All observations made with solar zenith angle less than  $90^\circ$  (i.e., daytime observations).
- All observations made with solar zenith angle greater than  $110^\circ$  (i.e., nighttime observations).

MERRA-2 [Gelaro *et al.*, 2017] reanalysis temperature fields (interpolated to each MLS observation point) are used to convert from pressure to potential temperature surfaces. Additionally MERRA-2 potential vorticity fields are used to construct equivalent latitude and vortex average information. The interpolated MERRA-2 fields used are taken from the MLS “Derived Meteorological Products” [Manney *et al.*, 2007, 2011]. Note that, for quantities on potential temperature surfaces, the MLS Level 3 profiles on pressure levels are first interpolated to the fixed potential temperature surfaces (from  $\log[p]$  to  $\log[\theta]$ ) before being binned (as opposed to directly binning Level 3 data points in potential temperature windows, which has the potential to introduce undesirable empty bins in the vertical). These interpolated values (and the interpolated L2GPPrecision field) are then used to construct all fields.

The vortex averages are defined using an altitude-dependent value of scaled potential vorticity (sPV) to demark the vortex edge. The values at each level are determined separately for each hemisphere, using the procedure described by Lawrence *et al.* [2018] wherein a constant sPV for each hemisphere and season is derived based on the climatological sPV at the location of the maximum high-latitude sPV gradient. While there are numerous methods of estimating the location of the vortex edge, this simple method with a value that is constant in time has been shown to avoid some common pitfalls such as large spurious day-to-day changes in vortex area and inappropriate values at the beginning and end of the cold season [see Lawrence and Manney, 2018, for a discussion of pros and cons of various vortex edge identification methods]. To estimate uncertainties in vortex edge definition, and to provide results for studies where more or less conservative estimates of the vortex edge are desirable, averages are also provided for “outer” and “inner” vortex edge values that are  $0.2 \times 10^{-4} \text{ s}^{-1}$  less and more, respectively, than the determined value for the vortex edge “center” [this also follows Lawrence *et al.*, 2018].

## 4.2 Level 3 data files

Two different temporal resolutions of Level 3 data are provided—daily (L3DB) and monthly (L3MB). The L3DB files are one file per day per Level 3 data product (with one time entry in each dataset in the file), and the L3MB files are one file per year per Level 3 data product (with twelve time entries in each dataset in the file). Both of these files contain latitude/longitude grids, zonal means, and polar vortex averages on various vertical coordinates, as described in section 4.1, above. To aid in the analysis of long-term datasets, the additional L3DZ files are a yearly rollup of all of the L3DB datasets except for the latitude/longitude grids, which are not included for file size considerations. The datasets in L3DZ files contain 365 or 366 time entries as appropriate. The filenames for these products using the following conventions, which differ mainly in the date format:

```

MLS-Aura_L3DB-<product>_v04-20-c01_<yyyy>d<ddd>.nc
MLS-Aura_L3MB-<product>_v04-20-c01_<yyyy>.nc
MLS-Aura_L3DZ-<product>_v04-20-c01_<yyyy>.nc
MLS-Aura_L3MB-<product>_v04-20-c01_<yyyy>m<mm>.nc (Mid-year forward processing only)
MLS-Aura_L3DZ-<product>_v04-20-c01_<yyyy>m<mm>.nc (Mid-year forward processing only)

```

Where <product> is the MLS standard product: CO, O<sub>3</sub>, Temperature, etc. The date(s) for the observations are given as a four-digit year <yyyy> with an optional three-digit day of year <ddd> (001 = 1 January) or

optional two-digit month <mm>. Files using the two-digit month will only be available during their current calendar year, as “forward processing” data are gathered, and will contain all data in the year up to and including the quoted month, with the remaining date entries present but consisting of values marked “bad” (i.e., with the netCDF `_FillValue`). Once all months are available, the complete dataset will be stored in the “<yyyy>” files.

Within each file, the datasets are stored in netCDF-4 groups. The L3DB and L3MB files contain six types of datasets: latitude/longitude grids on both pressure and potential temperature vertical coordinates, zonal means on both pressure and potential temperature vertical coordinates, means within equivalent latitude contours on potential temperature surfaces, and polar vortex averages as a function of potential temperature. As noted above, the L3DZ files omit the latitude/longitude maps.

These datasets are named as follows (where <product> is the same as listed in the filename):

<product> PressureGrid:	4°×5° geodetic longitude/latitude grid on pressure surfaces (L3DB and L3MB only)
<product> ThetaGrid:	4°×5° geodetic longitude/latitude grid on potential temperature surfaces (L3DB and L3MB only)
<product> PressureZM:	4° geodetic latitude zonal mean on pressure surfaces
<product> ThetaZM:	4° geodetic latitude zonal mean on potential temperature surfaces
<product> EqLZM:	4° equivalent latitude zonal mean on potential temperature surfaces
<product> VortexAvg:	Polar vortex average values for each hemisphere on potential temperature surfaces. The values are calculated in accordance with the “outer”, “center”, and “inner” vortex edge criteria documented in <i>Lawrence et al. [2018]</i> .

Diurnal product files have all of these groups repeated for day, night, ascending profiles only, and descending profiles only (with Day, Night, Asc, Desc, respectively added to the group name).

Each group contains the following data fields:

lon:	The longitude at center of the grid cell (PressureGrid and ThetaGrid groups only)
lon_bnds:	The longitude at the boundaries of the grid cell (PressureGrid and ThetaGrid groups only)
lat:	The latitude at center of the grid cell
lat_bnds:	The latitude at the boundaries of the grid cell
time:	The date of the grid cell (days since 1950-01-01)
time_bnds:	The boundaries of the time period (days since 1950-01-01)
lev:	The vertical coordinate (i.e. pressure/potential temperature values)
value:	The average value for each bin
nvalues:	The number of valid data points found in each bin
rms_uncertainty:	The root mean square of all the Level 2 L2GPPrecision values that contributed to each bin (note that this has <i>not</i> been divided by $\sqrt{nvalues}$ )
minimum:	The minimum value in each bin
maximum:	The maximum value in each bin
std_dev:	The standard deviation of the data in each bin

### 4.3 Guidance for users of Level 3 data

As discussed above, these Level 3 products are generated using only the Level 2 data points that meet all the screening criteria described in the earlier chapters of this document, providing a significant simplification for



users. In cases where there are no good Level 2 data available to populate a Level 3 data point, the nvalues field is set to zero and the other data fields are set to the \_FillValue (bad data flag) for the given netCDF variables.

When considering Level 3 data, as with every geophysical measurement, attention should be paid to the associated uncertainties. The averaging inherent in generating Level 3 data will act to reduce “precision”-related errors, those due to random noise in the MLS radiance measurements, by  $1/\sqrt{n}$ , where  $n$  is the number of Level 2 data points in the average (which is given by the nvalues field). We have chosen not to divide by  $\sqrt{n}$  in the files in order to make it easier for users who wish to perform further averaging. For example, when creating weekly averages from the daily L3 data, the final precision can be computed as the root-mean-square of the daily precisions divided by the square root of the total of the daily nvalues entries.

In contrast, the “accuracy”-related errors, those due to biases in the MLS measurement system, will in most cases be propagated through the averaging process unchanged, and should be assumed to apply to the Level 3 values in the same manner as they do to the values in the underlying Level 2 datasets.

Help

Overview

Table

S  
T

BRO

S  
TCH<sub>3</sub>ClS  
TCH<sub>3</sub>CNS  
TCH<sub>3</sub>OHS  
T

ClO

S  
T

CO

S  
T

GPH

S  
TH<sub>2</sub>OS  
T

HCl

S  
T

HCN

S  
THNO<sub>3</sub>S  
THO<sub>2</sub>S  
T

HOCl

S  
T

IWC

S  
T

IWP

S  
TN<sub>2</sub>OS  
TO<sub>3</sub>S  
T

OH

S  
T

RHI

S  
TSO<sub>2</sub>S  
T

## Bibliography

- Bernath, P. F., et al., Atmospheric chemistry experiment (ACE): mission overview, *Proceedings of SPIE*, 5542, 146–156, 2004.
- Butchart, N., and E. E. Remsburg, The area of the stratospheric vortex as a diagnostic for tracer transport on an isentropic surface, *J. Atmos. Sci.*, 43, 1319–1339, 1986.
- Cofield, R., and P. Stek, Design and field-of-view calibration of 114-660-ghz optics of the earth observing system microwave limb sounder, *IEEE Trans. Geosci. Remote Sens.*, 44(5), 1166–1181, doi: 10.1109/tgrs.2006.873234, 2006.
- Craig, C., K. Stone, D. Cuddy, S. Lewicki, P. Veefkind, P. Leonard, A. Fleig, and P. Wagner, HDF-EOS Aura file format guidelines, *Tech. rep.*, National Center For Atmospheric Research, 2003.
- Cuddy, D. T., M. Echeverri, P. A. Wagner, A. Hanzel, and R. A. Fuller, EOS MLS science data processing system: A description of architecture and capabilities, *IEEE Trans. Geosci. Remote Sens.*, 44(5), 1192–1198, 2006.
- Filipiak, M. J., N. J. Livesey, and W. G. Read, Precision estimates for the geophysical parameters measured by EOS MLS, *Tech. rep.*, University of Edinburgh, Department of Meteorology, 2004.
- Froidevaux, L., et al., Validation of Aura Microwave Limb Sounder HCl measurements, *J. Geophys. Res.*, 113(D15), D15S25, doi: 10.1029/2007JD009025, 2008a.
- Froidevaux, L., et al., Validation of Aura Microwave Limb Sounder stratospheric and mesospheric ozone measurements, *J. Geophys. Res.*, 113, D15S20, doi: 10.1029/2007JD008771, 2008b.
- Gelaro, R., et al., The Modern-Era Retrospective Analysis for Research and Applications, Version 2 (MERRA-2), *J. Climate*, 30(14), 5419–5454, doi: 10.1175/jcli-d-16-0758.1, 2017.
- Harrison, J. J., and P. F. Bernath, ACE-FTS observations of acetonitrile in the lower stratosphere, *Atmos. Chem. Phys.*, 13, 7405–7413, 2013.
- Hervig, M. E., et al., Validation of temperature measurements from the Halogen Occultation Experiment, *J. Geophys. Res.*, 101(10), 10 277–10,286, 1996.
- Hubert, D., et al., Ground-based assessment of the bias and long-term stability of 14 limb and occultation ozone profile data records, *Atmos. Meas. Tech.*, 9(6), 2497–2534, doi: 10.5194/amt-9-2497-2016, 2016.
- Hurst, D. F., W. G. Read, H. Vömel, H. B. Selkirk, K. H. Rosenlof, S. M. Davis, E. G. Hall, A. F. Jordan, and S. J. Oltmans, Recent divergences in stratospheric water vapor measurements by frost point hygrometers and the Aura Microwave Limb Sounder, *Atmos. Meas. Tech.*, 9(9), 4447–4457, doi: 10.5194/amt-9-4447-2016, 2016.
- Jarnot, R. F., V. S. Perun, and M. J. Schwartz, Radiometric and spectral performance and calibration of the GHz bands of EOS MLS, *IEEE Trans. Geosci. Remote Sens.*, 44(5), 1131–1143, 2006.
- Jiang, Y. B., et al., Validation of the Aura Microwave Limb Sounder ozone by ozonesonde and lidar measurements, *J. Geophys. Res.*, 112, D24S34, doi: 10.1029/2007JD008776, 2007.

- Khosravi, M., et al., Diurnal variation of stratospheric and lower mesospheric HOCl, ClO and HO<sub>2</sub> at the equator: comparison of 1-D model calculations with measurements by satellite instruments, *Atmos. Chem. Phys.*, *13*(15), 7587–7606, doi: 10.5194/acp-13-7587-2013, 2013.
- Kleinböhl, A., G. C. Toon, B. Sen, J.-F. L. Blavier, D. K. Weisenstein, and P. O. Wennberg, Infrared measurements of atmospheric ch<sub>3</sub>cn, *Geophys. Res. Lett.*, *32*, L23807, doi: 10.1029/2005GL024283, 2005.
- Kovalenko, L. J., et al., Validation of Aura Microwave Limb Sounder BrO observations in the stratosphere, *J. Geophys. Res.*, *112*, D24S41, doi: 10.1029/2007JD008817, 2007.
- Lambert, A., et al., Validation of the Aura Microwave Limb Sounder stratospheric water vapor and nitrous oxide measurements, *J. Geophys. Res.*, *112*(D24), D24S36, doi: 10.1029/2007JD008724, 2007.
- Lawrence, Z. D., and G. L. Manney, Characterizing stratospheric polar vortex variability with computer vision techniques, *J. Geophys. Res.*, *123*(3), 1510–1535, doi: 10.1002/2017jd027556, 2018.
- Lawrence, Z. D., G. L. Manney, and K. Wargan, Reanalysis intercomparisons of stratospheric polar processing diagnostics, *Atmos. Chem. Phys.*, *18*(18), 13,547–13,579, doi: 10.5194/acp-18-13547-2018, 2018.
- Livesey, N. J., and W. V. Snyder, EOS MLS retrieval processes algorithm theoretical basis, *Tech. rep.*, Jet Propulsion Laboratory, D-16159, available on the MLS web site <https://mls.jpl.nasa.gov>, 2004.
- Livesey, N. J., J. W. Waters, R. Khosravi, G. P. Brasseur, G. S. Tyndall, and W. G. Read, Stratospheric CH<sub>3</sub>CN from the UARS Microwave Limb Sounder, *Geophys. Res. Lett.*, *28*(5), 779–782, 2001.
- Livesey, N. J., W. V. Snyder, W. G. Read, and P. A. Wagner, Retrieval algorithms for the EOS Microwave Limb Sounder (MLS), *IEEE Trans. Geosci. Remote Sens.*, *44*(5), 1144–1155, doi: 10.1109/TGRS.2006.872327, 2006.
- Livesey, N. J., et al., EOS MLS version 1.5 Level 2 data quality and description document, *Tech. rep.*, Jet Propulsion Laboratory, D-32381, 2005.
- Livesey, N. J., et al., Validation of Aura Microwave Limb Sounder O<sub>3</sub> and CO observations in the upper troposphere and lower stratosphere, *J. Geophys. Res.*, *113*, D15S02, doi: 10.1029/2007JD008805, 2008.
- Livesey, N. J., et al., EOS MLS version 3.3 and 3.4 Level 2 data quality and description document, *Tech. rep.*, Jet Propulsion Laboratory, available from <https://mls.jpl.nasa.gov/>, 2013.
- Mahieu, E., et al., Recent Northern Hemisphere stratospheric HCl increase due to atmospheric circulation changes, *Nature*, *515*(7), 104–107, doi: 10.1038/nature13857, 2014.
- Manney, G. L., et al., Solar occultation satellite data and derived meteorological products: Sampling issues and comparisons with Aura Microwave Limb Sounder, *J. Geophys. Res.*, *112*(D24), D24S50, doi: 10.1029/2007JD008709, 2007.
- Manney, G. L., et al., Jet characterization in the upper troposphere/lower stratosphere (UTLS): Applications to climatology and transport studies, *Atmos. Chem. Phys.*, *11*, 6115–6137, doi: 10.5194/acp-11-6115-2011, 2011.
- Millán, L., N. Livesey, W. Read, L. Froidevaux, D. Kinnison, R. Harwood, I. A. Mackenzie, and M. P. Chipperfield, New Aura Microwave Limb Sounder observations of BrO and implications for Bry, *Atmos. Meas. Tech.*, *5*(7), 1741–1751, doi: 10.5194/amt-5-1741-2012, 2012.
- Millán, L., S. Wang, N. Livesey, D. Kinnison, H. Sagawa, and Y. Kasai, Stratospheric and mesospheric HO<sub>2</sub> observations from the Aura Microwave Limb Sounder, *Atmos. Chem. Phys.*, *15*(5), 2,889–2,902, doi: 10.5194/acp-15-2889-2015, 2015.

- Mlynczak, M., and J. M. Russell, III, An overview of the SABER experiment for the TIMED mission, NASA Langley Research Center, *Optical Remote Sensing of the Atmosphere*, 2, 1995.
- Nair, P. J., et al., Relative drifts and stability of satellite and ground-based stratospheric ozone profiles at NDACC lidar stations, *Atmos. Meas. Tech.*, 5(6), 1301–1318, doi: 10.5194/amt-5-1301-2012, 2012.
- Pardo, J. R., E. Serabyn, and J. Cernicharo, Submillimeter atmospheric transmission measurements on mauna kea during extremely dry el niño conditions: implications for broadband opacity contributions, *J. Quant. Spectrosc. Radiat. Transfer*, 68(4), 419–433, doi: 10.1016/S0022-4073(00)00034-0, 2001.
- Pickett, H. M., Microwave Limb Sounder THz Module on Aura, *IEEE Trans. Geosci. Remote Sens.*, 44(5), 1122–1130, 2006.
- Pickett, H. M., W. G. Read, K. K. Lee, and Y. L. Yung, Observation of night OH in the mesosphere, *Geophys. Res. Lett.*, p. L19808, doi: 10.1029/2006GL026910, 2006a.
- Pickett, H. M., et al., Validation of Aura MLS HO<sub>x</sub> measurements with remote-sensing balloon instruments, *Geophys. Res. Lett.*, 33(1), L01808, doi: 10.1029/2005GL024442, 2006b.
- Pickett, H. M., et al., Validation of Aura Microwave Limb Sounder OH and HO<sub>2</sub> measurements, *J. Geophys. Res.*, 113(D16), D16S30, doi: 10.1029/2007JD008775, 2008.
- Pumphrey, H. C., C. J. Jimenez, and J. W. Waters, Measurement of HCN in the middle atmosphere by EOS MLS, *Geophys. Res. Lett.*, 33(8), L08804, doi: 10.1029/2005GL025656, 2006.
- Pumphrey, H. C., W. G. Read, N. J. Livesey, and K. Yang, Observations of volcanic SO<sub>2</sub> from MLS on Aura, *Atmos. Meas. Tech.*, 8(1), 195–209, doi: 10.1002/2014JD021823, 2015.
- Pumphrey, H. C., et al., Validation of middle-atmosphere carbon monoxide retrievals from the Microwave Limb Sounder on Aura, *J. Geophys. Res.*, 112, D24S38, doi: 10.1029/2007JD008723, 2007.
- Read, W. G., Z. Shippony, and W. V. Snyder, Microwave Limb Sounder forward model algorithm theoretical basis document, *Tech. rep.*, Jet Propulsion Laboratory, JPL D-18130, 2004.
- Read, W. G., Z. Shippony, M. J. Schwartz, N. J. Livesey, and W. V. Snyder, The clear-sky unpolarized forward model for the EOS Microwave Limb Sounder (MLS), *IEEE Trans. Geosci. Remote Sens.*, 44(5), 1367–1379, doi: 10.1109/TGRS.2006.873233, 2006.
- Read, W. G., et al., EOS Aura Microwave Limb Sounder upper tropospheric and lower stratospheric humidity validation, *J. Geophys. Res.*, 112, D24S35, doi: 10.1029/2007JD008752, 2007.
- Rienecker, M. M., et al., The GEOS-5 data assimilation system: A documentation of GEOS-5.0, *Tech. rep.*, NASA, TM-104606, Technical report series on Global Modeling and Data Assimilation, 2007.
- Rodgers, C. D., Retrieval of atmospheric temperature and composition from remote measurements of thermal radiation, *Rev. Geophys.*, 14(4), 609–624, 1976.
- Rodgers, C. D., *Inverse Methods for Atmospheric Science, Theory and Practice*, 238 pp., World Scientific, 2000.
- Rodgers, C. D., and B. J. Connor, Intercomparison of remote sounding instruments, *J. Geophys. Res.*, 108(D3), 4116, doi: 10.1029/2002JD002299, 2003.
- Santee, M. L., N. J. Livesey, G. L. Manney, and W. G. Read, Methyl chloride from the Aura Microwave Limb Sounder: First global climatology and assessment of variability in the upper troposphere and stratosphere, *J. Geophys. Res.*, 118, 13,532–13,560, doi: 10.1002/2013/JD020235, 2013.

- Santee, M. L., et al., Validation of the Aura Microwave Limb Sounder HNO<sub>3</sub> measurements, *J. Geophys. Res.*, *112*, D24S40, doi: 10.1029/2007JD008721, 2007.
- Santee, M. L., et al., Validation of the Aura Microwave Limb Sounder ClO measurements, *J. Geophys. Res.*, *113*, D15S22, doi: 10.1029/2007JD008762, 2008.
- Schwartz, M. J., W. V. Snyder, and W. G. Read, MLS mesosphere-specific forward model algorithm theoretical basis document, *Tech. rep.*, Jet Propulsion Laboratory, JPL D-28534, 2004.
- Schwartz, M. J., W. G. Read, and W. V. Snyder, Polarized radiative transfer for Zeeman-split oxygen lines in the EOS MLS forward model, *IEEE Trans. Geosci. Remote Sens.*, *44*(5), 1182–1190, 2006.
- Schwartz, M. J., et al., Validation of the Aura Microwave Limb Sounder temperature and geopotential height measurements, *J. Geophys. Res.*, *113*, D15S11, doi: 10.1029/2007JD008783, 2008.
- Simmons, A., M. Hortal, G. Kelly, A. McNally, A. Untch, and S. Uppala, ECMWF analyses and forecasts of stratospheric winter polar vortex breakup: September 2002 in the southern hemisphere and related events., *J. Atmos. Sci.*, *62*(3), 668–689, 2005.
- Singh, H. B., et al., In situ measurements of HCN and CH<sub>3</sub>CN over the Pacific Ocean: Source, sinks and budgets, *J. Geophys. Res.*, *108*(D20), 8795, doi: 10.1029/2002HD003006, 2003.
- Tegtmeier, S., et al., SPARC Data Initiative: A comparison of ozone climatologies from international satellite limb sounders, *J. Geophys. Res.*, *118*(2), 12,229, doi: 10.1002/2013JD019877, 2013.
- Toohey, M., and T. von Clarmann, Climatologies from satellite measurements: the impact of orbital sampling on the standard error of the mean, *Atmos. Meas. Tech.*, *6*(4), 937–948, doi: 10.5194/amt-6-937-2013, 2013.
- von Clarmann, T., et al., Global stratospheric HOCl distributions retrieved from infrared limb emission spectra recorded by the Michelson Interferometer for Passive Atmospheric Sounding (MIPAS), *J. Geophys. Res.*, *111*, D05311, doi: 10.1029/2005JD005939, 2006.
- Wang, S., et al., Validation of Aura Microwave Limb Sounder OH measurements with Fourier Transform Ultra-Violet Spectrometer total OH column measurements at Table Mountain, California, *J. Geophys. Res.*, *113*, D22301, doi: 10.1029/2008JD009883, 2008.
- Wang, S., et al., Midlatitude atmospheric OH response to the most recent 11-y solar cycle, in *Proc. Natl. Acad. Sci.*, pp. 2023–2028, doi: 10.1073/pnas.1117790110, 2013.
- Waters, J. W., et al., The UARS and EOS Microwave Limb Sounder (MLS) experiments, *J. Atmos. Sci.*, *56*, 194–217, 1999.
- Waters, J. W., et al., An overview of the EOS MLS experiment, *Tech. rep.*, Jet Propulsion Laboratory, D-15745, 2004.
- Waters, J. W., et al., The Earth Observing System Microwave Limb Sounder (EOS MLS) on the Aura satellite, *IEEE Trans. Geosci. Remote Sens.*, *44*(5), 1075–1092, doi: 10.1109/TGRS.2006.873771, 2006.
- Wickert, J., et al., Atmosphere sounding by GPS radio occultation: First results from CHAMP, *Geophys. Res. Lett.*, *28*(17), 3263–3266, 2001.
- Wu, D. L., and J. H. Jiang, EOS MLS algorithm theoretical basis for cloud measurements, *Tech. rep.*, Jet Propulsion Laboratory, JPL D-19299, 2004.

- Wu, D. L., J. H. Jiang, and C. P. Davis, Aura MLS cloud ice measurements and cloudy-sky radiative transfer model, *IEEE Trans. Geosci. Remote Sens.*, 44(5), 1156–1165, 2006.
- Wu, D. L., J. H. Jiang, W. G. Read, R. T. Austin, C. P. David, A. Lambert, G. L. Stephens, D. G. Vane, and J. W. Waters, Validation of Aura MLS cloud Ice Water Content (IWC) measurements, *J. Geophys. Res.*, 113, D15S10, doi: 10.1029/2007LD008931, 2008.
- Wu, D. L., et al., Comparison of global cloud ice from MLS, CloudSat and correlative data sets, *J. Geophys. Res.*, 113, D00A24, doi: 10.1029/2008JD009946, 2009.

Help

Overview

Table

S  
BRO  
TS  
CH<sub>3</sub>Cl  
TS  
CH<sub>3</sub>CN  
TS  
CH<sub>3</sub>OH  
TS  
ClO  
TS  
CO  
TS  
GPH  
TS  
H<sub>2</sub>O  
TS  
HCl  
TS  
HCN  
TS  
HNO<sub>3</sub>  
TS  
HO<sub>2</sub>  
TS  
HOCl  
TS  
IWC  
TS  
IWP  
TS  
N<sub>2</sub>O  
TS  
O<sub>3</sub>  
TS  
OH  
TS  
RH  
TS  
SO<sub>2</sub>  
TS  
T  
T